Investigating Notch4 signalling mechanisms to inhibit Breast Cancer Stem Cells

A thesis submitted to The University of Manchester for the degree of Doctor of Philosophy in the Faculty of Biology, Medicine and Health

2022

Megan E G Thompson

School of Medical Sciences

Division of Cancer Sciences

Table of Contents

Final word count: 47,969

List of Figures

List of Tables

List of Abbreviations

Abbreviation	Full Name
AI	Aromatase Inhibitor
ALDH	Aldehyde dehydrogenase
ANK	Ankyrin repeats
BCSC	Breast Cancer Stem Cell
BSA	Bovine Serum Albumin
cDNA	Complementary DNA
CNA	Copy Number Aberration
CSC	Cancer Stem Cell
DLL	Delta-like ligand
DMFS	Distant Metastasis Free Survival
DNA	Deoxyribonucleic Acid
ECD	Extracellular Domain
EGF	Epidermal Growth Factor
EGFR	Epidermal Growth Factor Receptor
ELDA	Extreme Limiting Dilution Assay
EMT	Epithelial Mesenchymal Transition
ER	Estrogen Receptor
FACS	Fluorescence Activated Cell Sorting
FBS	Fetal Bovine Serum
FULVR	Fulvestrant Resistant
GSI	Gamma Secretase Inhibitor
GWAS	Genome Wide Association Studies
HER2	Human Epidermal Growth Factor 2
HOPS	Homotypic fusion and vacuole protein sorting
HR	Hormone Receptor
ICD	Intracellular Domain
IF	Immunofluorescence
IHC	Immunohistochemistry
JAG	Jagged
KEGG	Kyoto Encyclopedia of Genes and Genomes

LNR	Lin/ Notch Repeat
MFE	Mammosphere Forming Efficiency
mRNA	Messenger Ribonucleic Acid
N4KO	Notch4 Knockout
NECD	Notch Extracellular Domain
NEXT	Notch Extracellular Truncation
NICD	Notch Intracellular Domain
NSG	Nod Scid Gamma
P Value	Probability Value
PBS	Phosphate Buffered Saline
PCR	Polymerase Chain Reaction
PDX	Patient Derived Xenograft
PR	Progesterone Receptor
qPCR	Quantitative PCR
qRT-PCR	Quantitative Reverse Transcription PCR
RAM	RBP-jkappa-associated module
RNA	Ribonucleic Acid
RT	Reverse Transcription
SDS	Sodium Dodecyl Sulfate
SEM	Standard Error of the Mean
SERD	Selective Estrogen Receptor Downregulator
SERM	Selective Estrogen Receptor Modulator
siRNA	Small Interfering RNA
SNPs	Single Nucleotide Polymorphisms
SRB	Sulforhodamine
TAD	Transactivation Domain
TAMR	Tamoxifen Resistant
TNBC	Triple Negative Breast Cancer
TMR	Transmembrane Region
UT	Untransfected
WB	Western Blot
WT	Wildtype

Abstract

Breast cancer stem cell (BCSC) activity is enhanced following anti-estrogen treatment of Estrogen Receptor positive (ER+) breast cancer, leading to endocrine therapy resistance. Notch4 receptor signalling is highly activated in these BCSCs, linking Notch4 activity to endocrine therapy resistance (Simões, O'Brien, et al., 2015). In *Drosophila*, the Notch AxE2 mutant is involved in ligand-independent, Deltex-dependent signalling (Shimizu et al., 2014). Human Notch4 possesses the equivalent residue change to this mutant (Y914), diverging from Notch1/2/3. It is therefore hypothesised that Notch4 may signal in a Deltex-dependent or ligand-independent manner, increase BCSC activity and drive endocrine resistance. Notch4 mutants selected during endocrine therapy may further increase Deltex-dependent signalling.

Immunofluorescence and gene expression analysis showed that Notch4 signals via an endocytic pathway mechanism in breast cancer cells, passing through endosomes and lysosomes as a full length receptor for activation. We found that Deltex1, Deltex4 and Rab7a are specifically involved in this signalling pathway. Deltex4 is essential for BCSC activity of Notch4 cells and TRPML (facilitates fusion of endosomes and lysosomes) was found to be required for viability and BCSC activity of endocrine resistant and Notch4 reliant cells, whilst ADAM10 (undertakes a cleavage of Notch in the canonical signalling pathway) was not. Creation of a stable Notch4 overexpressing cell line demonstrated that Notch4 increases Hey2 expression preferentially over the other Notch target genes Hes1 and Hey1. This Notch4 cell line was found to have increased Notch signalling, BCSC activity and resistance to endocrine therapy. Analysis of breast cancer genomic databases identified increased numbers of Notch4 mutations in metastatic breast cancers compared to primary breast cancers. Investigating selected breast cancer associated Notch4 mutations using site-directed mutagenesis identified unique signalling and trafficking roles. Through its reversion to the residue found in Notch1/2/3, the Y914 Notch4 residue was discovered to be required for Notch4 endocytic trafficking and BCSC activity.

In conclusion, we have shown that Notch4 can signal via an endocytic pathway route, which requires Deltex. Deltex4 and TRPML are required for Notch4 mediated/ endocrine resistant BCSC activity. These actions are linked to the Notch4 Y914 residue which has been linked to ligand independent Notch activation in *Drosophila*. Using knowledge gained about Notch4 signalling mechanisms in BCSCs, the future aim is identification of therapeutic targets to reduce Notch4 activity and treat breast cancer stem cells, to be used in combination with endocrine therapy.

Declaration

I declare that no portion of the work referred to in the thesis has been submitted in support of an application for another degree or qualification of this or any other university or other institute of learning.

Copyright Statement

i. The author of this thesis (including any appendices and/or schedules to this thesis) owns certain copyright or related rights in it (the "Copyright") and s/he has given the University of Manchester certain rights to use such Copyright, including for administrative purposes.

ii. Copies of this thesis, either in full or in extracts and whether in hard or electronic copy, may be made only in accordance with the Copyright, Designs and Patents Act 1988 (as amended) and regulations issued under it or, where appropriate, in accordance with licensing agreements which the University has from time to time. This page must form part of any such copies made.

iii. The ownership of certain Copyright, patents, designs, trademarks and other intellectual property (the "Intellectual Property") and any reproductions of copyright works in the thesis, for example graphs and tables ("Reproductions"), which may be described in this thesis, may not be owned by the author and may be owned by third parties. Such Intellectual Property and Reproductions cannot and must not be made available for use without the prior written permission of the owner(s) of the relevant Intellectual Property and/or Reproductions.

iv. Further information on the conditions under which disclosure, publication and commercialisation of this thesis, the Copyright and any Intellectual Property and/or Reproductions described in it may take place is available in the University IP Policy (see http://documents.manchester.ac.uk/DocuInfo.aspx?DocID=24420), in any relevant Thesis restriction declarations deposited in the University Library, the University Library's regulations (see http://www.library.manchester.ac.uk/about/regulations/) and in the University's policy on Presentation of Theses.

Acknowledgements

I would like to firstly thank my supervisors, Rob Clarke and Martin Baron, for the opportunity to carry out this research. I am very grateful for all of their support and guidance in person and via zoom over the 4 ½ years. I also really appreciate all of the opportunities I have had to present my results at conferences and meetings across the world.

Thank you to the members of Breast Biology, past and present, for all of their encouragement, help in the lab and kindness. I will miss seeing them every day.

I'd like to thank Abby, Ailsa and Adam, who I would not have met if it had not been for this PhD, and who I could not have completed it without.

And finally, I continue to forever be thankful for my family. This thesis is dedicated to them.

1 Introduction

1.1 Breast cancer

Breast cancer is the most common cancer in women in the UK and it is estimated that 1 in 7 women will develop it in their lifetime. It accounts for 15% of female cancer related deaths, making it the second most common cause of cancer death after lung cancer (Smittenaar et al., 2016). Detection, treatment and management methods have greatly improved over time, leading to earlier diagnosis and therefore 70-80% survival rate in those with early, non-metastatic disease (Harbeck et al., 2019). The majority of cancer deaths result from relapse or metastatic spread of the cancer following therapy resistance, highlighting a key area for development and further research.

1.1.1 Risk factors

There are many risk factors that contribute to an individual's risk of developing breast cancer, with the most predominant and unavoidable being age. 95% of diagnosed breast cancers occur in women above the age of 40. After menopause, risk decreases due to the lower exposure to hormones. Approximately 69% of cases are diagnosed between the ages of 45 and 75 (Rojas & Stuckey, 2016). Other major risk factors include mammographic density, reproductive history, lifestyle, family history and genetics.

1.1.1.1 Mammographic density

A high mammographic density is the most significant risk factor after age. The density of the breast can be identified by a mammogram and is often quantified to assess risk (Sherratt et al., 2016). Dense breasts arise from a higher percentage of stromal and epithelial cells compared to fatty adipose tissue. The reason that dense breasts lead to a higher risk of breast cancer is not fully understood. Some links that have been identified include environmental influences, inherited factors and molecular players including collagen type-1, TGF-β and COX-2 (Nazari & Mukherjee, 2018).

1.1.1.2 Reproductive history

Reproductive history is linked to breast cancer risk because of the effects of estrogen and progesterone on the breast tissue. The situations that increase an individual's risk are those

that increase their exposure to estrogen and progesterone, particularly related to hormone receptor positive breast cancer (Anderson et al., 2014). Having children, and particularly having the first child at an earlier age, is protective against developing hormone receptor positive breast cancers. However, those with many children, or high parity, have a slightly increased risk over those with fewer children, due to a "recent" childbirth increasing the risk (Bladström et al., 2003). Breastfeeding has been found to be protective for developing breast cancer, and this protective effect is amplified the longer the time spent breastfeeding (Anderson et al., 2014; Ursin et al., 2005). Menopause related hormone replacement therapy can also play a part in increasing the risk of breast cancer (Rojas & Stuckey, 2016). Women who go through menarche at a younger age, as well as those that experience menopause at a later age have an increased risk of breast cancer (Hamajima et al., 2012).

1.1.1.3 Lifestyle

A high BMI is linked to an increased risk of developing hormone positive breast cancer in post-menopausal women (Biglia et al., 2013). This is thought to be linked to an increase in insulin and insulin-like growth factors which act both directly and via cross-talk with estrogen to increase risk (Renehan et al., 2004). IGF-1 may play a part in relation to diet as a high protein diet increases circulating levels of IGF-1, and so may contribute to a greater risk of breast cancer (Levine et al., 2014). A high frequency of exercise decreases an individual's breast cancer risk (McTiernan et al., 2003). Smoking and alcohol also both have a link to increasing breast cancer risk, with the effects varying depending on age, amount consumed and whether it is current or historical (Rojas & Stuckey, 2016).

1.1.1.4 Family history / genetics

Family history of breast cancer can contribute significantly to an individual's risk. One well known factor is inheritance of mutations that lead to dysfunction of the BRCA1 and BRCA2 genes. Mutations of these genes can lead to a 60% lifetime risk of developing breast cancer (Mavaddat et al., 2013). As well as mutations in these genes, other genetic factors have been used to predict an individual's inherited risk, including Single Nucleotide Polymorphisms (SNPs). Genome Wide Association Studies (GWAS) have contributed greatly to this field, identifying SNPs that are linked to an increased risk of developing breast cancer (Fanfani et al., 2021). Approximately 300 SNPs associated with breast cancer risk have been identified (Evans et al., 2018). Ongoing research into the distribution of SNPs could help identify more

high risk women than in the past, stratifying them according to risk, allowing for earlier intervention and more effective treatment.

1.1.2 Subtypes of breast cancer

In the past, breast cancers were only classified in terms of histological appearance. These histological classifications are constantly changing as there is a lot of crossover between subtypes, leading to differing analysis from different individuals. One of the most recent histological classifications was published in a report by Weigelt et al in 2010. This study found that 25% of cancers can be categorised into 17 histological 'special' types. The remaining cancers did not fit into these categories and can be classified as invasive ductal carcinomas not otherwise specified (IDC-NOS). The most prevalent of these subtypes are listed in Table 1-1 (Weigelt et al., 2010).

Histological type	**Prevalence (%)**
Invasive ductal carcinoma (IDC-NOS)	50-80
Invasive lobular carcinomas	5-15
Tubular carcinoma	2-4
Medullary carcinoma	1-7
Mucinous carcinoma	1.5-2.2
Invasive cribriform carcinoma	0.3-3.5
Neuroendocrine carcinoma	0-5

Table 1-1: Summary of the most prevalent histological subtypes of breast cancer (Weigelt et al., 2010).

As well as histology, there are five subtypes of cancer that can be defined by their molecular make-up. These are defined in Table 1-2 and include triple negative (basal-like), HER2+, normal breast-like, luminal A and luminal B (Dai, Li, et al., 2015). Although these are definable types of breast cancer, they all show genetic heterogeneity. These classifications were originally defined by Perou et al using 65 breast cancer samples from 42 patients. Gene expression patterns were identified from these samples and it was speculated that molecular subtypes could be identified from these (Perou et al., 2000). Sørlie et al further validated this to determine molecular subtypes related to the differences in gene expression, as well as

confirm the distinction between the two ER+ luminal subtypes (Sørlie et al., 2001). The molecular subtypes are mainly defined using expression levels of three receptors- estrogen receptor (ER), progesterone receptor (PR) and human epidermal growth factor receptor (HER2). Further classification comes from the expression of Ki67 which is an antigen associated with proliferation (Scholzen & Gerdes, 2000).

Subtype	**Receptor expression**	**Prevalence** (Perou et al., 2000; Voduc et al., 2010)
Triple negative (Basal-like)	ER- PR- HER2-	15%
HER2+	ER- PR- HER2+	10%
Normal breast-like	ER+ PR+ HER2- Ki67-	5-10%
Luminal A	ER+ PR+ HER2- Ki67-	40-50%
Luminal B	ER+ PR+ HER2-/+ Ki67+	15-20%

Table 1-2: Molecular subtypes of breast cancer (Dai, Li, et al., 2015). ER – Estrogen Receptor, PR – Progesterone Receptor, HER2 – human epidermal growth factor receptor 2.

Luminal breast cancers tend to express the two steroid receptors, ER and PR. The prognoses of luminal A breast cancers are significantly better than other subtypes and they are usually treated with endocrine therapy (Brenton et al., 2005). Luminal B tumours have a worse prognosis than luminal A and are often of a higher tumour grade. The two luminal subtypes have different gene expression profiles and prognostic gene signatures have been developed to distinguish between them (Paik et al., 2009; Van't Veer et al., 2002)

HER2+ cancers include tumours in which the HER2 receptor is overexpressed due to gene amplification and are frequently ER and PR negative. They are also categorised by the high level of expression of HER2 target genes including GRB7 and PGAP3 (Dai, Chen, et al., 2015; Z. Hu et al., 2006). The majority of these tumours also have a mutation in the tumour suppressor gene TP53 (Dai, Li, et al., 2015).

Basal or triple negative tumours do not express ER, PR or HER2. They are associated with a very poor prognosis, showing little to no response to endocrine therapies, but can respond to chemotherapy. There are many reports that show a link between basal breast cancers and

cancers that lack BRCA1 function due to a gene mutation (Turner & Reis-Filho, 2006). Both cancer types have a poor prognosis and share basal markers including p53, P-cadherin and Epidermal Growth Factor Receptor (EGFR) (Rakha et al., 2008). Compared to luminal and HER2 subtypes of breast cancer, basal tumours are more common in African-American women at a young age (Carey et al., 2006).

The different molecular subtypes are linked to different prognoses, with basal breast cancers correlated with a worse prognosis and luminal cancers with a better prognosis (summarised in Figure 1-1). The correlation of ER expression level and better prognosis can be explained by additional factors correlated with ER expression, including lower proliferation of the tumour, lower tumour grade and differentiation status (Dai, Li, et al., 2015).

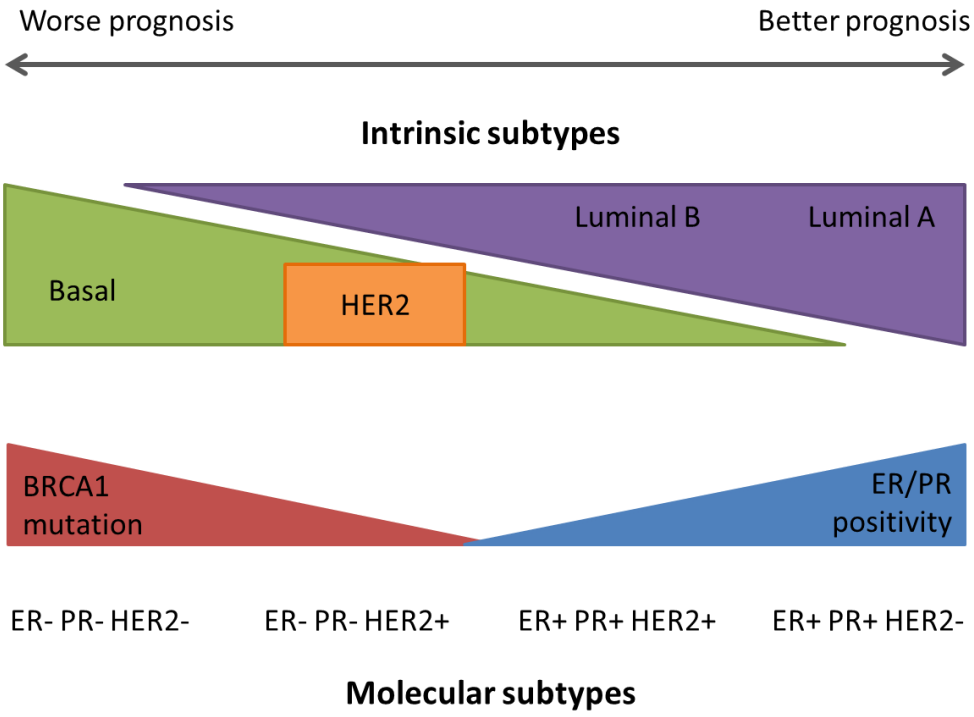

Figure 1-1: Intrinsic and molecular subtypes of breast cancer correlated with prognosis. A better prognosis of breast cancer is associated with the luminal A subtype and Estrogen Receptor (ER)/ Progesterone Receptor (PR) positivity. A worse prognosis of breast cancer is associated with the basal subtype, receptor negativity and BRCA1 mutations. Adapted from (Dai, Li, et al., 2015).

Gene expression profiling can be predictive or prognostic. Predictive gene expression profiling is used before treatment to predict how the tumour will respond. Prognostic gene

expression profiling is used to estimate the prognosis of the cancer, with or without treatment (Mallmann et al., 2010). A popular prognostic gene signature is PAM50, which identifies intrinsic subtypes based on the expression of 50 genes. It has been found to be able to predict for long term survival in hormone receptor positive breast cancers. Combining this gene signature with others including hypoxia signatures has been suggested to improve risk stratification (Pu et al., 2020).

Integrative clustering is another detailed way to characterise breast cancers and combines genetic information and transcriptomic features of tumours, such as Single Nucleotide Polymorphisms (SNPs) and Copy Number Aberrations (CNA). These are usually categorised by clinical outcome and can allow greater insight into personalisation of treatment (Curtis et al., 2012; Dawson et al., 2013).

Another way of subtyping breast cancer comes from the analysis of somatic mutations. Nik-Zainal et al published a study analysing the mutational landscape of 560 breast cancers, investigating driver mutations as well as identification of potential novel subtypes (Nik-Zainal et al., 2016). This study identified that the most commonly mutated genes across the breast cancers sampled were TP53, PI3KCA, CCND1, PTEN and ERB2, suggesting these genes play the most important roles in breast cancers (Nik-Zainal et al., 2016). More recent studies have provided more detail into this area. Tegally et al used a driver selection method, which allowed identification of mutations associated with the most differentially expressed genes, which were then validated through clinical data analysis and pathway analysis. Many novel, potentially cancer driving mutations were identified across a pan-cancer landscape, including breast cancer (Tegally et al., 2020). Others have created gene panels for use in identifying targetable mutations, known as Mammaseq. This panel can be used on advanced tumour biopsies and liquid samples, allowing for subtyping of the tumour in order to identify appropriate treatment strategies (N. G. Smith et al., 2019).

1.1.3 Breast cancer treatments

Currently, breast cancer patients are treated with one or a combination of surgery, radiotherapy, chemotherapy, endocrine therapy or targeted therapy. Treatment decisions are decided based on the tumour subtype and gene expression profile, as well as the general health, age and treatment history of the patient. Treatment is often a dynamic process as every tumour and patient will react differently. If a tumour shows ER/ PR expression, endocrine therapies are usually administered (Dai, Li, et al., 2015). Breast cancers with HER2

positivity are often treated with chemotherapy or a HER2 receptor targeted treatment such as trastuzumab (Lopez et al., 2009). Tumours with a triple negative phenotype are usually treated with chemotherapies such as fluorouracil, epirubicin and cyclophosphamide (Wahba & El-Hadaad, 2015). TNBCs with a BRCA mutation are treated with PARP inhibitors (Layman & Arun, 2021). These different therapies can be administered in a neo-adjuvant way, in order to attempt to shrink the tumour pre-surgery; or in an adjuvant way, post-surgery, in order to prevent the cancer from recurring ((EBCTCG), 2018). Adjuvant radiotherapy is also sometimes given to destroy any remaining cancer cells after surgery ((EBCTCG), 2011).

These are the standard of care treatments that are currently used routinely to treat most primary breast cancers. However, there are many other more personalised, targeted therapies that are in various stages of research from early basic science research through to clinical trials. These include CDK4/6 inhibitors, immune checkpoint inhibitors, PARP inhibitors and Akt, PI3K and mTOR inhibitors (Cortesi et al., 2021; J. J. X. Lee et al., 2015; Martorana et al., 2021; Spring et al., 2019; Thomas et al., 2021; Z. Zhang & Richmond, 2021).

Endocrine therapies, also known as anti-estrogens, act directly on the estrogen receptors in signalling cells and block their downstream actions (Osborne & Schiff, 2011). They act in a cytostatic way, blocking the growth of tumour cells. Tamoxifen is an example of a Selective Estrogen Receptor Modulator (SERM). This type of drug is an antagonist to the ER, and binds directly in the binding site, blocking estrogen and its effect on target genes. Interestingly, tamoxifen has also been reported to act as an ER agonist in some tissues, perhaps causing off-target effects (Frasor et al., 2004; Osborne & Schiff, 2011). It is unknown whether this is the case for all SERMs. Aromatase inhibitors (AI), including anastrozole, are another treatment commonly used to deprive tumours of estrogen. They block the formation of estrogen from androgens by inhibiting the enzyme aromatase at the last step of synthesis and are mostly prescribed to post-menopausal women (Mokbel, 2002). The third class of endocrine therapies are the Selective Estrogen Receptor Downregulators (SERDs) that include fulvestrant. These drugs act as downregulators of the ER by targeting it for degradation with ubiquitination (S. J. Howell et al., 2004). This reduces the amount of ER in the tumour cells and therefore reduces the level of signalling and gene regulation (Dowsett et al., 2005). The actions of the endocrine therapies are summarised in Figure 1-2.

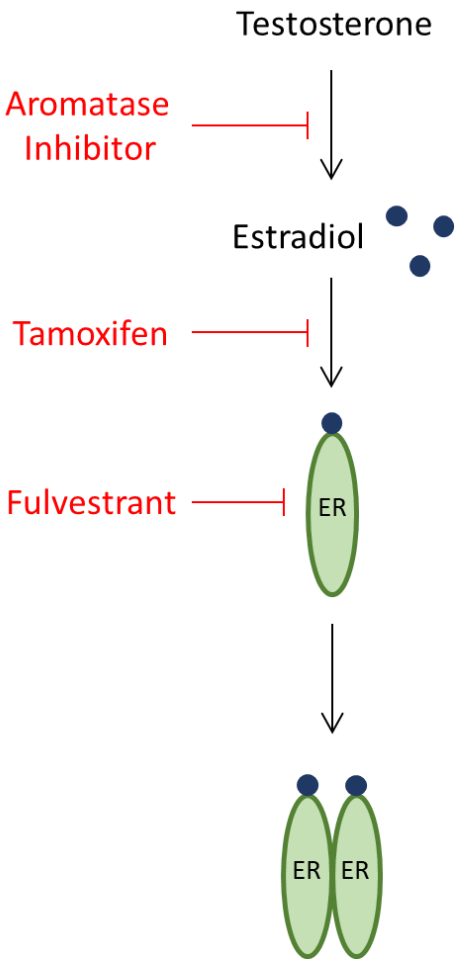

Figure 1-2: The effect of endocrine therapies on Estrogen Receptor (ER). Aromatase Inhibitors e.g. anastrozole block the conversion of androgens including testosterone to estrogen/estradiol. Tamoxifen is a Selective Estrogen Receptor Modulator (SERM). It is an antagonist of ER, blocking the binding of estrogen. Fulvestrant is a Selective Estrogen Receptor Downregulator (SERD). It binds directly to ER and targets it for degradation.

1.1.3.1 Endocrine resistance

ER+ breast cancers are generally treated successfully with anti-estrogen therapies. However, there is large population of women who develop resistance to the drugs (known as endocrine resistance), and subsequent recurrence or metastasis of the cancer occurs. In a large meta-analysis by C Davies et al it was shown that after 5 years of adjuvant tamoxifen treatment, up to 33% of cases resulted in recurrence or metastasis, suggesting these cancers are resistant to anti-estrogen therapies (Early Breast Cancer Trialists' Collaborative Group (EBCTCG) et al., 2011). This was significantly reduced from the control group with no adjuvant treatment, of which 46.2% recurred, but represents the ferocity of resistance to anti-estrogen treatment (Figure 1-3) (Early Breast Cancer Trialists' Collaborative Group (EBCTCG)

et al., 2011). A further analysis by Pan et al sorted breast cancer recurrence events by grade and node status, among other factors, and found that the 5-20 year recurrence risk after adjuvant therapy ranges from 10% to 40% risk. The higher end of the risk corresponds to cancers with a larger tumour diameter and involvement of many nodes, and the lower end corresponds to cancers with a smaller tumour diameter and no involvement from lymph nodes (Pan et al., 2017).

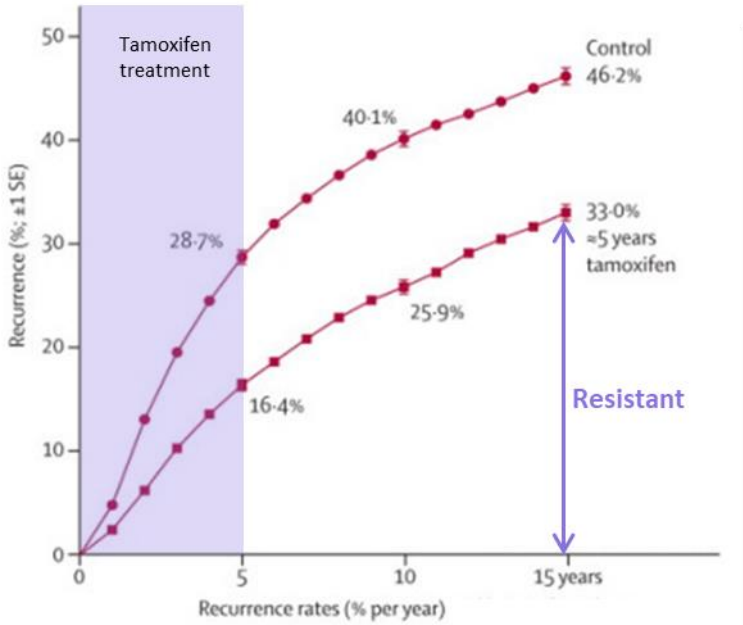

Figure 1-3: Results from a meta-analysis of more than 10,000 women investigating recurrence of ER+ breast cancer after 15 years following 5 years of treatment with tamoxifen. Graph sourced from (Early Breast Cancer Trialists' Collaborative Group (EBCTCG) et al., 2011).

Multiple studies have classified ER+ tumours into groups that predict for the level of resistance and metastasis. These classifications use gene expression profiling and split tumours in terms of likelihood of recurrence and aggressiveness. Two of the main gene profiles that have been developed are 21-gene and 70-gene lists (Paik et al., 2009; van de Vijver et al., 2002). Generally, the tumours more resistant to endocrine therapy will have a more aggressive phenotype, be highly proliferating, have a lower comparative expression of ER and PR and possess a high-risk gene profile. Gene signatures have also been used to predict for the response to aromatase inhibitors. This gene signature is made up of genes involving proliferation, apoptosis and immune signalling (Turnbull et al., 2015). EndoPredict

is another gene expression signature that tests for the likelihood of a woman with ER+/HER2- breast cancer developing metastasis within 10 years of diagnosis (B. M. Müller et al., 2013).

1.1.3.2 Mechanisms of endocrine resistance

There have been multiple reports investigating the mechanisms of resistance in tumours following endocrine therapy. In some cases, resistance can already be present in the tumours before any therapy but only become apparent once treatment has been administered (*de novo* resistance). The resistant population will not show any response to the initial treatment. They are often ER- cells and will dominate the tumour following treatment. Acquired resistance during treatment can happen for various reasons, of which some are explored below. Some cancer cells can remain dormant for extended periods of time and then emerge from dormancy by a particular signal and repopulate the tumour. It has been hypothesised that the treatments used on cancers can push the cells into a dormant state by inducing a growth arrest that becomes epigenetically imprinted (Clarke et al., 2015). This suggests that the dormant cells are also resistant to treatment. Increases in angiogenesis and signals from the immune system have been suggested as mechanisms that may allow exit from dormancy (Clarke et al., 2015).

ER+ tumours can develop resistance to endocrine therapy via complex mechanisms (Hanker et al., 2020):

- Loss of expression of ER. Tumours are no longer sensitive to antagonists of the receptor. This occurs in about 10% of the tumours that develop endocrine resistance. This can happen epigenetically, via multiple different methylation routes (Shiino et al., 2016).
- Upregulation of HER2 expression. Provides an alternative pathway for growth and proliferation signalling. Can also further reduce the expression of ER, reducing the effect of antagonists (Arpino et al., 2004).
- Ligand independent ER reactivation, rendering anti-estrogens ineffective (Miller et al., 2011):
    - Mutation of ERα at key sites, including Y537 and/or D538. Present in 20% of breast cancers (Toy et al., 2013).
    - ERα gene fusions (Basudan et al., 2019).
    - Changes in crosstalk with other cancer driving pathways (HER2, EGFR, Ras, FGFR). For example, loss of NF1 in the Ras pathway (Z. Y. Zheng et al., 2020).

- IL-6-STAT3 pathway leads to endocrine resistance by hijacking ER enhancers (Siersbæk et al., 2020).
- Alterations in the tumour microenvironment- CAFs (cancer associated fibroblasts), Extracellular Matrix, exosomes, inflammatory cells, immune cells.
    - Hypoxia- interplay between ER and HIF1α via SNAT2, which leads to resistance to endocrine therapies (Morotti et al., 2019).

After many years of treatment, if not fully ablated, all tumours subject to endocrine therapy will become resistant, with not all mechanisms known (Osborne & Schiff, 2011). Each tumour is unique and different treatments have different levels of success in different patients. There are some rare cases that confirm that resistance and response are not fully understood. For example, one patient showed response to repeated endocrine therapy followed by estrogen deprivation over eight years, without developing resistance (Osborne & Schiff, 2011).

Another pathway to endocrine resistance is the progesterone induced pathway, often caused by the loss of the progesterone receptor. As well as reflecting and exacerbating the loss of the ER and therefore decreasing estrogen signalling, this may also act as an independent mechanism, decreasing the signalling that occurs via the progesterone receptor. The expression of PR may be decreased by the crosstalk between ER and growth factor signalling, via the PI3K pathway (Cui et al., 2005). Cancers that are ER positive and lack expression of PR (both *de novo* and acquired) have more responsiveness to aromatase inhibitors but specifically develop resistance to SERMs (Cui et al., 2005).

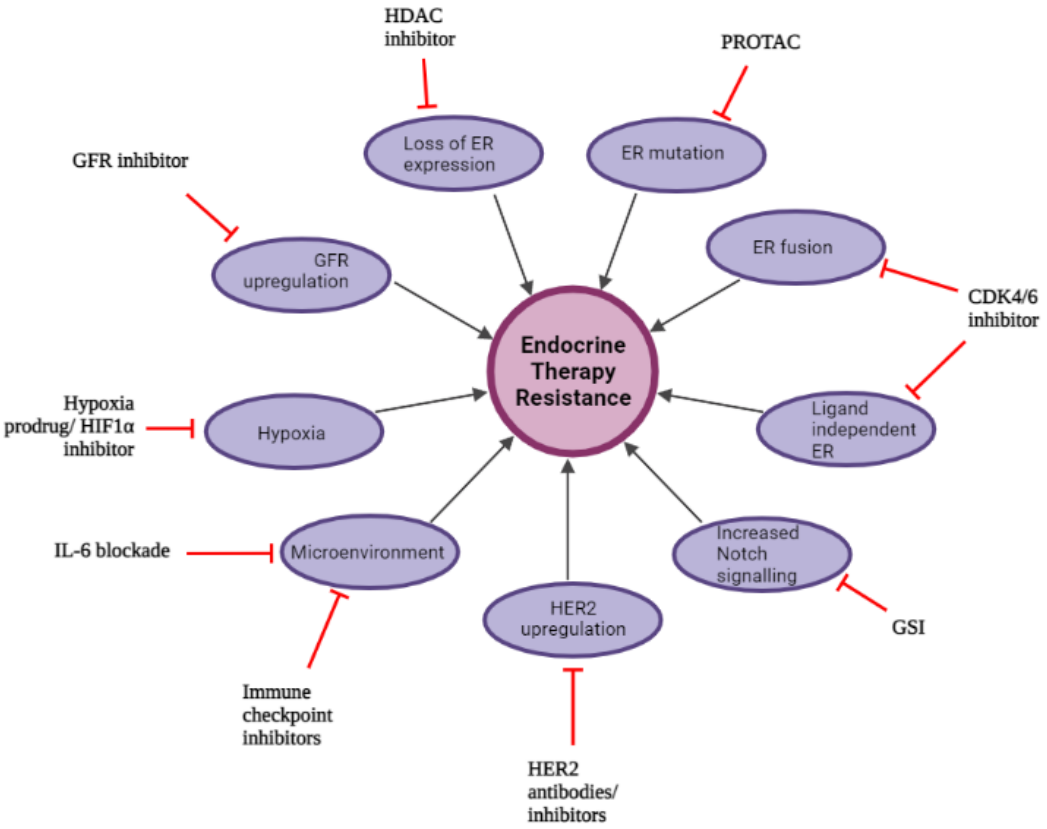

Figure 1-4: Mechanisms of endocrine therapy resistance and the treatments utilised to overcome it. PROTAC drugs target resistance caused by ER mutations. CDK4/6 inhibitors target resistance caused by ER fusion and ligand independent ER signalling. GSIs target resistance caused by upregulation of Notch signalling. HER2 antibodies or inhibitors target resistance caused by HER2 activation. Immune checkpoint inhibitors and IL-6 blockade may reduce the effect of the microenvironment. Hypoxia prodrugs or HIF1α inhibitors target resistance caused by hypoxia. Growth factor receptor upregulation can be targetted with Growth Factor Receptor inhibitors and ER expression could be restored with HDAC inhibitors. Created with BioRender.com. Adapted from (Hanker et al., 2020).

1.1.3.3 Overcoming endocrine resistance

The approaches for targeting endocrine therapy resistance depend on the method by which the resistance has been acquired. The main mechanisms of endocrine therapy resistance and the route each of these may be targeted is explored in Figure 1-4, adapted from Hanker et al, 2020.

If resistance develops due to a mutation in ER, a feasible alternative treatment could be a PROTAC (Proteolysis targeting chimera). PROTACs are bi-functional endocrine therapies that target both wild-type and mutated ER. These drugs include an ER ligand crosslinked to a ligand for E3 ligase, allowing for the recruitment of E3 ligase to the ER. This results in the ER

being ubiquitylated and targeted for degradation, in spite of any resistant mutations being present (Hanker et al., 2020).

If a mutation or amplification in another signalling pathway has been acquired, a specific targeting antibody or treatment towards that pathway may work synergistically with the endocrine therapy, preventing any further resistance e.g. FGFR1 TKIs, HER2 antibodies, MEKis or GSIs to target the Notch pathway (Hanker et al., 2020). PAK4 has been shown to be amplified in some endocrine resistant, metastatic ER+ breast cancers. It correlates with BCSC activity and progression in ER+ breast cancer samples. Targeting PAK4 has promising effects in reducing BCSC activity and reversing endocrine resistance (Santiago-Gómez et al., 2019).

CDK4/6 inhibitors are proven to effectively treat endocrine resistant breast tumours and may also prevent resistance from occurring. ER reactivation that involves the mitogenic pathway is dependent on CDK4/6, demonstrating inhibition of CDK4/6 may prevent this from occurring (Miller et al., 2011). The combination of CDK4/6 inhibitors with anti-estrogens has lengthened progression free survival, showing a successful preventative measure for resistance (Spring et al., 2019). CDK4/6 inhibitors can also be used to treat cancers after becoming endocrine therapy resistant, particularly those that acquire ESR1 gene fusion as these cancers stay sensitive to CDK4/6 inhibition (Lei et al., 2018). The field of CDK4/6 inhibitors in breast cancer has progressed to the point that they are currently in the first-line treatment for metastatic ER+ breast cancer. Current approved combination therapies are palbociclib, ribociclib and abemaciclib. These are individually combined with the administration of fulvestrant or an aromatase inhibitor (Baselga et al., 2012; Dickler et al., 2017; Finn et al., 2016; Hortobagyi et al., 2016; Turner et al., 2015). However, as with most treatments, not all patients will respond. A marker of CDK4/6 inhibitor resistance is cyclin E overexpression (Min et al., 2018). This fortifies the need for targeted treatment, but also the need to identify those individuals who will respond (Lei et al., 2019).

PARP inhibitors are also used to treat locally advanced or metastatic tumours that have developed resistance to conventional therapy. Olaparib and talazoparib are approved for treatment in such settings (Cortesi et al., 2021). PI3K/Akt/mTOR inhibitors are used to target endocrine resistant breast cancers- alpelisib is approved in combination with fulvestrant to treat PIK3CA mutated, as well as advanced and metastatic breast cancers (Narayan et al., 2021). Everolimus, an mTOR inhibitor, is currently approved for treatment of endocrine resistant/ metastatic hormone receptor positive breast cancers (Royce & Osman, 2015).

Other drugs have been investigated in clinical trials in combination with endocrine therapy but are not yet approved for treatment. These include PI3K/Akt inhibitors- taselisib in combination with fulvestrant increases progression-free survival (Dent et al., 2021), capivasertib, which was successfully trialled in combination with fulvestrant to treat metastatic ER+ breast cancers (Jones et al., 2020), as well as the currently approved everolimus in combination with various treatments including endocrine therapies and chemotherapies (Jerusalem et al., 2018). Several trials are also investigating the combination of three or more drugs, including the approved CDK4/6 inhibitor ribociclib and a conventional anti-estrogen therapy along with an additional inhibitor (Maurer et al., 2017).

If the microenvironment was found to be driving endocrine resistance, different components could be targeted. This could include inhibiting IL-6 with tocilizumab if aberrant activation was observed, or the use of immune checkpoint inhibitors (ICIs) in situations with increased immune infiltrate (Hanker et al., 2020). Inflammation is another key factor driving breast cancer progression and contributing to resistance. ERK5 is highly involved in this and it has been shown that it can be directly targeted, reducing cancer associated inflammation, potentially improving prognosis and allowing synergistic treatment of resistant tumours with other agents (Finegan et al., 2015). The microenvironment could also be targeted in order to prevent metastasis. For example, Il-1β has been found to stimulate bone metastatic colonisation of breast cancer. It is also linked to the ALDH+ population of cells that are key for endocrine resistance. IL1-R1, another player in this pathway, is closely linked to endocrine resistance and poor prognosis clinically. This Il-1β/IL1-R1/NFκB signalling pathway could be targeted to help reduce endocrine resistance and bone metastasis (Eyre et al., 2019; Sarmiento-Castro et al., 2020).

Cancer stem cells are another key driver of resistance in breast cancer which could be targeted at the same time as the tumour bulk population to prevent the stem cells from repopulating the tumour and leading to resistance. Cancer stem cells can be driven by multiple targetable pathways including the Notch pathway. Breast cancer stem cells and Notch will be explored in more detail in later sections.

1.2 Mammary stem cells

Mammary stem cells are the source of all cell types within the mammary gland, including ductal, alveolar and myoepithelial cells. They provide the massive expansion of cells for the remodelling processes that take place in the breast tissue during puberty, pregnancy and involution (Woodward et al., 2005). They also act in rare occasions to provide a resource for tissue repair after damage (Woodward et al., 2005). Mammary stem cells were first discovered in 1959 by DeOme et al in mouse experiments showing that small epithelial samples of the mammary gland can regenerate the entire structure, including all cell types (DeOme et al., 1959). However, the source of this regeneration wasn't understood to be mammary stem cells until 1991, when one mouse mammary epithelial cell was proved to be able to reconstitute the entire population, supporting the presence of multipotent mammary stem cells (Kordon & Smith, 1998; G. H. Smith et al., 1991).

Multiple markers have been used over the years to identify the mammary stem cell population. Initially, cells with an expression profile of $Lin^-/CD29^{high}/CD24^+$ were shown to be able to repopulate the mouse mammary gland (Shackleton et al., 2006). Meanwhile, Sleeman et al showed in humans that it was specifically the $CD24^{low}$ basal cell population that contained the mammary stem cells (Sleeman et al., 2005). $CD49f^{high}$ has also been identified as an expression marker for a population of cells that have the ability to regenerate mammary duct structures *in vivo* and possess proliferative activity *in vitro* (Eirew et al., 2008). More recently, studies have used a range of different markers to sort mammary stem cells into subpopulations through the stem cell hierarchy. The different combinations of these markers in each subpopulation highlights the heterogeneity of mammary stem cells (Taurin & Alkhalifa, 2020). This also supports the theory that stem cells exhibit a high level of plasticity and don't come from one singular source, with cells instead able to differentiate and de-differentiate.

Many signalling pathways act with a high importance in mammary stem cells. These include the Hedgehog pathway, the Wnt pathway and the Notch pathway. Hedgehog signalling is important in these cells in embryonic mammary gland development, as well as alveolar development (S. Liu et al., 2005). Wnt signalling has been linked to mammary stem cells through its actions in transgenic mice (B. Y. Liu et al., 2004). Notch signalling is closely linked with mammary stem cells and its roles in mammary gland development are explored in section 1.4.3.2.

Dontu et al first demonstrated the link between mammary stem cells and Notch using a Notch activating peptide which increased the self-renewal ability of normal human mammary tissue by 10-fold (Dontu et al., 2004). This same stimulation also led to an increased ability of mammary progenitor cells to produce 3D structures in Matrigel culture. In particular, it was observed that the increased action of the Notch4 receptor has the most pronounced effect on both mammary stem cells and progenitor cells, compared to the other Notch receptors (Dontu et al., 2004).

1.3 Breast Cancer Stem Cells (BCSCs)

1.3.1 Cancer stem cells

Cancer stem cells have been identified in many cancers as a population of cells with the ability to self-renew and generate more differentiated cells (Garza-Treviño et al., 2015; Huntly & Gilliland, 2005; S. Liu et al., 2014). This population of cells can reproduce an entire tumour.

There are different theories to describe the hierarchy of cancer stem cells. The single cell of origin theory maintains that there is one fully multipotent progenitor. This cell gives rise to discreet populations of further progenitors which can differentiate into different subsets of cells which make up the tumour. These populations may be overlapping, allowing plasticity between the different levels of progenitors (Cole et al., 2020). It has also been hypothesised that non-cancer stem cells could give rise to cancer stem cells, thereby repopulating the diversity of the tumour (Gupta et al., 2009).

As well as the cancer stem cell model of tumour heterogeneity, there are also two other theories used to explain the development of tumours. These are the clonal evolution model and the plasticity model. The clonal evolution model describes that all malignant cells begin biologically equivalent but acquire mutations which may increase tumour aggressiveness and invasiveness. These characteristics will drive tumour heterogeneity. The plasticity model ties together the cancer stem cell and clonal evolution theories, proposing that stem and differentiated cell states can interconvert. This plasticity could be driven by stimuli within the tumour or from the surrounding microenvironment (Rich, 2016). The plasticity model is the most relevant as it explains the great heterogeneity of cells within a breast tumour, as well as maintaining that some cells are genetically more “stem-like”.

Cancer stem cells are usually termed by the name of the cancer, for example stem cells that are the source of breast cancer are Breast Cancer Stem Cells (BCSC). Breast cancer stem cells were first discovered by Al-Hajj et al in 2003 with the identification of specific cells within the breast tumour with the ability to repopulate the tumour (Al-Hajj et al., 2003).

1.3.2 BCSCs and resistance

Resistance is thought to arise from Breast Cancer Stem Cells (BCSCs). It is thought that treatment causes regression of the bulk tumour, leaving behind resistant BCSCs. These cells can survive in the body and may remain dormant for an extended length of time. At a later

date they can then repopulate the tumour, leading to a local relapse of the breast cancer or travel to a distant site, resulting in metastasis (Figure 1-5A) (Bozorgi et al., 2015).

Evidence has suggested that the number of BCSCs in tumours increases following anti-estrogen treatment. *In vitro*, BCSC activity in the form of mammosphere forming efficiency (MFE) and percentage of cells positive for ALDH increased following anti-estrogen treatment (Piva et al., 2014; Simões et al., 2011). Anti-estrogens have shown the same effects *in vivo* (Simões, Alferez, et al., 2015). BCSC genes including NANOG, OCT4, SOX2 and CK5 have also been shown to increase following treatment in ER+ breast cancer cell lines (Creighton et al., 2010; Kabos et al., 2011; Piva et al., 2014; Simões et al., 2011) and *in vivo* in human cancer tissue (Creighton et al., 2010; Kabos et al., 2011). These actions could be due to a selection of BCSCs following treatment or by a switch of cell phenotype to a stem-like phenotype (Simões, Alferez, et al., 2015). Dormancy is also a key feature of BCSCs. BCSCs can remain quiescent and dormant within tumours or in the metastatic setting, until a signal induces them to exit dormancy. Dormant cells have key links with endocrine therapy, as discussed in section 1.1.3.2 (Clarke et al., 2015). Early metastatic breast cancer cells have been found to have a distinct stem cell gene signature, higher tumour initiating capacity and can differentiate to form advanced metastatic disease. It was found that BCSCs isolated from primary samples can also lead to metastases (Lawson et al., 2015; L. Liu et al., 2018). These findings all confirm that the BCSC population are involved in the development of endocrine resistance and are therefore important in recurrent and metastatic breast cancer.

1.3.3 Subpopulations of BCSCs

Two main subpopulations of BCSCs can be defined by their gene expression, those with the expression profile CD44+/CD24- and those with a high activity of the protein ALDH (Al-Hajj et al., 2003; Ginestier et al., 2007).

The CD44+/CD24- expression profile in BCSCs was first defined by Al-Hajj when these cells were found to have a greater *in vivo* tumour initiating ability in mice (Al-Hajj et al., 2003). Tumour initiating cells isolated from breast cancer patients and propagated *in vitro* were also found to be CD44+/CD24-, and had links with mesenchymal markers (Creighton et al., 2009; Ponti et al., 2005). CD44 is a transmembrane protein which activates many signalling pathways, increasing survival, motility and proliferation of cells, greatly contributing to the action of breast cancer stem cells (Chen et al., 2018).

Aldehyde dehydrogenases (ALDH) are a family of internal cellular enzymes involved in oxidation of aldehydes and are established as a marker of BCSCs (Ginestier et al., 2007). The most prominent of these is ALDH1 and its high activity in cells has been associated with a strong tumour initiating ability and correlates with other stem and progenitor markers. Cancers with a high ALDH1 expression also tend to have a poor prognosis (Ginestier et al., 2007). A method to separate/ identify these cells with high ALDH activity is the Aldefluor assay. The substrate BODIPY aminoacetaldehyde (BAAA) is converted, by the activated ALDH, to the fluorescent product BODIPY amino acetate (BAA). The cells that have a high activity level of ALDH can then be separated by flow cytometry (Tirino et al., 2013).

These two expression profiles were initially thought to be two ways of defining the same population, but it has been shown that these two markers represent two sub-populations or states of BCSCs and it has been proposed that cells can transition between the two due to their enhanced plasticity. This flexibility could be regulated by the tumour microenvironment including signals from growth factors and hormones, allowing for optimal metastatic colonisation. The CD44+/CD24- population are mesenchymal-like cells and are dormant. The $ALDH^{high}$ population represents the epithelial-like and proliferative state (S. Liu et al., 2014). The same study also identified a smaller sub population which is an overlap of the two, expressing both expression profiles, CD44+/CD24- and $ALDH^{high}$ (S. Liu et al., 2014).

Other markers have been used to identify BCSCs. These include CD133+, CD49f+, MUC1, and CK5+ (Brugnoli et al., 2019; Krawczyk et al., 2014; Ye et al., 2017). These proteins directly and indirectly upregulate signalling pathways involved in survival and metastasis, key features of BCSCs. Stemness factors and stem cell signalling pathways are also upregulated in BCSCs. These include Notch, Wnt, Hedgehog and Sox (Domenici et al., 2019; Y. Li et al., 2003; S. Liu et al., 2006). A splice variant of the estrogen receptor, ERα36, is linked to the BCSC population as it is correlated with an increase of the BCSC population following tamoxifen and fulvestrant treatment (Deng et al., 2014; Z. Wang et al., 2005). This splice variant activates the MAPK/ERK pathway when estrogen binds (Simões, Alferez, et al., 2015).

Markers are a good way to identify BCSCs, but even more important are the methods of functionally characterising them. This has been done in many ways, with the most common *in vitro* method being the mammosphere assay. In non-adherent, serum-free culture conditions, the BCSCs in a population will survive anoikis. These then divide and create floating colonies or mammospheres that can be quantified (Dontu et al., 2003; Farnie et al., 2007; Ponti et al., 2005) This method originated within neural stem cell research, whereby

the isolation of stem cells could be achieved by growing them in suspension as neurospheres (Reynolds & Weiss, 1996). Mammospheres have since been used to investigate breast cancer stem cell activity *in vitro* to study both cancer cell lines and patient derived tumour samples (Dontu et al., 2003, 2004; Harrison, Simões, et al., 2013; Simões, O'Brien, et al., 2015; Woodward et al., 2005). Another functional characterisation method involves the measurement of activity of the enzyme ALDH1 by the Aldefluor assay, described previously. Dyes can also be used to label cells with stem-like characteristics, including the PKH26 dye which labels cells which are dormant, and the exclusion of Hoechst dye in tumourigenic cells (Patrawala et al., 2005; Pece et al., 2010).

The 'gold standard' methods for studying the BCSCs within a tumour are *in vivo* studies as they allow the analysis of how BCSCs behave within an organism. Patient derived xenografts (PDXs) involve the subcutaneous transplantation of portions of a human breast cancer sample into an immune-compromised organism, usually a mouse. BCSCs within the transplanted sample initiate tumour development, enabling the identification and study of tumour initiating cells. This was utilised by Eyre et al in a study that found that metastatic breast cancer samples had a significantly greater *in vivo* tumour initiating ability compared to early breast cancers, suggesting the proportion of BCSCs in metastatic tumours is higher (Eyre et al., 2016). PDXs can also be used as a model for an individual's cancer, allowing treatments to be tested directly on the mice, leading the breakthrough in personalised medicine (Bhimani et al., 2020). Limiting dilution assays can also be used to study the proportion of BCSCs in cell lines or patient derived cancer cells. This method is similar to the formation of PDXs, but involves the injection of a limiting dilution of single cells in order to directly measure the tumour initiating capacity of cells (Simões, O'Brien, et al., 2015). Methods used to characterise BCSCs, including functionally and by expression are shown in Figure 1-5B.

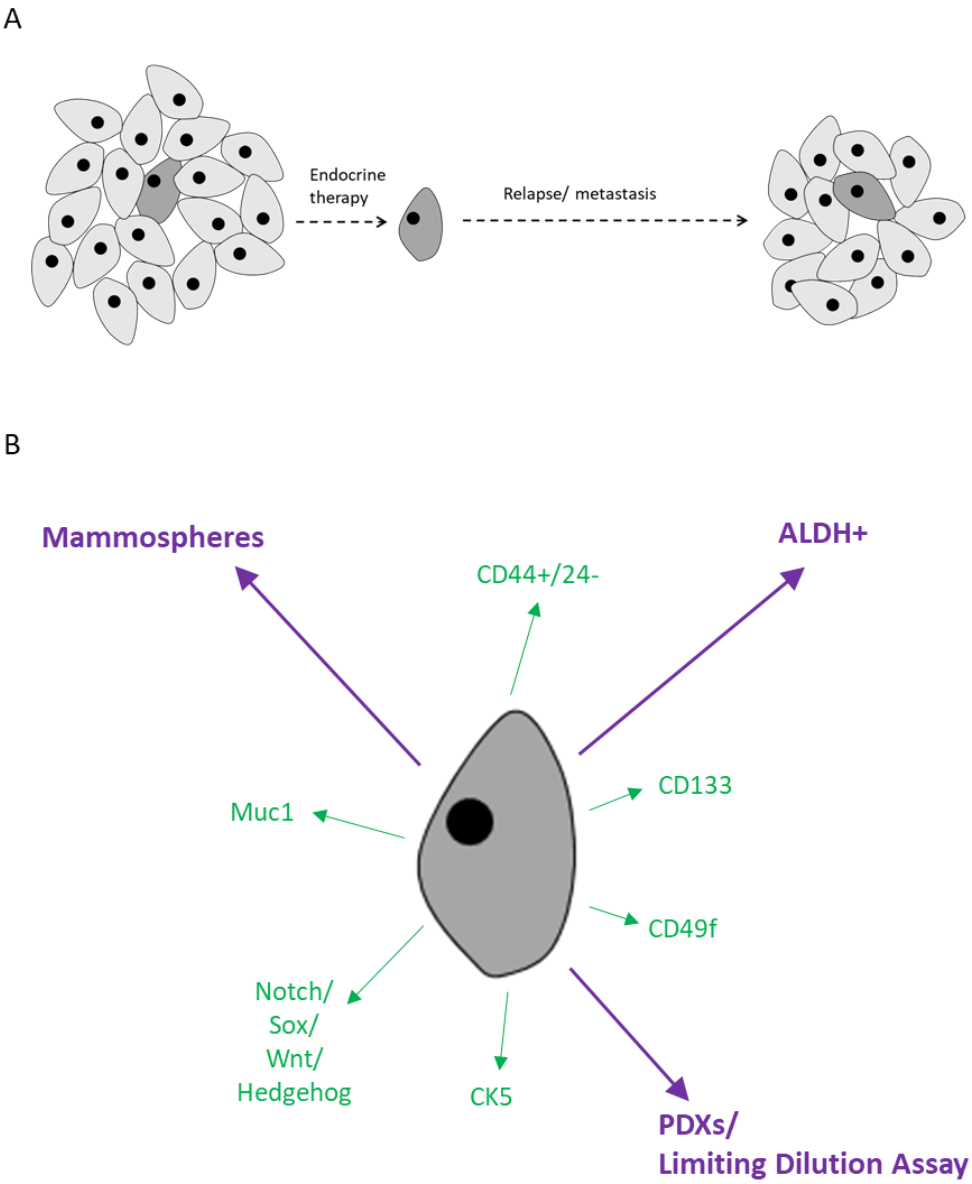

Figure 1-5: Breast Cancer Stem Cells (BCSCs). A) Breast Cancer Stem cells survive treatment with endocrine therapies. The cells lay dormant and can repopulate the tumour later, causing relapse or metastasis. B) BCSCs can be characterised by marker expression (green), including expression of CD49f, CD133, Mac1, Ck5, CD44+/24- or stem cell markers Notch/Sox/Wnt/Hedgehog. They can also be characterised functionally (purple) using the Mammosphere assay, Aldefluor assay, through Patient Derived Xenografts (PDXs) or Limiting Dilution Assay.

1.3.4 Hormone receptors and BCSCs

The hormone receptors Estrogen Receptor (ER) and Progesterone Receptor (PR) are highly involved in crosstalk with BCSCs. BCSCs themselves have become independent from and resistant to internal hormone receptor signalling, but through paracrine actions, the hormone receptors drive stemness signalling, survival and self-renewal.

ERα promotes the expression of target genes that allow for cell survival and therefore tumour growth and proliferation. It is activated by its ligand, estrogen, and in normal cells it is involved in the control of cell proliferation and in the development of the reproductive system (H.-R. Lee et al., 2012). The dimerisation of ER allows the recruitment of its co-receptors and co-activators, which include ubiquitin and SUMO ligases (Schiff et al., 2004). The genes activated downstream of the ER go on to regulate BCSCs via paracrine mechanisms (Figure 1-6). The main secreted paracrine mediators are Epidermal Growth Factor (EGF) and Fibroblast Growth Factor (FGF). ER+ cells also present Notch ligands on their surface. These mediators bind to EGFR, FGFR and Notch receptors on BCSCs, facilitating proliferation and survival. All three signalling mechanisms initiated by estrogen have been shown to increase the number of $CD44^{+}/CD24^{-}$ cells (BCSCs) (Fillmore et al., 2010; Harrison, Simões, et al., 2013).

The progesterone receptor is also involved in paracrine signalling mechanisms on BCSCs. PR is activated by progesterone, which dimerises the receptor and increases the expression of downstream targets. These signalling factors travel to adjacent BCSCs and bind to their receptors in order to stimulate proliferation and growth of the BCSCs. This regulation occurs via CXCL12/CXCR4, RANKL/RANK, GH/GHR and WNT4/FZD in paracrine signalling mechanisms (Figure 1-6) (Simões, Alferez, et al., 2015).

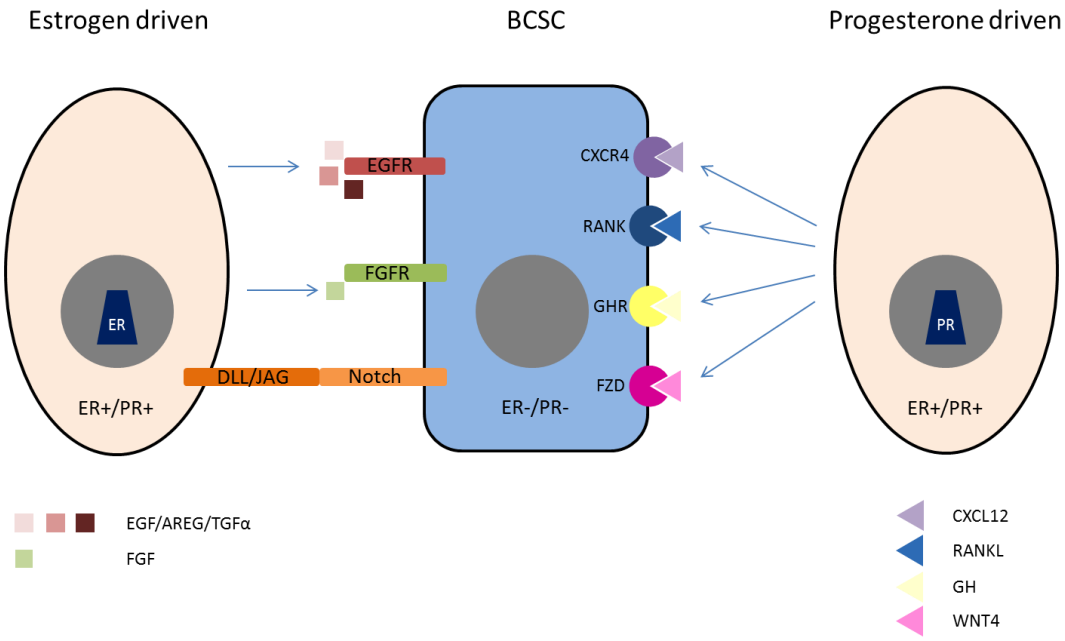

Figure 1-6: Hormones and hormone receptor driven paracrine signalling mechanisms that promote survival and self-renewal of BCSCs. Estrogen and progesterone bind to the estrogen receptor and progesterone receptor respectively and regulate target gene expression. Estrogen receptor regulation causes the release of Fibroblast Growth Factor (FGF) that stimulates Fibroblast Growth Factor Receptor (FGFR) in BCSCs. It also causes the release of Epithelial Growth Factor (EGF), Amphiregulin (AREG) and TGFα which stimulate the EGFR on BCSCs. Notch ligands are also expressed on the cell surface, which bind to the Notch receptors on the BCSC surface. In terms of progesterone regulation, cells release CXCL12, RANKL, Growth Hormone (GH) and WNT4 which bind to their receptors CXCR4, RANK, Growth Hormone Receptor (GHR) and Frizzled (FZD), respectively. These events will lead to downstream signalling that causes the upregulation of survival and self-renewal of the BCSCs. Adapted from (Simões, Alferez, et al., 2015).

1.3.5 Targeting BCSCs

Above are the main hormone driven, paracrine signalling mechanisms acting upon BCSCs. The three key signalling pathways that are involved within BCSCs are Notch, Wnt and Hedgehog. These pathways involve binding of an extracellular ligand to the receptor, leading to downstream signalling cascades. There is also lot of crosstalk and interactions between these BCSC signalling pathways in order to regulate the cells and maintain the tumour (Peng et al 2016). The most efficient way to target BCSCs is to inhibit a specific pathway to target the stem cells combined with standard treatments to regress the main bulk of the tumour. However, there is likely to be some functional redundancy between these main BCSC pathways as all are involved in the control of cell proliferation, differentiation and survival. There is therefore the argument that two or more of these pathways could be targeted at

once. Notch signalling inhibition will be covered in more detail in later sections. Briefly, gamma-secretase inhibitors (GSIs) that inhibit a key cleavage stage in the Notch pathway, have been explored in clinical trials with varying success. The Wnt pathway could be targeted with ursolic acid or LGK974, a porcupine inhibitor investigated in clinical trials for advanced cancer (J. Liu et al., 2013). The hedgehog pathway could be targeted with vismodegib, and the Hippo pathway with ciclesonide (S.-L. Kim et al., 2020). Some BCSCs efflux drugs at a higher rate and so could be targeted by inhibiting the pumps that remove drugs from cells, for example with lapatinib (Chun et al., 2015). Salinomycin is a another BCSC targeting drug which was identified using a library screen of current approved drugs. It has been reported to act in various ways to reduce drug resistance whilst allowing clinical regression of a breast tumour (Gupta et al., 2009; Versini et al., 2020).

Finally, the tumour microenvironment could also be targeted to treat BCSCs. CXCR1 has been targeted due to its high expression in BCSCs and activation by the inflammatory cytokine IL-8 (Ginestier et al., 2010). There have been promising results *in vitro* and in phase 1 clinical trials of the small molecule CXCR1 inhibitor Repertaxin (Q. Zheng et al., 2021). Targeting interleukins has also shown promising results in treating BCSCs. Inhibiting IL-1β reduces mice bone metastases resulting from breast tumours, via the inhibition of BCSCs (Eyre et al., 2019). IL-6 can also be targeted, which has been shown to significantly reduce BCSC activity (Heo et al., 2016; Simões et al., 2020).

The key BCSC pathway that will be explored here is the Notch signalling pathway.

1.4 Notch

The discovery of the Notch gene was made in *Drosophila* through the identification of a mutation in the gene affecting the wing phenotype, leading to a distinctive “Notch” in its shape (Dexter, 1914). Notch has been extensively studied in *Drosophila*, as well as other model organisms. In humans and mice, there are four Notch proteins and the structures and domains are shown schematically in Figure 1-7. (Kopan & Ilagan, 2009).

The Notch receptor in *Drosophila* and the four Notch receptors in humans have a modular structure with a separate extracellular domain and intracellular domain. All Notch proteins possess multiple EGF-like repeats at the N-terminus. *Drosophila* Notch, similarly to Notch1 and Notch2 in humans, has 36 EGF-like repeats, whereas Notch3 has 34 and Notch4 has 29 (Bellavia et al., 2008). Also in the extracellular domain there are a number of

Lin12/Notch/Glp-1 (LNG) repeats, which are known as the NRR (Negative Regulatory Region). This region controls the interaction between the ECD and ICD. The intracellular domain is made up of the RBP-Jkappa-associated module (RAM) domain, which forms a tightly folded binding domain, after which a nuclear localisation sequence is located (Kopan & Ilagan, 2009). This is followed by multiple ankyrin repeats and TAD domains. At the C-terminus is a PEST domain, which functions as a regulator of the stability of the protein, as well as leading to its ubiquitylation (Figure 1-7). An additional domain at the C-terminus of the *Drosophila* Notch is a glutamine-rich repeat (OPA) (Kopan & Ilagan, 2009).

The ligands of the Notch receptor include Delta and Serrate in *Drosophila* (Kopan & Ilagan, 2009). In mammals the main ligands are DLL1, 3 and 4 and Jagged 1 and 2 (Kopan & Ilagan, 2009). Due to the large number of combinations of Notch receptor-ligand interactions, it has been suggested that this could contribute to the variability in signalling output (Andersson et al., 2011). Ligands are presented on the cell surface, similarly to the receptors, and so cell-cell interactions are required for ligand dependent trans-activation. As well as being trans-activated by ligands presented on neighbouring cells, Notch receptors can also be cis-inhibited by ligands on the same cell as the receptor.

Non-canonical Notch ligands can also activate signalling. They include membrane tethered proteins (Delta-like homolog 1 (Dlk1), DNER and Jedi), GPI linked proteins (Contactin1/6) and secreted proteins (scabrous, wingless, OSM11 and MAGP-1/2) (D'Souza et al., 2010). Other proteins are involved in modulating Notch signalling. These include Fringe proteins that modify O-fucose residues on EGF repeats of Notch, allowing discrimination between different ligands (Kakuda & Haltiwanger, 2017).

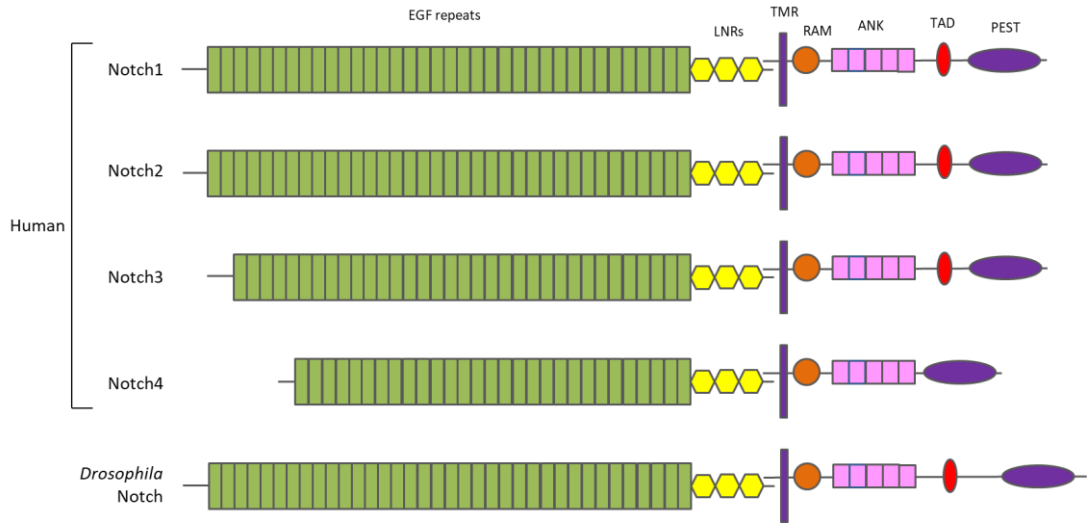

Figure 1-7: Structure homology of Drosophila Notch and the four human Notch receptors. Showing domains- EGF repeats, LNRs (Lin/Notch repeats), RAM (RBP-Jkappa-associated module), ANK (Ankyrin repeats), TAD (Transactivation domain), PEST (Contains amino acids proline, glutamic acid, serine and threonine).

1.4.1 Notch structure

Notch decoys have been used as a tool to study the interactions between Notch receptors and ligands. A Notch decoy includes a number of EGF repeats that mimic the Notch receptor and bind to Notch ligands, preventing ligand-receptor binding. They are particularly useful to determine which EGF repeats in the receptor are vital for the binding of particular ligands. A study by Kangsamaksin et al explores the use of these decoys to block the interaction of DLL4 and Jagged1 (JAG1) with Notch1 (Kangsamaksin et al., 2015). In this study, a decoy that included the EGF repeats 1-36 blocked the binding of both DLL4 and JAG1. A decoy composed of the EGF repeats 1-13 prevented DLL ligand induced Notch signalling. A decoy with EGF 10-24 blocked only JAG ligand induced signalling. This study concluded that the DLL ligands binding site is within EGF repeats 1-13 in Notch1 and the JAG ligands binding site is within EGF repeats 10-24 (Kangsamaksin et al., 2015).

The full structure of any of the four human Notch proteins is yet to be resolved, due to the size and complexity of the receptors. Recently, two studies by Luca et al have solved the crystal structure of the ligand binding region of Notch1 bound to two of its ligands- DLL4 and JAG1, both in an anti-parallel formation (Luca et al., 2015, 2017). These studies built on the work of Kangsamaksin et al. They showed that the region that binds to DLL4 is the EGF repeats 11 and 12 and the region that binds to JAG1 involves EGF repeats 8 and 12. This highlights the distinct roles of the different parts of the Notch ECD. The JAG1-Notch1

interface was found to have catch-bond behaviour, with JAG1 changing conformation upon binding, strengthening the interactions between the two proteins. This allows different cellular interactions to discriminate between ligands, leading to variability in Notch signalling output (Luca et al., 2017).

The Abruptex (Ax) domain, which is a portion of the receptor including the EGF repeats 24-29 in both *Drosophila* and mammalian Notch1, also has a distinct role (Figure 1-9). It is key for development in *Drosophila* and has been studied due to the myriad of mutations that lead to a gain of Notch function and phenotype in the fly wing (Brennan et al., 1997). The Abruptex domain has also been linked to alternative ligand independent pathways of Notch signalling.

1.4.2 Notch signalling pathways

Notch signalling is made up of multiple pathways that include activating and repressing pathways. These are ligand dependent or ligand independent (Figure 1-8). Notch is synthesised as a single polypeptide and is post-translationally processed by protein convertases with a cleavage coined "S1". The final structure of Notch is therefore made up of two non-covalently linked sections presented on the surface of the cell. The canonical Notch activation pathway involves the binding of one of the ligands to the EGF repeats of Notch. This changes the conformation of the Notch receptor from an inactive conformation, maintained by the NRR, to an active conformation allowing access to the cleavage site. A pulling mechanism is induced by the ligand (Gordon et al., 2009). An "S2" cleavage is then carried out by a metalloprotease Kuzbanian (*Drosophila*) or ADAM10/ADAM17 (human), releasing the Notch extracellular domain (NECD), which is endocytosed with the ligand into the ligand presenting cell. This leaves the transmembrane bound intracellular domain, often referred to as NEXT (Notch extracellular truncation) within the membrane of the Notch presenting cell (Kopan & Ilagan, 2009). The final, "S3" cleavage is then carried out by a gamma-secretase, releasing the Notch intracellular domain (NICD) into the cell. Cleavage sites shown in Figure 1-9.

Once released, the NICD translocates to the nucleus and binds with the protein complex CSL (CBF1/RBP/Su(H)/Lag-1), also known as RBP-Jκ (Wilson & Kovall, 2006). The binding of the NICD converts this complex from a transcriptional repressor, when in the resting state, to a transcriptional activator. In the repressor state, the complex is bound to the DNA. The binding of the ANK domain of NICD displaces co-repressors and recruits the co-activators

Mastermind (*Drosophila*) or Mastermind-like (humans), as well as Lag-3 (Kopan & Ilagan, 2009). This then allows recruitment of MED8 (Kopan & Ilagan, 2009). Signalling can be blocked by the hyper-phosphorylation of NICD and it will subsequently be degraded (Wilson & Kovall, 2006). The main transcriptional targets of the Notch receptors include the HES (Hes1, Hes5) and HEY (Hey1, Hey2, HeyL) genes. These target genes encode transcription factors that have key roles including in development of the nervous system and vessel system. Other target genes include Cyclin D1 (involved in cell cycle progression), c-myc (division and proliferation), Slug (differentiation and migration), p21 (DNA repair), GATA3 and Nanog. The products of these genes lead to control of further transcriptional targets (Nowell & Radtke, 2017). Once NICD has bound to its transcriptional target, its degradation is carried out by an F-box ubiquitin ligase, Archipelago in *Drosophila* and Fbw-7/SEL-10 in mammals (Kopan & Ilagan, 2009). Numb also negatively regulates Notch and has an important role in controlling the level of Notch signalling (Kopan & Ilagan, 2009).

The ligand independent mechanisms of Notch signalling are less widely studied, but they have been investigated in *Drosophila*. There are two main ligand independent Notch signalling pathways (Figure 1-8). Activation involves the endocytic trafficking of the full length Notch receptor, via a clathrin mediated pathway, induced by its mono-ubiquitylation by the E3 Ubiquitin ligase Deltex, after its binding to the ANK domain of Notch (Figure 1-9) (Guruharsha et al., 2012). It then travels from the endosomes to the lysosomes through the endocytic trafficking pathway. This requires proteins including Rab7, HOPS complex (including Carnation and Deep orange in *Drosophila*) and AP-3. The NICD is released from the lysosomal limiting membrane into the cytosol. From this point the pathway is the same as the ligand dependent activation pathway, with NICD translocating to the nucleus and inducing signalling (Wilkin et al., 2008).

The Notch repressing pathway is promoted by “Suppressor of Deltex” (Su(dx)) and involves internalisation of the Notch receptor by a clathrin-independent mechanism, followed by degradation via the multi vesicular bodies (MVB) (Figure 1-8) This pathway can alternatively lead to Notch activation if the Su(dx) hect domain is inactive (Shimizu et al., 2014; Wilkin et al., 2008). In *Drosophila*, it has been shown that Deltex and Su(dx) compete to promote each ligand independent pathway, providing a balance that is important for control within the cell (Shimizu et al., 2014).

In *Drosophila*, it has been shown that the Deltex stimulated activation pathway does not require ADAM10, whereas the Su(dx) degradation pathway does (Shimizu et al., 2014).

However, the method of ICD release into the cell in the ligand independent activation pathway could occur via multiple routes. The ECD may be fully proteolysed in the lysosome, or acidification of the lysosome may destabilise the NRR, with both routes allowing gamma-secretase to perform the "S3" cleavage (Steinbuck & Winandy, 2018). These insights are gained from *Drosophila* and little is known about the ligand independent routes of Notch activation in humans.

The Notch signalling pathway is involved in crosstalk with other important pathways. These include Wnt, NF-κB, HIF1α, YAP/TAZ, TGF-β, Akt and ERα (Edwards & Brennan, 2021; Rizzo et al., 2008). These crosstalks are implicated over the many normal functions of Notch in development, inflammation, and cell maintenance as well as in tumourigenesis.

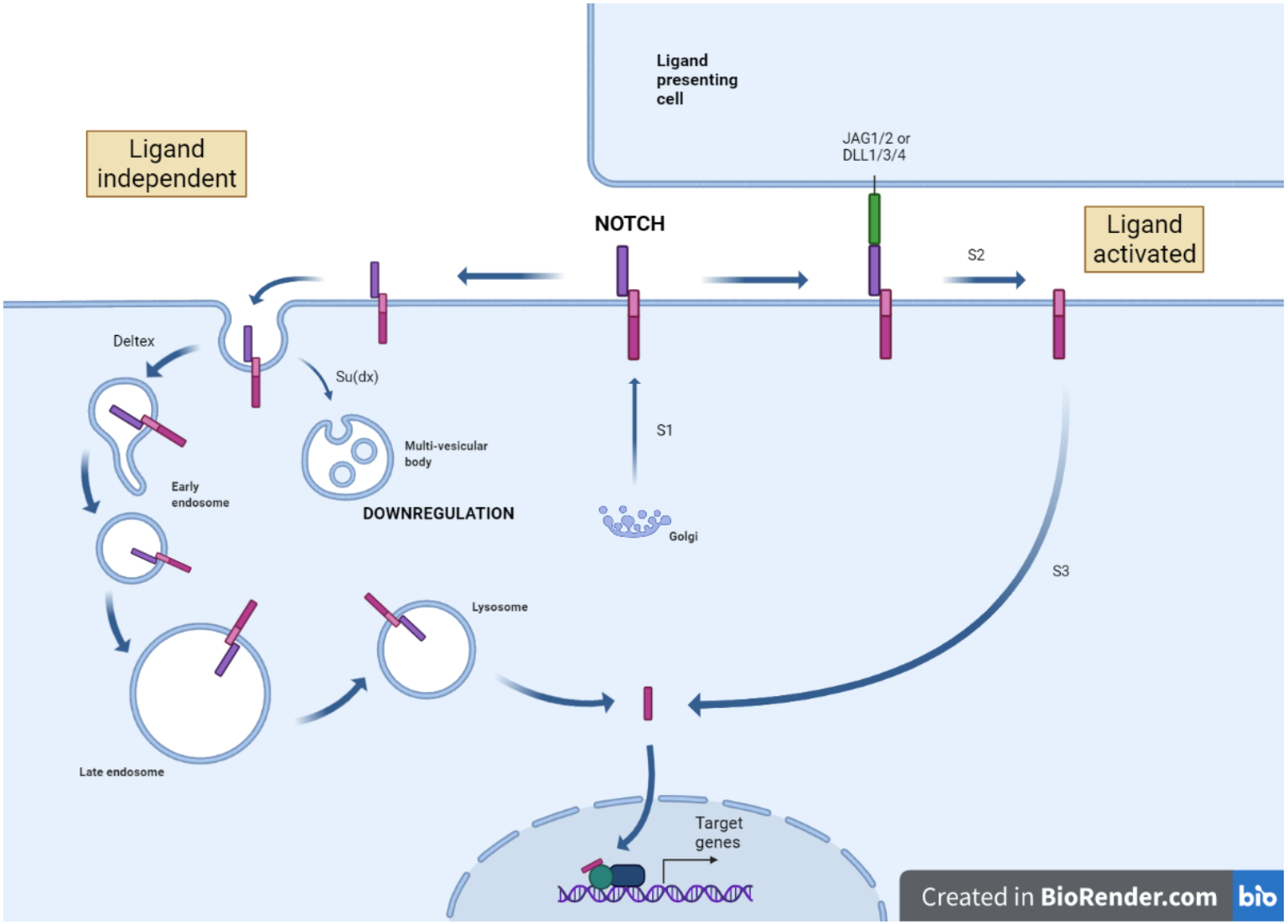
Ligand presenting cell
JAG1/2 or DLL1/3/4
Ligand independent
NOTCH
S2
Ligand activated
Deltex
Su(dx)
Multi-vesicular body
Early endosome
DOWNREGULATION
S1
Golgi
S3
Lysosome
Late endosome
Target genes
Created in BioRender.com

Figure 1-8: Signalling mechanisms of the Notch receptors. Prior to presentation on the surface, the Notch receptor is cleaved initially (S1) in the Golgi and travels to the surface as two domains connected non-covalently. In the ligand activated pathway, a ligand on the signal sending cell binds to the receptor on the signal receiving cell, causing another cleavage (S2), releasing the ligand and extracellular domain. The third cleavage (S3), facilitated by gamma-secretase, releases the Notch intracellular domain (NICD) into the cytosol. In the ligand independent activation pathway, the Notch receptor is internalised into the endocytic pathway without ligand binding, facilitated by Deltex. From here it is trafficked through the endosomes to the lysosomes where the NICD is released into the cytosol. The second ligand independent Notch signalling mechanism causes the downregulation of Notch. This pathway is controlled by Suppressor of Deltex (Su(dx)) and involves the trafficking of the Notch receptor to the multi-vesicular body (MVB) and subsequent degradation. After release of NICD into the cytosol, it translocates to the nucleus and localises with co-activators, causing transcription of target genes. Created with Biorender.com.

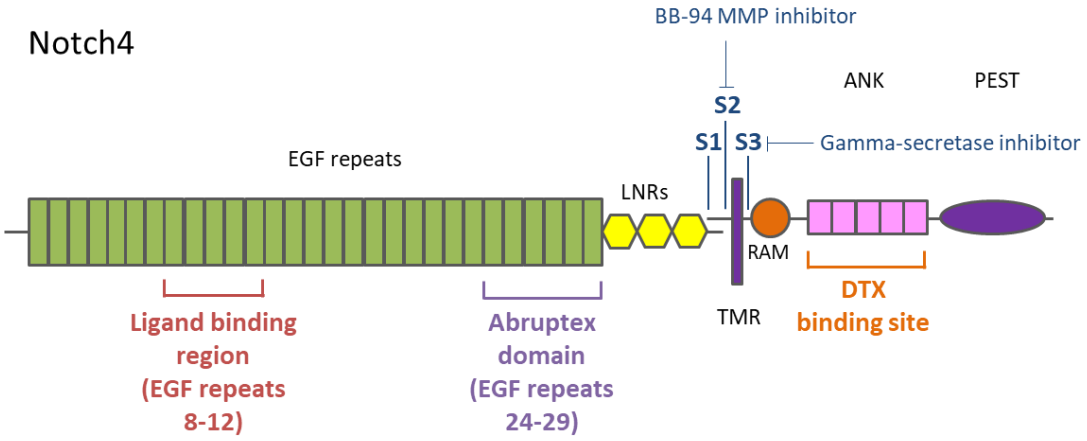

Figure 1-9: Structure of Notch4 with binding sites, cleavage sites and regions of interest. The ligand binding region of Notch4 is between EGF repeats 8-12. The Abruptex domain is between EGF repeats 24-29. Deltex binds to the ANK domain. The S1, S2 and S3 cleavage sites are near the transmembrane region. BB-94 MMP inhibitor prevents the S2 cleavage and gamma-secretase inhibitor prevents the S3 cleavage. Domains – EGF repeats, LNRs (Lin/Notch repeats), TMR (transmembrane region), RAM (RBP-Jkappa-associated module), ANK (Ankyrin repeats), PEST (Contains amino acids proline, glutamic acid, serine and threonine).

1.4.2.1 Deltex

Deltex is a key protein involved in the ligand independent activation mechanism of Notch. Its role was demonstrated in *Drosophila* using null mutations and overexpression experiments (Hori et al., 2011; Yamada et al., 2011). As well promoting the internalisation of Notch, it has also been established that Deltex has a key role stabilising Notch on the surface of the late endosome (Yamada et al., 2011). It additionally assists transmembrane proteins such as Crumbs to control the localisation of the Notch receptor (Nemetschke & Knust, 2016). Deltex and Su(dx) are involved in a fine balance, with Deltex promoting activation and Su(dx) promoting degradation of Notch. It has also been found that Deltex can have a negative control over Notch if expressed along with Su(dx). This is due to Deltex driving Notch endocytosis which Su(dx) could then divert to the MVB for degradation. This highlights the fine balance that gene expression changes can inflict upon Notch signalling (Shimizu et al., 2014; W. Yao et al., 2018). In terms of links to cancer in humans, Deltex1 (DTX1) has associations with tumourigenesis in glioblastoma (Huber et al., 2013) and has a tumour suppressive role in gastric cancer (Hsu et al., 2018). Mutations in DTX1 have been linked to certain lymphomas and non-small cell lung cancer (J. H. Lee et al., 2019; Meriranta et al., 2017). Deltex4 (DTX4) is linked to development and metastasis of hepatocellular carcinoma, melanoma and colorectal cancer (Lin et al., 2016; W. M. Liu et al., 2010; Viatour et al., 2011).

1.4.3 Normal functions of Notch

The outcome of Notch signalling varies depending on the developmental stage of the cell, the tissue of origin and crosstalk with other signalling pathways, including differentiation, cell survival/proliferation or cell death. These normal functions of Notch are summarised in Figure 1-10.

1.4.3.1 Asymmetric division

The main functions that Notch signalling fulfils are in situations where asymmetric division and boundary formations are key. During development, in situations where cells have different ratios of Notch and ligand, some cells become signal sending and some signal receiving. This allows for the beginning of a boundary to be formed, leading to definition between tissue compartments (Guruharsha et al., 2012; Sprinzak et al., 2010). Notch has a key role in the stem cell niche in *Drosophila* and is involved in its formation and maintenance (Song et al., 2007).

1.4.3.2 Mammary development

An important setting that Notch-led asymmetric division control comes into play is in cell fate determination of mammary stem and progenitor cells. Self-renewal of mammary stem cells and proliferation of their progenitors have been shown to be promoted by Notch signalling, and are particularly dependent on Notch4 (Dontu et al., 2004). Myoepithelial lineage commitment and branching morphogenesis in the mammary gland is also controlled by Notch. Notch was found preferentially in the luminal epithelial cells, driving cells down the luminal cell lineage (Bouras et al., 2008). Notch4 specific signalling is involved in mammary gland duct formation in breast development and in the expansion of mammary gland alveoli during pregnancy (G. H. Smith et al., 1995). Notch4 expression is heightened at the tips of the ducts in the cap cells when not pregnant. It changes localisation during pregnancy to the basal cells (Politi et al., 2004). The involvement of Notch4 in the mammary gland was further backed up in experiments studying the MMTV int3 (discussed in section 1.5).

1.4.3.3 Vascular and neural development

Notch is involved in the development of the vascular and neural systems. The main roles of Notch in vascular development are in artery or vein differentiation and the coordination of the branching and sprouting of vessels (Gridley, 2003). Notch mutant mouse models to study neural development show that Notch assists with the maintenance of progenitor neural cells (Yoon & Gaiano, 2005). When both Notch1 and Notch4 genes are disrupted in mice, there is a much more severe phenotype of disrupted vascular morphogenesis than the Notch1 mutations alone (Krebs et al., 2000).

1.4.3.4 Stem cells

In addition to developmental roles, Notch also has roles in adult tissue. In *Drosophila*, it plays a part in the maintenance of stem cell niches and tissue repair (Song et al., 2007). In mammals, adult functions of Notch signalling include control of T cell production in the thymus and the maintenance of progenitor cells in the gut. Notch can act to prevent or promote differentiation of progenitor cells, enriching the gut epithelial stem cell pool or providing more differentiated gut cells (Pellegrinet et al., 2011). In the mammary gland, Notch and DLL1 contribute to crosstalk in the mammary stem cell niche. Stem cells express the DLL ligand which activates macrophages. This in turn induces Wnt signalling which feeds back to the mammary stem cells, creating a positive feedback loop (Chakrabarti et al., 2018).

1.4.3.5 *Cell proliferation*

Notch has an impact on cell proliferation via target gene expression and through downstream signalling pathways. As summarised in a recent review by Edwards and Brennan, multiple Notch target genes are cell cycle regulators but can act against one another, complicating the pathway. Hes1 and Hes6 are both Notch target genes, but Hes1 acts to inhibit cell proliferation by downregulating E2F1. Hes6 however, increases cell cycle progression through the upregulation of E2F1, but is also an inhibitor of Hes1, further increasing proliferation. Cyclin A, D and B1 are also all Notch target genes, and increase cell cycle progression (Edwards & Brennan, 2021). Crosstalk with Ras and Wnt signalling pathways are also involved in cell proliferation.

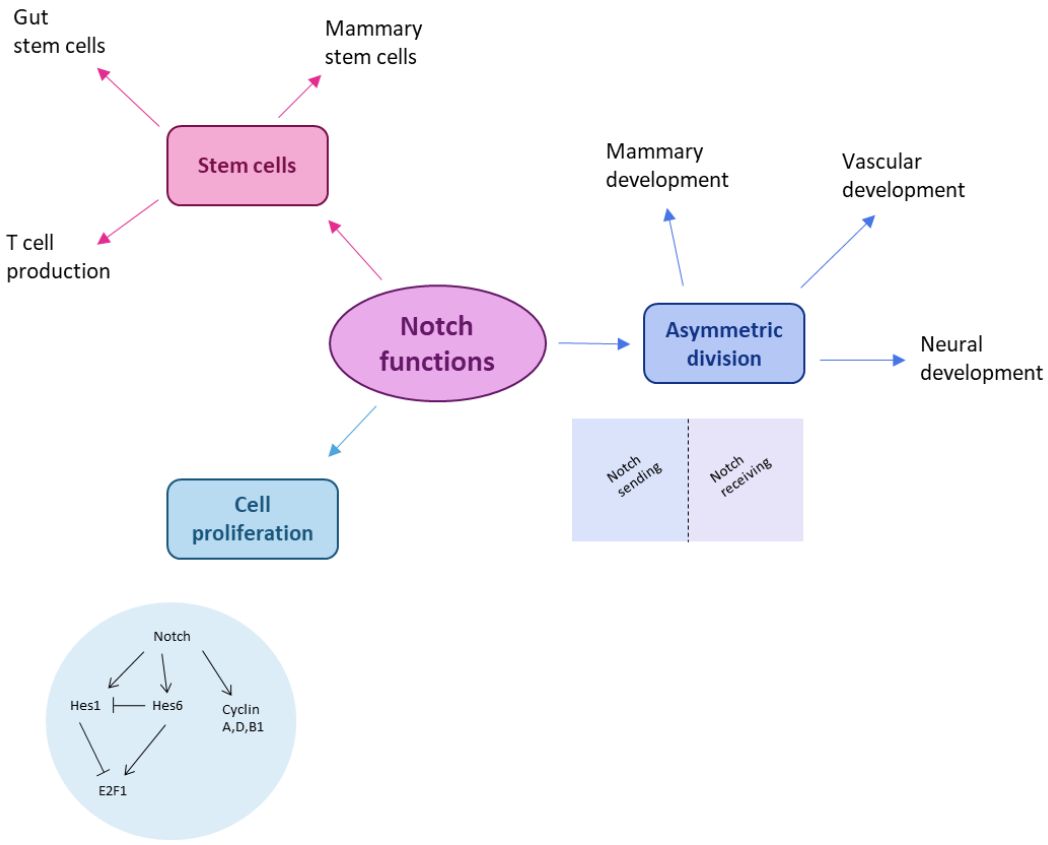

Figure 1-10: Normal functions of Notch. The main actions of Notch in development are due to its control over asymmetric division. This leads to it playing a key part in mammary, vascular and neural development. It also has a role in cell proliferation, via its impacts on E2F1 and cyclins. Notch is involved in regulation of adult stem cells. These include mammary stem cells, gut stem cells and stem cells involved in T cell production.

1.4.4 Notch in disease

Mutations in the Notch receptors can lead to multiple disorders and diseases. Many of these involve developmental defects such as familial aortic disease and alagille syndrome, which are diseases of the circulatory system (Garg et al., 2005; Gridley, 2003). The pathway is also associated with adult onset diseases involving defects in artery structure. Notch3 is linked to CADASIL which is a rare genetic disorder that acts upon the small blood vessels in the brain (Stojanov et al., 2014).

Notch has widely been implicated as an oncogene in many cancers. The first identified with a link to Notch was T cell acute lymphoblastic leukaemia (T-ALL). This oncogenic activity can occur via a translocation of the Notch gene with the T cell receptor B promoter-enhancer region, creating a dominantly active Notch1. Mutations within the NRR and PEST domains of Notch are also often found in T-ALL and lead to aberrant activation (Weng et al., 2004). Aberrantly activated Notch1 is found in approximately 60% of T-ALL cases (Tosello & Ferrando, 2013). Notch signalling is also activated in osteosarcoma (L. Yu et al., 2016). This is heightened after treatment with cisplatin, suggesting that the upregulation of Notch signalling is associated with resistance and therefore CSCs. A link has also been found in non-small-cell lung cancer, in mouse models where Notch signalling was shown as essential for tumour formation (Maraver et al., 2012). Links to oncogenic Notch have also been found in pancreatic cancer, colorectal cancer, melanoma and breast cancer (Nowell & Radtke, 2017).

In contrast, evidence has shown that Notch acts as a tumour suppressor in squamous cell carcinomas (SCC) in multiple epithelial tissues. Notch loss-of function mutations are one of the most common mutations found in lung SCC, head and neck SCC, bladder SCC and oesophageal SCC (Nowell & Radtke, 2017). These mutations have been found in Notch1, 2 and 3, in the ligands and other pathway components (Nowell & Radtke, 2017).

There are some cancers which have a strong link with the Notch signalling pathway but the role of Notch as either an oncogene or a tumour suppressor has not been defined. These include pancreatic ductal carcinoma (Miyamoto et al., 2003) and haematological cancers. T-ALL and chronic lymphocytic leukaemia demonstrate an oncogenic role for Notch1 and myeloid leukaemias show tumour-suppressive roles of Notch (Nowell & Radtke, 2017).

Notch signalling in cancer cells leads to crosstalk with the tumour microenvironment, acting on immune cells in a tumour promoting or suppressing manner, depending on the situation. Notch activation in a tumour can recruit immune cells and activate them, which will then activate tumour cells. For example, Notch mediated IL-6 secretion from myeloid derived

suppressor cells can lead to activation of tumour cells. Notch activation can also activate cancer associated fibroblasts (Meurette & Mehlen, 2018). In these and other ways, the microenvironmental actions of Notch have implications for most cancer types.

1.4.5 Notch in angiogenesis in cancer

Notch receptors and ligands are involved in the activation of angiogenesis. As Notch has a key function in normal vessel formation, tumours exploit this in order to aid their growth. It has been demonstrated that Jagged1 expression in tumours activates Notch signalling in neighbouring endothelial cells to activate vessel growth. This was also indicated in breast tumours, with estrogen upregulating Notch signalling, leading to increased vessel growth (Shi & Harris, 2006). However, the Notch ligands DLL4 and JAG1 were found to have different effects on Notch signalling and vessel formation, leading to differing effects on tumour growth. DLL4 caused growth of fewer bigger vessels, whilst JAG1 produced more smaller vessels (Oon et al., 2014). This solidifies the multiple roles that the different pathways of Notch signalling can play.

Research has begun to investigate the targeting of Notch signalling, whilst also targeting angiogenesis. This can be achieved by targeting VEGFR as well as Notch to stop the direct effect of Notch on the tumour as well as its effects on angiogenesis. This has been achieved by the production of a breast cancer specific adenovirus that targets both DLL1 and VEGF. Infection with this virus successfully reduced tumour growth, angiogenesis and prolonged survival time (Bazan-Peregrino et al., 2013).

1.4.6 Notch4

The first link between Notch4 and breast cancer was made in 1992 by Robbins et al when investigating insertion sites by the mouse mammary tumour virus (MMTV) (Robbins et al., 1992). This study identified that the third insertion site (int3), was within a member of the Notch family. It was Gallahan et al in 1997 that moved on to identify that int3 was within the Notch4 gene (Gallahan & Callahan, 1997). All int3 insertions led to a high level of Notch4 ICD. Gallahan et al also confirmed whilst working with the intracellular domain that altered Notch4 ICD signalling is tumourigenic (Gallahan et al., 1996). This highlighted that the gene plays a key role in mouse mammary tumours.

Notch4 is a slightly shorter member of the Notch receptor family, with 29 EGF repeats as opposed to the 36 of Notch1 (Figure 1-7). Notch4 is a vital protein that in mammals is most highly expressed in the vasculature (James et al., 2014). Notch4 is known to contribute to mammary stem cell maintenance, vasculature control and development as well as lung, adrenal gland and brain development in mice (Ables et al., 2011; Dontu et al., 2004). In vasculature development it controls the specification of arterial cells, controlling the size and shape of the vessels. It also has a particularly heightened role during ischemia of the vessels (James et al., 2014). When the vascular plexus (newly formed networks of vessels) is forming, Notch4 signalling controls parallel and antiparallel cell division and prevents excess branching (Hellström et al., 2007). As well as being active in development, Notch4 signalling is present in the brain where it acts as an important regulator for neurones, controlling their migration, plasticity (both structural and synaptic) and survival during aging and following trauma (Ables et al., 2011). It also has a role in the inflammation response in the coordination of T-reg cells in asthma (Harb et al., 2020). Importantly, Notch4 is also involved in the formation and function of the mammary gland.

There are four phosphorylation sites in the Notch4 ICD which are able to be phosphorylated by Akt both *in vivo* and *in vitro* (Ramakrishnan et al., 2015). The phosphorylation sites allow the protein 14-3-3 to bind and prevent the NICD from translocating to the nucleus. This provides a control over the cellular location of the NICD, suggesting a potential regulation carried out by the PI3K/Akt pathway (Ramakrishnan et al., 2015). This is particularly interesting as the PI3K/Akt pathway is usually upregulated in breast cancer (Creighton et al., 2010). James et al also discovered a cis-inhibition ability of Notch4, to block the signalling of Notch1 when both receptors are expressed in the same cell (James et al., 2014). This would allow for selection for a certain type of Notch signalling, fine-tuning the role and action of cells.

1.5 Notch and breast cancer

After the identification of int3 of MMTV being within the Notch4 gene, further *in vivo* experiments in mice confirmed the importance of Notch4 in mouse mammary tumours. Mice that were altered to overexpress Notch1 ICD, Notch3 ICD and Notch4 ICD were found to have increased mammary tumour growth (C. Hu et al., 2006; Robbins et al., 1992). *In vitro*, an RBP-Jκ dependent increase in Notch signalling induces transformation of normal mammary

epithelial cells into cancerous cells. This transformation can be reversed with the suppression of Notch signalling (Stylianou et al., 2006).

Altered expression of Notch has been reported in many breast cancers. Accumulation of Notch1 ICD was found in many cases, along with aberrantly higher Notch activity (Stylianou et al., 2006). High expression of Notch1 and Notch4 receptors in breast tumours is associated with poor prognosis, poor survival rates and higher chance of recurrence (Reedijk et al., 2005, 2008; K. Yao et al., 2011). A positive correlation was found between Notch4 expression and proliferation measured by Ki67 levels in breast cancer samples (Rizzo et al., 2008). A high level of Notch1 expression also correlates with a higher grade and more EMT markers in ALDH+ breast tumours (Pal et al., 2017).

High expression level of Notch ligands is also linked to breast cancer progression. A particularly poor outcome was identified in breast cancers with a very high expression level of Jagged1 (Dickson et al., 2007). Jagged1 is also involved in a positive feedback loop between the tumour microenvironment and BCSCs. This action, via Zeb1, acts to increase Notch signalling (Jiang et al., 2020). DLL1 is also overexpressed in ER+ breast cancers. It is linked to poor prognosis, cellular invasion and cancer stem cell function and is stabilised by estrogen signalling (Kumar et al., 2018; Sales-Dias et al., 2019). DLL4 has been found to be highly expressed in the intratumoural endothelium of breast cancers, indicating its association and potential as a prognostic factor (Jubb et al., 2010).

Numb is a negative regulator of the Notch pathway and has been found to be lost in half of breast cancers (Pece et al., 2004). In normal tissue, Numb reduces the cell surface availability of Notch receptors, either by ubiquitination or increased endocytosis. Therefore, with a reduced level of Numb in the cell, the level of Notch available for signalling increases (McGill et al., 2009).

Mutations have been found in Notch genes in all subtypes of breast cancer. In triple negative breast cancer, mutations in the PEST domain stabilise the receptor, increasing Notch activation and signalling (K. Wang et al., 2015). Other mutations can be found in the extracellular domain, increasing ligand independent signalling, altering activation and changing crosstalks, leading to aberrant signalling (Mollen et al., 2018).

1.5.1 Roles in breast tumours

There are many roles that the Notch signalling pathway plays in the regulation of breast tumours, summarised in Figure 1-11. Notch signalling can act to promote proliferation of cancer cells via activation of the cyclin signalling pathways and prevent apoptosis via upregulation of Akt (Meurette et al., 2009; Rizzo et al., 2008; Stylianou et al., 2006). These roles would both allow for the survival of breast cancer. These dual roles of Notch have been found to be dose-dependent in mammary cells, with a high level of Notch activity causing growth arrest and prevention of apoptosis and a medium level of signalling causing a hyperproliferative state (Mazzone et al., 2010). Notch alters the microenvironment to make it advantageous to the tumour, through paracrine mechanisms leading to supportive angiogenesis (Dufraine et al., 2008; Shi & Harris, 2006; Zeng et al., 2005). Notch signalling is involved in hypoxia mechanisms in ER+ breast cancers, interacting with HIF-1α (Harrison, Rogerson, et al., 2013). Notch signalling is also involved in the spread of breast cancer, with cell migration of breast cancer cells increasing with Notch activation (Bolós et al., 2013). EMT is heightened via Slug through the activation of Jagged1 mediated Notch signalling, and has strong links to the advancement of triple negative breast cancer (Leong et al., 2007). Also via Jagged1 induced signalling, Notch plays a part in promoting bone metastatic colonisation (Sethi et al., 2011). Finally, Notch signalling has been linked heavily to the action of breast cancer stem cells (BCSCs). This will be explored in section 1.6, examining the role of Notch4.

1.5.2 Interactions with other signalling pathways

The Notch pathway can interact with other signalling pathways to promote breast cancer, simplified in Figure 1-11. Non-canonical Notch signalling interacts with IL-6 which can activate the Jak/STAT pathway, leading to a pro-inflammatory phenotype. This is caused by interaction with p53, a tumour suppressor gene (Jin et al., 2013). Myeloid derived suppressor cells (MDSCs) have an interesting role in upregulating BCSCs and downregulating T-cell activation. They enhance the crosstalk between Notch and STAT3. IL-6 phosphorylates STAT3 whilst Nitric oxide activates Notch, prolonging the STAT3 activation (Peng et al., 2016).

Another pathway that Notch has a particularly intricate crosstalk with is the NF-κB pathway. Both pathways are implicated highly in cancer, and Notch-1 mediated NF-κB activation is thought to contribute to oncogenic effects and cell survival in breast cancer (L. Li et al., 2014; Osipo et al., 2008). When cells are under oncogenic conditions with increased Notch signalling, the increased level of NICD in the cytosol will lead to some molecules forming

complexes with other proteins including NF-κB and Smad3 (J. Han et al., 2011). These complexes will promote alternative signalling pathways, leading to an altered phenotype of the Notch activated cell, potentially promoting a more tumourigenic phenotype.

Notch-Wnt crosstalk has been linked to breast tumour initiation, as the Wnt induced transformation of mammary epithelial cells is reliant on Notch (Ayyanan et al., 2006). Hypoxia in tumours leads to upregulation of HIF2α, which induces Notch and Wnt signalling. This leads to resistance to paclitaxel and an enhanced stem cell phenotype (Yan et al., 2018).

Crosstalk has also been observed between PKCα and Notch4 in endocrine resistant breast cancer cells. The expression of the two components correlates strongly in breast cancer samples and this correlation was less apparent with the other Notch receptors. Notch inhibitors successfully reduced PKCα-high tumour growth (Yun et al., 2013).

Finally, Notch1 acts synergistically with the Ras/MAPK pathway to promote breast cancer, leading to progression and a poor prognosis (Mittal et al., 2009).

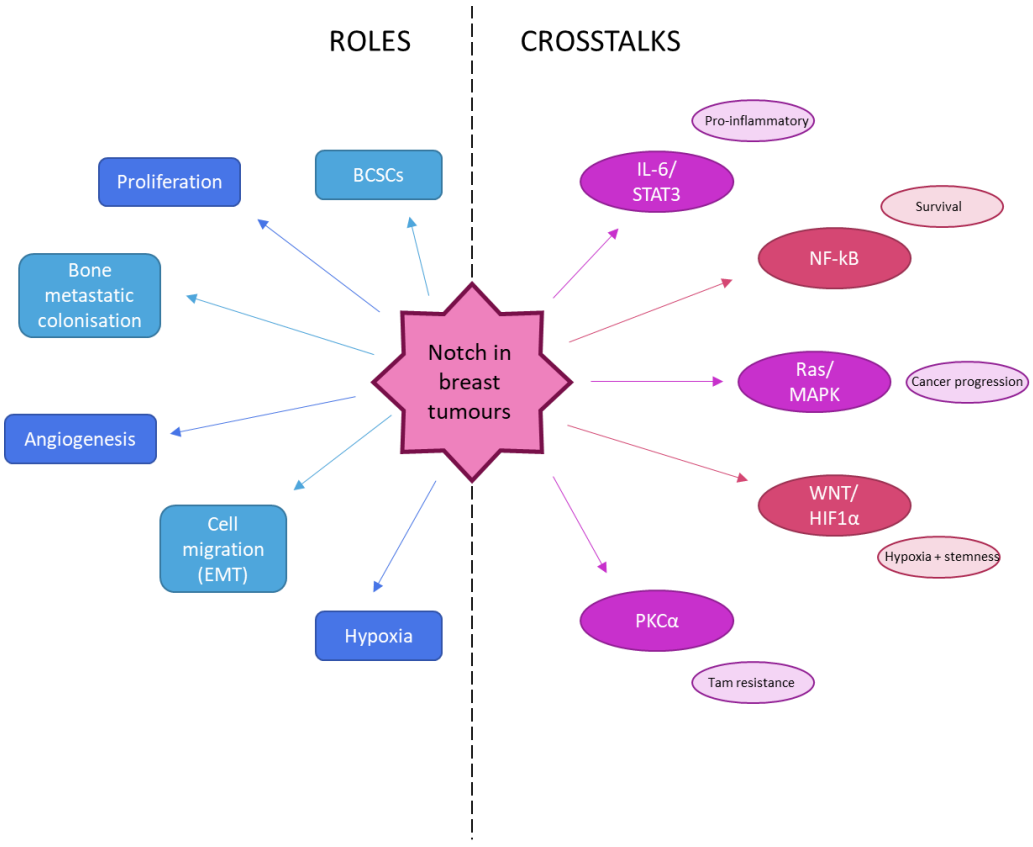

Figure 1-11: Roles and crosstalks of Notch in breast tumours. Notch is involved directly in many aspects of the progression of breast tumours. These include its roles in proliferation, progression (BCSCs, metastatic colonisation and cell migration (EMT)), and the microenvironment (angiogenesis and hypoxia). Notch also is involved in crosstalk with many pathways, including IL-6/STAT3, NF-κB, Ras/MAPK, Wnt/HIF1α and PKCα.

1.5.3 Notch and endocrine resistance

There is extensive evidence that BCSC activity and Notch signalling are enriched after treatment with endocrine therapies including tamoxifen. This is also the case following estrogen deprivation (Haughian et al., 2012; Piva et al., 2014; Simões et al., 2011; Simões, O'Brien, et al., 2015). High expression of Notch receptors also drives anti-estrogen treatment resistance, promoting cell survival processes. Notch inhibition can reverse endocrine resistance and stall tumour growth (Magnifico et al., 2009). In endocrine resistant breast cancers, the Notch pathway, and particularly Notch4, is activated. Notch4 also promotes tamoxifen resistance, leading to progression of breast cancer (Magnani et al., 2013; Yun et al., 2013).

1.6 Notch4 and BCSCs

The specific link between Notch4 and Breast Cancer Stem Cells (BCSCs) was first made by Harrison et al when they showed that in BCSCs Notch4 signalling is heightened, whereas Notch1 signalling is decreased. Knocking down or inhibiting the Notch4 receptor reduced BCSC activity, assessed by mammosphere forming efficiency, and abolished the tumour initiating capacity in mice (Harrison et al., 2010).

In TNBC, Notch4 has been found to play a key role in mesenchymal-like BCSCs. It is essential at maintaining the quiescence (through GAS1) and the invasiveness (through Snail) of BCSCs (Zhou et al., 2020). The inhibition of Notch4 in TNBC has been shown to reduce proliferation and invasiveness, highlighting its therapeutic potential as a BCSC target (Nagamatsu et al., 2014).

Other studies have shown that breast cancer cells with an increased level of Notch activity arising from acquisition of endocrine resistance have a greater Notch4 expression compared to other Notch receptors (D'Angelo et al., 2015; Lombardo et al., 2014). These cells also exhibit increased tumour-initiating capacity, mammosphere forming efficiency and expression of cancer stem cell markers. This suggests that these cells with increased Notch activity (particularly Notch4) are likely to be breast cancer stem cells. This is backed up by the fact that following the induction of Notch4 overexpression by nicastrin, resistance to tamoxifen is developed (Lombardo et al., 2014). Clinically, poor patient survival is correlated with increased Notch4 expression in cancers, further solidifying the link (D'Angelo et al., 2015). Mutations in the estrogen binding domain of ER drive cells to a BCSC phenotype

through ER/Notch4. This action is dependent on ERα phosphorylation at ser118 as inhibition of this phosphorylation blocked Notch4 and BCSC activity (Gelsomino et al., 2018).

Notch4 is also implicated in breast cancer progression and metastasis, as it has been reported that Notch4 plays a vital role in the epithelial-mesenchymal transition, an important step in the metastatic progression of cancer. This was identified in a tamoxifen resistant breast cancer cell line. It was also found that signalling via STAT3 was involved. An inhibitor to Notch4 was found to reduce splenic metastases, suggesting that targeting Notch4 in tamoxifen resistant breast cancers could help to reduce metastases (Bui et al., 2017).

The link between Notch4 and BCSCs in ER+ breast cancer was strengthened by Simões et al when work proved a vital link between Notch4-Jagged1 signalling and anti-estrogen treatment resistance. A strong Notch4/Hes/Hey signature predicted endocrine therapy resistance and a poor prognosis, similarly to cells with high ALDH1 expression. Anti-estrogen treatments increased BCSC activity and upregulated the Hes and Hey Notch target genes. This suggests an increase in Notch4 signalling in BCSCs following the development of endocrine resistance. An inhibitor of Notch4 then was employed which restored the treatment-induced increase in BCSC activity to a basal level. This inhibitor was also found to target BCSCs in long acquired tamoxifen resistant patient derived xenograft (PDX) models (Simões, O'Brien, et al., 2015). These results strongly link Notch4 to endocrine therapy resistance and therefore BCSCs.

1.7 Clinical relevance of targeting Notch in breast cancer

As shown, the Notch pathway is linked to endocrine resistance, BCSCs and therefore recurrence and metastasis of breast cancers. Targeting the Notch signalling pathway would also reduce its effects on angiogenesis, indirectly reducing tumour growth. Therefore, it is a key stem cell pathway to be targeted in therapy. It is a complex signalling pathway, providing multiple stages at which it could be targeted for inhibition.

For example, ligand-receptor binding could be targeted with molecules that block binding, such as Notch decoys or antibodies that bind to the receptor. These drugs would not inhibit ligand independent signalling pathways so may not be able to inhibit all Notch signalling. The cleavage events of "S2" or "S3" could be targeted by inhibiting the ADAM10 that carries out "S2" or the gamma-secretase that carries out "S3". The pathway could also be targeted further along by inhibiting the formation of the transcriptional activator complex to prevent

NICD from binding to the DNA and causing target gene expression (Edwards & Brennan, 2021). Specific Notch receptors could be targeted by exploiting differences between them, for example their length differences. Alternative Notch signalling pathways, such as the ligand independent pathway could also be targeted by inhibiting signalling components.

In reality, the only current Notch inhibitors that have been tested in the clinic are gamma-secretase inhibitors (GSIs), targeting the "S3" cleavage by gamma-secretase. There have been many GSIs explored in clinical trials for breast cancer, but after showing promising results *in vitro* and *in vivo* in mice, multiple trials have been aborted due to toxicities.

The general toxicities shown in trials could be due to multiple reasons. As discussed, Notch is a key signalling pathway involved in maintenance of many areas of the body, including the vasculature. When inhibited, effects are observed across many organ systems, particularly the gut (Milano et al., 2004). Moreover, gamma-secretases are key enzymes that are not exclusive to the Notch pathway. They cleave many other proteins including E-cadherin and ERB-B4 (Haapasalo & Kovacs, 2011). Inhibiting gamma-secretase would therefore affect many other pathways, increasing the risk of side effects and toxicities.

The toxicities observed when using GSIs clinically have been reduced by using smaller doses and spreading doses across a longer period of time. This can also be achieved by combination treatment with chemotherapy and endocrine therapy, inadvertently reducing dosage. These methods have shown some success as improvements in toxicity, increased treatment efficacy and reduction in metastases (Edwards & Brennan, 2021; Lamy et al., 2017; Meurette et al., 2009; Proia et al., 2015).

A GSI (RO492097) which has shown the ability to target Notch4 has recently been investigated in a Phase1b clinical trial to treat ER+ metastatic breast cancer. Inhibition of Notch4 was achieved, stability of disease was observed in some cases and it was determined that Notch inhibition should continue to be investigated in order to prolong life in the metastatic setting (Means-Powell et al., 2021). Another GSI clinical trial is underway, specifically to treat breast cancers that are Notch activated (*A Study of AL101 Monotherapy in Patients With Notch Activated Triple Negative Breast Cancer ClinicalTrials.gov*, 2022). Personalising GSI treatments to those that are most likely to benefit may be another approach to minimising GSI-related toxicities. This could be done by creating PDX's directly corresponding to a patient's cancer and testing therapies directly. This has been done recently with the GSI RO492097. Two PDX organoids were sensitive to the treatment,

suggesting that the corresponding tumour may also be sensitive, and RO492097 may be effective as a therapeutic strategy (Guillen et al., 2021).

Specific antibodies that target certain Notch receptors and ligands could provide an alternative way of inhibiting Notch signalling. This would discriminate from the potential tumour suppressing role that some Notch receptors may play. Anti-DLL4 monoclonal antibodies have shown success at targeting DLL4 binding with Notch1 and Notch4. This led to decreased Notch signalling and tumour growth (Brunner et al., 2016). Another DLL4 targeting antibody has been developed and investigated in solid tumours including breast. It was found to be tolerated well and responses were observed from reducing Notch signalling (Chiorean et al., 2015). Jagged1 has also been targeted with neutralising antibodies. These have been developed by Masiero et al and have been found to block JAG1-Notch breast cancer signalling *in vitro* and *in vivo*. They were also found to reduce brain metastases and did not show any toxicities, indicating promising clinical potential (Masiero et al., 2019). Specific monoclonal antibodies that target the individual Notch receptors have also been identified and investigated (Y. Wu et al., 2010).

A solution to the targeting Notch problem may also come from using a drug that simultaneously targets Notch signalling and other cancer signalling pathways. An example of this is the drug Sulforaphane, which has shown success at inhibiting Notch signalling and BCSCs *in vitro* and *in vivo* (Castro et al., 2019; Simões et al., 2020). It has also shown promising results in breast cancer clinical trials (S. J. Howell et al., 2019).

It can be agreed that further understanding on Notch signalling in BCSCs is needed to allow more targeted Notch therapies. Insight gained could allow the very specific inhibition of a particular Notch signalling pathway, abolishing its effects on BCSCs and endocrine resistance, whilst allowing the normal functions of Notch to continue.

1.8 Hypothesis and Aims

1.8.1 Hypothesis

Breast cancer stem cell activity is enhanced following anti-estrogen treatment of estrogen receptor positive breast cancer, leading to endocrine therapy resistance. Notch4 signalling is highly activated in these BCSCs, linking Notch4 activity to endocrine therapy resistance (Simões, O'Brien, et al., 2015). In *Drosophila*, the Notch AxE2 mutant (a single residue change H1167Y, Figure 1-12) leads to a Notch gain of function. This mutant is highly dependent on Deltex for activity determined by a more pronounced Notch loss of function when Deltex is deleted (compared to WT Notch) (T. Xu & Artavanis-Tsakonas, 1990). Deltex has been linked to ligand-independent/ endocytic pathway dependent Notch signalling. Human Notch4 possesses the equivalent residue change in its endogenous sequence (Y914), diverging from Notch1/2/3 (Figure 1-12). Research has also shown that Notch4 has been unable to be activated directly with ligand (James et al., 2014).

It is hypothesised that this evolutionary residue in Notch4 may enhance Deltex-dependent or ligand-independent Notch signalling, increase BCSC activity and drive endocrine resistance. Alongside this, Notch4 mutants selected during endocrine therapy may enhance Notch4 signalling and may further increase reliance on ligand independent/ Deltex-dependent signalling.

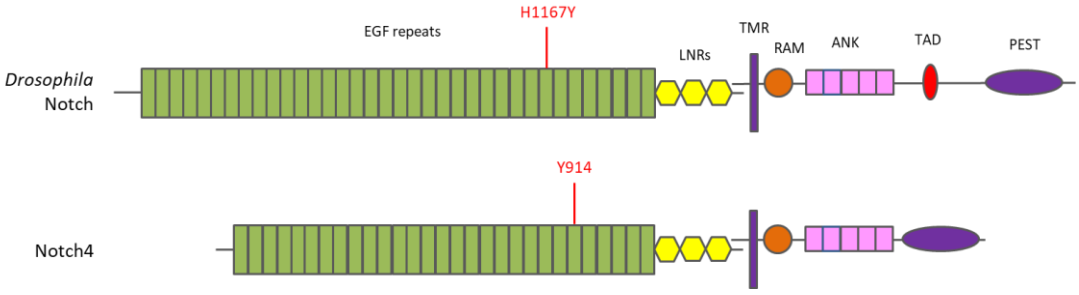

Figure 1-12: Drosophila Notch AxE2 mutant and Notch4. The *Drosophila* AxE2 mutation causes a gain of function for Notch to become more Deltex dependent. It also signals via the ligand independent pathway. Notch4 possesses this residue change in its endogenous sequence, diverging from Notch1/2/3. This suggests that Notch4 may signal in a Deltex dependent, ligand independent way.

1.8.2 Aims

1) To investigate Notch4 signalling by exploring requirements of trafficking proteins such as Deltex and identifying signalling pathways involved.
2) To investigate the effects that Notch4 signalling has on BCSC activity and endocrine resistance and to explore BCSC dependence on endocytic trafficking.
3) To investigate Notch4 mutations and the impact that they have on Notch4 signalling and BCSC activity.

Ultimately, the future clinical aim is to apply the mechanistic knowledge gained to target relevant parts of the Notch4 signalling pathway to treat breast cancer stem cells. The initial part of this aim is addressed in this thesis.

2 Materials and Methods

2.1 Materials

2.1.1 Antibodies

Name	Target	Host species	Source	Lot/ catalogue number	Final volume/ concentration to stain 100,000 cells/100µl
Notch4	Notch4	Human	MedImmune	ML01545-01	0.4µl
IgG	IgG	Human	MedImmune	555BO-130	0.4µl
Notch4 AlexaFluor647 conjugate	Notch4	Human	MedImmune	N/A	4µg/ml
IgG AlexaFluor647 conjugate	IgG	Human	MedImmune	N/A	4µg/ml

Table 2-1: Antibodies used for flow cytometry and FACS

Name	Target	Host species	Source	Dilution for IF	Dilution for WB	Catalogue number
Notch4	Notch4 C-terminus	Rabbit	Abcam	1/400	1/400	Ab91621
Notch4 AF647 conjugate	Notch4 NRR domain	Human	Med Immune	1/100	N/A	N/A
EEA1	Early endosomes	Mouse	Santa Cruz	1/500	N/A	sc365652
CD63	Late endosome	Mouse	Merk Millipore	1/500	N/A	CBL553
LAMP1	Lysosomes	Mouse	Santa Cruz	1/500	N/A	sc18821
KDEL	Endoplasmic Reticulum	Mouse	Enzo	1/500	N/A	ADI-SPA-827
GM130	Golgi	Mouse	Santa Cruz	1/500	N/A	sc55591
DYKDDDDK Tag mAb	FLAG tag	Mouse	Cell Signalling technology	1/400	N/A	8146S

B-actin	B-actin	Mouse	Sigma	N/A	1/10,000	A1978

Table 2-2: Primary antibodies used for immunofluorescence and western blot

Name	**Target**	**Host**	**Source**	**Fluorescent conjugate**	**Catalogue number**
Anti-rabbit	Rabbit antibodies	Goat	Invitrogen	AlexaFluor 488	A-21206
Anti-mouse	Mouse antibodies	Goat	Invitrogen	AlexaFluor 555	A-21422

Table 2-3: Secondary antibodies used for immunofluorescence

Name	**Target**	**Supplier**	**Catalogue number**	**Dilution**
Goat anti-mouse-HRP	Mouse antibodies	Dako	P0447	1/5000
Goat anti-rabbit-HRP	Rabbit antibodies	Dako	P0449	1/5000

Table 2-4: Secondary antibodies used for western blot

2.1.2 Drugs/inhibitors

Name	**Target**	**Source**	**Catalogue number**
RO4929097	Gamma-secretase	Cellagen technology	C7649
Batimastat (BB-94)	Matrix Metalloproteases	Stratech	S7155
GW-405833 (ML-SI1)	TRPML	Alfa-Aesar	J67425
ICI 182780 (Fulvestrant)	ER (downregulator)	TOCRIS	1047
4-OH-tamoxifen (Tamoxifen)	ER (antagonist)	Sigma	H7904

Table 2-5: List of drugs and inhibitors used

2.1.3 General Reagents

Reagent	**Supplier**
2-Mercaptoethanol	Sigma
Acetic acid	Honeywell Fluka
B-27 Supplement	Gibco
ProLong™ Gold Antifade Mountant	Thermo Fisher Scientific
Ethanol Absolute	VWR Chemicals
Fetal Bovine Serum (FBS)	Gibco
GeneJuice® Transfection Reagent	Novagen
Hexadimethrine bromide (polybrene)	Sigma
L-Glutamine	Thermo Fisher Scientific
4x Laemmli Sample Buffer	Bio-Rad
Library efficiency DH5α Competent Cells	Thermo Fisher Scientific
Lipofectamine RNAiMAX transfection reagent	Thermo Fisher Scientific
Luminata Classico Western HRP Substrate	Millipore
Luminata Forte Western HRP Substrate	Millipore
SuperSignal West Femto Maximum Sensitivity Substrate	Thermo Fisher Scientific
Matrigel (standard LDEV-free)	Corning
Nitrocellulose	Invitrogen
N,O-bis(trimethylsilyl)acetamide (BSA)	Thermo Fisher Scientific
Penicillin-Streptomycin	Thermo Fisher Scientific
Precision Plus Dual Colour Protein Standards	Biorad
Phosphate Buffered Saline (PBS)	N/A
Poly(2-hydroxyethylmethacrylate) (polyhema)	Sigma
Puromycin	Thermo Fisher Scientific
RNaseZap	Sigma
Taqman Transcription Reagents	Applied Biosystems
Taqman Universal PCR master mix	Roche
Trichloroacetic acid (TCA)	Sigma
TRIS-base	Sigma

Triton X-100	Sigma
Trypan blue (0.4 %)	Sigma
Trypsin-EDTA solution 0.05%: 0.5g porcine trypsin, 0.2g EDTA, 4Na/L HBSS, phenol red	Sigma

Table 2-6: List of general reagents

2.1.4 Buffers

Buffer	**Composition**
Lysis Buffer (for WB)	15mM EDTA, 10% glycerol, 25mM HEPES, 50mM NaCl, 50mM NaF, 30mM NaPP, 1µM PMSF, 1% Triton-X-100, 1 Complete Mini Protease Inhibitor Cocktail (Roche) tablet per 10 ml. 5µl of 200mM PMSF added per 1ml buffer before use.
Running buffer (for WB): NU Page Running Buffer	10x premixed electrophoresis buffer, contains 25 mM Tris, 192 mM glycine, 0.1% SDS, pH 8.3 following dilution to 1x with water
Transfer buffer for (for WB)	14.3g Glycine, 3g Tris-Base, 800ml distilled water, 200ml methanol
10x Tris-Buffered-Saline (TBS) wash buffer (for WB)	12.1g Tris base, 87.7g NaCl, distilled water to 1L. pH 7.4
TBS-Tween (TBST) wash buffer (for WB	100ml 10x TBS, 900ml distilled water, 1ml Tween
Ponceau red (for WB)	1% Ponceau s, 5% acetic acid
Tris-acetate-EDTA (TAE) Buffer	40mM Tris, 20mM acetic acid, 1mM EDTA
FACS Buffer	1% BSA, PBS

Table 2-7: List of buffers and composition

2.1.5 Cell culture media

Dulbecco's Modified Eagle's Medium (DMEM): +1000mg/L glucose +Sodium Bicarbonate -L-glutamine (Sigma)

DMEM F12 reduced serum media: +Non-essential amino acids +110mg/L sodium pyruvate -L-glutamine (Sigma)

DMEM F12 reduced serum media: -phenol red (Ham) (Sigma)

EBM-2 Basal Medium (Lonza)

Mammosphere media: DMEM F12 reduced serum media -phenol red, B27 supplement (Gibco), 20ng/ml Epidermal Growth Factor (EGF, Miltenyi)

Opti-MEM™ Reduced Serum Medium (Thermo Fisher Scientific)

2.1.6 Equipment

Flow cytometry: BD LSRII and BD AriaII

Tissue culture microscopy: Olympus CK2-TR 4x lens + 10x lens, Evos XL core (Life Technologies)

Nanodrop Spectrophotometer: Nanodrop One^{c} (Thermo Fisher Scientific)

Peltier thermal cycler PT-200 (MJ Research)

Qs5c qPCR machine (Thermo Fisher Scientific)

Tissue culture centrifuges: Heraeus™ Megafuge™ 40R centrifuge (Thermo Fisher Scientific) + centrifuge 5702 (eppendorf)

Main lab centrifuges: Centrifuge 5415 D (eppendorf) + microcentrifuge 154 (Camlab)

Fluorescent microscope: Axio imager M2 (Zeiss)

2.1.7 Primers

The following optimised TaqMan gene expression primer assays were used for qRT-PCR:

Target	**Amplicon length (nt)**	**Supplier**	**Assay ID**
DTX1	62	Thermo Fisher Scientific	Hs01092201_m1
DTX2	69	Thermo Fisher Scientific	Hs00539707_m1
DTX3	102	Thermo Fisher Scientific	Hs01595350_m1
DTX4	74	Thermo Fisher Scientific	Hs00392288_m1
DTX3L	97	Thermo Fisher Scientific	Hs00370540_m1
NOTCH4	60	Thermo Fisher Scientific	Hs00965889_m1

GAPDH	122	Thermo Fisher Scientific	Hs99999905_m1
18s rRNA	187	Thermo Fisher Scientific	Hs99999901_s1
B actin	75	Thermo Fisher Scientific	Hs00194899_m1
Hes1	78	Thermo Fisher Scientific	Hs00172878_m1

Table 2-8: Primer assays used in qRT-PCR reactions

The following primers were used for non-optimised qRT-PCR reactions:

Target	**Sequence**	**Supplier**
Hes1 FW	GAAGCACCTCCGGAACCT	eurofins
Hes1 RV	GTCACCTCGTTCATGCACTC	eurofins
Hey1 FW	CATACGGCAGGAGGGAAAG	eurofins
Hey1 RV	GCATCTAGTCCTTCAATGCT	eurofins
Hey2 FW	CCCGCCCTTGTCAGTATC	eurofins
Hey2 RV	TTGTTTGTTCCACTGCTGGT	eurofins

Table 2-9: Primers used in non-optimised qRT-PCR reactions

The following probes were used for non-optimised qRT-PCR reactions:

Probe name	**Fluorescent tag**	**Source**	**Gene that it corresponds to**
29	Taqman	CRUKMI MBCF	Hey1
60	Taqman	CRUKMI MBCF	Hes1
73	Taqman	CRUKMI MBCF	Hey2

Table 2-10: Probes used in non-optimised qRT-PCR reactions

The following primers were used for sequencing:

Target	**Sequence**	**Supplier**
NOTCH4 exon 2 FW	GGGTACCATGTGCAGAGTGG	eurofins
NOTCH4 exon 2 RV	CACAAGCTGGGTGTCAA	eurofins
DTX plasmid FW	GAACCCACTGCTTACTGGCTT	eurofins

DTX plasmid RV	ACGGTCGGTAGACAACAAACG	eurofins
DTX1 plasmid	GGTCCATCCGGCCCTGGCAGG	eurofins
DTX2 plasmid	GGGCGCAGCTCCTCCTTCCCT	eurofins
DTX3 plasmid	GAGCTCGGGGGCTCCCCCCTC	eurofins
DTX4 plasmid	AGGCACCATTCGAGGCCCACT	eurofins
hN4 plasmid start FW	AATATGTAATTTTCAGTGTTA	eurofins
hN4 plasmid start RV	CCACTGAGACACATAGCAGCA	eurofins
hN4 plasmid end FW	CTGTGGTCCCCCAGCCCTCCA	eurofins
hN4 plasmid end RV	TGTAATCCAGAGGTTGATTAT	eurofins
L491AFWseq	AAGTCCCTGTGAACATGGC	eurofins
E511KRVseq	ATATCCTCCTCACATCGGGT	eurofins
Y914HFWseq	TGCAACCTTCCACTGTCCT	eurofins
E1009QRVseq	CACAGGTCCCTCCATGAAA	eurofins
E1836KFWseq	AAGTAGCCCAGCTACTGCT	eurofins
E1836KRVseq	AAGTCTACGGACCAAGTCCG	eurofins

Table 2-11: Primers used for sequencing

The following primers were used for site-directed mutagenesis:

Target	**Sequence**	**Supplier**
L491A FW	ggaagcacctgtgcagacctacttgccaccttc	eurofins
L491A RV	gaaggtggcaagtaggtctgcacaggtgcttcc	eurofins
E511K FW	ggcttagaagggcagctctgtaaggtggagacc	eurofins
E511K RV	ggtctccaccttacagagctgcccttctaagcc	eurofins
Y914H FW	cagcggcccctcccatttctgccactg	eurofins
Y914H RV	cagtggcagaaatgggaggggccgctg	eurofins
G924V FW	ccctggattccaagtaagcctgtgccaggatc	eurofins
G924V RV	gatcctggcacaggcttacttggaatccaggg	eurofins
E1009Q FW	gggagacgtggaccagtgtctggacca	eurofins
E1009Q RV	tggtccagacactggtccacgtctccc	eurofins

E1836K FW	cacaaagccacgccgggccgcaaagctgggcccttcccgcgcgc	eurofins
E1836K RV	gcgcgcgggaagggcccagctttgcggcccggcgtggctttgtg	eurofins

Table 2-12: Primers used for site-directed mutagenesis

The following siRNA constructs were used for gene knockdown:

Type of siRNA	**Target**	**Species**	**Supplier**
Silencer® Select Pre-designed (Inventoried)	DTX1	Human	Ambion
Silencer® Select Pre-designed (Inventoried)	DTX4	Human	Ambion
Silencer® Select Pre-designed (Inventoried)	Rab7a	Human	Ambion
Silencer® Select Pre-designed (Inventoried)	VPS33A	Human	Ambion
Silencer® Select Pre-designed (Inventoried)	VPS18	Human	Ambion
Silencer® Select Pre-designed (Inventoried)	DTX2	Human	Ambion
Silencer™ Select Negative Control No. 1 siRNA	Negative control	Human	Ambion
Silencer™ Select Negative Control No. 2 siRNA	Negative control	Human	Ambion

Table 2-13: siRNA constructs used for knockdowns

2.1.8 Plasmids

Name	**Source**
hNOTCH4 lentiviral plasmid	VectorBuilder
Control lentiviral plasmid	VectorBuilder
DTX1 pcDNA3.1_C-DYK	Martin Baron, University of Manchester
DTX2 pcDNA3.1_C-DYK	Martin Baron, University of Manchester
DTX3 pcDNA3.1_C-DYK	Martin Baron, University of Manchester
DTX4 pcDNA3.1_C-DYK	Martin Baron, University of Manchester

Table 2-14: Plasmids obtained for use in the project

2.1.9 Kits

Kit	Supplier	Catalogue number
Endofree Plasmid Maxi Kit	Qiagen	12362
RNAeasy Mini	Qiagen	74104
RNAeasy Micro	Qiagen	74004
TaqMan Universal PCR Master-mix	Thermo Fisher Scientific	4304437
TaqMan™ Reverse Transcription Reagents	Thermo Fisher Scientific	N8080234
ALDEFLUOR™ Kit	STEMCELL Technologies	01700
Pierce™ BCA Protein Assay Kit	Thermo Fisher Scientific	23225
QuickChange II XL Site-directed Mutagenesis Kit	Agilent	200517

Table 2-15: List of pre-made kits used

2.1.10 Cell lines

Cell line	Tissue
MCF7	Breast
MCF7 (Cardiff)	Breast
TAMR (Tamoxifen resistant)	Breast
FULVR (Fulvestrant resistant)	Breast
MCF7 N4KO Clone control	Breast
MCF7 N4KO	Breast
HEK-293T	Embryonic kidney
RPE (hTert-RPE1)	Epithelial eye cell

Table 2-16: List of cell lines used

2.2 Methods

2.2.1 Database search

Mutations in primary and metastatic breast cancers were searched for using publicly available genomic databases and smaller study datasets. This was carried out methodically, excluding samples that are present in more than one database. The databases used are as follows: cBioPortal (Cerami et al., 2012; Gao et al., 2013), National Cancer Institute GDC Data Portal (Grossman et al., 2016), COSMIC (Tate et al., 2019) and Tumour Portal (Lawrence et al., 2014).

The studies that the mutations were sourced from are listed: "MSK-IMPACT Clinical Sequencing Cohort" (Zehir et al., 2017), "Breast Invasive Carcinoma" (Banerji et al., 2012), "Breast Invasive Carcinoma" (Ciriello et al., 2015), "Breast Invasive Carcinoma" (Koboldt et al., 2012), "Breast Invasive Carcinoma" (TCGA, Provisional), "Mutational profiles of metastatic breast cancer" (Lefebvre et al., 2016), "Sequence analysis of mutations and translocations across breast cancer subtypes" (Banerji et al., 2012), "Landscape of somatic mutations in 560 breast cancer whole-genome sequences" (Nik-Zainal et al., 2016), "A whole-genome sequence and transcriptome perspective on HER2-positive breast cancers" (Ferrari et al., 2016), "Diverse somatic mutation patterns and pathway alterations in human cancers" (Kan et al., 2010), "Genomic Evolution of Breast Cancer Metastasis and Relapse" (Yates et al., 2017), "Comparative genomic analysis of primary tumors and metastases in breast cancer" (Bertucci et al., 2016), "Breast Cancer" (Razavi et al., 2018), "Breast Cancer" (Nixon et al., 2019), "Breast Cancer" (Kan et al., 2018) and "Proteogenic landscape of breast cancer" (Krug et al., 2020).

2.2.2 Cell culture methods

2.2.2.1 Normal cell culture

All cell lines were grown in tissue culture flasks and maintained at 37°C and 5% CO_2. The flasks were passaged once they reached 80% confluency. Detachment from the flasks was performed using trypsin-EDTA (Sigma). Cell lines were tested regularly for mycoplasma infection and authenticated through the CRUKMI Molecular Biology Core Facility. Tamoxifen and Fulvestrant resistant cells (TAMR and FULVR) were a gift from Julia Gee (University of Cardiff) and were treated with 10^{-7}M 4OH-tamoxifen (Sigma) or 10^{-8}M ICI 182780

(fulvestrant) (TOCRIS), respectively, to maintain resistance (Knowlden et al., 2003; McClelland et al., 2001).

2.2.2.2 3+3 day treatment culture

Cells were seeded in 6 well culture plates at a density to provide 80% confluency after 3 days and treated with ethanol (vehicle), 10^{-6}M 4OH-tamoxifen (Sigma) or 10^{-7}M ICI 182780 (Fulvestrant) (TOCRIS). These were grown for 3 days, detached, and reseeded at the same confluency, with the same treatment. After another 3 days, the cells were detached and analysed.

2.2.2.3 Mammosphere assay

Resuspended cells were syringed with a 25G needle to ensure a single cell suspension was achieved. Cells were then seeded at the required density in Polyhema (Sigma) coated 6 well plates in mammosphere media. They were then incubated at 37°C for 5 days. The primary mammospheres formed were counted using an Olympus CK2-TR microscope, including only those that had reached 60µm diameter, using 4x lens. Mammosphere forming efficiency (MFE) was calculated using the following equation:

$$Mammosphere\ forming\ efficiency\ (MFE)(\%) = \left(\frac{No\ of\ mammospheres}{no\ of\ cells\ seeded}\right) * 100$$

2.2.2.4 Transfection

Cells were cultured to reach approximately 70% confluency. First, 4.5µl GeneJuice® Transfection Reagent (Novagen) was added to 225µl Opti-MEM™ Reduced Serum Medium and mixed by vortexing. 1.125µg of relevant plasmid was added and mixed by gentle pipetting. This was incubated at RT for 30 mins, after which, it was added to monolayer cells in Opti-MEM™ Reduced Serum Medium. Cells were analysed after 24 hours. Values for 1 well of 6 well plate.

2.2.2.5 siRNA knockdown

Cells were cultured to reach approximately 70% confluency. 7.5µl Lipofectamine RNAiMAX Transfection Reagent (Thermo Fisher Scientific) was added to 135µl Opti-MEM™ Reduced

Serum Medium. 25pmol of relevant Silencer Select Pre-Designed & Validated siRNA (Thermo Fisher Scientific) was added to a separate 135µl Opti-MEM™ Reduced Serum Medium. These solutions were combined gently by pipetting, incubated for 15 mins at RT, and added dropwise to monolayer cells in Opti-MEM™ Reduced Serum Medium. After 24h, knockdown was confirmed using qRT-PCR or western blot. Values for 1 well of a 6 well plate.

2.2.2.6 Lentivirus production

HEK293T cells were cultured to reach 70% confluency. Cells were then transfected following the calcium phosphate method using $CaCl_2$ and 2xHBS. 2xHBS was added to solution containing equimolar ratio of lentiviral gene expression plasmid (Vector Builder) (Figure 2-1) and 3 lentiviral packaging plasmids "gagpol", "env" and "vsvg" as well as $CaCl_2$ solution. This solution was mixed for 5 minutes, incubated for 12 minutes at RT and added dropwise to cells. Incubation was carried out at 37°C for 6 hours, after which, the media was switched for complete media. Virus particles were harvested 24h, 48h and 72h post-transfection. These virus particles were ultra-centrifuged in Beckman Coulter Avanti JXN-30 centrifuge at 20000rpm for 2 hours at 4°C. Virus titre was determined using a titration method using HEK293T cells. Serial dilutions of virus volume were added to cells with 8µg/ml Polybrene. Fresh media was added after 6 hours and Puromycin (2µg/ml) was introduced 48 hours later for selection. Colonies formed after 7 days were fixed and stained with 1% Giemsa stain. Virus titre was calculated using the formula below for each well and mean value was taken as the virus titre:

$$\frac{TU}{mL} = \left(\frac{Number\ of\ colonies}{total\ volume\ in\ well}\right) * dilution\ factor$$

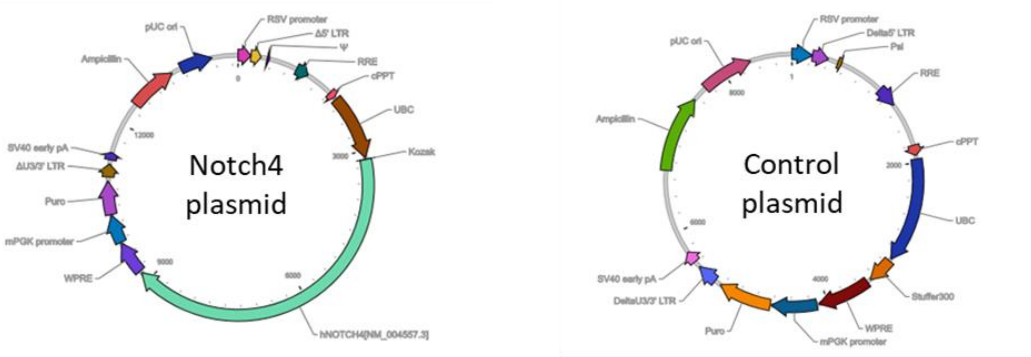

Figure 2-1: Plasmids obtained from VectorBuilder for lentivirus production

2.2.2.7 Stable cell line production

Required parental cells were plated out at 10,000 cells/well in a 96 well plate. Once the virus titre had been calculated, the virus could be added at the required MOI (Multiplicity of Infection). Virus was added at a MOI of 0.5 with 8µg/ml polybrene 24 hours after seeding cells. 6 hours later, virus containing media was switched for complete media. 48 hours after this, Puromycin (2µg/ml) containing media was added to the cells for selection. Once selected for, the transduced cells were expanded and used as required.

2.2.3 Imaging methods

2.2.3.1 Flow cytometry for Aldefluor assay and Notch4 antibody

Aldefluor assays were carried out using the ALDEFLUOR™ Kit (Stemcell Technologies) as per manufacturer's instructions. Cells were resuspended in FACS buffer at a density of $1x10^6$ cells/ml. 0.4µl of Notch4 ECD antibody (MedImmune) was added per 100,000 cells and cells incubated for at 4°C for 1 hour. Cells were washed in PBS and resuspended in ALDEFLUOR™ assay buffer. 2.5µl ALDEFLUOR™ reagent was added to half of the cell suspension. To the other half, 5µl DEAB and 2.5µl ALDUFLUOR reagent was added. Following mixing, these cells were incubated at 37°C for 40 minutes, mixing periodically. Cells were resuspended in ALDEFLUOR™ assay buffer. Analysis was carried out using a BD LSRII flow cytometer and BD FACSDIVA software using lasers and filters at (488)530/30 to detect Aldefluor reagent and (640)660/20 to detect Notch4. Compensation was also carried out using single stained controls. Further data analysis was carried out using FlowJo software (FlowJo).

2.2.3.2 Flow cytometry and sorting for Notch4 antibody

Cells were resuspended in FACS buffer at a density of $1x10^6$ cells/ml. 0.4µl of Notch4 ECD antibody (MedImmune) was added per 100,000 cells and cells incubated for at 4°C for 1 hour. Cells were washed in PBS and resuspended in FACS buffer. Analysis was carried out using a BD LSRII flow cytometer using lasers and filters at (640)660/20. Sorting was carried out using a BD AriaII flow cytometer. Cells were sorted using a gate drawn for the lasers and filters at (640)660/20, choosing the cells positive/ negative for Notch4. Cells were collected in DMEM media and lysed for use in RNAseq. Further data analysis was carried out using FlowJo software (FlowJo).

2.2.3.3 Immunofluorescence

Cells were cultured on 16mm diameter coverslips (FisherScientific) that had been autoclaved for sterility. Cells were fixed with 4% PFA, permeabilised with 0.2% Triton X-100 (in PBS) and blocked with 4% PBSA. Primary antibodies at the required concentration in 4% PBSA were added for the relevant time, followed by washes in PBS. Secondary antibodies at the required concentration in 4% PBSA were then added for 30 mins in the dark, followed by washes in PBS. After rinsing in ddH_2O, coverslips were mounted onto the slide with ProLong™ Gold Antifade Mountant (Thermo Fisher Scientific). Slides were imaged on an Axio imager M2 fluorescent microscope (Zeiss) at 100x magnification.

2.2.3.4 Immunofluorescence image analysis

Immunofluorescence images were initially deconvolved using Huygens software (CRUKMI) with appropriate settings. Images were then processed using Fiji (Image J) for viewing. Colocalisation of channels was analysed using Imaris software, accessed via CRUK Manchester Institute. The Imaris "coloc" function was used to create a colocalisation channel from two chosen channels, providing quantification details about colocalisation, including Pearson's coefficient. The "volume" function was also used to represent the structure of the compartments including endosomes. The intensity sum of certain channels that were present within those compartments could then be quantified.

2.2.3.5 SRB assay

SRB assays were used to assess cell density. Cells were fixed at desired timepoints using 50% Trichloroacetic acid (TCA, Sigma) for 1 hour at 4°C. Plates were washed 3-5 times with water. Following air drying, cells were stained with 0.04% sulforhodamine B (SRB) in 1% acetic acid for 1 hour at RT. Plates were washed 3-5 times with 1% acetic acid and air dried. Before visualisation, stain was solubilised with 10mM TRIS-base (pH 10.5, Sigma). After 20 minutes, optical density was measured at 570nm using VersaMax tuneable microplate reader and SoftMax Pro software.

2.2.4 Protein analysis - Western Blotting

Cells were lysed using lysis buffer and scraped with a cell scraper. The lysate was rotated for 1 hour at 4°C and centrifuged for 10 minutes at 4°C. The concentration of protein lysates was determined with a BCA assay using a Pierce™ BCA Protein Assay Kit (Thermo Fisher).

A pre-cast 10% Sodium Dodecyl Sulfate Polyacrylamide Gel Electrophoresis (SDS-PAGE) gel (BioRad) was used and loaded into a western blotting cassette. 80µg of protein was added to each well, after being mixed with 4x laemmli buffer (BioRad) and boiling at 95°C for 5 minutes. 8µl Precision Plus Protein™ Dual Colour Standards (BioRad) was also added to determine size of bands. The SDS-PAGE gel was run at approximately 150V for 30 minutes or until the blue dye front had travelled out of the gel.

The gel was transferred to Nitrocellulose blotting membrane with 0.45µm pores assembled in a cassette including transfer sponges and filter paper. The protein was then transferred in transfer buffer for 1 hour at 100V using the Trans-Blot Electrophoretic Transfer Cell.

Membranes were blocked using 5% BSA in TBS at RT for 1 hour on a shaker. They were then incubated with primary antibody overnight at 4°C. Primary antibody dilutions and timings were optimised for each antibody. Following three washes with TBS-Tween, membranes were incubated with the appropriate HRP conjugated secondary antibody for 1 hour at RT. Following another wash stage, the appropriate HRP substrate was added, depending on the approximate concentration of the protein of interest. Images of the membrane were taken using the BioRad ChemiDoc Touch Imaging System. If another protein was to be detected on the same membrane, antibodies were stripped using Stripping Buffer (BioRad) for 30 minutes. This was followed by a wash stage and the detection stages were repeated, starting with a blocking step.

2.2.5 Molecular biology methods

2.2.5.1 RNA extraction

RNA was extracted from cells using the RNeasy Mini Kit (Qiagen) and Qiashredder (Qiagen). Monolayer cells were washed with PBS and RLT buffer (+β-mercaptoethanol) was added directly to cells. Lysates were collected and RNA was extracted using columns as per manufacturer's instructions. Purity and yield were judged by a nanodrop spectrophotometer (Thermo Fisher Scientific).

2.2.5.2 qRT-PCR

2.2.5.2.1 Reverse Transcription

cDNA was produced from RNA using the TaqMan® Reverse Transcription Reagents (Applied Biosystems). Reagents provided in the kit and RNase free water (Ambion) were added to 1µg RNA as described by manufacturer. The reaction took place on a Peltier thermal cycler (MJ Research) with the following settings: 25°C 10 minutes, 48°C 30 minutes, 95°C 5 minutes.

2.2.5.2.2 qPCR and quantification of mRNA expression

qPCR was carried out in a 384 well PCR plate (Thermo Fisher Scientific) using the Qs5c qPCR machine (Thermo Fisher Scientific). Taqman Universal PCR Mastermix (Thermo Fisher Scientific), optimised TaqMan Gene expression primer assays or unoptimised primers and relevant probes (section 2.1.7), and cDNA produced from reverse transcription were added to each well. Assays were designed and analysed using the Thermo Fischer Scientific Cloud "Design and Analysis Application".

2.2.5.3 RNAseq

2.2.5.3.1 Library preparation and sequencing

Library preparation and sequencing was carried out by the CRUK Manchester Institute Molecular Biology Core Facility. This was carried out with double-ended polyA sequencing using a Novaseq SP system (Illumina).

2.2.5.3.2 Bioinformatic analysis

Bioinformatic analysis and production of user-accessible shiny app was carried out by Matthew Roberts (CRUK). Bioconductor packages AnnotationDbi (1.48.0) (Pagès et al., 2020) and org.Hs.eg.db (3.10.0) (Carlson, 2019) were used to retrieve additional gene IDs. Gene set enrichment analysis and pathway analysis was performed using Bioconductor packages ideal (1.10.0) (Marini, 2020), fgsea (1.14) (Korotkevich et al., 2019) with MSigDB gene set collections (McCarthy et al., 2012) limma (3.42.2), pathview (1.26.0) (Luo & Brouwer, 2013), enrichR (3.0) (Jawaid, 2021), gage (2.36.0) (Luo et al., 2009) with gageData (2.24.0) (Luo, 2020) and ReactomePA (1.30) (G. Yu & He, 2016). ggplot2 (3.3.3) (Wickham, 2009), pheatmap (1.0.12) (Kolde, 2019) and RColorBrewer (1.1-2) (Neuwirth, 2014) were used for making plots. tidyr (1.1.3) (Wickham, 2021), tibble (3.1.2) (K. Müller & Wickham, 2021), dplyr (2.0.6) (Wickham et al., 2021) and magrittr (2.0.1) (Bache & Wickham, 2020) were used for general data processing and formatting. The analysis was presented in a web application using shiny

(1.5.0) (Chang et al., 2021) hosted on a server running R (3.6.0) (R Core Team, 2020). Code was written using RStudio Workbench (1.4.1717.3) (R Studio Team, 2021) using R (4.0.3). Fastq files were processed with Nextflow (19.10.0) nf-core/rnaseq (1.3) pipeline. Gene count normalisation was performed with DESeq2 (1.26.0).

Genes of interest were determined by calculating the log2 fold change between samples and filtering for genes that met a certain, user defined threshold. Figures were created using shiny (1.5.0) with user-defined parameters.

2.2.5.4 Genomic DNA purification

Genomic DNA was extracted from cells using the Wizard® Genomic DNA purification Kit as per manufacturer's instructions. Cells were detached from culture dishes and centrifuged at 16000g and then lysed using Nuclei lysis solution. RNA and proteins were removed with RNase Solution and Protein Precipitation Solution. The DNA was then precipitated using isopropanol and rehydrated with DNA Rehydration Solution.

2.2.5.5 Transformation

DH5α competent cells (Invitrogen) were used for transformations. 10ng plasmid DNA was added to 50µl DH5α cells and incubated for 30 mins. A 45 second heat shock at 42°C was used to allow DNA to enter the cells. Cells were incubated at 37°C for 1 hour at 225rpm and spread on LB + Ampicillin plates. Plates were incubated overnight at 37°C and stored at 4°C until needed.

2.2.5.6 Plasmid amplification and purification

Following transformation, clones were picked from stored LB + Ampicillin plates and pre-cultured in LB broth with 100µg/ml Ampicillin at 37°C, 225rpm for 8 hours. Following this, the preculture was added to the expansion culture (also LB broth with 100µg/ml Ampicillin). Cells were harvested by centrifugation at 6000g 4°C for 15 minutes. A Qiagen Plasmid Maxi kit (Qiagen) was used to purify plasmids according to manufacturer's instructions. Pelleted bacteria was resuspended in Buffer P1, followed by the addition of Buffer P2, incubation at room temperature for 5 minutes, addition of Buffer P3 and then centrifugation at 6000g at 4°C for 15mins. A QIAfilter cartridge was used to clear the lysate. Buffer ER was then added

followed by 30 minutes incubation on ice. A QIAGEN-tip was used to collect the plasmid DNA and multiple washing rounds were carried out with Buffer QC. Buffer QN was used to elute the DNA. Plasmid DNA was then precipitated with isopropanol, washed with ethanol and rehydrated with RNase and DNase free water.

2.2.5.7 Site-directed mutagenesis

Site-directed mutagenesis was carried out using a QuickChange II XL Site-directed Mutagenesis Kit as per manufacturer's instructions. Primers to correspond to each mutation were designed using Snapgene software and synthesised by Eurofins. Mutated plasmids were created using a modified PCR reaction, followed by a digestion of the original plasmid with Dpn-1. Mutated plasmids were transformed into XL10-Gold ultracompetent cells and amplified and purified as above.

2.2.5.8 DNA sequencing

DNA samples were sequenced using the CRUKMI Molecular Biology Core Facility. Each tube contained 15ng DNA for genomic DNA or 300ng for plasmids and 15pmoles of primer.

2.2.6 *In vivo* methods

2.2.6.1 Limiting dilution assay

The resource equation was used to estimate optimal mouse number for the experiment. "Experimental units = total degrees of freedom – treatments degrees of freedom". For this experiment, E = 23 – 5, E = 18. For optimal conditions, E should be between 10 and 20, so this number of mice is an appropriate number to test this hypothesis (Mead, 1988).

Serial cell dilutions of N4KO-CON and N4KO-N4 cells were made according to Table 2-17. 100µl cell suspension in mammosphere media was added to 100µl Matrigel (Corning) to create a 1:1 dilution. Cells were injected subcutaneously into the left and right flanks of NSG mice as described in Table 2-17. These mice had previously had a 90-day release 0.36mg 17-ß estradiol pellet (Innovative Research of America) implanted subcutaneously 7 days prior to cell injection. Tumours (if formed) were measured 3 times a week. Tumour size was calculated using 0.5 x length x width^2. At endpoint (total tumour volume per mouse 1250mm^3 or 77 days post injection) tumours and lungs for groups 4a and 4b were collected and fixed for 24 hours with formalin.

Group number	Mouse	Number of cells per injection	Left flank	Right flank
1	1-5	10,000	N4KO-CON	N4KO-N4
2	6-10	1000	N4KO-CON	N4KO-N4
3	11-15	100	N4KO-CON	N4KO-N4
4a	16-19	100,000	N4KO-CON	N4KO-CON
4b	20-23	100,000	N4KO-N4	N4KO-N4

Table 2-17: Experiment design for Limiting dilution assay

The Extreme Limiting Dilution Analysis (ELDA) is an online application that was used to calculate tumour initiating cell frequency (Y. Hu & Smyth, 2009).

2.2.7 Statistical analysis

All statistical analyses were carried out using GraphPad Prism 9.0. Normality of datasets was determined using Agostino-Pearson, Shapiro-Wilk and Kolmogorov-Smirnov normality tests. Normal parametric tests included the unpaired two-tailed t-test, Ordinary one-way ANOVA and Two-way ANOVA with Tukey's or Šidák's multiple comparisons, specified in figure legend. $p<0.05$ (*), $p<0.01$ (**), $p<0.001$ (***), $p<0.0001$ (****). Error bars are shown as ±SEM unless stated otherwise.

3 Notch4 signals via a endocytic pathway signalling mechanism

3.1 Introduction

This chapter will investigate signalling by the Notch4 receptor and identify which endocytic vesicle components are involved in the pathway. This was carried out using *in vitro* methods including immunofluorescence, analysis of gene expression and knockdown of genes.

Canonical Notch signalling involves the binding of a Notch ligand expressed on the membrane of a signal sending cell to a Notch receptor on the membrane of a signal receiving cell. "S2" and "S3" cleavages that take place after ligand binding, release the Notch intracellular domain into the cytoplasm, which translocates to the nucleus (Figure 1-8). Here, it binds with the protein complex RBP-Jκ and other co-activators and induces expression of target genes including those of the Hes and Hey families (Kopan & Ilagan, 2009). In the ligand-independent pathway, Notch is internalised into the cell via the actions of Deltex. It is trafficked through the endocytic pathway via early endosomes, late endosomes and lysosomes. The NICD is released and can travel to the nucleus, inducing target gene expression in a similar manner to the ligand dependent pathway (Shimizu et al., 2014).

In *Drosophila*, a Notch mutant (AxE2) that contains one amino acid residue change in the Abruptex (Ax) domain, from a histidine to a tyrosine, alters this signalling pathway. It alters Notch function so that it becomes less ligand-dependent and more ligand-independent (T. Xu & Artavanis-Tsakonas, 1990). This mutant Notch is also reliant on the protein Deltex for signalling. The amino acid sequence of mammalian Notch4 is generally well conserved with Notch1, 2 and 3 but significantly, Notch4 diverges from Notch1, 2 and 3 to match the *Drosophila* AxE2 mutant described above. This leads to our hypothesis that Notch4 might signal similarly to this mutant Notch, in a ligand-independent and Deltex-dependent way. This would suggest less ligand control over the amount of Notch signalling in the cell and NICD would be released into the cytoplasm at a greater rate, without the limiting step of ligand binding for receptor activation.

Deltex is an E3 protein ubiquitin ligase and assists in the internalisation of various proteins from the cell membrane, including Notch. In the non-canonical Notch signalling pathway it generally acts as a positive regulator, both inducing internalisation of the full length Notch receptor from the cell surface, as well as stabilising the receptor in the late endosome, preventing degradation (Yamada et al., 2011). However, its role switches to a negative regulator of the pathway when co-expressed with Su(dx) (L. Wang et al., 2021; Wilkin et al.,

2008). The role of Deltex is further complicated by the fact that there are four Deltex proteins in mammalian cells (DTX1-4).

The ligand-independent pathway has been studied in *Drosophila*, but very little is known about this signalling pathway or its action in mammalian cells, including humans. Using transient transfection of Notch4 into cell lines including breast cancer cell lines, this chapter will investigate the Notch4 signalling pathway, looking for evidence of Notch4 endocytic pathway activation. By use of immunofluorescence staining of Notch4, the cellular localisation of full length or cleaved forms of the protein will be investigated. siRNA knockdown will then be used to dissect the involvement of the members of the Deltex family and various components of the endocytic pathway and gene expression of target genes will be analysed.

3.2 Successful transient transfection of Notch4 into breast cancer cells increases gene expression of Notch4 and Notch target genes

From previous work in the lab, it has been found that Notch4 is only present at a very low level in the ER+ breast cancer cell line MCF7. In order to study Notch4 signalling in breast cancer cells, Notch4 was transiently transfected into MCF7 cells. Due to the large size of the Notch4 plasmid (14.7kb) (Figure 3-1A), GeneJuice® was selected as the optimal transfection reagent which allowed a balance between transfection efficiency and health of the cells. The plasmid used is a lentiviral gene expression vector, also applicable for transient transfection. The optimal length of time after transfection to analyse the expression of the Notch4 receptor on the cell surface was determined using flow cytometry. The cells were collected 24, 48 and 72 hours after transfection and cell surface Notch4 expression was analysed. They were stained using the Notch4-AlexaFluor647 antibody, (a gift from MedImmune). Notch4 transfected cells maintain a significantly higher AF647 fluorescence level than untransfected after 24 hours. This returns to a similar level to untransfected cells after 48 and 72 hours (Figure 3-1B+C). At 24 hours after transfection, approximately 10% of cells are positive for Notch4, which reduces to 2.4% after 48 hours and to 1.2% after 72 hours (Figure 3-1D). These data suggest transient transfection of Notch4 causes expression and membrane presentation of the receptor, but turnover and loss of cell surface expression after 24 hours.

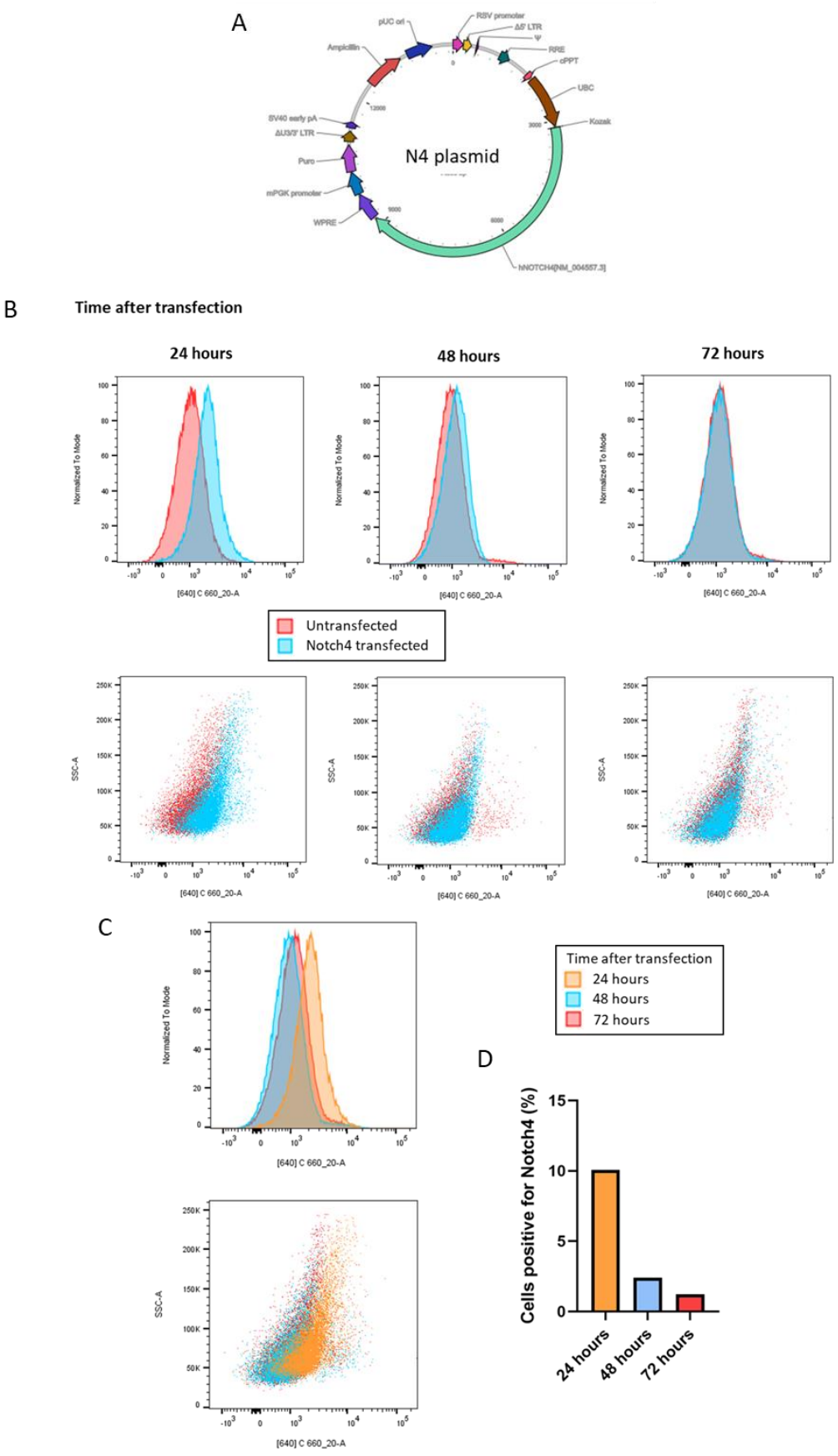
A
N4 plasmid
pUC ori
Ampicillin
RSV promoter
Δ5' LTR
Ψ
RRE
cPPT
UBC
Kozak
hNOTCH4[NM_004557.3]
WPRE
mPGK promoter
Puro
ΔU3/3' LTR
SV40 early pA
B
Time after transfection
24 hours
48 hours
72 hours
Normalized To Mode
[640] C 660_20-A
Untransfected
Notch4 transfected
SSC-A
C
Time after transfection
24 hours
48 hours
72 hours
D
Cells positive for Notch4 (%)
24 hours
48 hours
72 hours

Figure 3-1: Transient transfection of Notch4 into MCF7 cells leads to a significant population of cells expressing Notch4 at the membrane after 24 hours. A) Plasmid map of the construct containing Notch4 that was used here for transient transfection of MCF7 cells using GeneJuice®. B) Flow cytometry results using Notch4-AF647 fluorescently conjugated antibody 24, 48 and 72 hours after transfection of MCF7 cells with Notch4 plasmid. Histograms and scatter plots include untransfected (red) cells and transfected (blue) cells and histograms have been normalised to allow for numbers of cells. C) Transfected MCF7 cells at 24 (orange), 48 (blue) and 72 (red) hours after transfection. Plotted using FlowJo. D) Graph to show percentage of cells positive for Notch4 from flow cytometry, 24, 48 and 72 hours after transfection. N=1.

Above, we demonstrate that the transiently transfected Notch4 is expressed and protein is detectible by flow cytometry at the cell surface of MCF7 cells. Next, we investigated whether it is being activated and inducing signalling and expression of its target genes. We also used a gamma-secretase inhibitor (GSI) to explore whether any signalling from the transiently transfected Notch4 was gamma-secretase dependent. For this experiment a GSI was used (RO4929097) that has been found to be more specific in blocking Notch4 signalling compared to other pan-GSIs such as DAPT (Simões, O'Brien, et al., 2015). To show that the transiently transfected Notch4 receptor was signalling, we measured expression levels of three Notch target genes, Hes1, Hey1 and Hey2. These three genes are used throughout this thesis as Notch target genes as they are common canonical targets of Notch signalling in most tissues, as well as in breast cancer. They encode for proteins involved in key cellular processes (Stylianou et al., 2006). MCF7 cells were transiently transfected with Notch4 plasmid using GeneJuice® as described above. After 24 hours, these cells were treated for 48 hours with vehicle or gamma-secretase inhibitor (GSI) RO4929097 (10μM). RNA was then collected, and a qRT-PCR was carried out to investigate Hes1, Hey1 and Hey2 gene expression levels. Transfecting Notch4 into MCF7s increased expression of Hes1, Hey1 and Hey2 genes (Figure 3-2A+B). These gene expression increases were reduced by treatment with the GSI for 48 hours. This establishes that the Notch4-induced increase of target genes is gamma-secretase dependent.

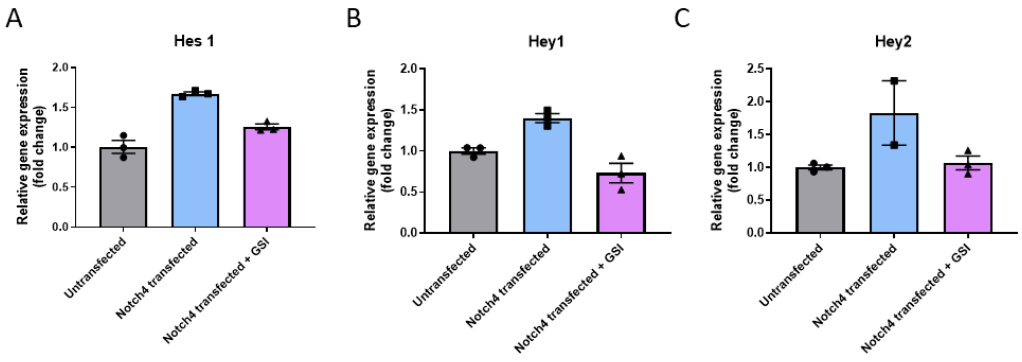

Figure 3-2: Notch4 transiently transfected into MCF7 cells induces Hes and Hey gene expression. MCF7 cells were transiently transfected with Notch4 plasmid for 24 hours and then treated with vehicle or the gamma-secretase inhibitor (GSI) RO4929097 (10µM) for 48 hours. After treatment was complete, RNA was collected and qRT-PCR was carried out to measure gene expression of Notch target genes Hes1 (A), Hey1 (B) and Hey2 (C). Fold change calculated from untransfected control. N=1. Data are represented as mean ±SEM.

3.3 Full length Notch4 is present within the endocytic trafficking pathway

In the ligand-independent, Deltex-dependent Notch activation pathway in *Drosophila*, Notch is internalised from the surface into the endocytic pathway as a full length protein. After internalisation, it travels from the early endosomes through the late endosomes and into the lysosomes, where the NICD is released into the cytoplasm (Shimizu et al., 2014; Steinbuck & Winandy, 2018). In order to determine whether Notch4 signals via this pathway, we investigated whether it is present in the cell as a full length protein. This was carried out using 3D immunofluorescence (with z-stacks at every 0.5mm) after transiently transfecting cells with Notch4. 24 hours after transfection, cells were fixed, permeabilised and stained with antibodies. The C-terminus (ICD) of Notch4 was labelled using a Notch4 ICD antibody (Figure 3-3). This was stained with an anti-rabbit AlexaFluor488 secondary antibody (green fluorescence in figures). The NRR domain (within the ECD) of Notch4 was labelled using the Notch4-AlexaFluor647 MedImmune antibody (red fluorescence in figures) (Figure 3-3). Colocalisation of these two antibodies observed in immunofluorescence of permeabilised cells indicated the presence of full length Notch4 receptor within the cell.

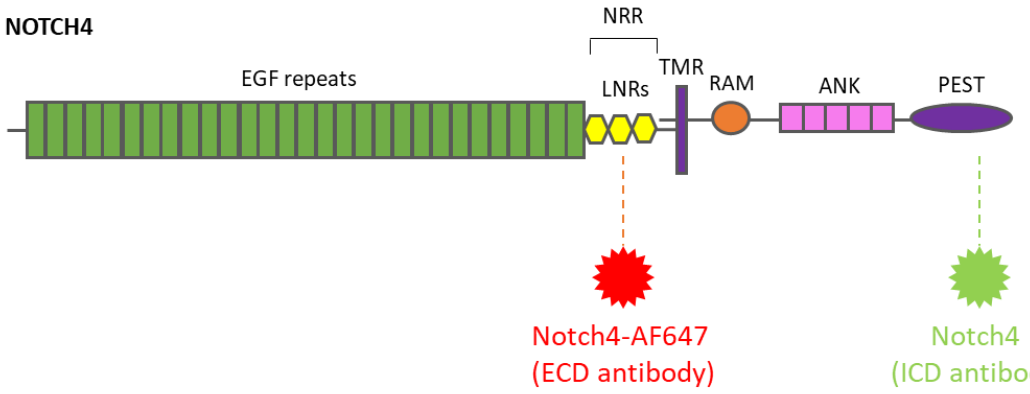

Figure 3-3: Binding regions of Notch4 antibodies used in immunofluorescence. Notch4-AF647 (ECD antibody) binds to the NRR (Negative regulator region). Notch4 (ICD antibody) binds to the C-terminus of Notch4. LNRs (Lin-12/Notch repeats), TMR (transmembrane region), RAM (RBP-Jkappa-associated module), ANK (ankyrin repeats).

hTert-RPE1 (RPE) cells were used initially as the optimisation cell line for the immunofluorescence as they are very flat, thin cells, with little background, to allow for more easy detection and imaging (Figure 3-4). In immunofluorescence of permeabilised cells, staining for both Notch4 ICD (green) and Notch4 ECD (red) can be seen to colocalise (merged panel, yellow), in punctate dots, suggesting that Notch4 is present within RPE cells as a full length protein (Figure 3-4A). There are also some points of ICD and ECD separate within the cell, indicating that intracellular separation of ICD and ECD is occurring. In non-permeabilised RPE cells, the immunofluorescence demonstrated that only Notch4 ECD was detectible at the surface of the cell, suggesting that the two antibodies are reliably binding and detecting the two different ends of the Notch4 protein (Figure 3-4B). No Notch4 ICD was detected at the surface (image not shown). Untransfected cells did not show ICD or ECD staining (data not shown).

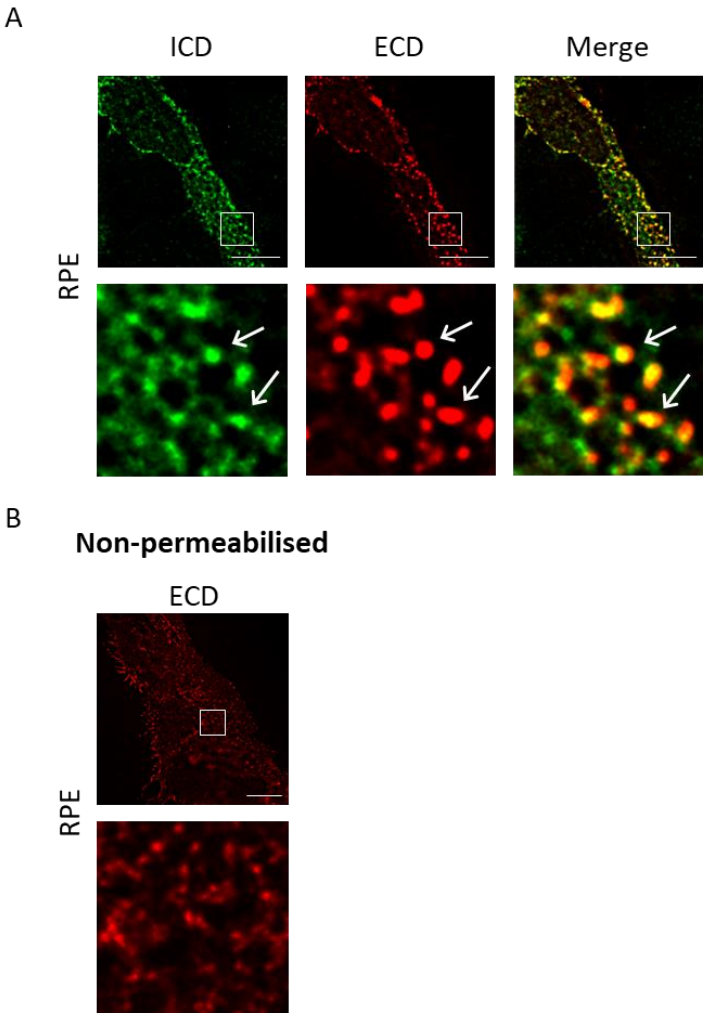

Figure 3-4: Notch4 is present as a full length protein inside RPE cells. RPE cells were used to optimise immunofluorescence staining for Notch4. Cells were transfected with Notch4 plasmid using GeneJuice® and after 24 hours were fixed, stained with antibodies, and visualised using an Axio Imager M2 fluorescent microscope (Zeiss) at 100x magnification. Images were also deconvolved using Huygens software. Immunofluorescence pictures show one plane of Notch4 intracellular domain (ICD) (green) and Notch4 extracellular domain (ECD) (red) and a merge of the two channels to demonstrate colocalisation. Areas of key colocalisation are indicated with arrows. A) Immunofluorescence using permeabilised cells shows full length Notch4 protein inside the cell. B) Immunofluorescence using non-permeabilised cells shows that only the Notch4 ECD is present at the surface of the cell. Areas zoomed in to show detail in higher magnification, indicated by the white squares. Scale bars: 5µm.

The distribution of the colocalised "spots" of full length Notch4 in Figure 3-4 indicates that the protein is located within an internal compartment. The compartments of the endocytic trafficking pathway were investigated with antibodies. EEA1 antibody was used to stain the early endosomes, CD63 antibody was used to stain the late endosomes and LAMP1 antibody

was used to stain the lysosomes. These endocytic pathway antibodies are shown in blue in Figure 3-5. They were used along with the Notch4 ICD (green) and Notch4 ECD (red) antibodies used previously, and colocalisation between all three channels was analysed to determine if the full length Notch4 receptor was present within the three endocytic compartments in RPE cells. Figure 3-5A shows colocalisation of ICD, ECD and EEA1 antibodies establishing that full length Notch4 is located in early endosomes. Figure 3-5C shows colocalisation of ICD, ECD and LAMP1 antibodies, indicating that full length Notch4 is present in lysosomes. There is also some colocalisation of ICD and LAMP1 without ECD (cyan dots), indicating that in some situations ICD is present in lysosomes without ECD, suggesting processing of Notch4 has occurred within the lysosome. In Figure 3-5B, although Notch4 ICD and ECD consistently colocalise, there is only a little cross over with CD63, suggesting full length Notch4 may be found in some subregions of the late endosomes, but not as consistently within the compartment as in early endosomes or lysosomes. Additional immunofluorescence experiments showed that full length Notch4 was not mainly remaining within the ER or Golgi during synthesis and processing (no full colocalisation between ICD, ECD and KDEL (ER marker) and GM130 (Golgi marker)) (Appendix Figure 8-1).

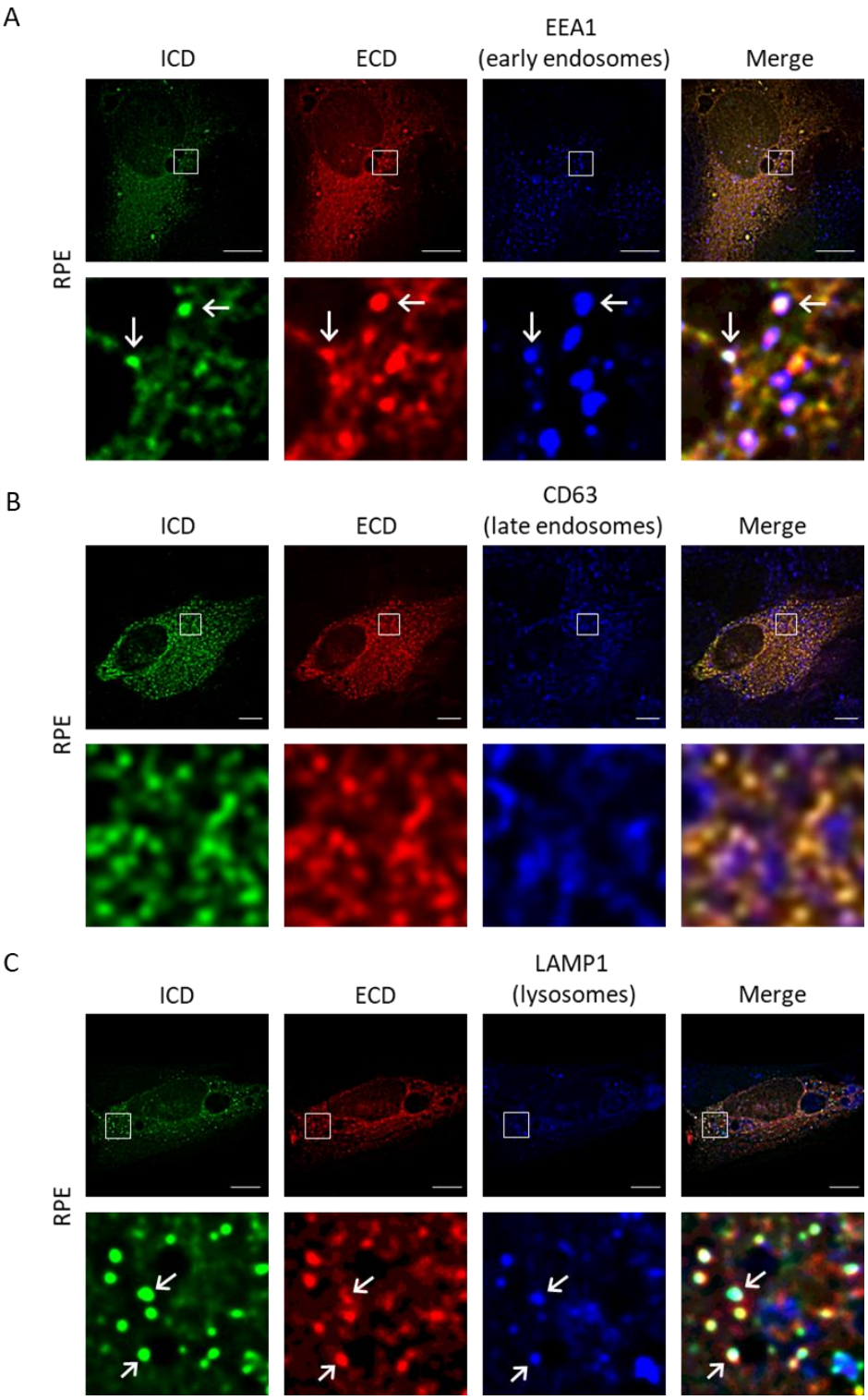

Figure 3-5: Full length Notch4 is located in early endosomes and lysosomes in RPE cells. Immunofluorescence images of RPE cells 24h after transiently transfecting with a Notch4 plasmid showing one plane of Notch4 ICD (green), Notch4 ECD (red) and EEA1-early endosomes (blue) (A), CD63-late endosomes (blue) (B), LAMP1-lysosomes (blue) (C) and a merge of the three channels to demonstrate colocalisation. Areas of key colocalisation are indicated with arrows. Areas zoomed in to show detail in higher magnification, indicated by the white squares. Scale bars: 5µm.

Equivalent immunofluorescence experiments were carried out in ER+ MCF7 breast cancer cells to confirm whether the presence of the full length Notch4 receptor in the endocytic pathway was apparent in breast cancer cells. It was observed that the Notch4 ICD and ECD antibodies colocalised in permeabilised MCF7 cells (Figure 3-6A), suggesting full length Notch4 is present. This colocalisation was further analysed using Imaris software with its embedded "coloc" feature and the level of colocalisation between the two channels was quantified using the Pearson's correlation. Pearson's correlation was used to measure the colocalisation of two channels in an image and supplies a correlation score depending on the colocalisation of the channels. These scores range from 0 with no colocalisation to 1 with full colocalisation. The result of the analysis of fourteen images of MCF7 cells transfected with Notch4 is shown in Figure 3-6B. The mean of these correlations is 0.66 showing a medium to high colocalisation between the ICD and ECD channels. The spread of Pearson's correlation between the different images was from 0.51 to 0.82.

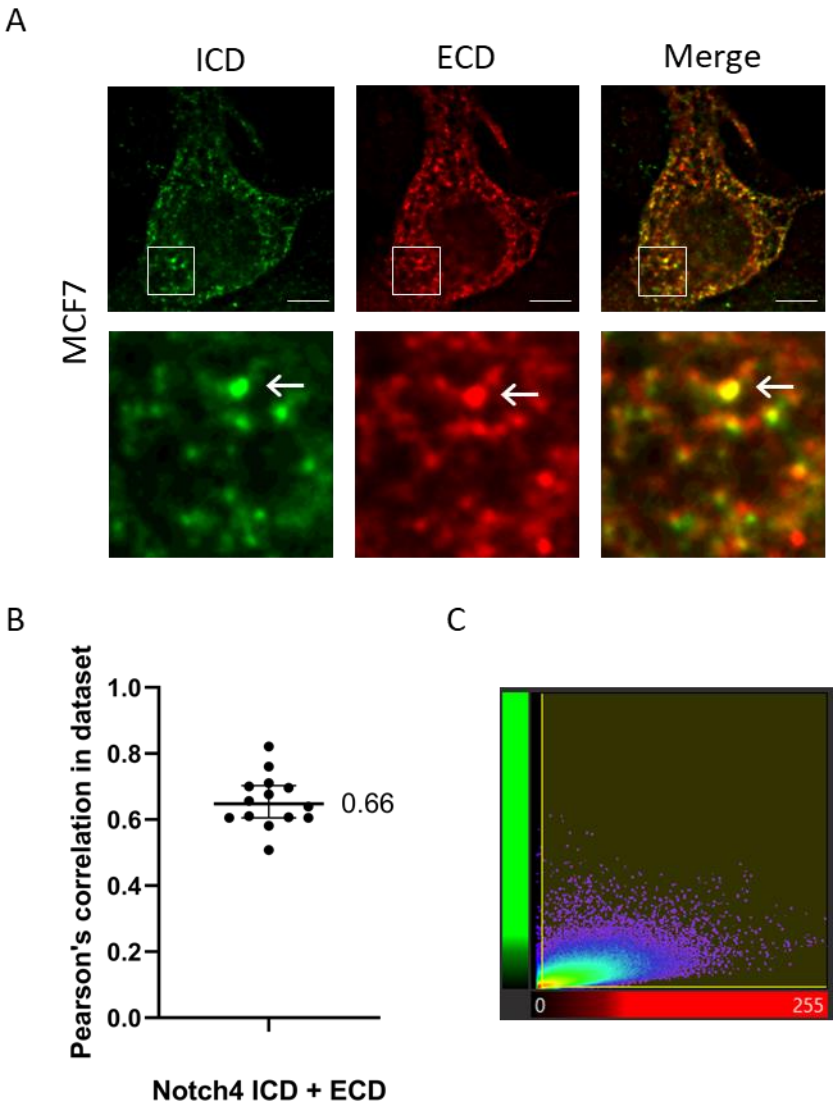

Figure 3-6: Notch4 is present as a full length protein inside MCF7 cells. (A) Immunofluorescence images of permeabilised MCF7 cells 24h after transiently transfecting with a Notch4 plasmid, showing one plane of Notch4 intracellular domain (ICD) (green) and Notch4 extracellular domain (ECD) (red) and a merge of the two channels to demonstrate colocalisation. Areas of key colocalisation are indicated with arrows. Areas zoomed in to show detail in higher magnification, indicated by the white squares. Scale bars: 5µm. (B) Pearson's correlation of the colocalisation of Notch4 ICD and ECD channels in full 3D immunofluorescence images. Graph shows spread between different images. Mean Pearson's correlation is 0.66. (C) Representative 2D scatter plot for colocalisation calculation of one image with the green channel (Notch4 ICD) on the y axis and the red channel (Notch4 ECD) on the x axis. N=14.

MCF7 cells were also investigated by immunofluorescence to explore Notch4 colocalisation with endocytic pathway components. The same endocytic compartment antibodies that were used in Figure 3-5 were used here- EEA1 to stain early endosomes, CD63 to stain late endosomes and LAMP1 to stain lysosomes (Figure 3-7). Colocalisation between ICD, ECD and EEA1 antibodies indicates full length Notch4 can be found in early endosomes (Figure 3-7A). Colocalisation is also observed between ICD, ECD and CD63 antibodies, establishing that full length Notch4 is located in late endosomes in MCF7s (Figure 3-7B). Figure 3-7C shows colocalisation of ICD, ECD and LAMP1 antibodies, indicating full length Notch4 is present in the lysosomes of MCF7 cells (Figure 3-7C). The immunofluorescence imaging of MCF7 cells together establish that in MCF7 cells, full length Notch4 can be found in endocytic compartments from early and late endosomes, through to lysosomes.

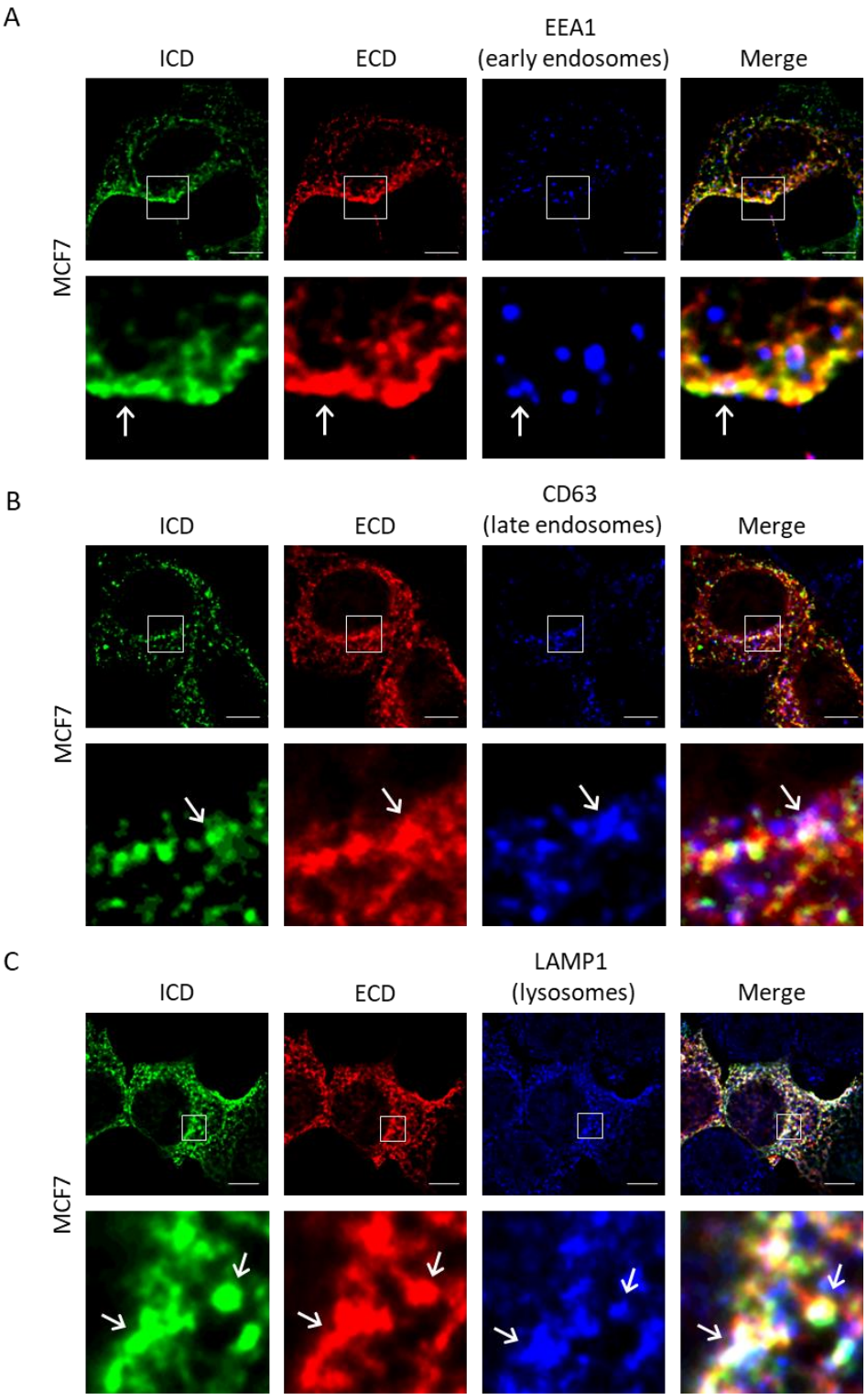

Figure 3-7: Full length Notch4 is found in early endosomes, late endosomes and lysosomes in MCF7 cells. Immunofluorescence images of MCF7 cells 24h after transiently transfecting with a Notch4 plasmid using GeneJuice® showing one plane of Notch4 ICD (green), Notch4 ECD (red) and EEA1-early endosomes (blue) (A), CD63-late endosomes (blue) (B), LAMP1-lysosomes (blue) (C) and a merge of the three channels to demonstrate colocalisation. Areas of key colocalisation are indicated with arrows. Areas zoomed in to show detail in higher magnification, indicated by the white squares. Scale bars: 5µm.

3.4 Full length Notch4 colocalises with DTX1 and DTX4 in MCF7 cells

In *Drosophila*, Deltex is involved in the ligand independent Notch activation pathway. It binds to the Notch receptor at the surface inside the cell and is involved in its monoubiquitylation, leading to its internalisation as a full length protein. Previous studies have shown that Deltex is essential for this alternative Notch signalling pathway (Guruharsha et al., 2012; Hori et al., 2011; Wilkin et al., 2008; Yamada et al., 2011). In humans, there are four Deltex proteins, Deltex 1-4. DTX1 and DTX4 are mainly found in the cytoplasm, whilst DTX2 and DTX3 are usually found in the nucleus. DTX1 has the highest homology with Deltex in *Drosophila* and has been studied the most in human cells (L. Wang et al., 2021). However, it is unknown which, if any of the human Deltex proteins are involved in Notch signalling. Due to the involvement of Deltex in the ligand independent Notch activation pathway in *Drosophila*, it was investigated if any of the human Deltex proteins contribute to Notch4 signalling in human breast cancer cells.

To investigate which of the Deltex proteins are most likely to be involved, MCF7 cells were co-transfected with Notch4 and Deltex 1/2/3/4. Cells were stained for Notch4 ICD and ECD in a similar manner as before, with the addition of a FLAG-tag antibody to bind to the FLAG labelled DTX protein (shown in blue in Figure 3-8) and visualised by immunofluorescence. The level of colocalisation between DTX and Notch4 was observed, by imaging and by using the Imaris "coloc" function for quantification. Extensive colocalisation can be observed between ICD, ECD and DTX1 (Figure 3-8A) as well as between ICD, ECD and DTX4 (Figure 3-8D). There are a few areas of colocalisation between ICD, ECD and DTX2 (Figure 3-8B) and little to no colocalisation between ICD, ECD and DTX3 (Figure 3-8C). This suggests that full length Notch4 can be found together in the cell with DTX1 and DTX4, suggesting some involvement of these two proteins, as well as a potential role of DTX2.

Quantification of results using the Imaris "coloc" function show that the Pearson's correlation of full length Notch4 with DTX4 is the highest, with an average value of 0.66 (Figure 3-9). DTX2 and DTX3 both have a lower average Pearson's correlation of 0.39. The three images analysed for DTX1 have varied values for Pearson's correlation (Figure 3-9B), giving them an average of 0.52. These results support the colocalisation observed by imaging in Figure 3-8 and suggest that DTX colocalisation may vary from cell to cell.

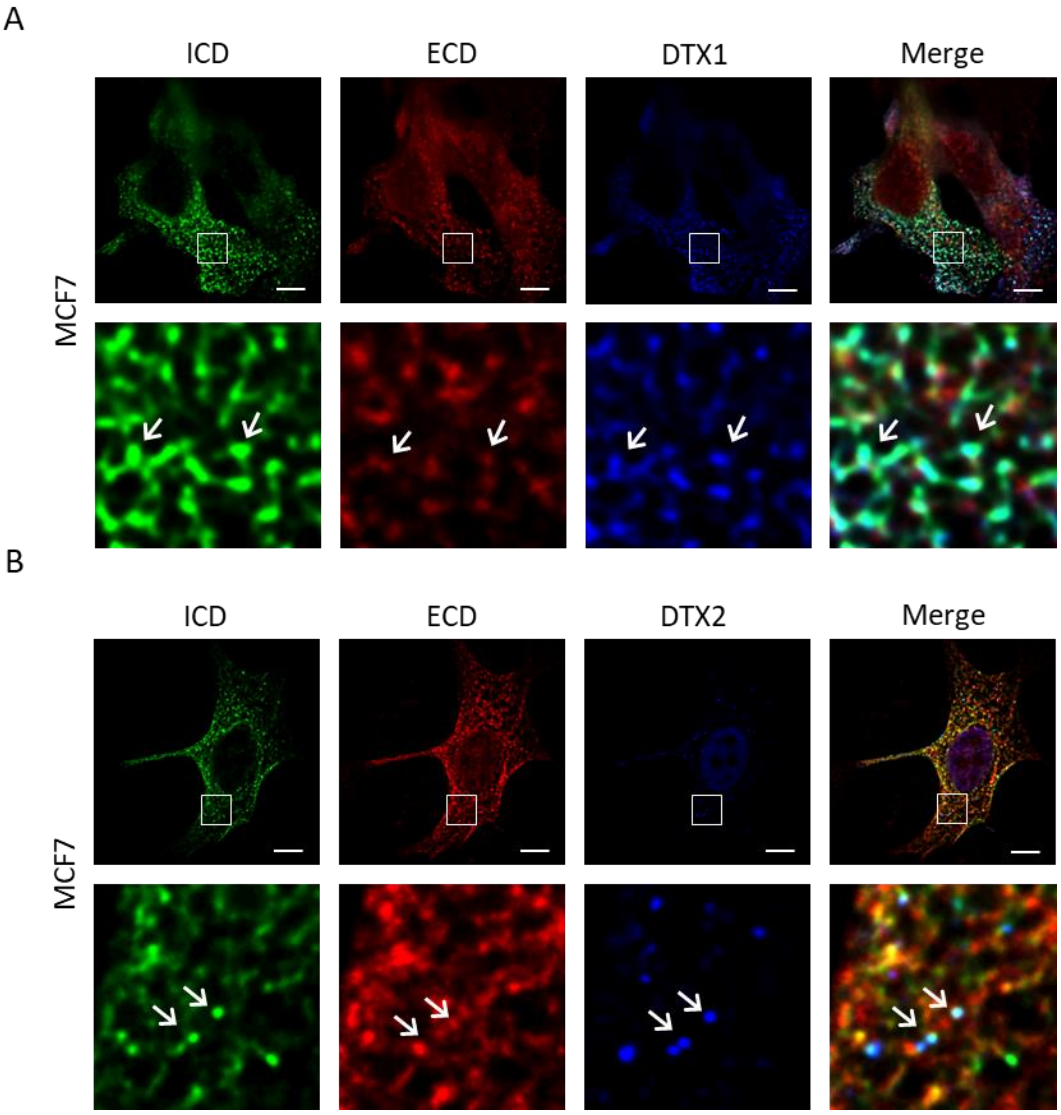
A
ICD
ECD
DTX1
Merge
MCF7
B
ICD
ECD
DTX2
Merge
MCF7

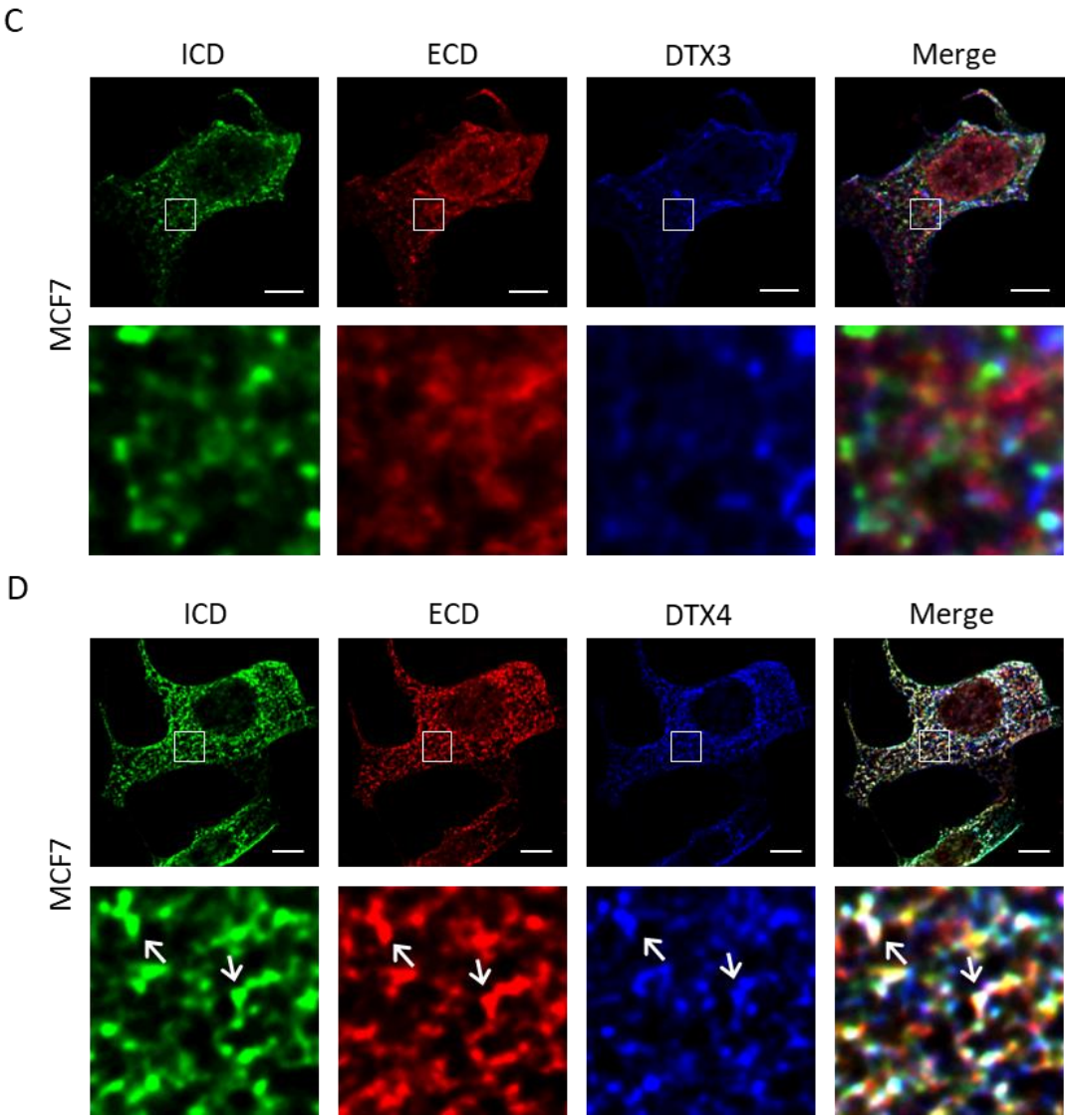

Figure 3-8: Full length Notch4 colocalises with DTX1 and DTX4 in breast cancer cells. Immunofluorescence images of MCF7 cells 24h after transiently transfecting with a Notch4 plasmid and a DTX1 (A), DTX2 (B), DTX3 (C), or DTX4 (D) plasmid. Images show one plane of Notch4 ICD (green), Notch4 ECD (red) and DTX1-4 (blue), and a merge of the three channels to demonstrate colocalisation. Areas of key colocalisation are indicated with arrows. Areas zoomed in to show detail in higher magnification, indicated by the white squares. Scale bars: 5µm.

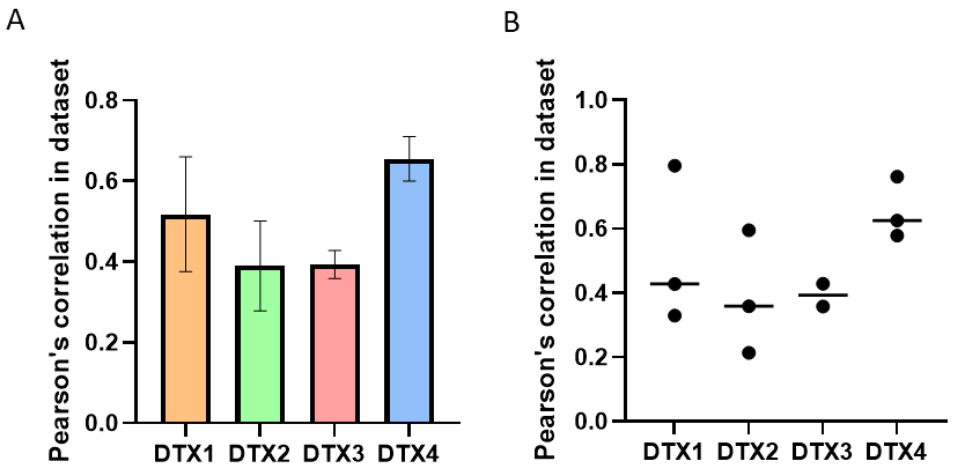

Figure 3-9: Quantification of colocalisation between full length Notch4 and DTX in MCF7 cells. Quantification was carried out using the Imaris "coloc" function on full 3D immunofluorescence images. A new channel was created using colocalising voxels between Notch4 ICD and Notch4 ECD and this was used as "full length Notch4" The colocalisation between this channel and the DTX channel was then quantified and Pearson's correlation plotted. A) Data are represented as mean ±SEM.

3.5 DTX1 and 4 knockdown reduces Notch4 ICD and ECD colocalisation

To further investigate the role of Deltex in Notch4 signalling, the Deltex genes were knocked down using siRNA. DTX1 and DTX4 were selected due to their colocalisation with full length Notch4 observed in immunofluorescence (Figures 3-8 and 3-9). The genes were knocked down separately as well as both simultaneously, using Silencer Select pre-designed siRNAs and lipofectamine RNAiMAX transfection reagent. RNA was isolated after 24 hours and levels of DTX1 and DTX4 gene expression were analysed by qRT-PCR to confirm knockdown. With both siDTX1 and siDTX1+4, levels of DTX1 gene expression were reduced at a rate of 4-fold compared to untransfected control (Figure 3-10A). In siDTX4 and siDTX1+4, the gene expression level of DTX4 was reduced by 5.5-fold and 4.1-fold, respectively (Figure 3-10B). The controls in this case were untransfected cells. All knockdowns were significant $p<0.0001$.

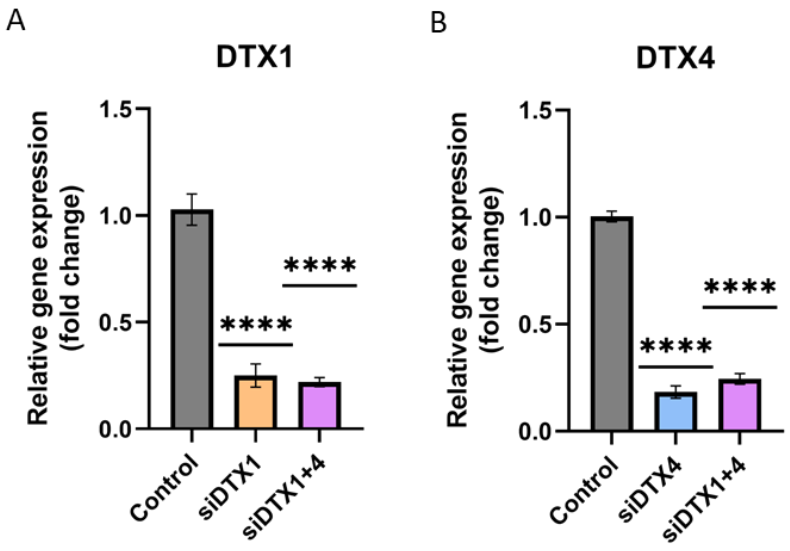

Figure 3-10: DTX1 and 4 genes were knocked down in MCF7 cells using siRNAs specific to each gene. RNA was isolated 24 hours after transfection and gene expression analysed by qRT-PCR. A) Knockdown of DTX1 was achieved at a rate of 4-fold when knocking down DTX1 alone and a rate of 4.6-fold when knocking down DTX1 and DTX4 together. B) Knockdown of DTX4 was achieved at a rate of 5.5-fold when knocking down DTX4 alone, and a rate of 4.1-fold when knocking down both DTX1 and 4. Shown as fold change compared to untransfected control. Data are represented as mean ±SEM. Statistical tests: Unpaired t-tests. ****p<0.0001. N=3.

The effect that knocking down DTX1, DTX4 and both DTX1+4 has on the location and full-length/ cleaved status of Notch4 in MCF7s was investigated using immunofluorescence. The same experiment and staining procedure was carried out as that shown in Figure 3-7, with the addition of the siRNA when transfecting Notch4 into the MCF7s. Knocking down DTX1 led to a dramatic change in phenotype and there was little to no colocalisation between the ICD and ECD of Notch4 (Figure 3-11). This was even more pronounced when knocking down DTX4 (Figure 3-12), as well as when both DTX1 and DTX4 were knocked down simultaneously (Figure 3-13).

The colocalisation of Notch4 ICD and ECD when knocking down DTX was analysed using the Imaris "coloc" function and is quantified in terms of Pearson's correlation (Figure 3-14A+B+C). When quantified including the whole image, the Pearson's correlation does not differ significantly between control, siDTX1, siDTX4 or siDTX1+4 (Figure 3-14A). However, when calculating the Pearson's correlation between Notch4 ICD and ECD within a defined Region of Interest (ROI) corresponding to the Notch4 ICD stained area, siDTX4 caused a significantly reduced level of colocalisation (Figure 3-14B) ($p<0.01$). This was also the case

when calculating the Pearson's correlation within the colocalised area, with siDTX4 leading to a significantly reduced colocalisation (Figure 3-14C) ($p<0.05$). Contrarily to the images, the calculated Pearson's correlation for Notch4 ICD and ECD when DTX1 or DTX1+4 were knocked down, was not reduced in any case compared to the control.

When staining for EEA1, CD63 and LAMP1, Notch4 ICD and ECD were not colocalised with any of the three markers, suggesting little to no full length Notch4 is present in early endosomes, late endosomes or lysosomes when DTX1 and 4 are knocked down (Figure 3-11+12+13). This is quantified in Figure 3-14D+E+F. Analysis in this case was carried out in Imaris by creating a "surface" to represent each endocytic compartment and the intensity of the full length Notch4 channel within that compartment was quantified and compared between control and knockdown of DTX1, DTX4 or DTX1+4 (Figure 3-14D+E+F). Amount of full length Notch4 in early endosomes was greatly reduced when DTX1, DTX4 and both DTX1+4 were knocked down (Figure 3-14D). The amount of full length Notch4 in lysosomes was also greatly reduced after DTX knockdown (Figure 3-14F). Knocking down DTX1 increased intensity of full length Notch4 in late endosomes, whilst knocking down DTX4 reduced it (Figure 3-14E). These did not reach significance due to the small sample size of some groups.

Together, these results suggest that knocking down DTX1 and DTX4 prevents Notch4 being internalised into the endocytic pathway as a full length protein in MCF7 cells. The quantification results mostly back this up, whilst suggesting that DTX1 may alter the Notch4 internalisation/ processing in some way.

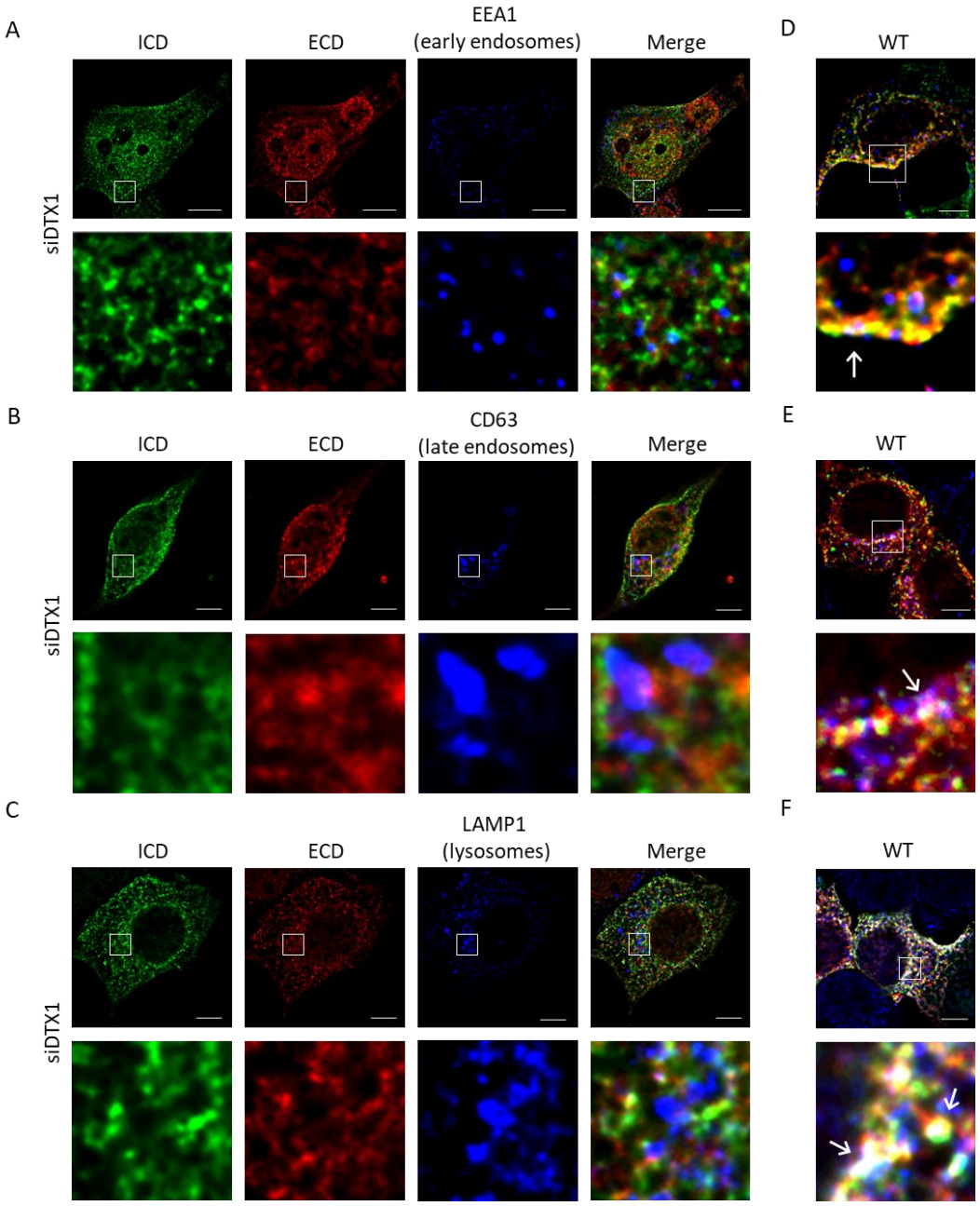

Figure 3-11: Immunofluorescence images of MCF7 cells 24h after transiently transfecting with a Notch4 plasmid and an siRNA targeting DTX1. Images show one plane of Notch4 ICD (green), Notch4 ECD (red) and EEA1- early endosomes (blue) (A), CD63- late endosomes (blue) (B), LAMP1- lysosomes (blue) (C) and a merge of the three channels to demonstrate colocalisation. Areas of key colocalisation are indicated with arrows. Areas zoomed in to show detail in higher magnification, indicated by the white squares. Scale bars: 5µm. D-F) Panels from Figure 3-7 for comparison.

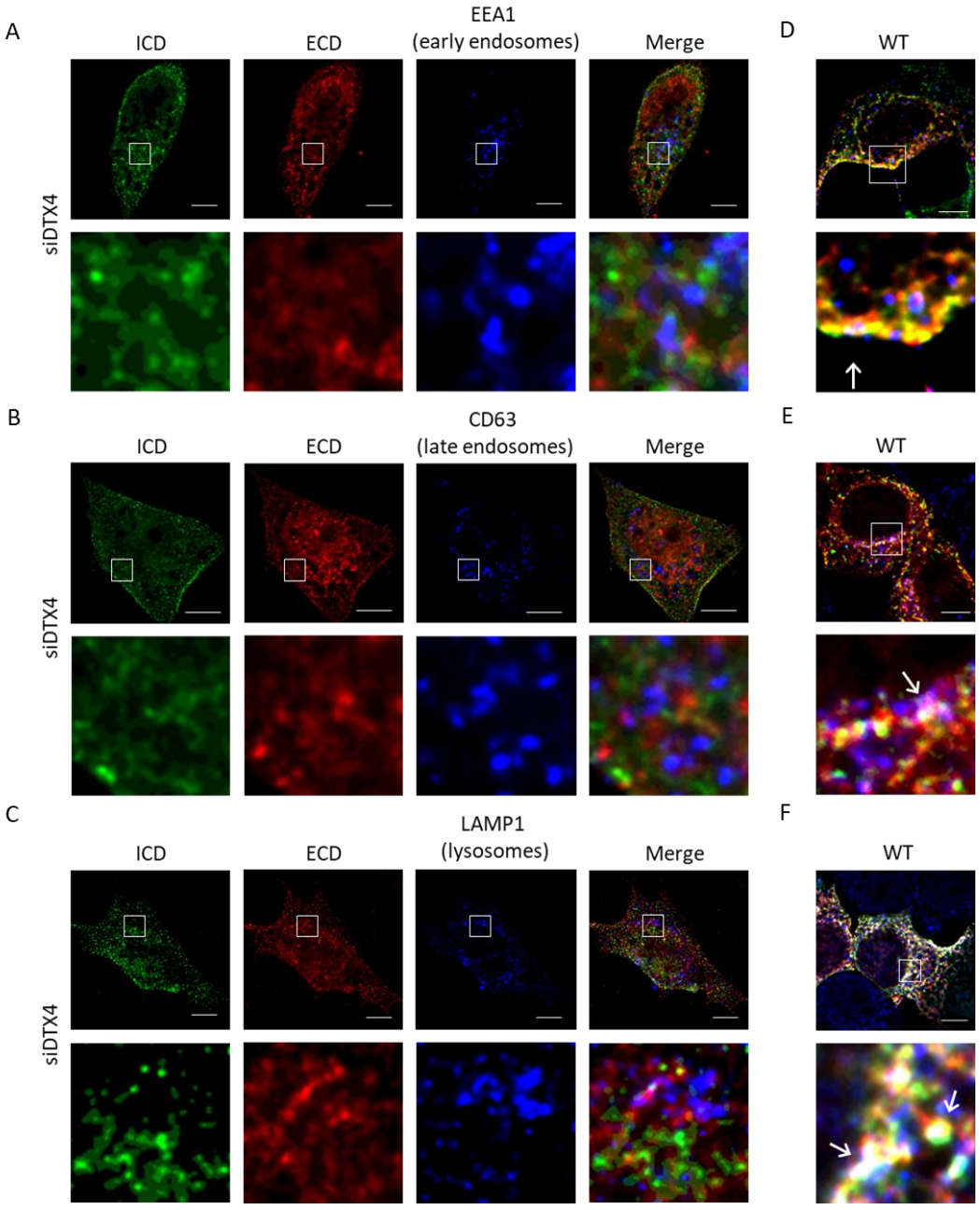

Figure 3-12: Immunofluorescence images of MCF7 cells 24h after transiently transfecting with a Notch4 plasmid and an siRNA targeting DTX4. Images show one plane of Notch4 ICD (green), Notch4 ECD (red) and EEA1- early endosomes (blue) (A), CD63- late endosomes (blue) (B), LAMP1- lysosomes (blue) (C) and a merge of the three channels to demonstrate colocalisation. Areas of key colocalisation are indicated with arrows. Areas zoomed in to show detail in higher magnification, indicated by the white squares. Scale bars: 5µm. D-F) Panels from Figure 3-7 for comparison.

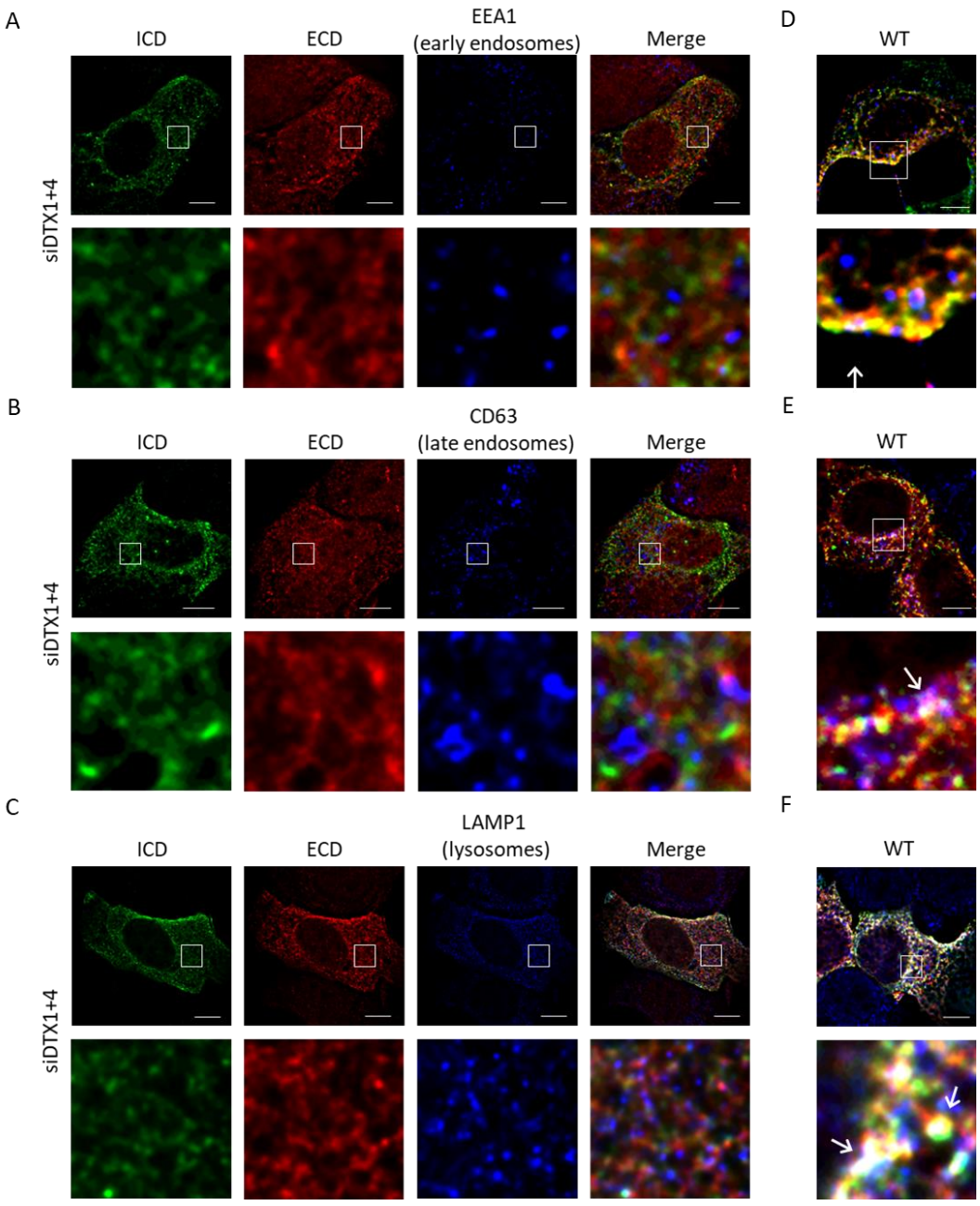

Figure 3-13: Immunofluorescence images of MCF7 cells 24h after transiently transfecting with a Notch4 plasmid and siRNAs targeting DTX1 and DTX4. Images show one plane of Notch4 ICD (green), Notch4 ECD (red) and EEA1- early endosomes (blue) (A), CD63- late endosomes (blue) (B), LAMP1- lysosomes (blue) (C) and a merge of the three channels to demonstrate colocalisation. Areas of key colocalisation are indicated with arrows. Areas zoomed in to show detail in higher magnification, indicated by the white squares. Scale bars: 5µm. D-F) Panels from Figure 3-7 for comparison.

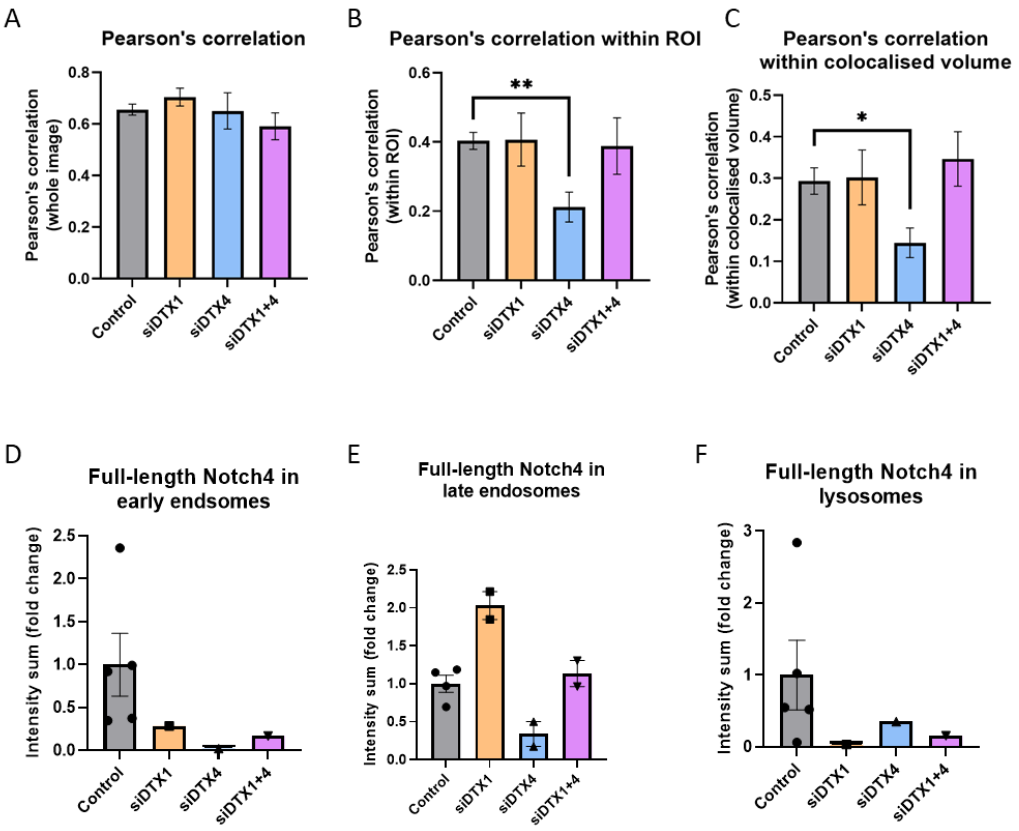

Figure 3-14: Quantification of colocalisation of Notch4 ICD and ECD and amount of full length Notch4 in endosomal compartments when knocking down DTX. A+B+C) Pearson's correlation of colocalisation between Notch4 ICD and ECD channels in the whole image (A), within a defined Region of Interest (ROI) (B) and within the colocalised volume (C). D+E+F) Data intensity sum of full-length Notch4 within "surfaces" created to represent endosomal compartments early endosomes (D), late endosomes (E) and lysosomes (F). The values for Notch4 when DTX1, DTX4 or both DTX1+4 are knocked down are compared to control images transfected with Notch4 alone. Data are represented as mean ±SEM. Statistical tests: Unpaired t tests. *$p < 0.05$. **$p < 0.01$. A+B+C) N=4. E) N=2. D+F) N=1.

3.6 Knocking down DTX affects the gene expression of Notch target genes Hes1, Hey1 and Hey2 and BCSC activity

Due to the dramatic change that knocking down DTX1 and DTX4 has on the colocalisation and location of Notch4, the effect of knocking down these genes on Notch target gene expression was investigated. DTX2 was also knocked down to investigate whether it is involved in Notch4 signalling. DTX3 was not investigated as it does not contain a Notch binding motif (L. Wang et al., 2021). The experiment was optimised and stable Notch4 expressing breast cancer cells were used (stable cell line explored fully in Chapter 4). DTX was knocked down using Silencer Select siRNAs and the RNA was isolated 72 hours later. Gene expression levels were analysed by qRT-PCR.

Firstly, with both siDTX1 and siDTX1+4, levels of DTX1 gene expression were reduced down to a level undetectable by qRT-PCR, achieving a consistent knockdown (Figure 3-15B). With siDTX4 and siDTX1+4, the gene expression level of DTX4 was reduced by 3.1-fold and 2.7-fold, respectively (Figure 3-15D). Knockdown of DTX2 was achieved at an average rate of 5.6-fold (Figure 3-15C). Knocking down DTX1 significantly increased the gene expression of Notch4 by 2.4-fold ($p<0.0001$) (Figure 3-15A). The gene expression of Hes1 and Hey1 was unchanged, but the gene expression of Hey2 was significantly reduced ($p<0.0001$) (Figure 3-15E+F+G). Knocking down DTX4 did not affect expression of Notch4 or Hey2. However, it increased expression of Hey1 ($p<0.05$) and decreased expression of Hes1 ($p<0.01$). Knocking down both DTX1 and DTX4 together increased the expression of Notch4 ($p<0.05$) and Hey2 ($p<0.001$) but did not affect Hes1 or Hey1. Knocking down DTX2 did not affect Notch4 gene expression but significantly increased expression of Hey1 and Hey2 ($p<0.05$ and $p<0.0001$), whilst decreasing Hes1 expression ($p<0.05$). These results suggest that DTX1, DTX2 and DTX4 have complex and contrasting roles on the expression of Notch target genes.

The effect that knocking down Deltex has on the mammosphere forming efficiency of breast cancer cells was also investigated. The relevant DTX genes were knocked down in MCF7 cells and after 24 hours cells were seeded out for mammospheres at 3000 cells/well in non-adherent conditions. After 5 days, the mammospheres formed in each case were counted and mammosphere forming efficiency (MFE) was calculated. Knocking down DTX4 and DTX1+4 decreased the mammosphere forming efficiency of MCF7 cells, with DTX4 knockdown having the greatest effect, reducing the MFE by 2.2-fold (Figure 3-15H). Knockdown of DTX1 and DTX2 did not affect the mammosphere forming efficiency. These

results suggest that DTX4 plays an important role in the stem cell activity of breast cancer cells.

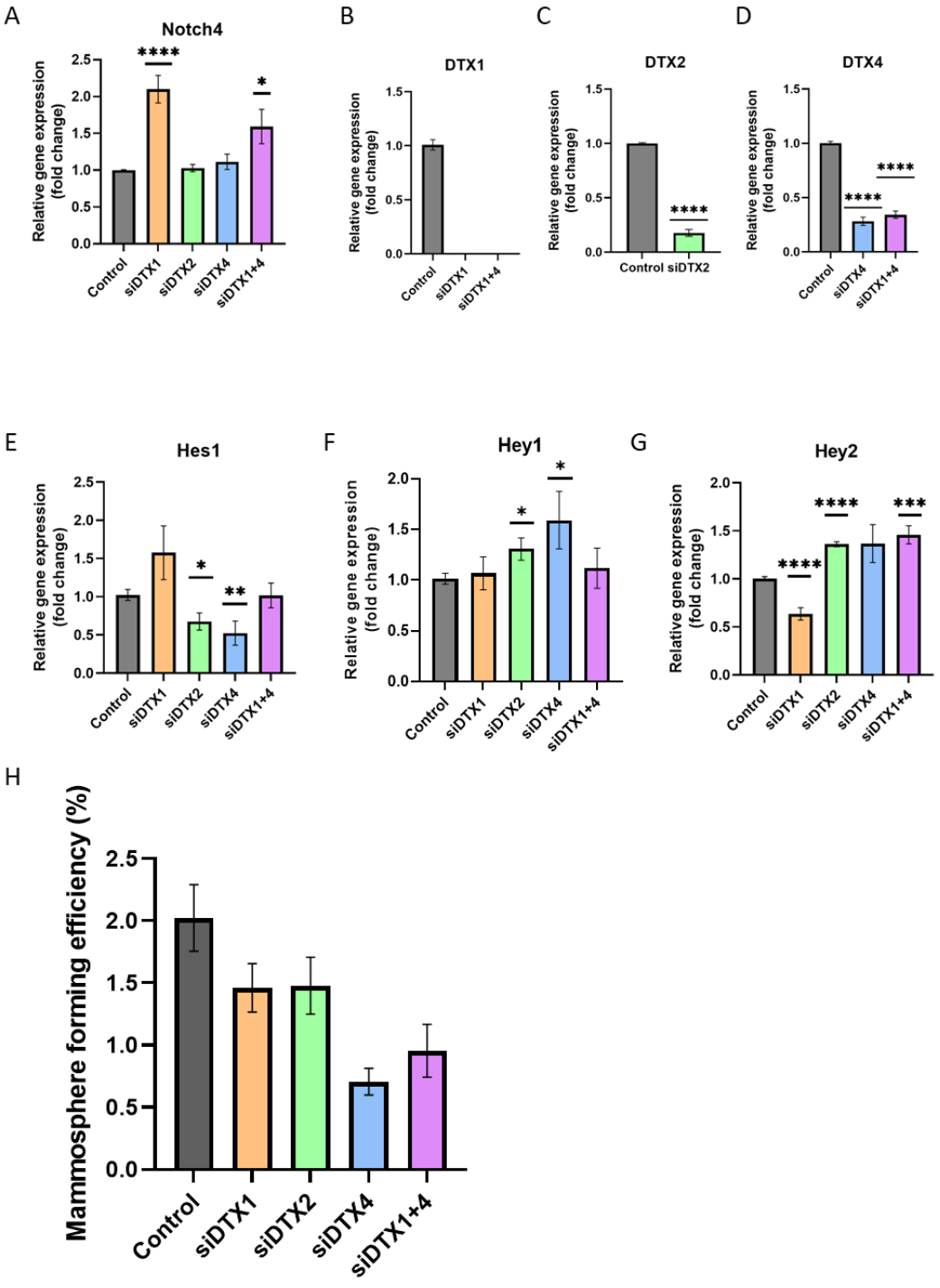

Figure 3-15: Knocking down DTX affects the gene expression of Notch4, Notch target genes Hes1, Hey1 and Hey2 and reduces mammosphere forming efficiency. Knockdown was carried out using Silencer Select siRNAs and lipofectamine RNAiMAX in Notch4 expressing cells. Control is a pre-made negative control #2 siRNA and data is shown as fold change to

this control. Relative gene expression of Notch4 (A), Hes1 (E), Hey1 (F) and Hey2 (G) when knocking down DTX1, DTX2, DTX4 and DTX1+4 together. B) Knockdown of DTX1 was achieved to a level where it was no longer detectable by qRT-PCR when knocking down DTX1 alone and when knocking down DTX1 and 4 together. C) Knockdown of DTX2 was achieved at a rate of 5.6-fold. D) Knockdown of DTX4 was achieved at a rate of 3.1-fold when knocking down DTX4 alone, and a rate of 2.7-fold when knocking down both DTX1 and 4. H) Mammosphere forming efficiency of Notch4 expressing cells when DTX1, 2, 4 and 1+4 together are knocked down. Data are represented as mean ±SEM. Statistical tests: Unpaired t tests. *p < 0.05. **p < 0.01. ***p<0.001. ****p<0.0001. N=3 (H: N=2).

3.7 Overexpressing DTX increases the gene expression of Notch4 and Notch target gene Hes1

To further explore the role of DTX in Notch4 signalling, each of the DTX genes in turn were overexpressed in Notch4 expressing breast cancer cells using GeneJuice® and Notch target genes were analysed. RNA was isolated 72 hours after transfection and gene expression was analysed by qRT-PCR. Significant overexpression was achieved with DTX1 (53,000-fold increase) (Figure 3-16A), DTX2 (34-fold increase) (Figure 3-16B) and DTX4 (78-fold increase) (Figure 3-16C). Overexpression of DTX1, 2 and 4 increased gene expression of Notch4 significantly ($p<0.01$, $p<0.05$ and $p<0.0001$, respectively) (Figure 3-16D). Overexpression of DTX1, 2 and 4 significantly increased gene expression of Hes1 ($p<0.0001$, $p<0.0001$ and $p<0.01$, respectively) (Figure 3-16E). However, overexpression did not affect Hey2 expression (Figure 3-16G), and only DTX1 overexpression increased expression of Hey1 ($p<0.05$) (Figure 3-16F).

Overexpressing DTX 1, 2 and 4 increases the gene expression of the other DTX genes (Figure 3-16H-J). Overexpressing DTX1 increased expression of DTX2 and DTX4 ($p<0.0001$ and $p<0.01$); overexpressing DTX2 increased expression of DTX1 ($p<0.05$); and overexpressing DTX4 increased expression of DTX1 and DTX2 ($p<0.001$ and $p<0.0001$).

Taken together, these results suggest that DTX1, 2 and 4 work together in a positive feedback mechanism to increase expression of each other. They also act directly on the expression of Notch4 to positively regulate it and this feeds back to increase Hes1 expression.

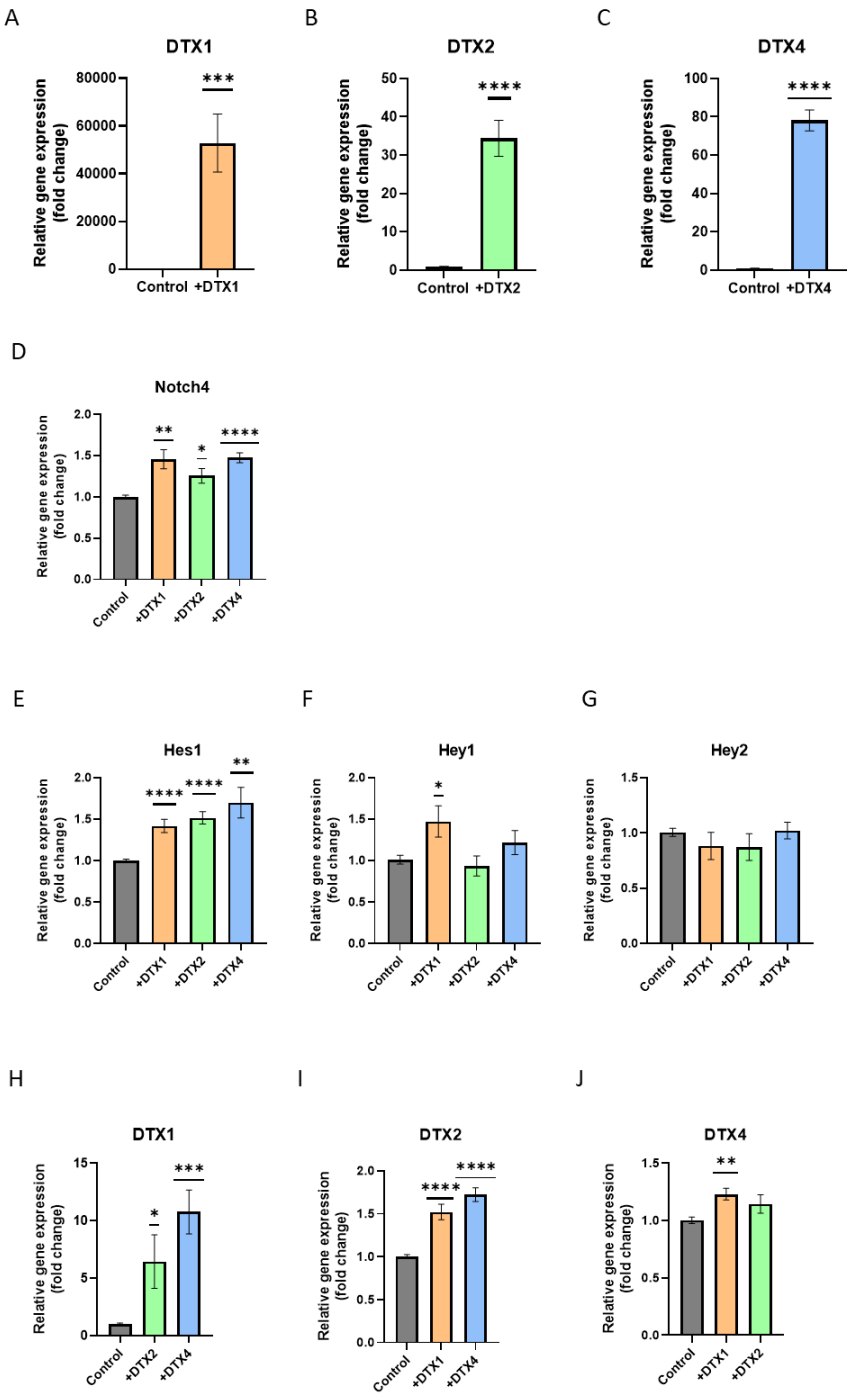

Figure 3-16: Overexpression of DTX increases the gene expression of Notch4, Notch target gene Hes1 and increases the expression of the other DTX genes. Transfection was carried out in Notch4 expressing cells. RNA was taken 24 hours after transfection and qRT-PCR was carried out to assess gene expression. Control is untransfected cells and data is shown as fold change to this control. Overexpression of DTX1 (A), DTX2 (B) and DTX4 (C) was achieved at a rate of 53,000-fold, 34-fold and 78-fold, respectively. A-C) Relative gene expression of Notch4 (D), Hes1 (E), Hey1 (F) and Hey2 (G) after transfection with DTX. (H-J) Gene expression changes of other DTX genes when each is overexpressed. Data are represented as mean ±SEM. Statistical tests: Unpaired t tests. *p < 0.05. **p < 0.01. ***p<0.001. ****p<0.0001. N=3.

3.8 Knocking down components essential in the endocytic pathway affects expression of Notch target genes Hes1, Hey1 and Hey2.

In *Drosophila*, Notch ligand-independent/ Deltex-dependent signalling also involves other components including the HOPS complex and Rab7a, among others reviewed in Chapter 1 (Wilkin et al., 2008). These particular components are involved because their function is to regulate endocytic trafficking, and so are essential in the trafficking of the Notch receptor within the cell. Deep orange and carnation in *Drosophila* (VPS18 and VPS33a in humans) have been found to be required for lysosomal activation of Notch (Wilkin et al., 2008). Notch has also been found to be colocalised extensively with Rab7a on vesicles in *Drosophila*, indicating it has an important role (Shimizu et al., 2014).

To investigate what parts of the endocytic pathway might be involved in Notch4 signalling in breast cancer, Rab7a and the HOPS components VPS18 and VPS33a were knocked down using Silencer Select siRNAs. This took place in Notch4 expressing breast cancer cells, as above. RNA was isolated 72 hours after knockdown and qRT-PCR was used to analyse gene expression. Significant knockdown was achieved of Rab7a (3.5-fold decrease), VPS18 (3.2-fold decrease) and VPS33a (7.5-fold decrease) (Figure 3-17A-C). Knocking down Rab7a increased gene expression of Notch4 more than 2-fold ($p<0.0001$), increased Hey1 expression ($p<0.05$) and decreased Hey2 expression ($p<0.0001$) (Figure 3-17D+F+G). Knocking down VPS18 increased Notch4 expression ($p<0.05$) and increased Hes1 expression ($P<0.05$). Knocking down VPS33a did not affect Notch4 expression, but increased expression of Hey1 ($p<0.01$). In summary, knocking down Rab7a increases Notch4 gene expression and decreases Hey2 gene expression, suggesting it acts on Notch4 in a similar way to DTX1. VPS18 may act on Notch4 in a different way as its knockdown increases Notch4 gene expression but increases expression of a different target gene, Hes1.

Mammosphere analysis took place after knockdown of Rab7a, VPS18 and VPS33a. Cells were isolated 24 hours after knockdown and plated out to form mammospheres, which were counted after 5 days. Knockdown of Rab7a and VPS18 did not affect Mammosphere Forming Efficiency (MFE). Knocking down VPS33a slightly decreased MFE, although this did not reach significance (Figure 3-17H).

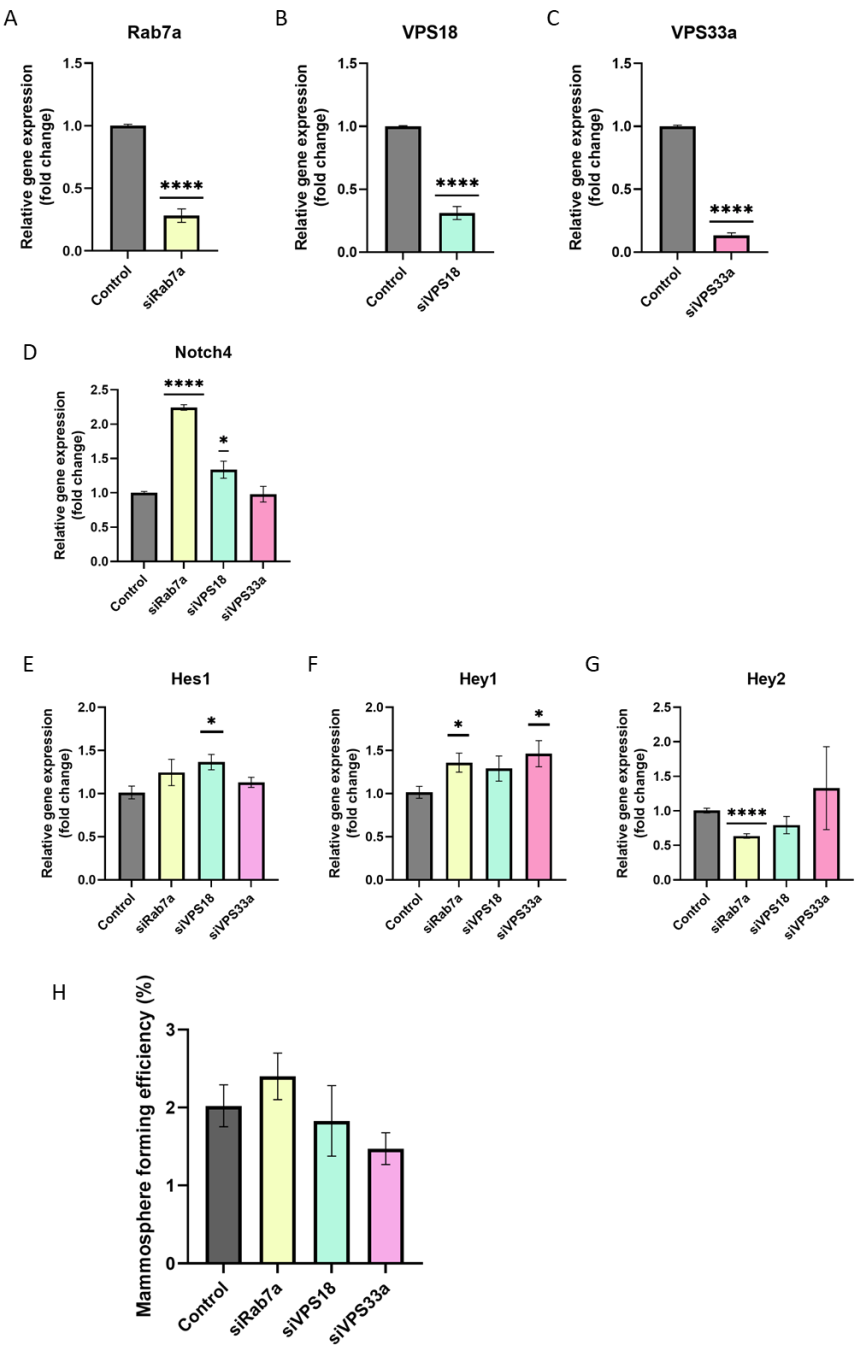

Figure 3-17: Knocking down Rab7a and components of the HOPS complex affects the gene expression of Notch4 and Notch target genes Hes1, Hey1 and Hey2 and mammosphere forming efficiency. Knockdown was carried out using Silencer Select siRNAs and lipofectamine RNAiMAX in Notch4 expressing cells. Control is a pre-made negative control #2 siRNA and data is shown as fold change to this control. (A-C) Knockdown of Rab7a (A), VPS18 (B), VPS33a (C) was achieved at a rate of 3.5-fold, 3.2-fold and 7.5-fold, respectively. Relative gene expression of Notch4 (A), Hes1 (B), Hey1 (C) and Hey2 (D) when knocking down Rab7a, VPS18 and VPS33a. E) Mammosphere forming efficiency of Notch4 expressing cells when Rab7a, VPS18 and VSP33a are knocked down. Data are represented as mean ±SEM. Statistical tests: Unpaired t tests. *$p < 0.05$. **$p < 0.01$. ****$p<0.0001$. N=3.

3.9 High Notch4 and DTX4 expression correlates with reduced distant-metastasis-free survival, particularly in endocrine therapy treated breast cancer

Previous studies show that high Notch4 expression is linked with breast cancer progression, resistance, recurrence, and metastasis (Bui et al., 2017; D'Angelo et al., 2015; Harrison et al., 2010; Simões, Alferez, et al., 2015; Yun et al., 2013). Previous research and results from this chapter led to us investigating whether Notch4, DTX1 and DTX4 expression correlates with breast cancer progression and metastasis clinically. KMPlotter software (Győrffy, 2021) was used to compare mRNA expression levels of genes to survival of 7830 breast cancer patients. Patients can be sorted for various characteristics including subtype of the tumour and treatment type. They are split in terms of gene expression of a certain gene at the median of expression and the survival for each group is plotted. This is the most unbiased approach to splitting the data, demonstrating that any correlation observed can be relied upon. All graphs shown here specifically explore distant metastasis free survival (DMFS).

Notch4 was investigated first. Notch4 was plotted against DMFS in ER+ breast cancer patients, which showed that a high expression of Notch4 correlates with reduced DMFS in ER+ breast cancers (p=0.067) (Figure 3-18A). This was also the case for Grade 3 breast cancers (p=0.054) (Figure 3-18B), for those that were both ER+ and classed as Grade 3 (p=0.054) (Figure 3-18C) and for breast cancers that are both Grade 3 and have had previous treatment with endocrine therapy (p=0.061) (Figure 3-18D). However, these correlations did not reach significance. A significant negative correlation was found between Notch4 expression and DMFS when analysing breast cancers that were Grade 3 and had been treated previously with Tamoxifen (HR=3, p=0.003) (Figure 3-18E).

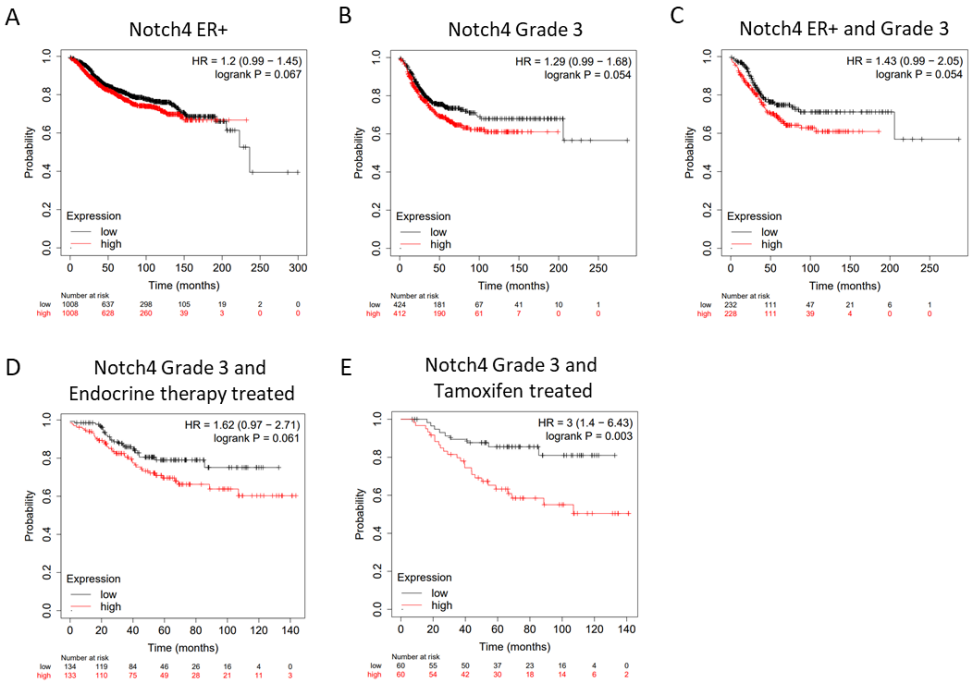

Figure 3-18: High Notch4 expression correlates with reduced distant metastasis free survival (DMFS). Notch4 expression plotted against probability of DMFS using KMPlotter software in ER+ breast cancers (A), Grade 3 breast cancers (B), ER+ and Grade 3 breast cancers (C), Grade 3 and previous endocrine therapy treated breast cancers (D), and Grade 3 and Tamoxifen treated breast cancers (E).

Next, DTX1 was investigated. DTX1 expression plotted against DMFS for ER+ breast cancers demonstrates that low DTX1 expression correlates with reduced DMFS (p=0.0054) (Figure 3-19A). This suggests that DTX1 may have a protective effect in ER+ breast cancers. There is also a correlation between low DTX1 expression and reduced DMFS in ER+ breast cancers that have undergone endocrine therapy, although this did not reach significance (p=0.11) (Figure 3-19B).

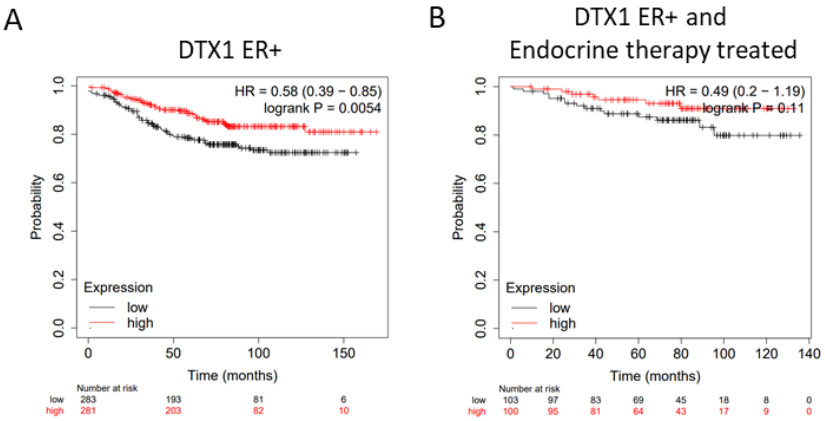

Figure 3-19: Low DTX1 expression correlates with reduced distant metastasis free survival (DMFS). DTX1 expression plotted against probability of DMFS using KMPlotter software in ER+ breast cancers (A) and ER+ and previous endocrine therapy treated breast cancers (B).

DTX4 expression was also explored. In all breast cancers, high DTX4 expression correlates significantly with reduced DMFS (p=0.048) (Figure 3-20A). However, in ER+ breast cancers, this correlation did not reach significance (p=0.29) (Figure 3-20B). In Grade 3 and both endocrine therapy and tamoxifen treated breast cancers, there is a correlation between DTX4 expression and reduced DMFS up to the point of 60 months in endocrine treated and 80 months in Tamoxifen treated, where the two groups converge. Due to this, neither correlation reaches significance, but suggests DTX4 may play a part in the early metastasising breast cancers (Figure 3-20C+D).

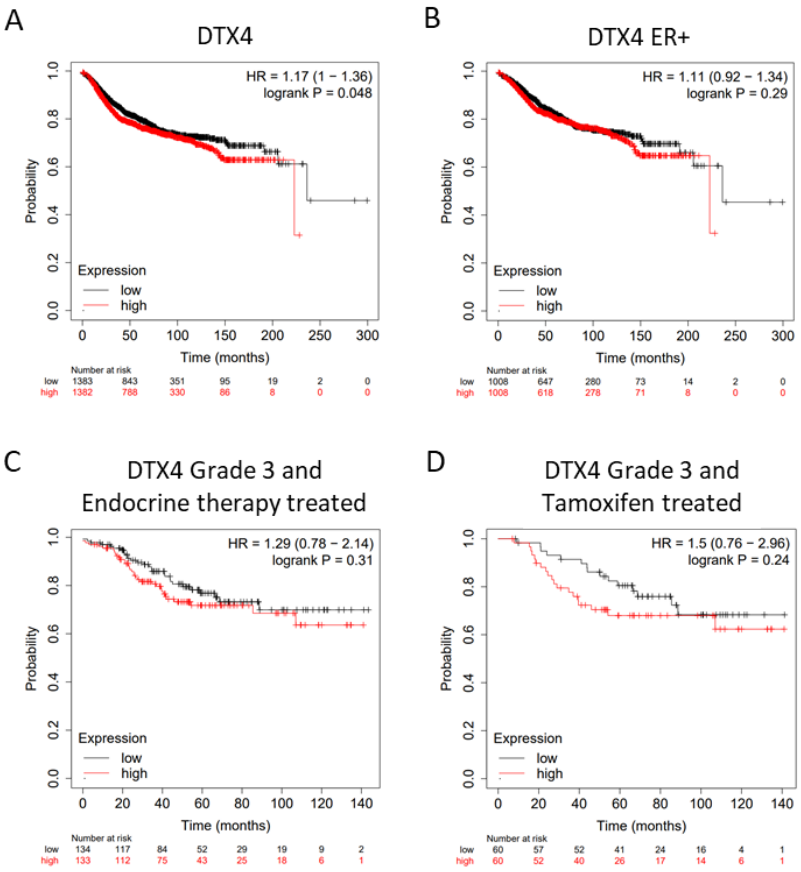

Figure 3-20: High DTX4 expression correlates with reduced distant metastasis free survival (DMFS). DTX4 expression plotted against probability of DMFS using KMPlotter software in all breast cancers (A), ER+ breast cancers (B), Grade 3 and previous endocrine therapy treated breast cancers (C), and Grade 3 and Tamoxifen treated breast cancers (D).

3.10 Discussion

The aim of this chapter has been to investigate Notch4 signalling in breast cancer cells. It has been established that in ER+ MCF7 cells, Notch4 signals via an endocytic pathway mechanism. It was also demonstrated that Deltex is essential for Notch4 signalling. We hypothesised that this may be due to a tyrosine residue in Notch4, which is divergent from the histidine in human Notch1/2/3 and *Drosophila* Notch. This change is equivalent to a *Drosophila* Notch mutant AxE2 which is dependent on Deltex and signals in a ligand independent manner. These are novel findings for the Notch field and shows a possible mechanism for how Notch4 regulates BCSCs and endocrine resistance in ER+ breast cancer.

Firstly, we demonstrated that transient transfection of Notch4 plasmid leads to a consistent level of cell surface expression of the Notch4 receptor at 24 hours after transfection. Despite successful optimisation, the final transfection efficiency was never higher than 10%. In the future, to increase the percentage of these cells that express Notch4, they could be sorted with FACS to isolate the Notch4 expressing cells, which could then be analysed. This transient transfection also upregulated Notch target genes Hes1, Hey1 and Hey2 (displayed in the summary gene expression figure below, Figure 3-21A). To date, the signalling capacity of Notch4 has not been demonstrated in breast cancer cells in this way, highlighting this novel finding. These findings made use of a novel Notch4 conjugated antibody, gifted by MedImmune, which we have demonstrated can be reliably used to detect the surface expressed Notch4 receptor in flow cytometry. The highest surface expression of the transiently transfected Notch4 was found to occur at 24 hours, whilst the target gene expression increase was highest 72 hours after transfection. This was not measured after 72 hours, leaving the possibility that greater induction of gene expression could have been detected after this. This would likely depend on the stability of the protein as well as the speed of its processing. The induction of gene expression by Notch4 was also shown to be dependent on gamma-secretase. However, these data are from only one biological repeat, requiring it to be further validated in the future.

We also demonstrated that the Notch4 antibody can be reliably used to detect the extracellular domain (ECD) of the Notch4 receptor in immunofluorescence through its binding to the NRR domain of Notch4. Use of this antibody alongside a Notch4 ICD antibody showed that Notch4 is present in MCF7 cells as a full length protein, confirming internalisation of the receptor. Full length Notch4 can be found in early endosomes, late endosomes, and lysosomes in MCF7 cells, establishing that it is internalised into the endocytic pathway and trafficked through it. These findings in mammalian cells corroborate

the *Drosophila* ligand independent Notch activation pathway. This previous work showed that *Drosophila* Notch can signal via a ligand independent signalling route, and in particular that the AxE2 mutant is partly dependent on this signalling pathway (Shimizu et al., 2014). The fact that Notch4 signals via an endocytic pathway, likely to be similar to this *Drosophila* one, is a novel finding for Notch4 in mammalian cells and breast cancer cells. However, we do not know how much Notch4 signals via this route, or even whether this pathway is required for Notch4 signalling. This could be explored by fully blocking this endocytic pathway and observing Notch4 signalling.

These data support the hypothesis that full length Notch4 is trafficking through the endocytic pathway for ICD release at the lysosomes, but there are some aspects that should be explored further in the future. There is little to no LAMP1 colocalisation with ECD alone or ICD alone, suggesting no presence of either ECD or ICD portions of Notch4 in the lysosome. However, this could be the case if the ECD is degraded simultaneously to ICD release. There are various other endocytic compartment markers that could be stained and explored in a similar way to investigate Notch4 colocalisation and dissect the exact pathway of Notch4 trafficking in breast cancer cells. This would help to identify if Notch4 is present in a specific subset or part of the compartments. These include Rab5 (a marker for early endosomes) Rab7 (a marker for late endosomes), and GPI (a marker for membrane microdomains) which have been explored in the lysosomal Notch activation pathway in *Drosophila* (Shimizu et al., 2014).

When the role of DTX in Notch4 endocytic signalling was explored by immunofluorescence, DTX1 and DTX4 were found to be likely candidates for involvement as when they were overexpressed with Notch4, they consistently colocalised. When knocking down these genes, the colocalisation of Notch4 ICD and ECD was dramatically reduced, with little to no full length Notch4 observed. The punctate dots of full length Notch4 that are observed when DTX is present are abrogated when DTX is knocked down, leaving a more dispersed distribution of Notch4 ICD and Notch4 ECD. It is likely that the knockdown of DTX1 and 4 prevents Notch4 from localising to the endocytic compartments, leaving some in the cytoplasm of the cell. Due to this “blurry” appearance, the whole image Pearson’s correlation is more difficult to compare, as there is more background colocalisation from the cytoplasm located Notch4. However, the ROI and colocalised volume Pearson’s correlation was decreased with knockdown of DTX4 compared to control, showing consistency with the images. This was not reflected with the knockdown of DTX1, perhaps highlighting the different roles of the two DTX proteins. Quantification of full length Notch4 within endocytic compartments agreed

with observation of images, although the knockdown of DTX1 led to an increase in intensity of full length Notch4 in late endosomes when quantifying, whereas the images suggested a decrease. This could be due to a role of DTX1 in downstream compartment sorting, although further replicates would be needed in order to be confident of a link.

Knocking down DTX1, 2 and 4 had varying effects on Notch target gene expression. These effects have been summarised in Figure 3-21A below. Results indicate that DTX1 acts conversely to DTX2 and DTX4, which have similar effects. DTX1 upregulates Hey2 and DTX2 and DTX4 downregulate Hey2 and Hey1 and upregulate Hes1. Results also indicate that DTX1 downregulates Notch4 gene expression (Figure 3-22A). These actions may be happening directly via these genes, indirectly via Notch4 or independently through another unspecified mechanism or signalling pathway. To investigate this, the Notch4 and DTX promoter regions could be studied to identify any binding sites for each other.

The signalling results are contrasted with the immunofluorescence results as the actions of DTX1 and DTX4 knockdown on reducing the colocalisation of Notch4 ICD and ECD are very similar, whereas the signalling gene expression effects are very different.

The complexity of the effects of DTX on Notch target genes are further demonstrated when investigating the overexpression of the DTX proteins. These gene expression results have also been summarised in Figure 3-21B below. Overexpression of DTX1, DTX2 and DTX4 all upregulate Notch4 and Hes1 gene expression (Figure 3-22B). In most cases these results support the data from knockdown experiments, although knockdown of DTX1 suggests it plays a negative role on Notch4 gene expression and overexpression suggests it has a positive effect. Again, there is the possibility that different signalling pathways are playing a role, including potential interaction with the other Notch receptors 1, 2 and 3. The interaction of each DTX with the other Notch receptors has not been explored and would be an interesting future perspective on the signalling pathway. Each DTX also shows signs that it controls and promotes the other DTX proteins, which may occur via the Notch signalling pathway or via a separate pathway and mechanism.

One way to explain the contrasting results could be that the two different situations, with and without DTX, represent two separate signalling mechanisms of Notch4, with different distributions of Notch4 observed by immunofluorescence as well as different downstream consequences on which target genes are activated. The DTX proteins may also play more than one role in these pathways, explaining the varying effects when knocked down and overexpressed. One role of both DTX1 and 4 may be to induce internalisation of the full

length Notch4 receptor. Their roles may then diverge further on in the trafficking pathway, explaining their different effects on gene expression.

Something to take into consideration is that the overexpression and knockdown of DTX alters their gene expression but not proportionally. The large overexpression could force the DTX to act in an abnormal role or promote one particular role of it (if it has multiple roles in the normal situation). In *Drosophila*, Deltex is involved in a very fine balance with other components of the Notch pathway including Su(dx), pushing it towards a negative regulatory role if this balance is changed (Shimizu et al., 2014). This could be happening in this situation with the abnormal expression levels. Other components including Su(dx), AP-3 or Numb could be investigated in the future in order to further explore this.

We have shown that DTX4 has a role in BCSCs as its knockdown reduced mammosphere forming efficiency of Notch4 cells. In the future this role could be confirmed by investigating how the overexpression of DTX4 affects mammosphere formation. Other methods of BCSC activity analysis could also be explored, such as the Aldefluor assay.

These results agree with current published data in *Drosophila* that show Deltex is required for Notch signalling (Hori et al., 2011; Shimizu et al., 2014; Wilkin et al., 2008). In mammalian cells, some links to DTX being involved in Notch trafficking have been identified. DTX1 has been connected to Notch1 endosomal recycling, blocking ligand dependent signalling (L. Zheng & Conner, 2018). DTX4 has been shown to promote ligand independent signalling of Notch1 by inducing its endocytosis (Chastagner et al., 2017). Our data agree with these results showing that DTX has a key role to play in Notch4 signalling and particularly in the endocytosis driven, ligand independent activation pathways. To date, no studies have been published exploring the involvement of DTX in Notch4 signalling in breast cancer cells, highlighting the novelty of these results.

When knocking down other components of the endocytic pathway, Rab7a was found to have a very similar effect on gene expression as DTX1. Results show that it acts to downregulate Notch4 and upregulate Hey2 gene expression. The HOPS complex components VPS18 and VPS33a (Deep Orange and Carnation in *Drosophila*) had less distinct roles on gene expression, neither confirming nor refuting previous studies that show that they are required for lysosomal Notch activation in *Drosophila* (Wilkin et al., 2008). These components have key roles in the regulation of all endocytic trafficking in the cell and are not directly related to Notch, meaning that results, although indicative of some role in the Notch4 signalling pathway, should be taken cautiously.

Applied clinically, high Notch4 gene expression was found to correlate with metastasis in ER+ and grade 3 breast cancers. This correlation was increased in endocrine therapy treated breast cancers. DTX4 also had a similar correlation, although effects were less pronounced. DTX1 had the inverse correlation, being correlated with a reduced risk of metastasis in ER+ and endocrine therapy treated breast cancers. These results from breast cancer patient samples support the hypothesis that DTX1 and DTX4 are acting conversely to each other, suggesting that their opposing effects on Notch target gene expression and signalling may translate to risk of metastasis in ER+ endocrine therapy treated breast cancer patients. These results also suggest that DTX could be a promising target clinically. Its targeting could reduce BCSCs, as its knockdown reduced BCSC activity and metastasis, as its expression is negatively correlated with DMFS.

In conclusion, we have found that in ER+ human breast cancer cells Notch4 can signal via an endocytic pathway route by being internalised into the cell and trafficking through the endocytic pathway. DTX1 and DTX4 are also required for this pathway and are involved in the full length receptor internalisation. DTX1 and DTX4 have opposing effects on Notch target gene expression, indicating that they play multiple roles in Notch4 signalling and these roles depend on Notch4, DTX gene expression level and the cellular context. Now that results have confirmed that Notch4 can signal via this mechanism in breast cancer cells, and DTX4 is required for BCSC activity, the role of this Notch4 signalling pathway will be investigated in BCSCs and endocrine resistance, explored in the next chapter.

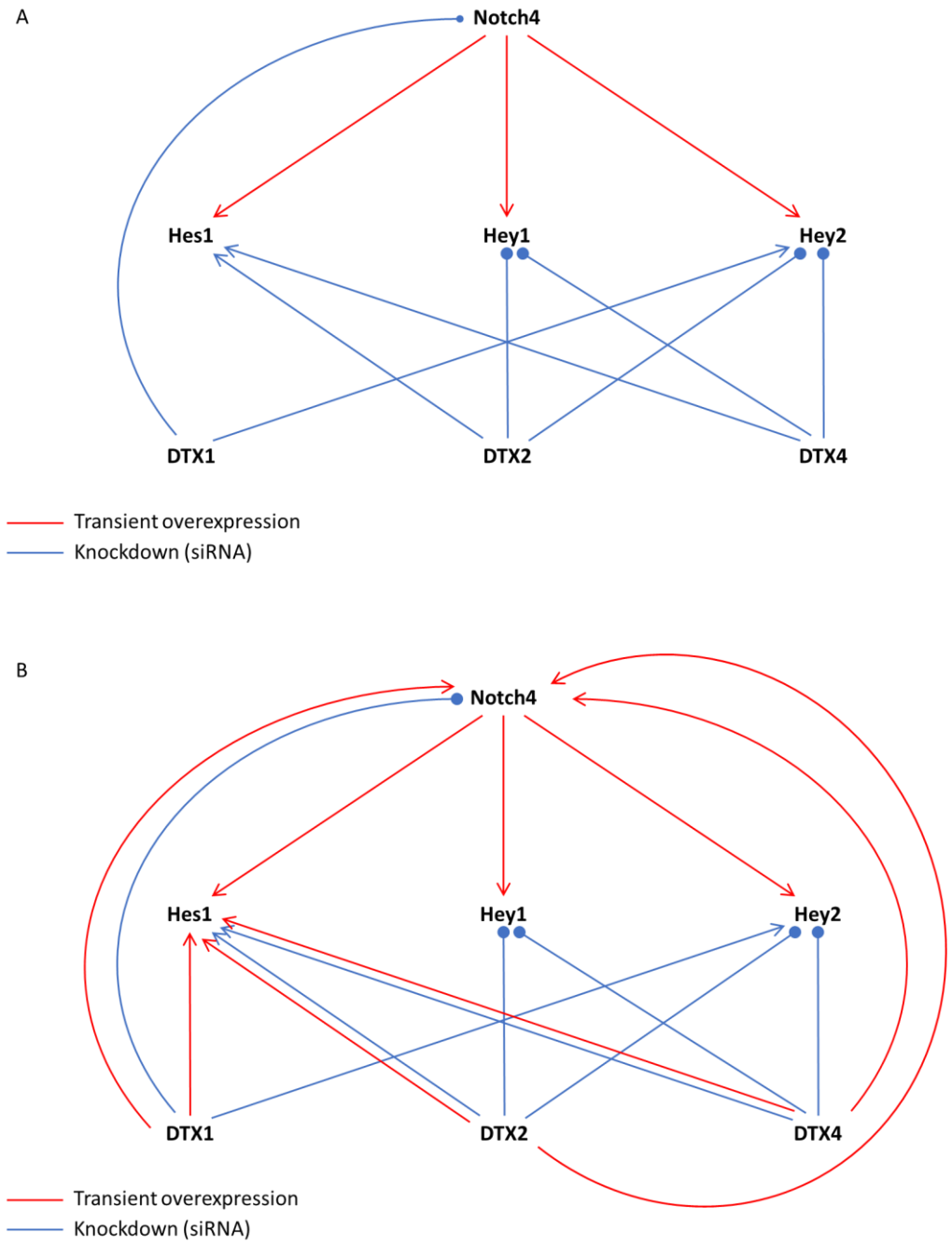

Figure 3-21: Summary of signalling results from Notch4 and DTX transient overexpression and DTX knockdown experiments to visualise a potential signalling pathway. Schematic includes significant results from gene expression experiments in Chapter 3. A) Results from Notch4 transient overexpression and DTX knockdown. B) Schematic in A with results from DTX transient overexpression added.

4 How BCSC activity / resistance to endocrine therapy is reliant on endocytic Notch4 signalling

4.1 Introduction

This chapter will investigate Notch4 signalling further and will focus specifically on how its endocytic pathway signalling is linked to endocrine resistance and Breast Cancer Stem Cells (BCSCs) using lentivirus created cell lines, BCSC activity analysis, RNAseq analysis and specific inhibitors.

Notch4 has been knocked out in breast cancer cell lines previously. For example, shRNA and siRNA have been used in the ER+ T47D cell line to transiently knockdown Notch4 expression (Rizzo et al., 2008; Yun et al., 2013). Harrison et al have used Notch4 siRNA for knockdown in MCF7 cells, as well as a stable MCF7 cell line with a doxycycline-inducible, shRNA Notch4 knockdown (Harrison et al., 2010). In our group, a Notch4 knockout MCF7 breast cancer cell line was previously created with CRISPR. It has very low expression of the Notch4 protein and has been used in previous research to show that Notch4 is vital for breast cancer stem cell activity, made more significant after endocrine treatment (Simões, O'Brien, et al., 2015). Although this cell line has its limitations (discussed further in section 4.2), it can be used as a reliable stable ER+ "knockdown" of Notch4.

Previously, Notch4 intracellular domain (ICD) has been transiently overexpressed using plasmid transfection in various breast cancer cell lines, including MCF7s (Harrison et al., 2010; Simões, O'Brien, et al., 2015). Stable cell line overexpression of the full length Notch4 receptor has not previously been investigated in any breast cancer cell line although Zhou et al used stable overexpression of Notch4 ICD (N4ICD) in triple negative SUM149 and MDA-MB-231 cells as well as in ER+ MCF7s using a lentivirus overexpression method (Zhou et al., 2020).

In the clinic, endocrine therapies are regularly used to treat estrogen receptor positive (ER+) breast cancers. One of the most common of these is tamoxifen which acts as an antagonist to the ER, blocking its downstream effects. Another endocrine therapy used in the clinic is fulvestrant. Fulvestrant acts to directly downregulate the ER, targeting it for degradation (A. Howell et al., 2004). Both drugs act to reduce ER signalling, acting cytostatically to prevent growth of cells and therefore are effective on ER+ breast cancers.

In the canonical Notch signalling pathway, the binding of a ligand creates a conformational change in the Notch receptor, allowing the matrix metalloprotease (MMP) ADAM10/17 to

carry out the cleavage “S2”. This releases the ligand-ECD portion of the receptor outside of the cell and leaves the membrane-bound Notch extracellular truncation (NEXT). Next, gamma-secretase will carry out cleavage “S3”, releasing NICD into the cytoplasm (Kopan & Ilagan, 2009). However, in the ligand independent activation pathway in *Drosophila*, ADAM10 is not required for “S2” cleavage, but gamma-secretase is required for “S3” cleavage (Shimizu et al., 2014). From previous studies in *Drosophila*, it is thought that the fusion of endosomes and lysosomes is required for ICD release at the lysosomal limiting membrane. These requirements in the ligand independent signalling pathway are unknown for human cells.

In this chapter, the investigation will be carried out involving the production and characterisation, as well as functional analysis of a stable Notch4 overexpressing ER+ breast cancer cell line, produced by a lentivirus method. BCSC activity assays including mammosphere assay, Aldefluor assay and limiting dilution assay will analyse this cell line functionally. These cell lines will also be analysed preliminarily by RNAseq, to allow a overall look at gene expression changes. Secondly, we explore the use of specific inhibitors, in order to gain insight on the inner workings and connections between Notch4 endocytic signalling, endocrine resistance and BCSCs.

4.2 N4KO cells have reduced breast cancer stem cell activity, increased Hes1 and Hey1 and decreased Hey2 gene expression

A Notch4 knockout (N4KO) cell line in MCF7s was created previously in the lab (Simões, O’Brien, et al., 2015). This cell line has lower levels of the active Notch4 protein than the parental clone. The knockout was achieved by CRISPR-targeted deletions in the NOTCH4 gene in both of the two alleles present in MCF7s. There is a 19 base pair deletion in exon 2 in one of the alleles and a 170bp deletion spanning exon 2 and some of exon 1 in the other allele (Appendix Figure 8-2B+C). These deletions were classed as abrogating the function of the Notch4 gene and therefore this cell line was labelled as a knockout. However, there is still some protein detectible by western blot (Appendix Figure 8-2A). This could be explained by exon skipping since in the possible reads, there could be in-frame splice variants of Notch4 created between the end of exon 1 and the beginning of exons 4 or 5 These would allow an almost full length Notch4 protein to be synthesised and therefore detected via western blot. This slightly shorter Notch4 would not be functional in the same way as the full length receptor. Due to the dramatic differences in phenotype and BCSC activity observed with the

N4KO cell line by Simões et al, as well as the markedly reduced expression detected by western blot, this cell line can be classed as a Notch4 knockdown (Simões, O'Brien, et al., 2015). Therefore, the results must be treated in the knowledge that this CRISPR "knockout" may be a functional knockout rather than a complete loss of gene.

To confirm previous findings, the N4KO cell line and control cell line were treated with vehicle, tamoxifen (10^{-6}M) or fulvestrant (10^{-7}M) for 6 days and then investigated for BCSC activity. Drug concentrations were determined from previous experiments in the group. After treatment, cells were plated out in low attachment conditions and mammospheres were counted after 5 days (Figure 4-1A). N4KO cells had approximately 2-fold lower mammosphere forming efficiency than control without treatment ($p<0.01$), as well as after tamoxifen and fulvestrant treatments ($p<0.0001$ and $p<0.05$). Cells that had undergone treatment with vehicle, tamoxifen or fulvestrant were also analysed by Aldefluor assay to assess the ALDH activity, which is another measure of stemness (Figure 4-1B). An Aldefluor assay was chosen as BCSCs have a high expression of the enzyme ALDH1 and is used alongside the mammosphere assay to investigate BCSC activity. N4KO cells had reduced numbers of ALDH+ cells, which was significantly reduced after no treatment ($p=0.05$). After tamoxifen and fulvestrant treatment the results were too varied to achieve significance.

The gene expression of Notch target genes Hes1, Hey1 and Hey2 were analysed in N4KO and control cell lines (Figure 4-1C+D+E). N4KO cells had increased Hes1 expression ($p<0.0001$) and Hey1 expression (2.8-fold increase, $p<0.0001$). N4KO cells also had greatly reduced Hey2 gene expression (8.7-fold decrease, $p<0.0001$), suggesting that Hey2 is the best gene of the three for measuring Notch4 signalling.

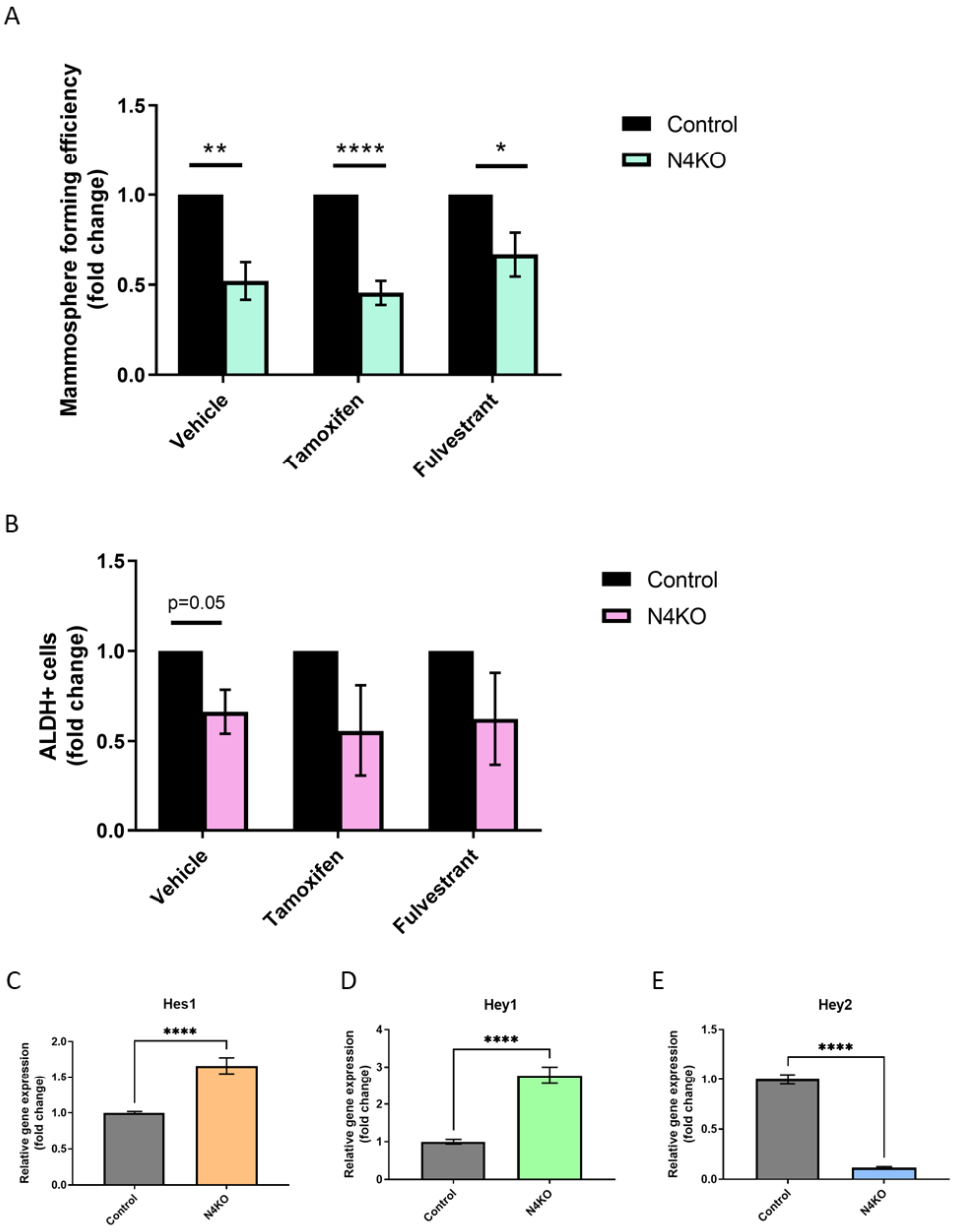

Figure 4-1: N4KO cells have reduced breast cancer stem cell activity, increased Hes1 and Hey1 gene expression and decreased Hey2 gene expression. The N4KO (Notch4 knockout) cell line was created prior to this project and has two gene deletions, creating a non-functional protein (Simões, O'Brien, et al., 2015). A) Mammosphere forming efficiency of Control and N4KO cells after 6-day treatment with vehicle, tamoxifen (10^{-6}M) or fulvestrant (10^{-7}M). B) ALDH+ cells determined by Aldefluor assay in Control and N4KO cells after treatment with vehicle, tamoxifen (10^{-6}M) or fulvestrant (10^{-7}M). C+D+E) Relative gene expression of Hes1 (C), Hey1 (D) and Hey2 (E) in Control and N4KO cells. N=3. Data are represented as mean ±SEM. Statistical tests: Unpaired t tests. *p < 0.05. **p < 0.01. ***p<0.001. ****p<0.0001.

4.3 Creation of Notch4 overexpressing ER+ breast cancer cell line

In order to comprehensively investigate the actions of Notch4 and the connections between Notch4 endocytic pathway signalling and Breast Cancer Stem Cells (BCSCs), a stable cell line overexpressing Notch4 was needed. This was in part due to the duration of the assays to determine stem cell activity, as well as the need for analysis of stemness with a consistent and reliable Notch4 expression (rather than the rapidly changing gene expression of Notch4 when transiently transfecting).

Two stable cell lines were produced with the N4KO cell line used as a parental cell line. A Notch4 expressing cell line (N4KO-N4) and a control cell line (N4KO-CON) were created using a lentivirus transduction of Notch4 and control virus, respectively. The lentivirus expression plasmids used to create the lentiviral particles are shown in Figure 4-2A+B. The plasmids were acquired from VectorBuilder. The plasmids are identical, but the control plasmid has a "stuffer" region in place of the Notch4 gene. The Notch4 gene is controlled by a UBC promoter. The plasmids have a Puromycin resistance gene, controlled by a mPGK promoter, to allow for antibiotic selection of the transduced cells. Other components of the plasmid include an Ampicillin resistance gene for bacterial selection and RRE, Ψ and WPRE to facilitate and improve efficiency of viral packaging.

Firstly, the plasmids shown in Figure 4-2A+B were amplified along with three other plasmids expressing the genes required for packaging a lentivirus. These are "rev", "gagpol" and "vsvg" (Appendix Figure 8-3). Cells were transfected with the lentiviral gene expression plasmid and each of the lentivirus packaging plasmids using the calcium phosphate method. Virus particles produced were collected and concentrated. A titration was carried out using HEK293T cells to determine the concentration of the viral particles. The determined titre for Control and Notch4 viruses were $5.3x10^4$ TU/ml and $5.5x10^4$ TU/ml, respectively. To make the stable cell lines, N4KO cells were transduced with a MOI (Multiplicity of Infection) of 0.5 using polybrene to aid transduction efficiency and selected for with Puromycin treatment. Previously, a kill curve was carried out to determine the optimal concentration of Puromycin to use, which was determined to be 2µg/ml. Finally, the cells were selected with Puromycin for 4 weeks whilst expanding (Figure 4-2C).

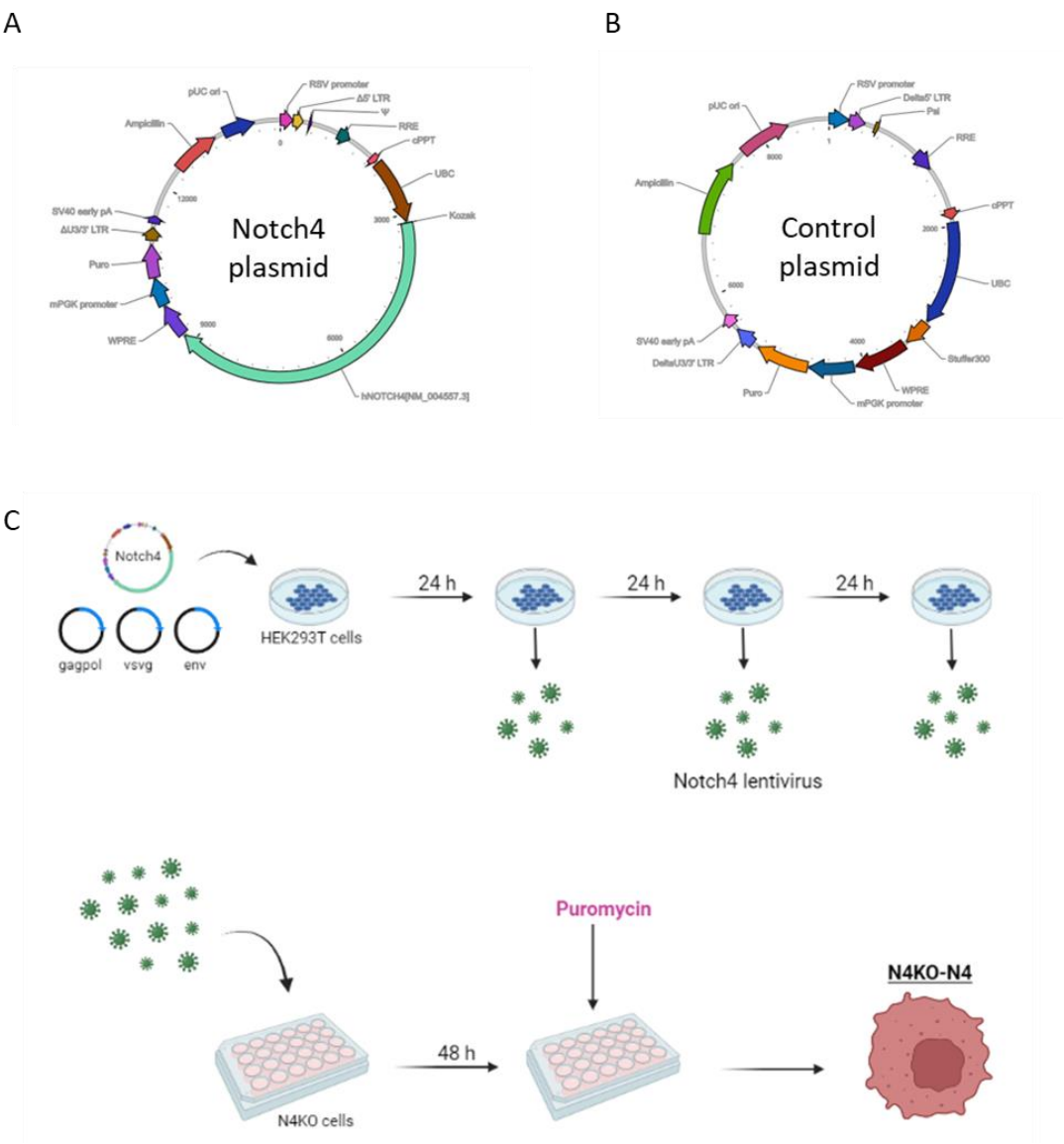

Figure 4-2: N4KO-CON and N4KO-N4 are two stable cell lines created using lentivirus and are a control and Notch4 expressing cell lines, respectively. Plasmids used to create stable cell lines Notch4 (N4KO-N4) (A) and Control (N4KO-CON) (B) (VectorBuilder). C) Workflow of how the cell lines were created. Figure created with BioRender.com.

4.4 N4KO-N4 (Notch4 expressing) stable cell line expresses more Notch4 than N4KO-CON (control)

To characterise the cell lines created, western blots were used to measure the expression level of the Notch4 protein. The N4KO-N4 cell line had more detectable protein than the N4KO-CON control cell line (Figure 4-3A+B+C), for full length Notch4 as well as Notch4 ICD, although this did not reach significance.

The cell lines were also analysed by flow cytometry and stained with Notch4-AlexaFluor647 conjugated antibody. Unstained (orange), N4KO-CON (blue) and N4KO-N4 (red) cells are shown in Figure 4-3 D+F as histograms normalised to allow for cell number. The Notch4 cell line has a clear shift to the right, indicating more surface expression of Notch4 compared to control. The Mean Fluorescence Intensity (MFI) of the three groups of cells corroborates this (Figure 4-3E). N4KO-CON and N4KO-N4 cells are also shown as a scatter plot demonstrating that 13.9% of the N4KO-N4 cells have a high level of surface expression of Notch4 (Figure 4-3G). Finally, RNA was taken from both N4KO-N4 and N4KO-CON cells and analysed by qRT-PCR (Figure 4-3H). The gene expression of Notch4 was significantly higher in the N4KO-N4 cells, with an increase of 13.7-fold compared to control ($p<0.0001$).

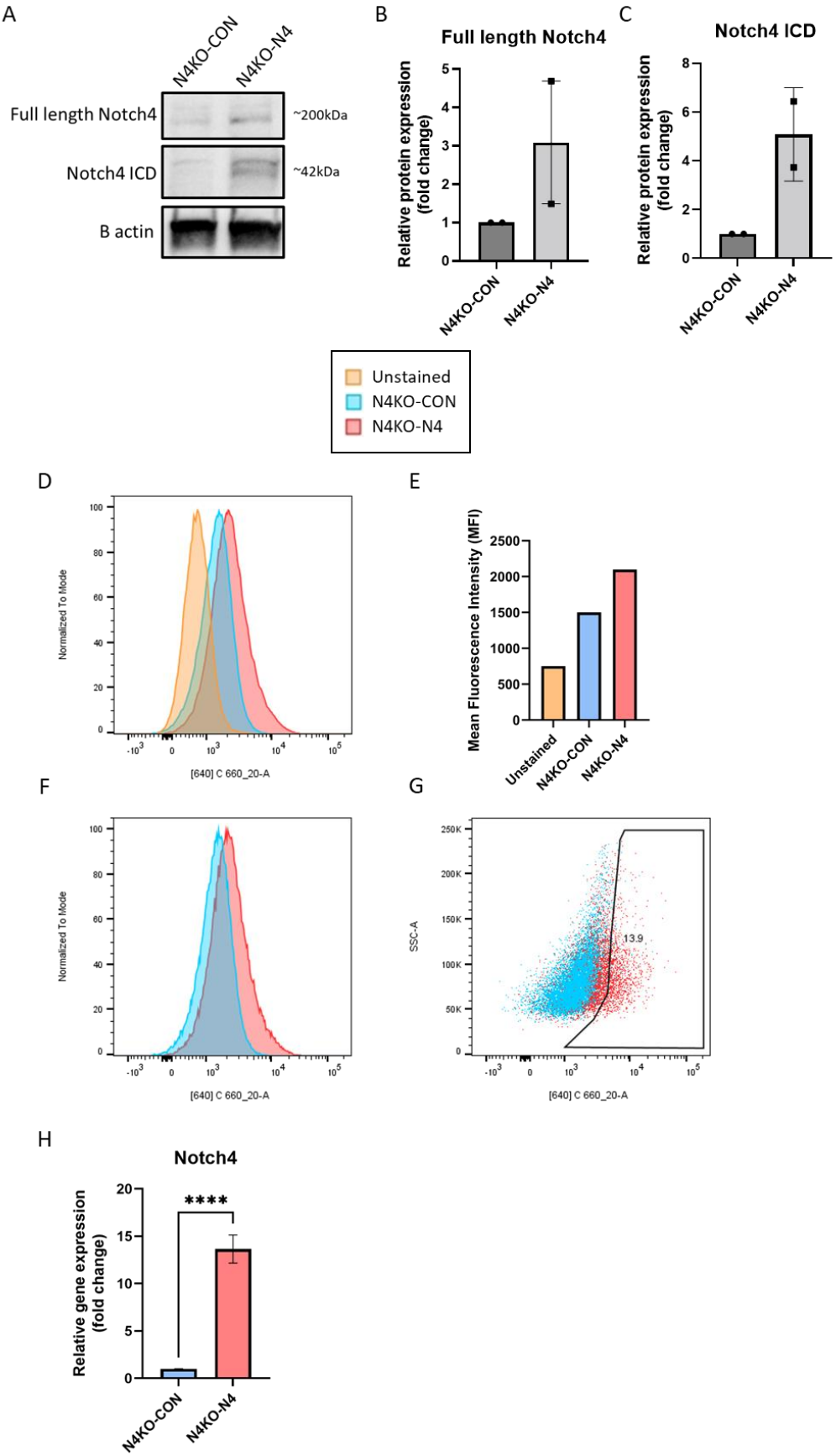
A
N4KO-CON
N4KO-N4
Full length Notch4
~200kDa
Notch4 ICD
~42kDa
B actin
B
Full length Notch4
Relative protein expression (fold change)
N4KO-CON
N4KO-N4
C
Notch4 ICD
Relative protein expression (fold change)
N4KO-CON
N4KO-N4
Unstained
N4KO-CON
N4KO-N4
D
Normalized To Mode
[640] C 660_20-A
E
Mean Fluorescence Intensity (MFI)
Unstained
N4KO-CON
N4KO-N4
F
Normalized To Mode
[640] C 660_20-A
G
SSC-A
13.9
[640] C 660_20-A
H
Notch4
Relative gene expression (fold change)
****
N4KO-CON
N4KO-N4

Figure 4-3: N4KO-N4 stable cell line expresses more Notch4 than N4KO-CON (control). A) Representative western blot showing more Notch4 protein expression in the N4KO-N4 cell line than in the N4KO-CON cell line. B+C) Quantification of the densitometry from western blots of full length Notch4 (B) and Notch4 ICD (C). N=2. D) Flow cytometry results of Notch4 levels on the surface of unstained (orange), N4KO-CON (blue) and N4KO-N4 (red) cells stained with Notch4-AF647 conjugated antibody. E) Mean Fluorescence Intensity from histogram. N4KO-CON and N4KO-N4 are compared directly in histogram (F) and scatter plot (G), with the latter showing an appropriate gate, demonstrating 13.9% of the cells have a high Notch4 surface expression. Histograms normalised to allow for numbers of cells. N=1. (H) N4KO-N4 cells have higher Notch4 gene expression than N4KO-CON cells. N=3 Data represented as mean ±SEM. Statistical test: Unpaired t-test. ****p<0.0001.

4.5 N4KO-N4 cells have increased Hey1 and Hey2 gene expression and decreased Hes1, DTX1, DTX2 and DTX4 gene expression

As well as measuring the gene expression of Notch4 in the N4KO-N4 and N4KO-CON cells by qRT-PCR, expression of Notch target genes and DTX genes were measured. Hey2 gene expression was significantly increased in N4KO-N4 cells up to a level 3.8-fold higher than control (P<0.0001) (Figure 4-4C). Hey1 gene expression was increased in the Notch4 cells (P<0.05) (Figure 4-4B). Conversely, Hes1 gene expression was reduced in the Notch4 cells compared to control (p<0.001) (Figure 4-4A). The gene expression of DTX1, DTX2 and DTX4 were reduced in Notch4 cells (Figure 4-4D+E+F).

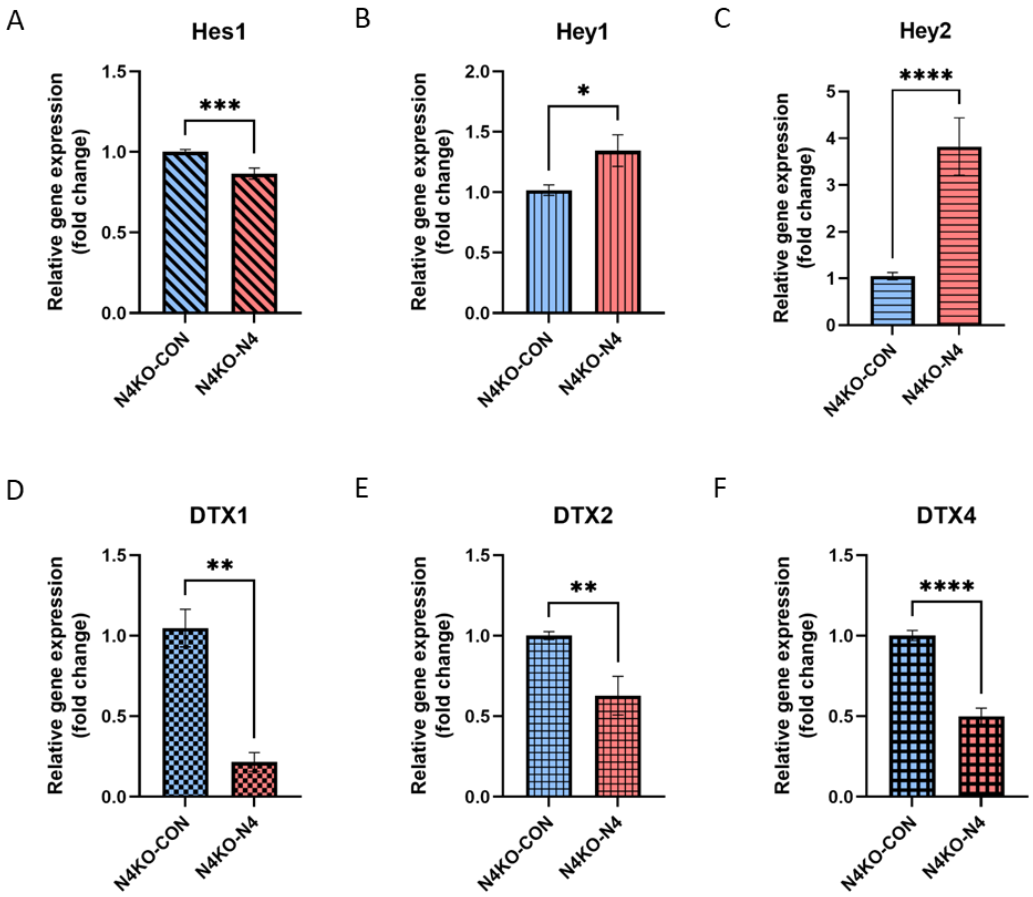

Figure 4-4: Notch4 overexpressing (N4KO-N4) cells have increased gene expression of Hey1 and Hey2 and decreased gene expression of Hes1, DTX1, DTX2 and DTX4. Relative gene expression of Hes1 (A), Hey1 (B), Hey2 (C), DTX1 (D), DTX2 (E) and DTX4 (F). N=3. Data are represented as mean ±SEM. Statistical tests: Unpaired t-tests. *p < 0.05. **p < 0.01. ***p<0.001. ****p<0.0001.

4.6 N4KO-N4 cells have increased breast cancer stem cell activity

Notch4 has been linked extensively to Breast Cancer Stem Cells (Simões, O'Brien, et al., 2015) and so the BCSC activity of the Notch4 expressing cells was investigated. This was explored firstly with a mammosphere assay. N4KO-N4 and N4KO-CON cells were treated with vehicle or a gamma-secretase inhibitor (GSI) RO4929097 (10µM) for 48 hours, before being seeded out for mammospheres in low attachment conditions. After 5 days, mammospheres were counted and mammosphere forming efficiency (MFE) was calculated. Untreated N4KO-N4 cells have significantly increased MFE, an average of 1.06%, up from 0.40% in N4KO-CON cells ($p<0.01$) (Figure 4-5A). Both N4KO-CON and N4KO-N4 cells have decreased MFE after treatment with the GSI, and the N4KO-N4 increased MFE is reduced down to the level of control, proving that this MFE increase by Notch4 is gamma-secretase dependent. As well as the N4KO-N4 cells producing more mammospheres, the mammospheres were also much larger in size compared to the N4KO-CON mammospheres (representative images of mammospheres formed shown in Figure 4-5B).

A

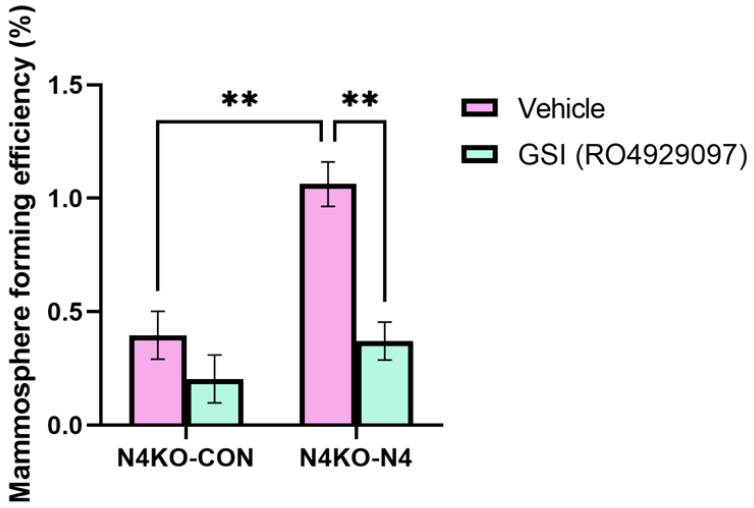

B

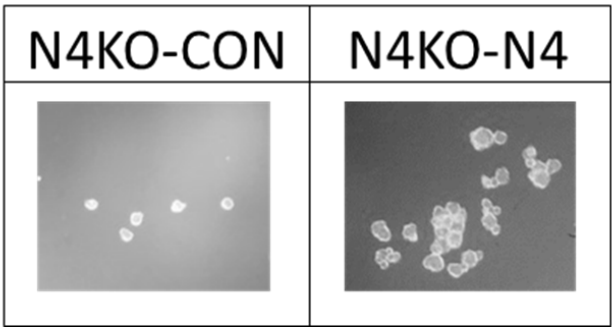

Figure 4-5: N4KO-N4 cells have increased mammosphere forming efficiency. A) Mammosphere forming efficiency of N4KO-CON and N4KO-N4 cells with and without 48 hour treatment with the gamma-secretase inhibitor (GSI) RO4929097 (10µM). N=3. B) Representative images of mammospheres from N4KO-CON and N4KO-N4 cells. Data are represented as mean ±SEM. **p < 0.01. Statistical tests: two-way ANOVA with Tukey's multiple comparisons.

Another BCSC activity assay carried out was the Aldefluor assay. MCF7 cells were transiently transfected with the Notch4 plasmid. After 24 hours, these cells were stained with the Notch4-AF647 conjugated antibody before undergoing an Aldefluor assay. They were then analysed by flow cytometry using laser and filter settings of (488)530/30 to detect Aldefluor reagent and (640)660/20 to detect Notch4 antibody. Using FlowJo, cells were gated to exclude debris and doublet cells, to allow analysis only on single cells (Figure 4-6A). Cells transfected with Notch4 had a higher proportion of ALDH positive cells than untransfected cells. DEAB inhibitor was used to discriminate ALDH positive cells from negatives (Figure 4-6B+C). After gating for ALDH, the cells positive for ALDH were measured for Notch4 positivity and 4.85% of these cells were deemed positive, compared to 5.21% of the whole population (Figure 4-6D). This suggests that after transfecting with Notch4, although indirectly enriching the ALDH+ population, cells do not co-express both Notch4 and ALDH at high levels.

To confirm this, transfected cells and untransfected inhibited cells were plotted to show Notch4 vs ALDH (Figure 4-6E). The Notch4 positive population can be clearly observed, as well as the ALDH positive population. The double positive population, although present (0.47% of cells vs 0% in untransfected), is very small, confirming that Notch4 expression does not always lead to a high expression of ALDH. The Notch4 positive, ALDH positive and the double positive populations were then plotted onto a FACS plot of FSC vs SSC to observe the distribution of the populations (Figure 4-6F). Mostly, the Notch4+ and ALDH+ populations are discreet, with the Notch4 cells being smaller and the ALDH cells being larger. There is also an area of crossover, where the Notch4 and ALDH cells have similar sizes and granularity. The double positive population is mostly distributed in an area that indicates that they are slightly larger and more granular than the majority. Together, these results suggest that transfecting with Notch4 slightly increases the population ALDH positivity. However, a high Notch4 expression does not directly lead to an increase in activity of ALDH, with the Notch4 positivity of the ALDH+ cells reflecting that of the main population. The ALDH positivity of the Notch4 positive cells also reflects that of the main population (inverse analysis, data not shown). The distribution of the populations suggests that the Notch4 positive cells represent a different population of cells to the ALDH positive ones, although these populations do overlap.

A

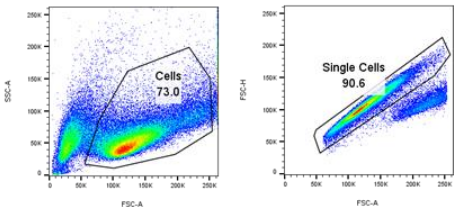
Cells
73.0
Single Cells
90.6
SSC-A
FSC-A
FSC-H
FSC-A

B

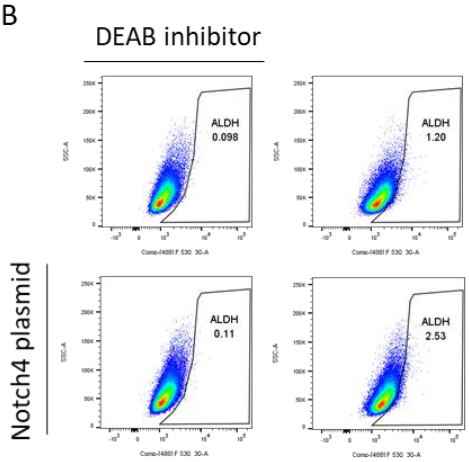
DEAB inhibitor
ALDH
0.098
ALDH
1.20
Notch4 plasmid
ALDH
0.11
ALDH
2.53

C

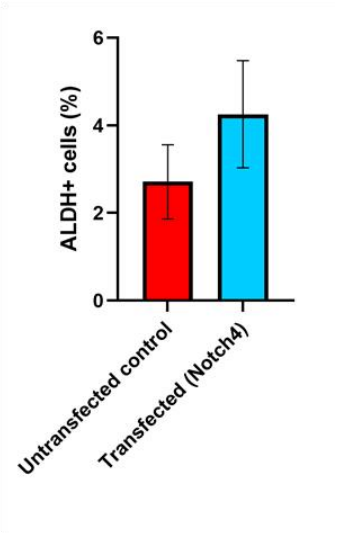
ALDH+ cells (%)
6
4
2
0
Untransfected control
Transfected (Notch4)

D

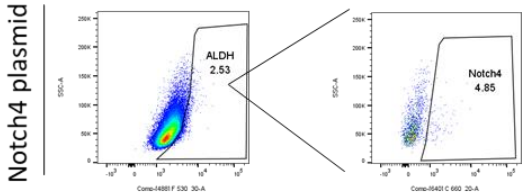
Notch4 plasmid
ALDH
2.53
Notch4
4.85

E

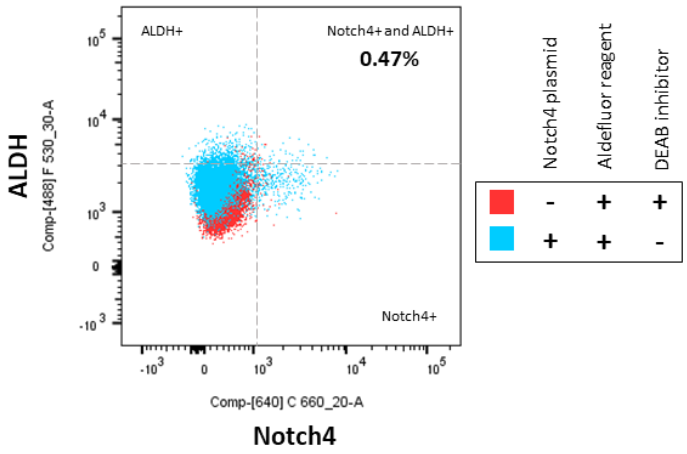

F

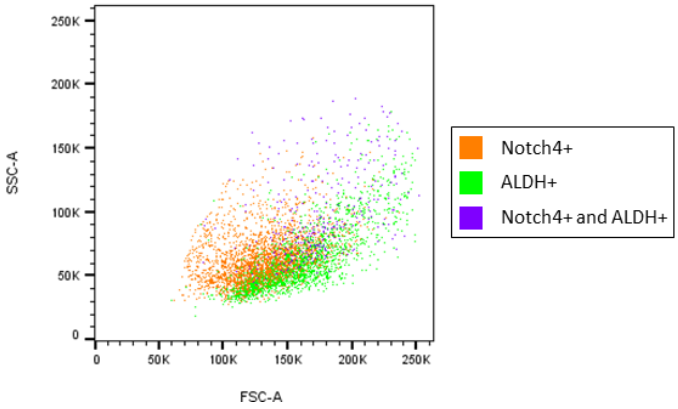

Figure 4-6: Notch4 transfection increases ALDH activity of MCF7 cells. MCF7 cells were transiently transfected with Notch4, stained with Notch4-AF647 antibody, stained with Aldefluor reagent and analysed by flow cytometry. DEAB inhibitor was used as a control to prevent efflux of Aldefluor reagent. A) Gating strategy to include only single cells and exclude debris and doublets. B) Representative FACS plots of cells with and without the Notch4 plasmid. ALDH positive cells (gate outlined) were discriminated from ALDH negative cells using the DEAB inhibitor. 2.83% of the cells transfected with Notch4 were positive for ALDH (bottom right panel). C) Bar chart representing proportion of ALDH positive cells in Untransfected control and Notch4 transfected cells. Data is represented as mean ±SEM. N=3. D) Representative FACS plots showing the distribution of Notch4 staining of the ALDH+ positive cells from B. Gate used is a standard gating strategy showing cells positive for Notch4. 4.85% of this population were positive for Notch4. E) Representative FACS plot showing the single positive and double positive populations for ALDH and Notch4 in cells that have been transfected with Notch4 and have no inhibitor (blue) and untransfected cells with inhibitor (red). 0.47% of the former cells are double positive for Notch4 and ALDH, compared to 0% of the latter. F) FACS plot showing the Notch4 positive, ALDH+ and double positive populations of the transfected cells plotted onto a scatter plot of FSC vs SSC. Plot shows distribution of these populations according to size and granularity. Plotted using FlowJo software.

The gold standard assay for measuring BCSC activity is an *in vivo* limiting dilution assay. This was carried out in NSG mice (Nod Scid Gamma, immunodeficient mice) to compare the tumour forming capacity of N4KO-CON and N4KO-N4 cells. Serial dilutions of cells in 1:1 mammosphere media and Matrigel were injected subcutaneously into both flanks of mice (as described in Table 2-17). Cell numbers were decided based on our group's previous publications (Harrison et al., 2010; Sarmiento-Castro et al., 2020). For groups 1,2 and 3 (10,000, 1000 and 100 cells per flank, respectively), control cells were injected into the left flank and Notch4 cells were injected into the right flank. This was to reduce variability between different mice having different cell lines injected. Groups 4a and 4b (100,000 cells per flank) however, had only Control cells (4a) or Notch4 cells (4b) injected into both flanks. This was so that the lungs could be collected and analysed for these groups to assess lung metastasis developed by Notch4 cells compared to control cells. The lung metastasis data has yet to be analysed and quantified. Appropriate mice numbers for each group was determined using previous publications in our group (see above), using a resource equation analysis (Methods) as well as taking into account the impact on each group of losing mice due to natural causes.

Mice were implanted with 90-day release 0.36mg 17-ß estradiol pellets 7 days before injection of cells. Following injection, the mice were monitored for tumour growth 3 times a week. The growth of N4KO-N4 tumours vs N4KO-CON tumours in groups 4a and 4b (100,000 cells per flank) was plotted as a 7-day moving average and it was found that all mice in both groups formed tumours (Figure 4-7A+B). Both sets of cells maintained a similar rate of growth for the first 4 weeks after implantations. After this point, the tumours formed by the N4KO-CON cells grew at a faster rate, reaching significantly greater average volumes at week 7 and beyond (Figure 4-7A).

The Extreme Limiting Dilution Analysis (ELDA) is an online application that was used in this situation to analyse the tumour initiating cell frequency of the N4KO-N4 and N4KO-CON cells (Figure 4-7C). The results show that the two sets of cells did not have a significant difference in tumour initiating capacity.

A

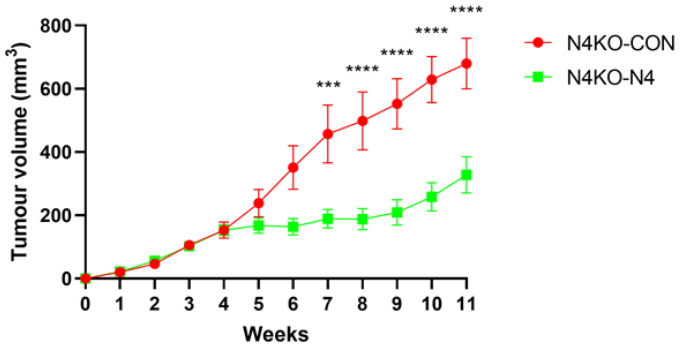

B

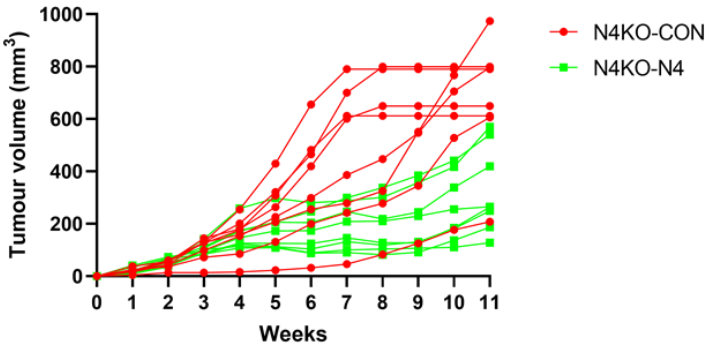

C

		N4KO-CON	N4KO-N4
Cell number	**100,000**	8/8	8/8
	10,000	2/2	1/2
	1000	2/5	1/5
	100	0/5	1/5
Tumour initiating cell frequency (95% CI)		**1:2121**	**1:6217**
P value between groups		**0.221**	

Figure 4-7: In vivo tumour growth and Extreme Limiting Dilution Analysis (ELDA) of N4KO-N4 and N4KO-CON cells. Cells were injected subcutaneously into mice as described in methods section. A+B) Growth curves of tumours from 100,000 injected cells showing moving 7-day values for tumour volume (mm^3). Average values (A) and individual tumour values (B). C) ELDA analysis was carried out for 100,000 cells, 10,000 cells, 1000 cells and 100 cells and corresponds to tumours greater than $100mm^3$ at week 10. 1000 cells group has N=2 due to unexpected mouse deaths at an early stage of the experiment. Statistical test: Two-way ANOVA with Šidák's multiple comparisons test (A) and Chi-squared (χ^2) (C). ***p<0.001. ****p<0.0001.

4.7 Notch4 expressing cell line is resistant to fulvestrant treatment while the Notch4 knockout cell line is more susceptible

Notch4 has been linked extensively to endocrine resistance (D'Angelo et al., 2015; Lombardo et al., 2014; Simões, O'Brien, et al., 2015). In order to investigate this, N4KO-N4 and N4KO-CON cells were treated with vehicle or endocrine therapies tamoxifen 10^{-6}M or fulvestrant 10^{-7}M. Drug concentrations were determined by previous experiments in the lab. The treatment spanned 14 days, with media changes at regular points. The cell density throughout the treatment was assessed by SRB assay and these data were processed relative to vehicle control and day 0.

No difference in cell density was observed between the cell lines after treatment with tamoxifen (data not shown). After treatment with fulvestrant (10^{-7}M), it was found that N4KO-N4 was slightly more resistant to treatment than N4KO-CON, with a higher relative cell density from day 5 through to day 14 (Figure 4-8A).

The Notch4 knockout cell line (N4KO) was also investigated for resistance to fulvestrant (10^{-7}M) treatment, compared to its control cell line. It was found that N4KO was more susceptible to fulvestrant treatment compared to control, with much less cell density detected (Figure 4-8B).

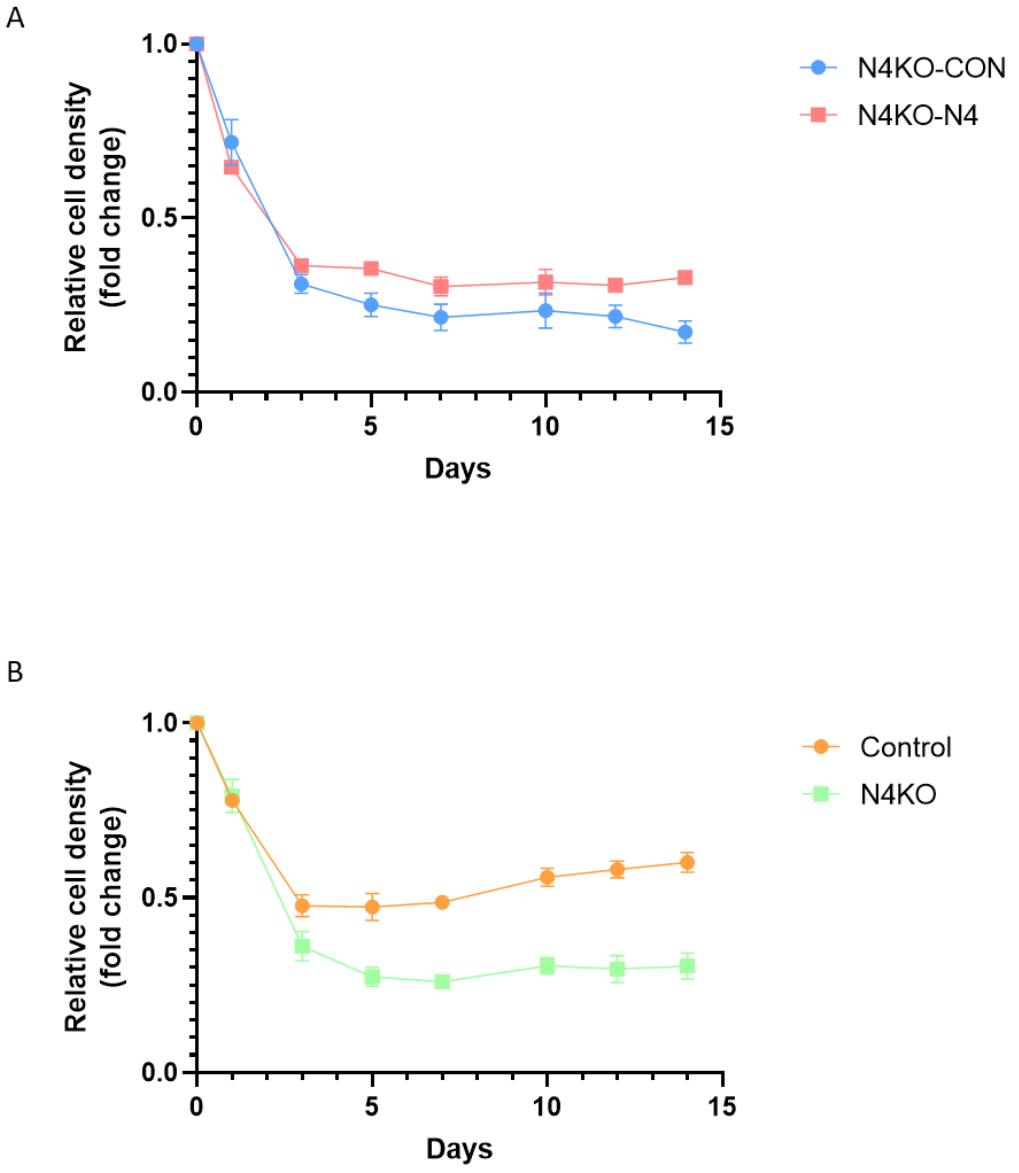

Figure 4-8: Notch4 expressing cell line is resistant to fulvestrant treatment while the Notch4 knockout cell line is more susceptible. Cells were treated with 10^{-7}M fulvestrant over 14 days and the cell density was determined using SRB assay. A) N4KO-CON and N4KO-N4. B) Control and N4KO cells. Data is plotted relative to vehicle control and relative to day 0 and is shown as mean ±SEM. N=2.

4.8 Analysis of putatively differentially expressed genes in N4KO-N4 cells

Next, we aimed to identify genes and pathways that might be responsible for the differences observed between N4KO-N4 and N4KO-CON cells. The gene expressions of the two sets of cells were analysed using RNAseq. Analysis was carried out by Matthew Roberts (CRUK) and detailed methods are included in the methods section. The genes that were found to have the greatest difference in expression between N4KO-N4 and N4KO-CON are plotted in heatmaps (Figure 5-9). Due to the low number of samples (N=1), a high fold change threshold was chosen to increase confidence around differences. 91 genes were identified that were putatively differentially expressed with a log2 fold change of greater than 3.25, which corresponds to a fold change of 9.51. 43 genes were identified that were putatively differentially expressed with a log2 fold change of greater than 4, which corresponds to a fold change of 16. Some of these genes that are highly upregulated in the Notch4 cells compared to the control have an association with cancer. These are listed in Table 4-1. CD36 was a gene in this group with a significant link to this project as it has been found to drive proliferation and metastasis of tamoxifen resistant breast cancers (Liang et al., 2018), although this was a highly downregulated gene in the Notch4 cells.

A user defined list of genes was queried for within the RNAseq data. This Notch related gene list included the genes for Notch receptors, Notch ligands, Notch target genes and other genes of interest including the DTX genes and genes involved in endocytic trafficking. The heatmap for gene expression of N4KO-N4 vs N4KO-CON of this set of genes is shown in Figure 4-10. From this set, genes that were upregulated, in order from most upregulated to least upregulated are JAG1, HEY1, HES2, JAG2, HES6, DLL1, NOTCH1, HES1, NOTCH4, CDKN1A, VPS18. HES4, DLL4, GATA3, RAB7A, DTX2 and VPS33A. Genes that were downregulated, from most downregulated to least downregulated are HEY2, DTX3, DTX3L, HEYL, DTX4, CCND1, NOTCH3 and NOTCH2. Calculated fold change values of these genes are found in Appendix Table 8-1.

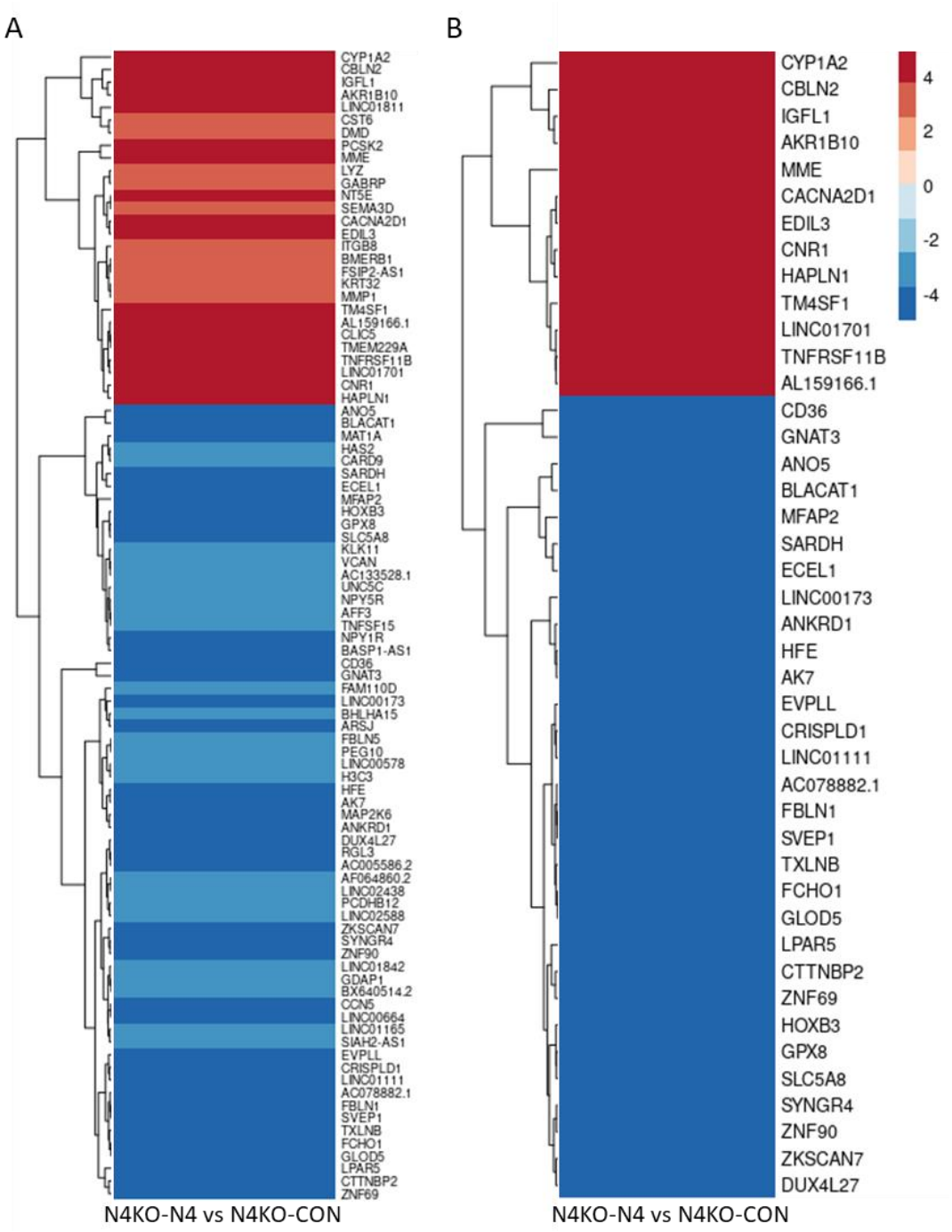

Figure 4-9: Genes putatively differentially expressed in N4KO-N4 compared to N4KO-CON. Includes genes with a log2 fold change greater than 3.25 (A) and 4 (B). Red corresponds to upregulated genes and blue to downregulated genes.

Gene ID	Gene name	Relevance/ association with cancer/
TNFRSF11B	TNF Receptor Superfamily Member 11b	Activates Wnt/ β-catenin signalling. Associated with gastric cancer (Luan et al., 2020).
CYP1A2	Cytochrome P450 1A2	May contribute to lifestyle risk of breast cancer (Hong et al., 2004).
Cacna2d1	Calcium Voltage-Gated Channel Auxiliary Subunit Alpha2delta 1	Associated with epithelial ovarian cancers (D. Yu et al., 2016)
EDIL3	EGF Like Repeats And Discoidin Domains 3	Involved in angiogenesis and EMT (Gasca et al., 2020).
CD36		Proliferation, tumourigenesis and endocrine resistant growth and metastasis in ER+ breast cancer (Liang et al., 2018)

Table 4-1: Relevance/ association with cancer of some of the putatively differentially expressed genes identified in Figure 4-9.

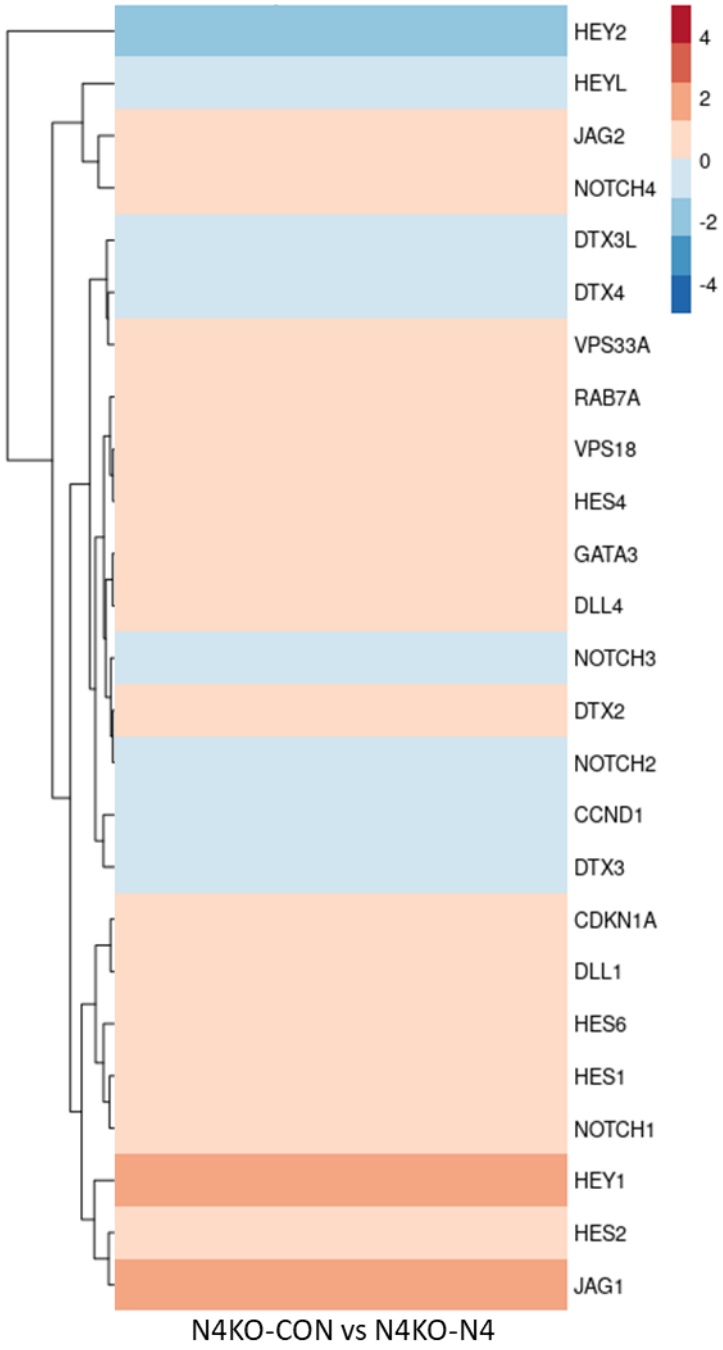

Figure 4-10: Expression level of genes related to Notch signalling including target genes and related genes. Expression level displayed as log2 fold change in N4KO-N4 compared to N4KO-CON. Red corresponds to upregulated genes and blue to downregulated genes.

Next, we identified signalling pathways and networks that were associated with the Notch4 cells compared to the control cells. KEGG pathway analysis was performed using the R package limma (v3.42.2) (McCarthy et al., 2012). Genes with a log2 fold change greater than 1 were used for the comparison between N4KO-N4 and N4KO-CON, and they were compared to gene sets that correspond to a certain cellular/ molecular signalling pathway. The pathways that have enough matching genes present in the dataset that leads to a p value of less than 0.01 are displayed in Table 4-2. Pathways of significance to this research are highlighted in pink and these include the TGFβ, MAPK, Wnt, Hippo and HIF-1 signalling pathways.

Pathway	Number of genes	Putatively differentially expressed genes in N4KO-N4	P value
Rap1 signalling pathway	210	32	0.000099
Cytokine-cytokine receptor interaction	295	39	0.00040
Axon guidance	182	27	0.00053
cAMP signalling pathway	221	31	0.00057
TGF-beta signalling pathway	94	17	0.0006
MAPK signalling pathway	294	38	0.00074
Gap junction	88	16	0.00081
Pathways in cancer	531	60	0.00094
Inflammatory bowel disease	65	13	0.00099
Cellular senescence	156	23	0.0015
C-type lectin receptor signaling pathway	104	17	0.0019
Calcium signalling pathway	240	31	0.0022
Oxytocin signalling pathway	154	22	0.0027
Cocaine addiction	49	10	0.0032
AGE-RAGE signaling pathway in diabetic complications	100	16	0.0032
cGMP-PKG signalling pathway	167	23	0.0036
Wnt signalling pathway	167	23	0.0036
Colorectal cancer	86	14	0.0049
Arachidonic acid metabolism	61	11	0.0055
Glucagon signalling pathway	107	16	0.0064
Hippo signalling pathway	157	21	0.0073
HIF-1 signalling pathway	109	16	0.0076
Estrogen signalling pathway	138	19	0.0077
Phospholipase D signalling pathway	148	20	0.0078

Glycine, serine and threonine metabolism	40	8	0.0091
Chagas disease	102	15	0.0094
FoxO signalling pathway	131	18	0.0095

Table 4-2: Pathways identified by KEGG pathway analysis that have an association with the N4KO-N4 cell line. Putatively differentially expressed genes with a log2 fold change of more than 1 identified in N4KO-N4 vs N4KO-CON were included in the analysis. Pathways that had an association with these genes leading to a p value of less than 0.01 are shown in the table. Those that are of particular interest are highlighted in pink.

We performed gene set enrichment analysis (GSEA) using genes of interest, defined by log2 fold change. The R package ideal (v1.10.0) (Marini, 2020) was used to generate enrichment analysis results using Gene Ontology terms from two domains- Biological Processes and Molecular Functions. Gene sets which correspond to these processes/ functions were compared to the differentially expressed genes between N4KO-N4 that were above a log2 fold change of 1.5 for Biological processes (Table 4-3) and 1 for Molecular functions (Table 4-4). Of note, this identified the biological processes "regulation of MAPK cascade", "positive regulation of ERK1 and ERK2" and "positive regulation of cell communication". It also identified key molecular functions involved in receptor coordination.

Next, we performed GSEA using the R package fgsea (c1.14) (Korotkevich et al., 2019) and gene set collections from the molecular signature database (MSigDB) were compared to genes of interest defined by a log2 fold change of greater than 1. Hallmark genes sets that overlap with these genes with a p value of less than 0.05 are included in Figure 4-11A. This data showed that the N4KO-N4 cells have a positive association with Notch signalling and epithelial mesenchymal transition, and a negative association with estrogen response late genes. Using the "C2" curated gene sets, those that overlap with a p-adjusted value of less than 0.05 are included in Figure 4-11B. The data showed that N4KO-N4 cells have a positive association with endocrine therapy resistance and "squamous breast tumour" gene sets but a negative association with estradiol response and metastasis gene sets.

Together, these data suggest a complex role for Notch4 that enriches for endocrine resistance and EMT but is not classically associated with estrogen signalling. The enriched genes associated with Notch4 identifies novel molecules to investigate further in Notch signalling and breast cancer. There are multiple signalling pathways that have enrichment when Notch4 expression is high, including MAPK, TGF-β, HIF-1 and ERK signalling pathways.

Biological Process	Number of genes	Differentially expressed genes in N4KO-N4	P value
Biological adhesion	1426	102	2.6E-07
Cell adhesion	1419	100	4.7E-07
Anatomical structure development	5987	282	2.6E-06
Regulation of multicellular organismal process	3260	169	1.2E-05
Developmental process	6407	293	1.2E-05
Multicellular organism development	5489	258	1.4E-05
Homophilic cell adhesion via plasma membrane adhesion molecules	168	27	1.7E-05
System development	4917	234	2.8E-05
Animal organ development	3584	180	5.6E-05
Cell-cell adhesion via plasma-membrane adhesion molecules	274	33	8.9E-05
Extracellular structure organization	421	38	0.00011
Multicellular organismal process	7718	332	0.00011
Tissue development	2064	115	0.00014
Cell-cell adhesion	839	61	0.00021
Cell surface receptor signalling pathway	2947	150	0.00024
Positive regulation of protein phosphorylation	1015	67	0.00024
Extracellular matrix organization	367	34	0.00025
Positive regulation of phosphorylation	1066	69	0.00028
Positive regulation of phosphorus metabolic process	1139	72	0.00033
Positive regulation of phosphate metabolic process	1139	72	0.00033
Positive regulation of MAPK cascade	545	43	0.00045
Skeletal system development	517	41	0.0014
Anatomical structure morphogenesis	2737	139	0.0014
Negative regulation of multicellular organismal process	1317	74	0.0023
Regulation of ossification	201	21	0.0030
Regulation of protein phosphorylation	1463	83	0.0035
Positive regulation of protein modification process	1234	73	0.0036
Animal organ morphogenesis	1067	67	0.0057
Positive regulation of ERK1 and ERK2 cascade	213	21	0.0058
Regulation of MAPK cascade	768	50	0.0095
Regulation of secretion by cell	753	49	0.0096
Positive regulation of cell communication	1847	97	0.0096

Table 4-3: Biological processes identified by GSEA that have an association with the N4KO-N4 cell line. Processes that have differentially expressed genes with a log2 fold change of more than 1.5 in N4KO-N4 vs N4KO-CON with a p value of less than 0.01 are included.

Molecular Function	Number of genes	Differentially expressed genes in N4KO-N4	P value
Calcium ion binding	702	113	1.3E-10
Signalling receptor binding	1547	170	3.1E-05
Molecular function regulator	1808	191	3.2E-05
Receptor regulator activity	528	68	0.00088
Peptidase regulator activity	217	36	0.00090
Receptor ligand activity	484	63	0.0010
Peptidase inhibitor activity	180	31	0.0014
Serine-type endopeptidase inhibitor activity	93	19	0.010
Endopeptidase inhibitor activity	173	28	0.010
Growth factor activity	164	28	0.011
Syndecan binding	7	5	0.015
Endopeptidase regulator activity	180	28	0.017
Sialyltransferase activity	21	8	0.021
Chemorepellent activity	27	9	0.046

Table 4-4: Molecular functions identified by GSEA that have an association with the N4KO-N4 cell line. Processes that have differentially expressed genes with a log2 fold change of more than 1 in N4KO-N4 cell vs N4KO-CON with a p value of less than 0.05 are included

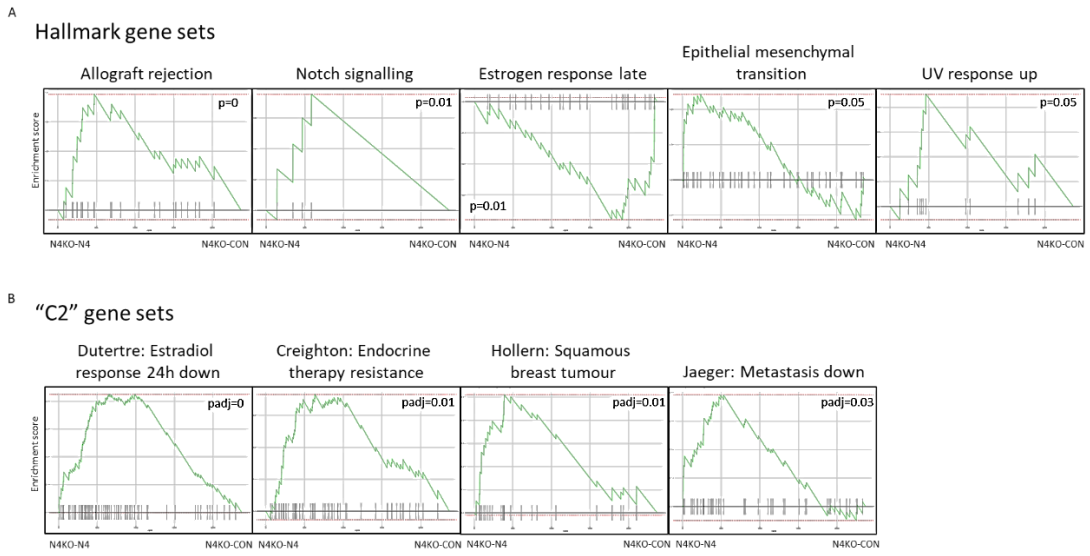

Figure 4-11: GSEA plots of N4KO-N4 vs N4KO-CON using MSigDB gene sets. Gene sets that corresponded to differentially expressed genes between N4KO-N4 and N4KO-CON with a log2 fold change of more than 1 were included for the analysis. Plots shown are A) Hallmark gene sets that overlap with the N4KO-N4 cell line with a p value of less than 0.05 and B) Relevant C2 curated gene sets that overlap with the N4KO-N4 cell line with a p-adjusted value of less than 0.05.

4.9 Tamoxifen and Fulvestrant resistant cell lines are more sensitive to ML-SI1 (TRPML inhibitor) treatment than control

Next, we investigated the use and effect of two inhibitors on Notch4 signalling and BCSC activity in ER+ breast cancer cells. These inhibitors were used to further explore the pathway of Notch4 signalling as they each inhibit a key component of Notch signalling.

Batimastat (BB-94) is an inhibitor of matrix metalloproteinase (MMP) activity and acts by binding a zinc ion in the MMP's catalytic site, blocking its action (Low et al., 1996). An important MMP in Notch signalling is ADAM10 which is involved in the canonical Notch pathway. It facilitates the "S2" cleavage event in the cell membrane, which allows the "S3" cleavage event to happen and NICD to be released. Previous studies have shown that BB-94 successfully inhibits ADAM10 (Abel et al., 2004; Leriche et al., 2016). BB-94 has also been implicated in breast cancer by inhibiting tumour progression, although clinical trials were not successful (Low et al., 1996; Macaulay et al., 1999). The main evidence for using BB-94 as a specific ADAM-10 inhibitor comes from studies by Shimizu et al in *Drosophila*, showing that it successfully inhibited ligand dependent Notch signalling, but not Deltex-driven ligand independent signalling (Shimizu et al., 2014) (Baron et al, unpublished). It is unknown whether Notch4 signalling (and Notch4 endocytic pathway signalling) requires ADAM10. Use of this inhibitor whilst studying the effects on Notch4 signalling could help us to answer that question.

Another inhibitor used in this part of the chapter is ML-SI1. This inhibitor blocks the action of TRPML (Samie et al., 2013). The TRPML group of proteins, of which the main one is TRPML1 (also known as MLN1), are mucolipins that act as cation channels within the endocytic pathway (Zeevi et al., 2007). They are located in the cell in the late endosomes and lysosomes and they are essential for the fusion of these compartments (Venkatachalam et al., 2015). The TRPML channels have been implicated in cancers as they are essential for regulating lysosomes and therefore autophagy. They have also specifically been linked to breast cancer, playing a part in tumour progression and cell survival (Huang et al., 2013; M. Xu et al., 2019). One of two identified TRPML inhibitors, ML-SI1 has also been investigated in *Drosophila*. It has been found that due to its actions on blocking late endosome-lysosome fusion, it is successful at inhibiting the Deltex-driven ligand independent, endocytic pathway dependent mechanism of Notch signalling (Baron et al, unpublished). Use of this inhibitor whilst studying Notch4 signalling, will further explore the requirements of the endocytic pathway in Notch4 activation.

Tamoxifen resistant and fulvestrant resistant ER+ cell lines (TAMR and FULVR, respectively) as well as their control (Cardiff), were used to explore the action of inhibitors BB-94 and ML-SI1. These cell lines were a gift from Julie Gee (University of Cardiff) and were derived from MCF7 cells that underwent long term treatment with a low concentration of tamoxifen or fulvestrant until resistance was acquired (Knowlden et al., 2003; McClelland et al., 2001). In previous studies it was found that these cell lines have an increased level of Notch4 expression, linking Notch4 to endocrine resistance and suggesting that these cells have a high level of Notch4 signalling (Simões, O'Brien, et al., 2015). These cells were therefore used to investigate the effects of these inhibitors in the context of endocrine resistance, when Notch4 levels are high. The Notch4 overexpressing cell line N4KO-N4 and its control (N4KO-CON) discussed previously were used to specifically look at the inhibitor's effects on Notch4.

TAMR, FULVR and Cardiff cells were treated with vehicle, 10µM Batimastat (BB-94, MMP inhibitor), 50µM ML-SI1 (TRPML inhibitor) or both BB-94 and ML-SI1 for 24 hours, before being counted using a haemocytometer method. The concentrations of the inhibitors used was determined prior to use by Baron et al. After treatment with BB-94, the cell number of the three cell lines did not change. However, after treatment with ML-SI1 all three cell lines decreased in cell number to 50% (Cardiff), 6% (TAMR) and 20% (FULVR) compared to vehicle. Although cell number was reduced by ML-SI1 in control cells, the reduction was markedly greater in the TAMR and FULVR cells, reaching significance in the TAMRs ($p<0.05$) (Figure 4-12A). When both inhibitors were used in combination, cell number was reduced below 50% of vehicle in all three cell lines, although no differences were observed between cell lines. When plotting these cell numbers relative to Cardiff for each of the treatment regimes, these differences are more apparent (Figure 4-12B+C+D). Little to no difference was seen between cell lines after BB-94 treatment, but a dramatic decrease in cell number of TAMRs and FULVRs after ML-SI1 treatment was observed, suggesting tamoxifen and fulvestrant resistant cells are more susceptible to ML-SI1 and therefore more dependent on TRPML.

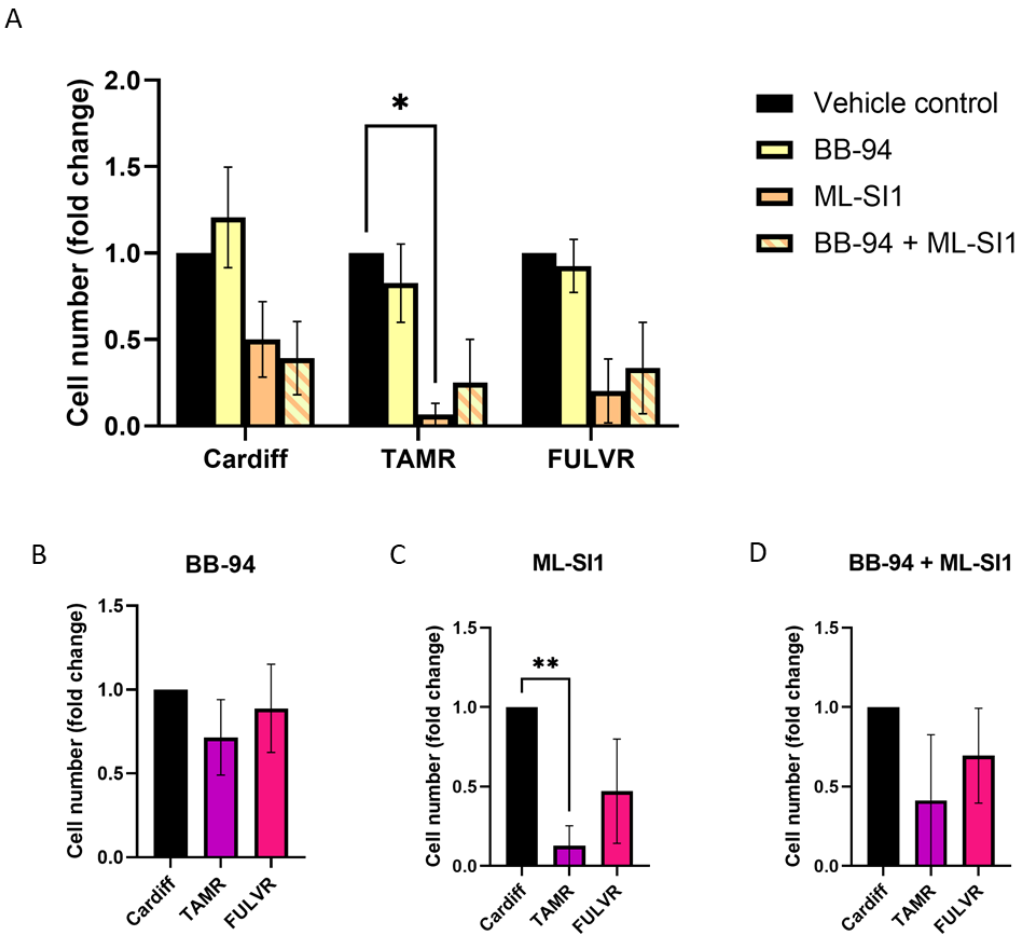

Figure 4-12: Tamoxifen and Fulvestrant resistant cell lines are more sensitive to ML-SI1 (TRPML inhibitor) treatment than control. Cardiff, TAMR and FULVR cells were treated with vehicle, 10µM Batimastat (BB-94, MMP inhibitor), 50µM ML-SI1 (TRPML inhibitor) or both BB-94 and ML-SI1 for 24 hours, after which cells were counted using a haemocytometer method. A) Cell number plotted relative to vehicle control for each cell line. B) Cell number relative to Cardiff after treatment with 10µM BB-94 (B), 50µM ML-SI1 (C), and both BB-94 and ML-SI1. N=3 Statistical tests: Two-way ANOVA with Tukey's multiple comparisons (A) Unpaired t-tests (B+C+D). *$p < 0.05$. **$p<0.01$.

4.10 Adding in ML-SI1 to BB-94 treatment decreases cell number in Notch4 overexpressing cells more than in control cells

When treating N4KO-CON cells and N4KO-N4 cells with BB-94 and ML-SI1, the same treatment protocol was carried out as above. In both cell lines, BB-94 treatment did not change cell number compared to control (Figure 4-13). ML-SI1 treatment reduced cell number significantly compared to vehicle ($p<0.01$ in N4KO-CON and $p<0.05$ in N4KO-N4). However, this reduction was similar for both control and Notch4 cell lines (to 38% and 49% of vehicle, respectively). When comparing combination treatment of BB-94 and ML-SI1 together across the two cell lines, the reduction compared to control is quite similar, to 26% of vehicle for control and 21% of vehicle for Notch4. However, in combination treatment compared to the single treatment of BB-94 alone, there is a greater reduction in cell number in the Notch4 cells when adding in ML-SI1 into treatment. This may suggest that there is a greater susceptibility to ML-SI1 treatment in Notch4 cells, and more of a reliance on TRPML, compared to control.

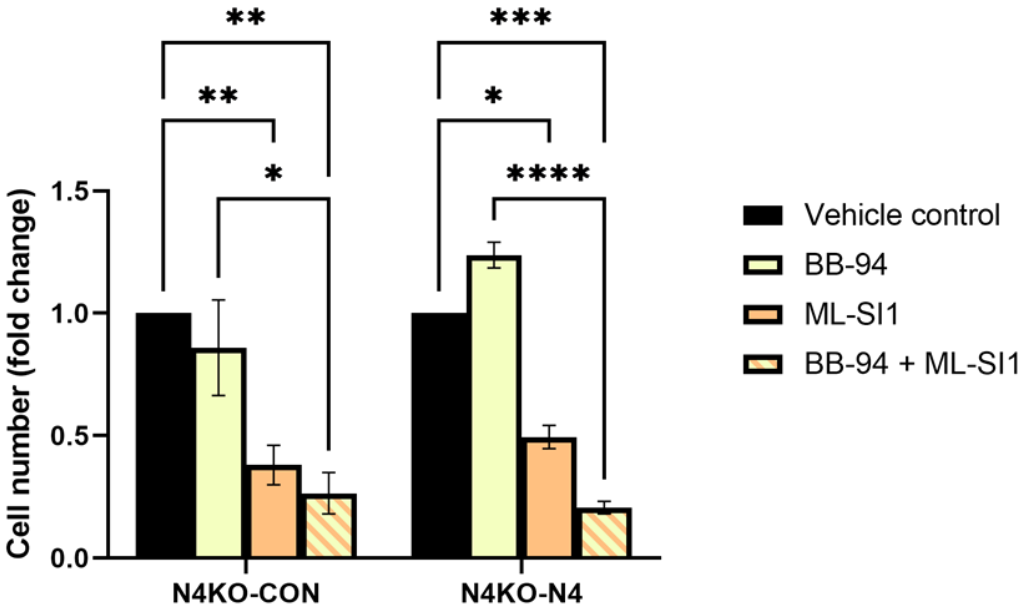

Figure 4-13: Adding in ML-SI1 to BB-94 treatment decreases cell number in Notch4 cells more than in control cells. N4KO-CON and N4KO-N4 cells were treated with vehicle, 10µM Batimastat (BB-94, MMP inhibitor), 50µM ML-SI1 (TRPML inhibitor) or both BB-94 and ML-SI1 for 24 hours, after which, cells were counted using a haemocytometer method. Cell number plotted relative to vehicle control for each cell line. N=3 Statistical tests: Two-way ANOVA with Tukey's multiple comparisons. $p < 0.05$. **$p < 0.01$. ***$p<0.001$. ****$p<0.0001$.

4.11 Batimastat (BB-94) treatment affects mammosphere forming efficiency differently in different cell lines

Mammosphere forming efficiency was used to determine any affect that TRPML and MMP inhibition has on BCSC activity. TAMR, FULVR and Cardiff cells were treated for 24 hours with vehicle, 10µM Batimastat (BB-94, MMP inhibitor), 50µM ML-SI1 (TRPML inhibitor) or both BB-94 and ML-SI1 and then plated out in low attachment conditions for mammospheres. Mammospheres were counted after 5 days. Due to the death of almost all of the ML-SI1 and combination treated TAMRs (Figure 4-12), only BB-94 treated cells were able to be plated out for mammospheres. After treatment with BB-94, control cells do not create as many mammospheres, with the mammosphere forming efficiency reducing to 36% of that of vehicle treated cells ($p<0.01$). TAMR cells are seemingly resistant to this BB-94 induced reduction in MFE, maintaining a similar MFE as TAMR vehicle treated cells. In FULVR cells, treatment with BB-94 increases MFE ($P<0.05$) (Figure 4-14). The differences between these cell lines in the effects of BB-94 treatment are apparent when mammosphere forming efficiency is compared directly to each other and plotted relative to Cardiff (Figure 4-14B). TAMR cells exhibit a 3.3-fold increase compared to Cardiff ($p<0.05$) and FULVR an 8.7-fold increase ($p=0.08$). These data indicate that MMP inhibition increases the BCSC activity of endocrine resistant cells.

Next, N4KO-CON and N4KO-N4 cells were treated in the same way for 24 hours and plated out for mammospheres. BB-94 treatment slightly reduced the MFE capacity of control and Notch4 cells. However, ML-SI1 treatment increased MFE of control cells by 1.7-fold but did not increase MFE of Notch4 cells. In combination treatment in control cells, addition of BB-94 to ML-SI1 reduced the MFE to a similar level as vehicle, apparently reversing the effect of ML-SI treatment alone ($p<0.05$ and 3.1-fold decrease of combination compared to BB-94 alone) (Figure 4-15A). When ML-SI1 treatment effect on MFE in Notch4 cells is plotted compared to control cells, the difference between the two cell lines is more apparent ($p<0.0001$) (Figure 4-15B). Compared to control, after treatment with ML-SI-1, Notch4 cells have a more reduced MFE, indicating they are resistant to the ML-SI1 induced MFE increase in control cells.

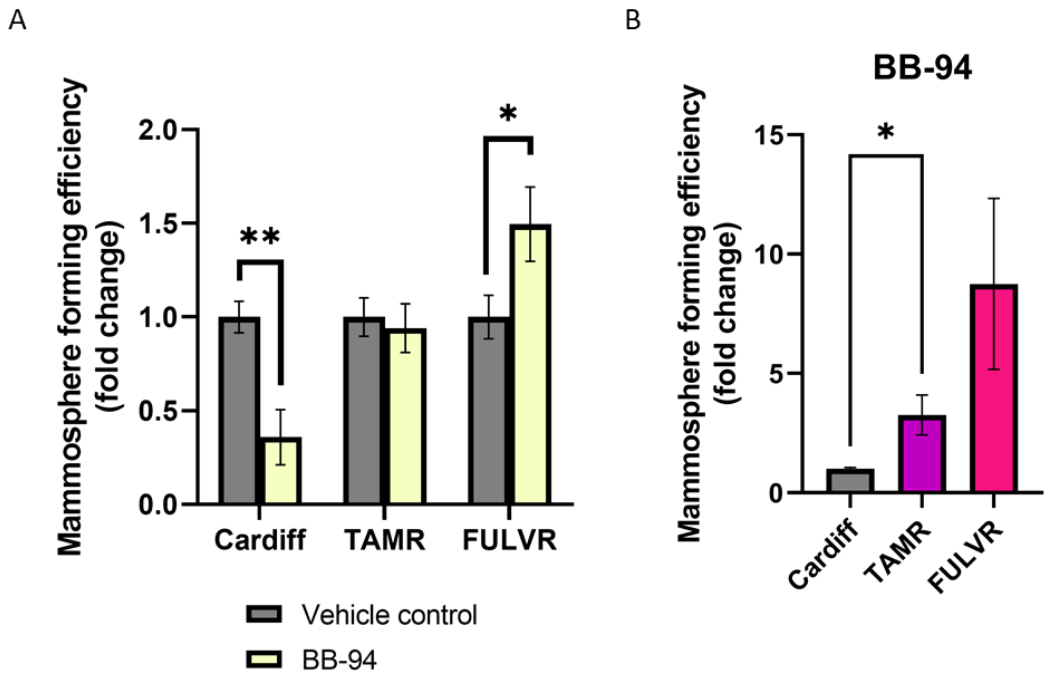

Figure 4-14: Tamoxifen and Fulvestrant resistance reverses the BB-94 induced decrease of MFE. Cardiff (control), TAMR (tamoxifen resistant) and FULVR (fulvestrant resistant) cells were treated for 24 hours with vehicle or 10µM Batimastat (BB-94, MMP inhibitor) and then plated out for mammospheres and counted after 5 days. A) Data plotted relative to vehicle control for each cell line. B) Data plotted relative to vehicle control and Cardiff control for BB-94 treatment. N=3 Statistical tests: Unpaired t-test. *$p < 0.05$. **$p<0.01$.

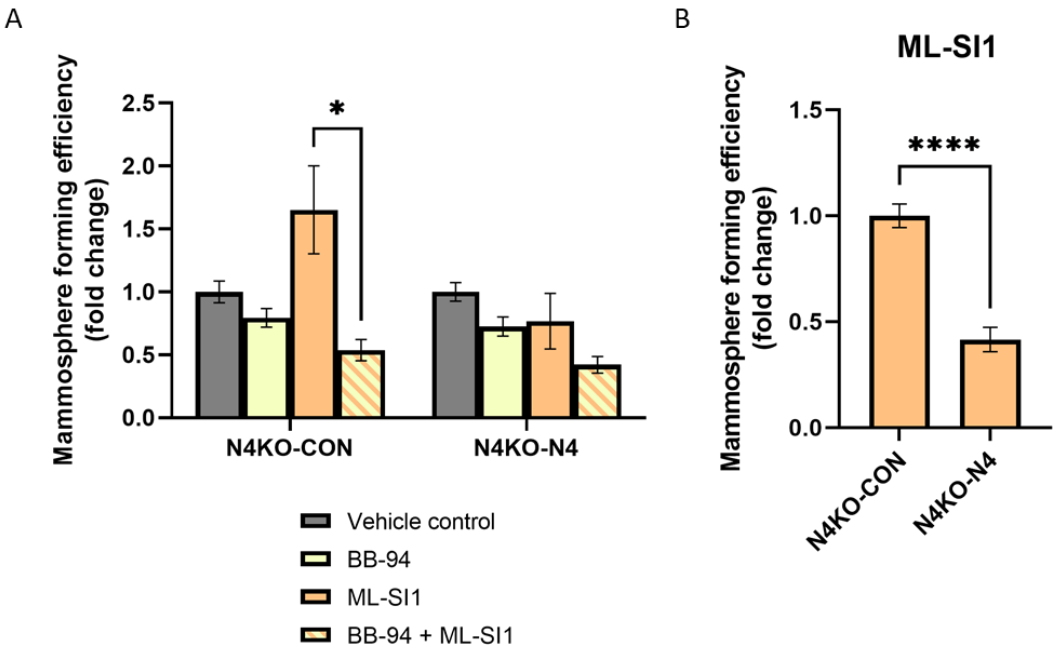

Figure 4-15: Notch4 expressing cells are resistant to the ML-SI1 treatment induced MFE increase in control cells. N4KO-CON and N4KO-N4 cells were treated for 24 hours with vehicle, 10µM Batimastat (BB-94, MMP inhibitor), 50µM ML-SI1 (TRPML inhibitor) or both BB-94 and ML-SI1 and then plated out for mammospheres and counted after 5 days. A) Data plotted relative to vehicle control for each cell line. B) Data plotted relative to vehicle control and N4KO-CON for ML-SI1 treatment. N=3 Statistical tests: Two-way ANOVA with Tukey's multiple comparisons (A). Unpaired t-test (B). *p < 0.05. **p < 0.01. ****p<0.0001.

4.12 BB-94 treatment increases Hey2 gene expression while ML-SI1 increases Hes1 and Hey1 and decreases Hey2 gene expression

MCF7 cells were treated with vehicle, 10µM Batimastat (BB-94, MMP inhibitor), 50µM ML-SI1 (TRPML inhibitor) or both BB-94 and ML-SI1 for 24 hours and then RNA was isolated. The RNA was analysed for gene expression of Notch target genes Hes1, Hey1 and Hey2 and DTX2 and DTX4 by qRT-PCR. BB-94 treatment increased gene expression of Hey2 ($p<0.05$) (Figure 4-16C). ML-SI1 treatment increased Hes1 ($p<0.0001$) and Hey1 ($p<0.0001$) gene expression (Hey1 by 10.8-fold compared to vehicle) (Figure 4-16A+B). It also decreased gene expression of Hey2 ($p<0.01$) (Figure 4-16C). When ML-SI1 is added to BB-94 treatment, the Hey2 gene expression increase reduced to a similar level of reduction as ML-SI1 alone ($p<0.0001$). When BB-94 treatment is added to ML-SI1, the Hes1 gene expression increase reduced down to match the reduction after BB-94 treatment ($p<0.0001$).

BB-94 treatment reduces gene expression of DTX2 and DTX4, as well as in combination (although this did not reach significance), whilst ML-SI1 treatment has no effect on their expression (Figure 4-16D+E).

Taken together, these results indicate that MMP inhibition increases Hey2 Notch target gene signalling. TRPML inhibition increases Hes1/Hey1 Notch target gene signalling and reduces Hey2 Notch target gene signalling. This suggests that Hey2 signalling is reliant on TRPML and Hes1/Hey1 signalling is reliant on MMP (ADAM10/17), and in the absence of each other, the other Notch target genes are upregulated.

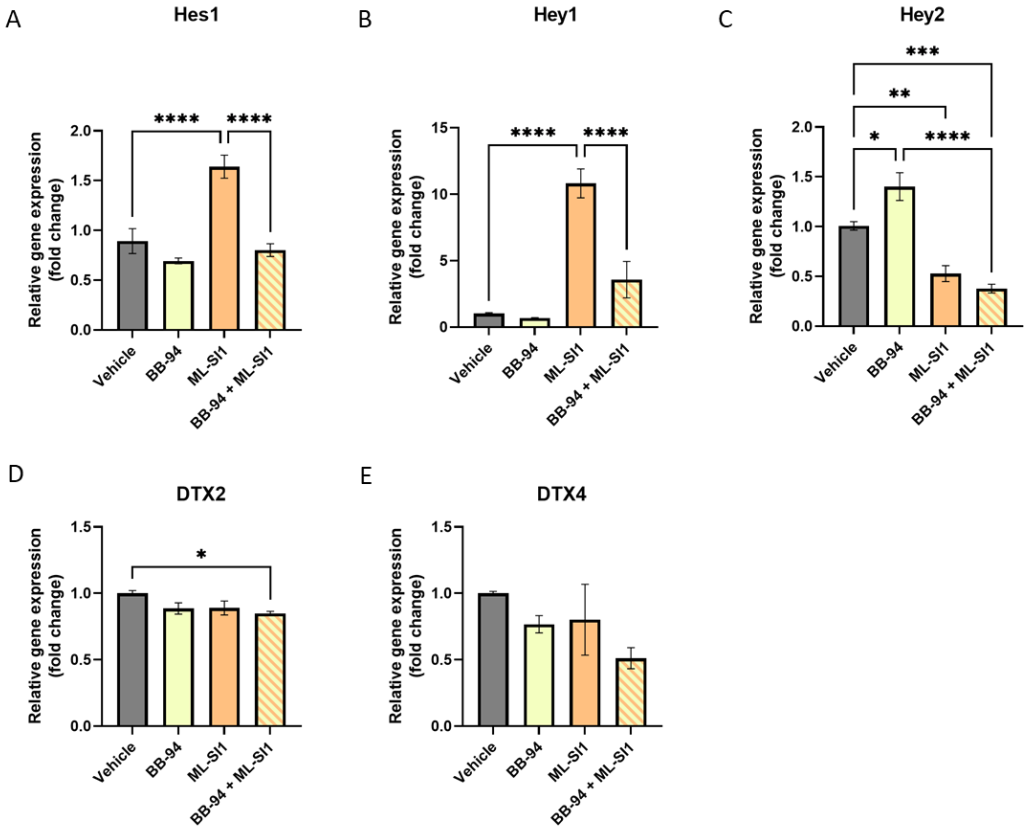

Figure 4-16: BB-94 treatment increases Hey2 expression. ML-SI1 increases Hes1 and Hey1 and decreases Hey2 expression. MCF7 cells were treated for 24 hours with vehicle, 10µM Batimastat (BB-94, MMP inhibitor), 50µM ML-SI1 (TRPML inhibitor) or both BB-94 and ML-SI1. RNA was then taken for qRT-PCR to calculate gene expression of Hes1 (A), Hey1 (B), Hey2 (C), DTX2 (D) and DTX4 (E). N=3. Data are represented as mean ±SEM. Statistical tests: One-way ANOVA with Tukey's multiple comparisons. *p < 0.05. **p < 0.01. ***p<0.001. ****p<0.0001.

4.13 Discussion

The aim of this chapter has been to explore how the Notch4 endocytic signalling pathway relates to Breast Cancer Stem Cell (BCSC) activity and resistance to endocrine therapy. This has been achieved via the creation of a stable Notch4 overexpressing cell line using lentivirus. This stable overexpression increases BCSC activity, Notch target gene expression and resistance to endocrine therapy treatment. Preliminary RNAseq analysis of this cell line has also identified signalling pathways and genes that are associated with increased Notch4 expression. The other aim of this chapter has been to gain new insight into the action and interaction of two inhibitors, the MMP inhibitor BB-94 and the TRPML inhibitor ML-SI1, with Notch4 and its endocytic trafficking. The use of these inhibitors has helped to explore Notch target gene signalling further as well as solidify the link between endocrine therapy resistance and endocytic trafficking. This novel research impacts on resistant and metastatic breast cancers, linking Notch4 and endocytic trafficking to BCSCs and resistance.

The Notch4 knockout cell line that was created prior to this project has some limitations (discussed in section 4.2). However, it had a very low level of Notch4 expression so is used as a reliable “knockdown” of Notch4. It was found to have reduced BCSC activity compared to control, measured by mammosphere forming efficiency and Aldefluor assay. This agreed with Simões et al (Simões, O’Brien, et al., 2015). However, endocrine therapies were not observed to have synergistic effects on BCSC activity, as seen by Simões et al. These differences could be explained by drift in clonality of cell lines over time, as well as a difference in treatment protocols. These problems could be improved in the future with the streamlining and optimisation of protocols and precise use of certain passages of cell lines.

The Notch4 knockout cell line has a large decrease in Hey2 gene expression and an increase in Hes1 and Hey1 gene expression compared to control (summarised in the gene expression schematic diagram below, Figure 4-17). This establishes that Hey2 is the main target gene of Notch4, as when Notch4 is knocked out there is little to no expression. The increase of Hes1 and Hey1 could be explained by the actions of other Notch receptors. Perhaps when Notch4 is not present, they compensate for the reduced Hey2 expression by increasing Hes1 and Hey1 expression. These results may also indicate that Hey2 is not controlled by the other Notch proteins as the decrease is quite dramatic. This could be explored further by observing how the expression of these target genes are affected after knockdown of the other Notch receptors. Some cross-regulation has been observed previously between the Notch1 and Notch4 receptors (James et al., 2014).

Creation of a stable Notch4 cell line was an effective way of studying long term expression of Notch4. The N4KO cell line was used as a parental cell line to create the Notch4 and Control cell lines to ensure that they had a very low endogenous expression of Notch4. The Notch4 overexpressing stable cell line was found to have a higher protein (full length and ICD) and gene expression of Notch4. It also had more surface Notch4 expression, detectable by flow cytometry.

The stable Notch4 overexpression increased gene expression of target genes Hey1 and Hey2, whilst decreasing Hes1. It also decreased expression of DTX1, 2 and 4 (all included in summary Figure 4-17 below). These data, along with results from the N4KO cell line suggest that over the long term (in the case of stable cell lines with increased or decreased expression of Notch4), expression of Notch4 upregulates Hey2 expression and downregulates Hes1 expression. Hey1 is more complicated as the knockout suggests that Notch4 downregulates Hey1 whereas the overexpression suggests Notch4 upregulates it. Perhaps there is a variation on the effect of Hey1 at different levels of Notch4 gene expression. This case of different effects at different expression levels has been explored previously, showing that different expression levels of Notch has different effects on tumourigenic capacity and proliferation of breast cells (Mazzone et al., 2010). Hey1 could be a target gene that is upstream of these different consequences. This could also be explained by different signalling pathways taking over at different levels of Notch4 expression, leading to different target genes being induced. Over long term expression, Notch4 also has a negative effect on the expression of DTX genes.

The stable Notch4 overexpressing cell line was found to have greater BCSC activity, determined by mammosphere assay and Aldefluor assay. However, when analysed by limiting dilution assay, the Notch4 cells were not observed to have greater tumour initiating capacity, instead suggesting that they had similar BCSC activity to control cells. This may be due to the stem-like dormancy of these cells. Three out of five of the mice in one of the groups died unexpectedly in the early stages of the experiment. With these extra data the results could have been different. Although an increase in BCSC activity could be observed in the *in vitro* mammosphere assay, perhaps the level of Notch4 expression in this stable cell line was not enough to observe an increase in BCSC activity *in vivo*. Again, the expression level of Notch4, whether medium or high, can impact the tumourigenicity and proliferation of breast cells (Mazzone et al., 2010).

The tumour initiating rate was the same for both groups of cells until week 4, after which, the control cells had increased growth. This fits with the concept that the Notch4 cells are more stem-like and would be expected to have lower proliferation. Studies have reported that Notch4 cells are quiescent and have a phenotype that includes lower proliferation (Zhou et al., 2020). The Notch4 cells here may be able to lay dormant, repopulate the tumour and potentially lead to metastasis. To investigate if these Notch4 cells did form greater lung metastases, the lungs from the group of mice with the most injected cells were isolated and will be stained for Notch4 and imaged to detect metastases and micro-metastases. This will be done after the completion of this thesis and will provide greater insight into the BCSC activity and metastasis forming ability of Notch4 cells.

Previously, ALDH positive cells have been isolated by FACS and analysed for Notch4 protein expression. The analysis showed that the ALDH+ cells had an increased protein expression of Notch4 compared to the ALDH- cells (Simões, O'Brien, et al., 2015). The results in this thesis are contradictory to this, suggesting no enrichment of Notch4 surface expression in the ALDH+ cells. This could be explained by the fact that we measured the surface expression of Notch4 specifically compared to the total protein levels. The surface Notch4 is thought to represent the active signalling Notch4 receptor compared to total protein level within a cell. Here, the cells have also been transfected with Notch4, compared with untransfected MCF7s in the previous study, suggesting there could be a difference due to the endogenous or transfected expression level of Notch4 in the cells. However, this could be explored further in the future. This would help us to explore the precise interaction between Notch4+ and ALDH+ cells and whether these populations are discrete or overlap.

After treatment with the endocrine therapy fulvestrant over 14 days, it was found that the N4KO cell line had greater susceptibility to treatment compared to control. It was also found that the Notch4 overexpressing cell line showed greater resistance to the same treatment, compared to respective controls. The amount of resistance applied by the Notch4 expressing cell line did not reach that of N4KO's control, but this was to be expected as the N4KO-N4 was not a full "rescue" cell line as it did not reach the Notch4 expression of the parental MCF7 cells (data not shown). Further repeats are needed in order to confirm this resistance.

The RNAseq analysis undertaken on the N4KO-N4 cells to identify genes and pathways that have a particular association with the cell line compared to N4KO-CON was a preliminary analysis due to the fact that there was only one sample of each cell line. Because of this, differentially expressed genes are "putative" and high log2 fold change values are used to

discriminate for genes, to increase confidence in expression changes. A gene signature and Notch-related gene signature for N4KO-N4 were identified and would have to be confirmed in the future. In the Notch related user defined gene set, the reduction of CCND1 expression in the Notch4 cells fits in with the *in vivo* tumour growth results showing that the Notch4 cells have reduced proliferation. The higher level of CDKN1A expression also fits with this as it is an inhibitor of CCND1. CDKN1A is also associated with a higher risk of developing breast cancer (Akhter et al., 2021). From this RNAseq data, signalling pathways, biological processes and molecular functions that have been shown to be associated with the Notch4 cells include the MAPK, TGF-β, HIF-1, Wnt, Hippo and ERK signalling pathways. The Wnt, HIF-1, MAPK and TGF-β signalling pathways have been shown previously to have links to the Notch signalling pathway in breast cancer (Collu & Brennan, 2007; Ercan et al., 2012; L. Han et al., 2014; Mittal et al., 2009), with TGF-β having a link with Notch4 specifically, through Notch4's ability to bind Smad3 which inhibits TGF-β signalling (Sun et al., 2005). The Hippo pathway has been linked to BCSCs and metastasis, providing another link with Notch4 (L. Wu & Yang, 2018). The ERK signalling pathway has been linked to Notch signalling in pancreatic cancer, but not breast (Tremblay et al., 2013).

It was also shown with RNAseq that Notch may have a negative association with estrogen signalling (Rizzo et al., 2008). This negative crosstalk between ER and Notch4 has been observed previously in the lab and this association would suggest that although Notch4 has been extensively linked to ER positive breast cancers, the direct crosstalk between the receptors is a negative feedback.

In this chapter, the use of MMP inhibitor BB-94 (to inhibit the action of ADAM-10) and TRPML inhibitor ML-SI1 (to inhibit endosome-lysosome fusion) has gained insight into the link between Notch4, endocrine resistance and endocytic pathway signalling.

We showed that TAMR and FULVR cells are reliant on TRPML for growth and viability. They are also resistant to the BB-94 induced decrease of MFE in control cells. It can therefore be concluded that ADAM-10 is required for BCSC activity in control cells, but not in TAMR and FULVR cells.

Notch4 expressing cells are linked to TRPML for growth and viability but are not as reliant as the TAMR and FULVR cells are. Notch4 cells are resistant to the ML-SI1 induced increase in MFE in control cells. This shows that without TRPML, control cells increase their BCSC activity, but Notch4 cells do not. This could be the case if their BCSC activity happens through Notch4 and Notch4 requires TRPML for signalling through the endocytic pathway.

Current published data in *Drosophila* shows that BB-94 blocks base level Notch signalling, as well as ligand activated signalling, but not Deltex activated signalling (Shimizu et al., 2014). Our data aligns with this, suggesting that control cells require ADAM-10 for BCSC activity, but Notch4 cells do not. Taken together, this suggests that the Notch4 signalling leading to BCSC activity is DTX activated.

Unpublished previous research showed that ML-SI1 treatment inhibited Deltex driven ligand independent Notch signalling in *Drosophila*, determining that TRPML was required for this signalling (Baron et al, unpublished). Our data aligns with this, suggesting that Notch4 requires TRPML for signalling, highlighting the importance of late endosomal trafficking in Notch4 signalling.

Results from gene signalling experiments indicated that BB-94 and ML-SI1 act in opposing ways on Notch signalling. Hey2 signalling is reliant on TRPML and Hes1/Hey1 signalling is reliant on ADAM10. With the action of each inhibitor blocking each pathway, the other genes that have not been blocked are upregulated in order to compensate for the loss of the other signal. This agrees with the earlier data of Notch4 "knockout" leading to a decrease in Hey2 expression whilst increasing Hes1 and Hey1 expression to compensate. From this, it could be suggested that BB-94 treatment, or ADAM-10 inhibition mimics an increase in a Notch4 signal whereas ML-SI1 treatment, or TRPML inhibition mimics a decrease in Notch4 signal. BB-94 could be acting on the other Notch receptors with potential crosstalk to Notch4.

Further insight could be gained by studying the effect of these inhibitors on Notch4 internalisation by immunofluorescence. In the future, BB-94 and ML-SI1 could even be investigated clinically. ML-SI1 is the more promising due to its effects on viability of endocrine resistant cells suggesting it may have effects countering endocrine resistance clinically.

To summarise the insights gained from inhibitor experiments, Notch4 cells and endocrine resistant cells (that have higher Notch4 levels), need TRPML for growth, viability and BCSC activity. They also don't require ADAM-10 for growth, viability and BCSC activity. Hey2 signalling requires TRPML and Hes1/Hey1 signalling requires ADAM-10. These data together link Notch4, endocytic trafficking, endocrine resistance, BCSCs and Hey2 signalling which are novel insights.

In conclusion, we have created a Notch4 overexpressing cell line which provides novel insights into Notch4 signalling, building on the previous chapter by linking the endocytic pathway signalling to BCSC activity. The Notch4 stable cell line could continue to be used in

the future for further investigations into Notch4, endocrine resistance and BCSCs. The inhibitor experiments have also brought together endocytic trafficking and Notch4, showing that endocrine resistant cells require TRPML for growth, viability and BCSC activity, while not requiring ADAM10. Hey2 is further linked to Notch4, whilst Hes1 and Hey1, although linked, may be downstream of another Notch receptor or pathway. The next chapter will aim to apply these insights on Notch4 signalling clinically, by investigating genomic reasons for its actions, as well as exploring Notch4 mutations found in primary and metastatic breast cancer.

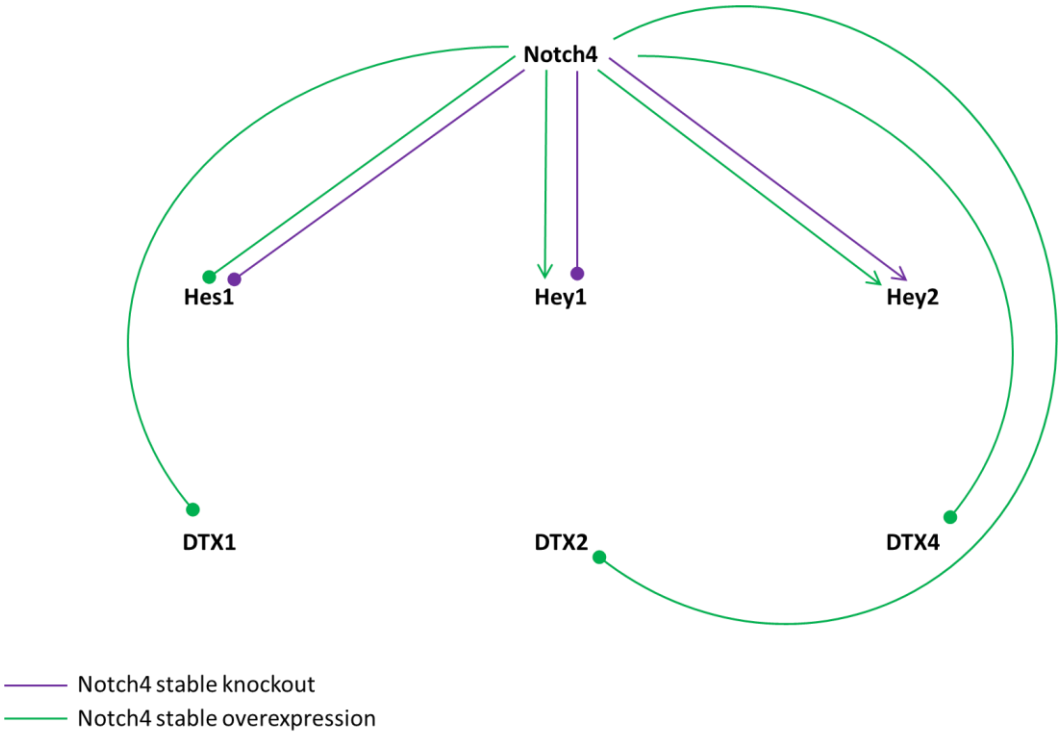

Figure 4-17: Signalling results from stable Notch4 knockout and overexpression experiments to visualise a potential signalling pathway. Schematic includes significant results from gene expression experiments in Chapter 4.

5 Investigating Notch4 mutations in breast cancer

5.1 Introduction

This chapter will focus on Notch4 mutations in *Drosophila* and breast cancer. This will be done by investigating how mutations affect Notch4 signalling and endocytic trafficking. The effects on BCSC activity will also be explored and preliminary gene expression analysis will be undertaken by RNAseq. Altering a residue present in Notch4 that has been studied in *Drosophila* will also add to data in previous thesis chapters to further dissect the Notch4 endocytic trafficking. These insights will aid research into how mutations affect the action of Notch4 in breast cancer, with the possibility of being able to apply this insight into clinical research.

Several databases collate genetic, proteomic and transcriptomic data on patient cancer samples from research studies. The most prominent of these for genomic data is cBioPortal, which is coordinated by the Broad Institute (Cerami et al., 2012; Gao et al., 2013). Others include the National Cancer Institute GDC Data Portal (Grossman et al., 2016), COSMIC (Tate et al., 2019) and Tumour Portal (Lawrence et al., 2014). Mutational information for all genes in any cancer of choice can be accessed in these databases and they were used to methodically search for mutations in Notch4 in breast cancers.

The Notch AxE2 mutant studied in *Drosophila* has a mutation which alters a histidine residue to a tyrosine in the Abruptex (Ax) region. This makes Notch act in a Deltex dependent way, which may be ligand independent (T. Xu & Artavanis-Tsakonas, 1990). Notch4 has this residue change in its endogenous wild-type protein sequence, diverging from Notch1/2/3. For this reason, it was hypothesised that Notch4 may act in a ligand independent/ Deltex dependent manner and signal via the endocytic pathway. This was investigated in Chapter 3 and it was established that Notch4 can signal via an endocytic pathway and that DTX1, 2 and 4 are involved. It was also confirmed in Chapter 4 that Notch4 is highly involved in BCSCs and endocrine resistance and this resistance is reliant on endocytic trafficking. Our hypothesis is that this unique endocytic signalling involving DTX and leading to BCSC upregulation and endocrine resistance is due to this Ax domain residue in Notch4 being different to the equivalent residue in Notch1/2/3.

The ligand binding domain of Notch is present between EGF repeats 8 and 12. Different ligands bind to different EGF repeats. This has been studied previously by resolving portions of the crystal structure of Notch1 bound to JAG1 or DLL4 and it was found that EGF repeats 8 and 12 of Notch1 are required for JAG1 binding and 11 and 12 for DLL4 binding (Luca et al.,

2015, 2017). Due to this it can be determined that EGF repeat 12 is required for the binding of most ligands to Notch. The ligand binding domain of Notch1 corresponds to the same EGF repeats of Notch4. The ligand binding domain of Notch in *Drosophila* has been even more extensively studied (Whiteman et al., 2013).

Gain of function mutations, which allow Notch to possess a new molecular function leading to an altered gene expression pattern, have been observed in Notch genes in various cancers including T-ALL, NSCLC and breast cancer (Mutvei et al., 2015). In breast cancer, mutations specifically in the PEST domain of Notch have been found to increase Notch stability, activity and therefore signalling (K. Wang et al., 2015). We have hypothesised that in breast cancer, mutations in Notch4 could increase its signalling and exacerbate its effects on BCSC activity and therefore increase resistance to therapy.

Using site-directed mutagenesis, this chapter will investigate the effect of Notch4 mutations found in breast cancers, a ligand binding disruption mutation, and the “reverted residue” mutation in the Abruptex region. The effect of these mutations on the signalling of Notch4 will be explored, as well as its trafficking activities, gene expression signatures and further effects on BCSC activity.

5.2 Identification of Notch4 mutations in breast cancers using genomic databases

Publicly available genomic databases were searched for all Notch4 mutations found in breast cancer. These databases included cBioPortal, The Cancer Genome Atlas (TCGA) and National Cancer Institute Genomic Data Commons (NCIGDC). Additional studies not accessible on these databases were also included. 24 studies were included overall and data from 10,011 primary breast cancer samples and 4028 metastatic breast cancer samples was analysed.

The frequency of mutations and their genomic location was mapped along the Notch4 protein length, compared to the schematic of the Notch4 domains (Figure 5-1). Overall, 190 samples contained at least one mutation in Notch4 with 2.89% of primary samples containing a mutation (97 out of 10,011) and 3.84% of metastatic samples (93 out of 4028). This indicates an increase in mutation frequency in Notch4 in metastatic samples, indicating these mutations may contribute towards the progression and metastasis of breast cancer. In primary breast cancer samples, Notch4 mutations were mostly clustered to the EGF repeats region in the extracellular domain of the receptor. In metastatic samples there were less EGF repeat mutations but more frequent PEST domain mutations. A mutation of key note with a particularly high frequency in the metastatic samples was the mutation E1836K/Q in the PEST domain. The PEST domain of Notch is a region of importance to the stability of the protein. Mutations or deletions in this area have been linked with increased stability and activity of the protein (K. Wang et al., 2015). The increase in this type of mutation in Notch4 could lead to a higher level of Notch signalling, which could drive the metastatic process.

Mutations found exclusively within the EGF repeats of Notch4 were plotted onto the typical structure of an EGF domain with conserved residues across Notch receptors illustrated. These mutations are separated into mutations found in primary and metastatic breast cancers and the EGF repeat that the mutation is found in is also included (Figure 5-2). Mutations found in the ligand binding domain are shown in red and those found in the Abruptex domain are in green. Mutations used later in the chapter are circled.

A


NOTCH4 structure
EGF repeats
LNRs
TMR
RAM
ANK
PEST

B

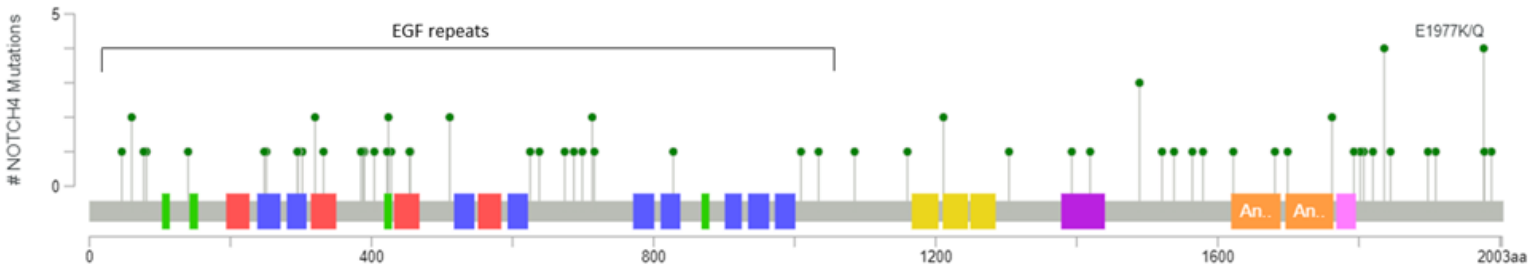
Primary breast cancer
NOTCH4 Mutations
5
0
EGF repeats
E1977K/Q
An..
An..
0
400
800
1200
1600
2003aa

C

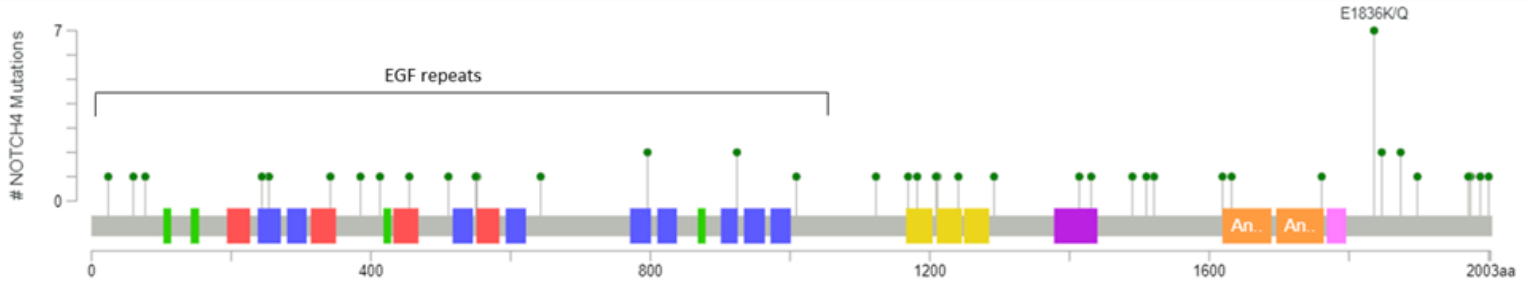
Metastatic breast cancer
NOTCH4 Mutations
7
0
EGF repeats
E1836K/Q
An..
An..
0
400
800
1200
1600
2003aa

Figure 5-1: Notch4 mutations in breast cancer. Open access databases including cBioPortal and COSMIC cancer browser were searched for all Notch4 mutations in breast cancer. 24 studies were investigated overall, with 14,039 breast cancer tumours analysed between them, 10,011 primary and 4028 metastatic. 190 of these samples contained a mutation in the Notch4 gene, with 2.89% of primary samples containing a mutation and 3.84% of metastatic samples. Mutations were plotted across the Notch4 structure using cBioPortal's mutation mapper (B+C). A) Schematic of Notch4 protein structure, showing domains. LNR (Lin-12/Notch repeats), TMR (Transmembrane Region), RAM (RBP-Jkappa-associated module), ANK (Ankyrin repeats). Domains in B and C correspond to the domains in A directly above.

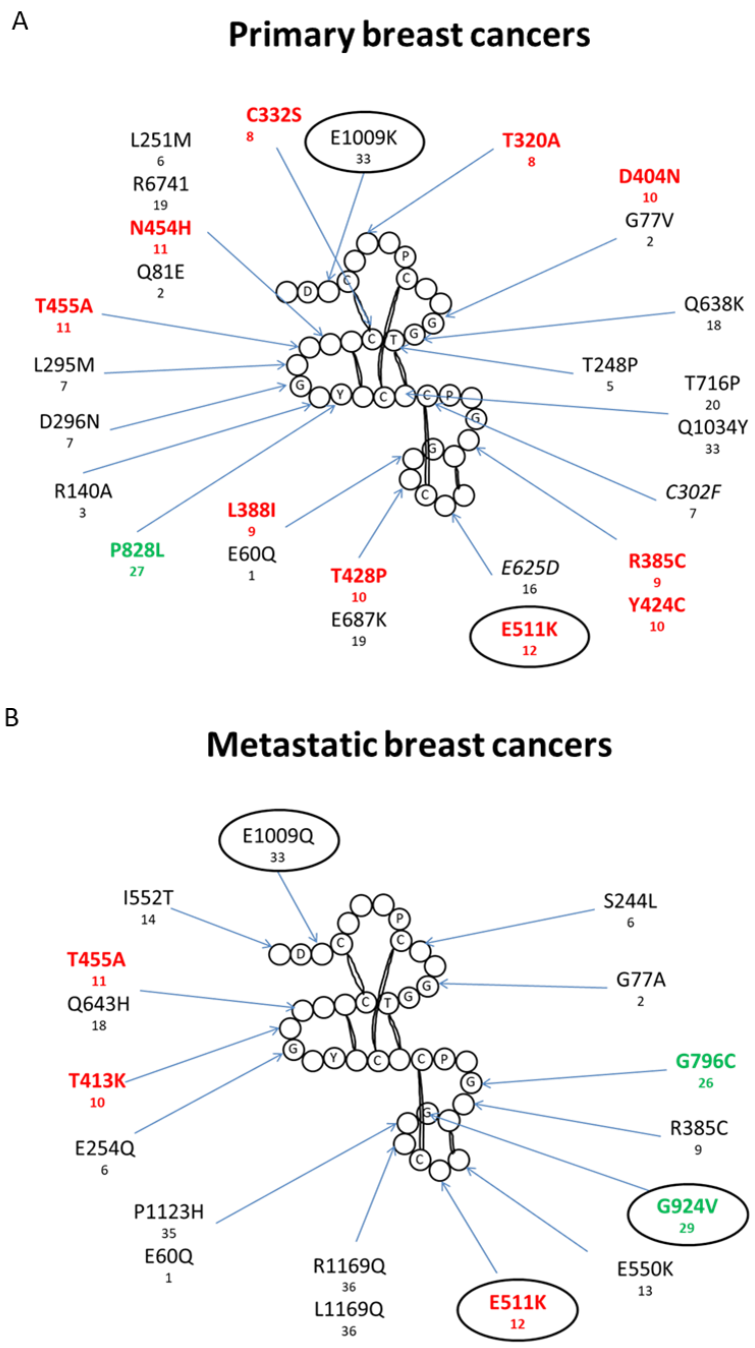

Figure 5-2: Notch4 mutations in primary and metastatic breast cancers mapped to a model EGF repeat peptide sequence. Conserved consensus residues between EGF repeats and key disulphide bonds are included in the diagram. Red corresponds to mutations in the ligand binding domain, EGF repeats 8-12. Green corresponds to mutations in the Abruptex region, EGF repeats 24-29. The number below the mutation is in which EGF repeat it is found. Mutations that are circled were used for further investigation.

5.3 Generation of Notch4 mutations using site-directed mutagenesis

Notch4 possesses a key tyrosine residue in the Abruptex domain at amino acid position 914 which differs from the equivalent histidine residue in *Drosophila* Notch and mammalian Notch 1, 2 and 3 (Sequence alignment in Figure 5-3). In *Drosophila* Notch mutation studies, that residue change leads to Notch signalling in a ligand independent and Deltex dependent way.

Figure 5-3: Amino acid sequence alignment of part of EGF 29 in the four human and *Drosophila* Notch proteins showing the key Y914 residue in Notch4 that will be mutated to match the conserved Histidine residue.

In order to study whether this residue is the reason that Notch4 signals in an endocytic pathway manner, the wild-type NOTCH4 gene in the plasmid used previously was mutated using site-directed mutagenesis. The codon that encodes a tyrosine at amino acid position 914 (TAT) in the wild-type Notch4 gene was changed to a codon that encodes a histidine (CAC) (Y914H).

Site-directed mutagenesis was also carried out to separately introduce five additional residue changes in the Notch4 gene, to generate five mutant versions of the Notch4 plasmid. These mutations are illustrated across the protein domain structure of Notch4 (Figure 5-4A). The mutations were chosen to test the functional consequences of certain mutations and to study any differences they caused in Notch4 signalling and activity (Figure 5-4B). For example, L491A was chosen to test its effect on the function of the ligand binding domain of Notch4 as it is a mutation of a conserved residue in EGF repeat 12. The equivalent residue has been identified and investigated in *Drosophila* and has been shown to be essential for ligand binding (Baron et al, unpublished) (Whiteman et al., 2013). The remaining four were discovered in breast cancer samples (Figure 5-1). E511K was chosen as it was found in multiple primary and metastatic breast cancers and changes a negatively charged residue to

a positive charge, therefore potentially having an impact on the structure of the protein (Figure 5-2). G924V is a mutation found in two metastatic breast cancer samples (and no primary samples). It is within the Abruptex region, very close to the key tyrosine residue (Y914). The endogenous glycine is also a consensus residue for the EGF domain structure. E1009Q was chosen due to its proximity to Y914 and because it is within the Abruptex domain, as well as because it is found in primary and metastatic breast cancer samples. Finally, the E1836K mutation within the PEST domain was chosen as it was found at high frequency in metastatic breast cancer samples and may be a stabilising mutation as it is within the PEST domain. Interestingly, this mutation reverts the Notch4 glutamic acid residue to a lysine to match Notch1, 2 and 3.

Following site-directed mutagenesis and sequencing to confirm the presence of required mutations, the mutated plasmids were then expanded ready for use.

A

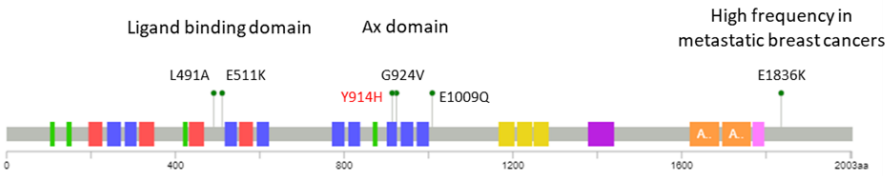

B

Mutation	Location	Role
L491A	EGF repeats (ligand binding domain)	Knocks out ligand binding domain
E511K	EGF repeats (ligand binding domain)	• Found in multiple primary and metastatic breast cancers • Puts a positive charge where is originally a negative
G924V	EGF repeats (Ax domain)	• Found in two metastatic breast cancers • Close to Y914 • Consensus residue for EGF structure
E1009Q	EGF repeats	• Found in primary and metastatic samples • At the very end of Ax region
E1836K	PEST domain	• Found in high frequency in primary and particularly metastatic breast cancers • Reverting to match Notch1,2,3
Y914H	EGF repeats (Ax domain)	Reverting the "ligand independent" residue from Drosophila studies to match WT Drosophila Notch (and mammalian Notch1,2,3)

Figure 5-4: Mutations targeted in site-directed mutagenesis. Six mutations were chosen to be targeted in site-directed mutagenesis experiments. A) Notch4 mutations for site-directed mutagenesis plotted along the schematic of domains of Notch4. Plotted using cBioPortal's mutation mapper. B) Details of each mutation, its domain location in Notch4 and the roles that the mutations investigate.

To study the Notch4 mutations, the plasmids containing the mutated Notch4 gene were transiently transfected into MCF7 cells as described previously. In order to confirm that the transfected mutated Notch4 was signalling, protein and RNA was collected 24 hours after transfection and analysed by western blot and qRT-PCR, respectively. Transfection with all six mutated Notch4 plasmids increased the protein expression of Notch4, compared to untransfected (Appendix Figure 8-4). Notch4 gene expression was also significantly increased after all transfections, compared to untransfected (Figure 5-5). This increase differed between mutations compared to WT Notch4. The protein expression of all six mutations is very similar, so this change is likely to be due to the action of the mutation on downstream Notch4 gene expression. The Y914H "reversion" mutation increased Notch4 gene expression compared to WT by approximately 2-fold. G924V and E1009Q mutations also had a higher Notch4 expression than WT. L491A, E511K and E1836K mutations had a lower Notch4 expression than WT, although all were more than 2000-fold higher than untransfected.

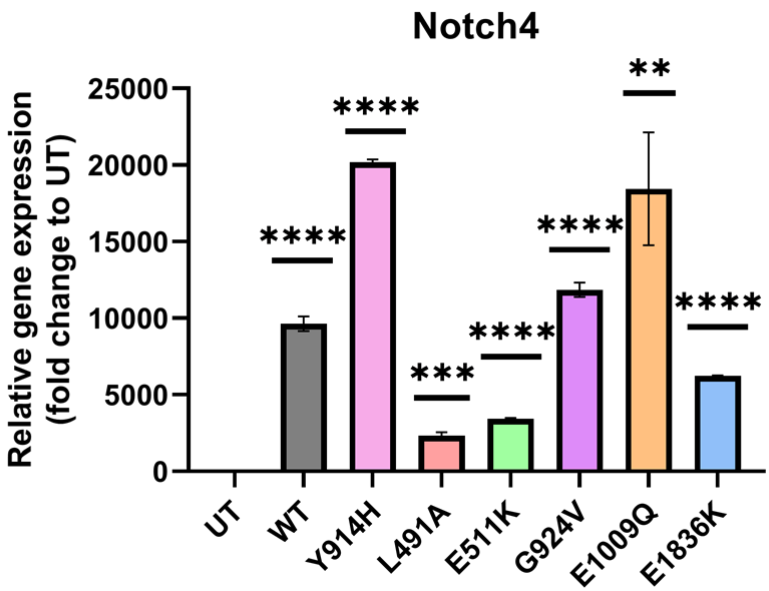

Figure 5-5: Transient transfection of plasmids containing mutated Notch4 genes leads to increased gene expression of Notch4. MCF7 cells were transiently transfected with a plasmid containing WT Notch4 or Notch4 with one of six mutations. After 24 hours, RNA was extracted. Relative gene expression of Notch4 in transfected cells, analysed by qRT-PCR, plotted relative to untransfected control. Data are represented as mean ±SEM. Statistical tests: Unpaired t tests. **p < 0.01. ***p<0.001. ****p<0.0001. N=3.

5.4 Y914H mutation of Notch4 gene reduced colocalisation of Notch4 ICD and ECD and reduced the full length Notch4 presence in the endocytic trafficking pathway

In chapter 3, it was found that Notch4 is present as a full length protein within MCF7 cells and inside early endosomes, late endosomes and lysosomes. From this, it was concluded that it is trafficked through the endocytic pathway for signalling. To investigate how the Y914H Notch4 mutation affects this trafficking action, wild-type (WT) and Y914H Notch4 plasmids were transiently transfected into MCF7 cells before being fixed and stained with Notch4 ICD antibody (green) and Notch4 ECD antibody (red) and visualised with permeabilised immunofluorescence. WT Notch4 ICD and ECD colocalised throughout the cell as observed by punctate dots of yellow (Figure 5-6A). However, Y914H Notch4 does not. There is little to no colocalisation of Notch4 ICD and ECD and most Notch4 can be observed as separate areas of green (Notch4 ICD) and red (Notch4 ECD) (Figure 5-6B). This colocalisation was analysed as described previously using the "coloc" function of the Imaris software (Figure 5-8A+B+C). The Pearson's correlation calculated for the whole image was significantly reduced in the Y914H Notch4 compared to wild-type ($p<0.05$) (Figure 5-8A). This quantification corroborates the reduced colocalisation that can be observed in the images with Y914H mutated Notch4.

Next, it was investigated whether the Y914H mutation altered the cellular distribution of Notch4. Compared to wild-type Notch4, very little Notch4 was colocalised with EEA1 antibody and CD63 antibody (Figure 5-7A+B). If any, it is the ECD portion of Notch4 that colocalises. This indicates that little to no Notch4 was located in the early or late endosomes. There is some colocalisation between Notch4 ICD and LAMP1 and also between Notch4 ECD and LAMP1 (Figure 5-7C). This suggests that although mostly the Notch4 ICD and ECD were separate within the cell, some of both parts could be found in lysosomes. However, these areas of colocalisation are greatly reduced compared to that observed using wild-type Notch4. This colocalisation was again quantified using the "surface" function of Imaris to represent the compartment and the intensity of the full length Notch4 channel within the compartment was measured (Figure 5-8D+E+F). No change in amount of full length Notch4 in early endosomes, late endosomes or lysosomes was observed (Figure 5-8F).

Taken together, these data indicate that the Y914 residue of Notch4 is a key residue for the endocytic pathway signalling action of Notch4. When this residue is altered so that it matches

Notch 1, 2 and 3, the endocytic pathway signalling is reduced and full length is Notch4 found within the cell at a lower rate.

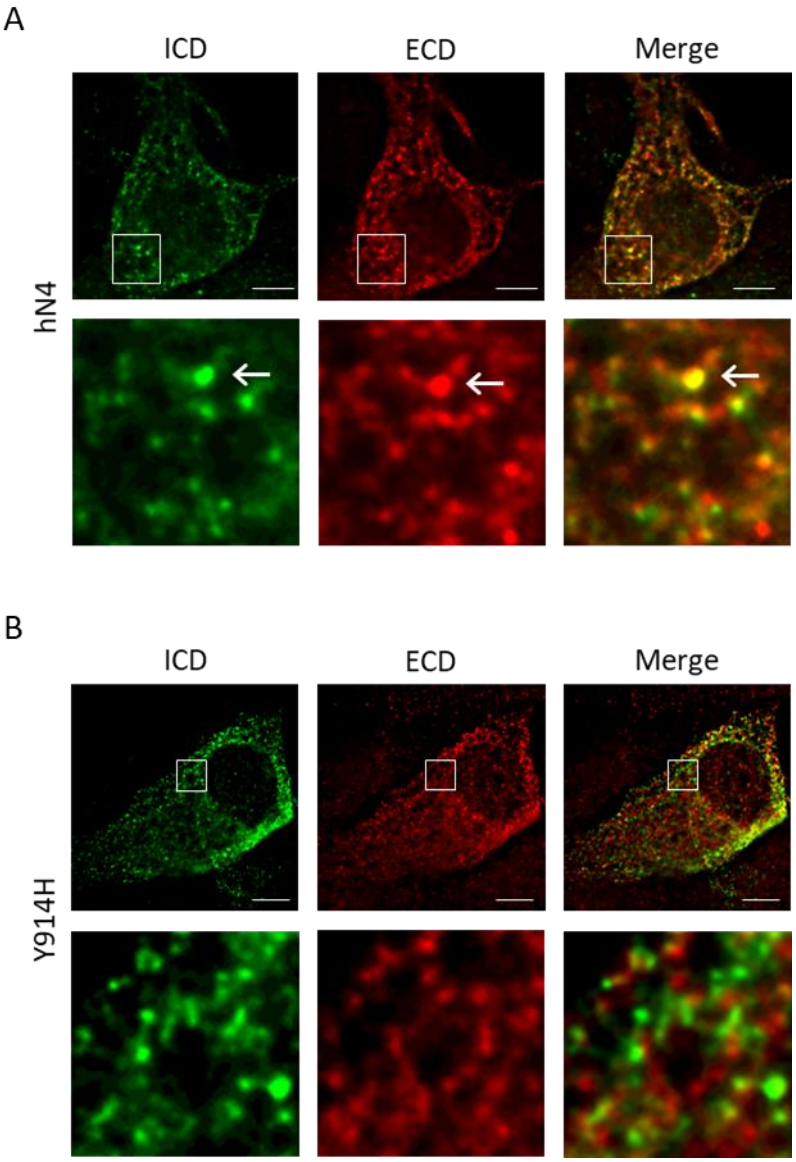

Figure 5-6: Y914H mutation of Notch4 reduced colocalisation of Notch4 ICD and ECD within the cell. Immunofluorescence images of MCF7 cells transiently transfected with a WT Notch4 plasmid (A) or a Notch4 plasmid with a mutation at Y914H (B). Images show Notch4 ICD (green), Notch4 ECD (red) and a merge of the three channels to demonstrate colocalisation. Areas of key colocalisation are indicated with arrows. Areas zoomed in to show detail in higher magnification, indicated by the white squares. Scale bars: 5µm.

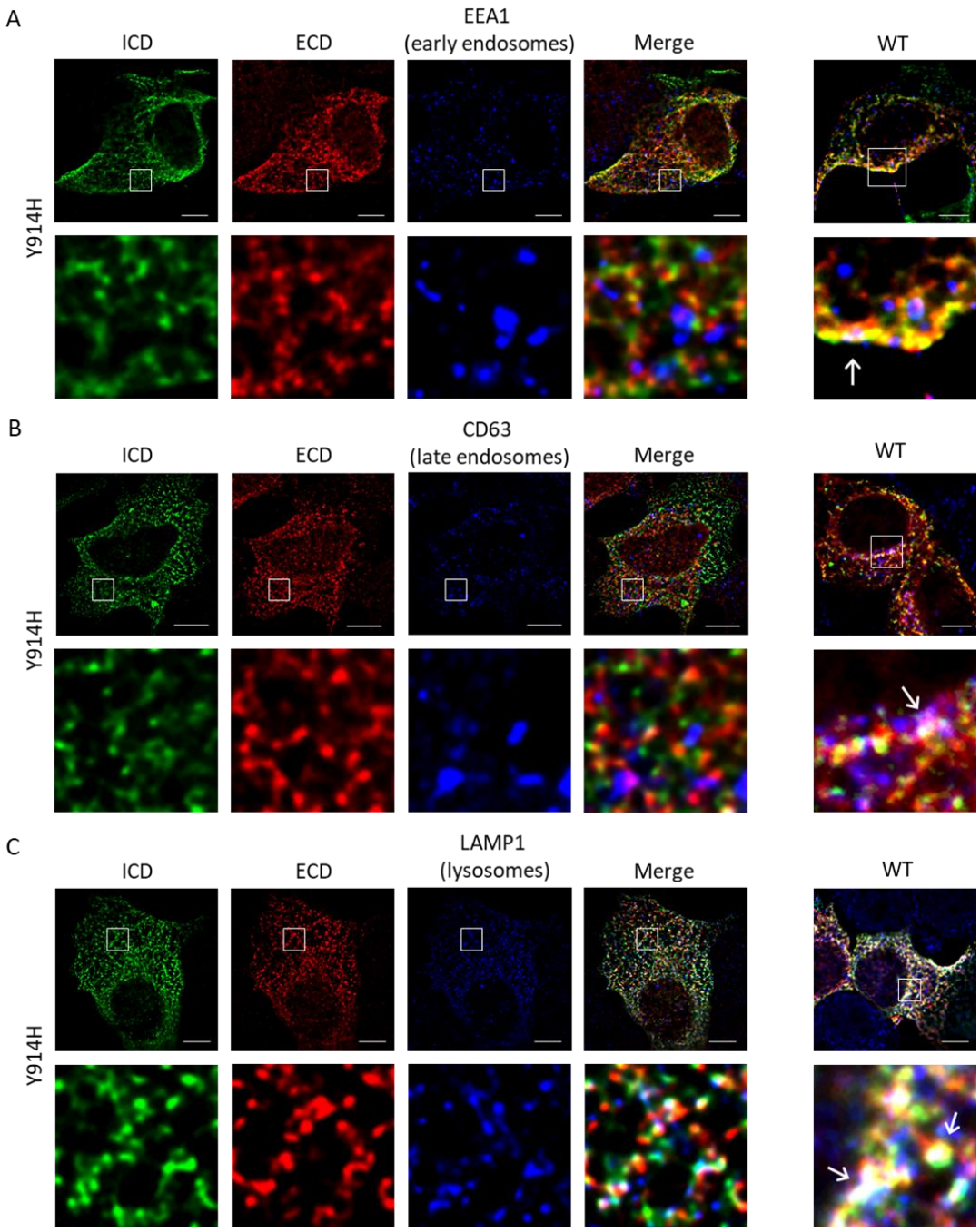

Figure 5-7: Immunofluorescence images of MCF7 cells transiently transfected with a Notch4 plasmid with a Y914H mutation. Images show Notch4 ICD (green), Notch4 ECD (red) and EEA1- early endosomes (blue) (A), CD63- late endosomes (blue) (B), LAMP1- lysosomes (blue) (C) and a merge of the three channels to demonstrate colocalisation. Areas of key colocalisation are indicated with arrows. Areas zoomed in to show detail in higher magnification, indicated by the white squares. Scale bars: 5µm. Panels from WT Notch4 from Figure 3-7 are shown for comparison.

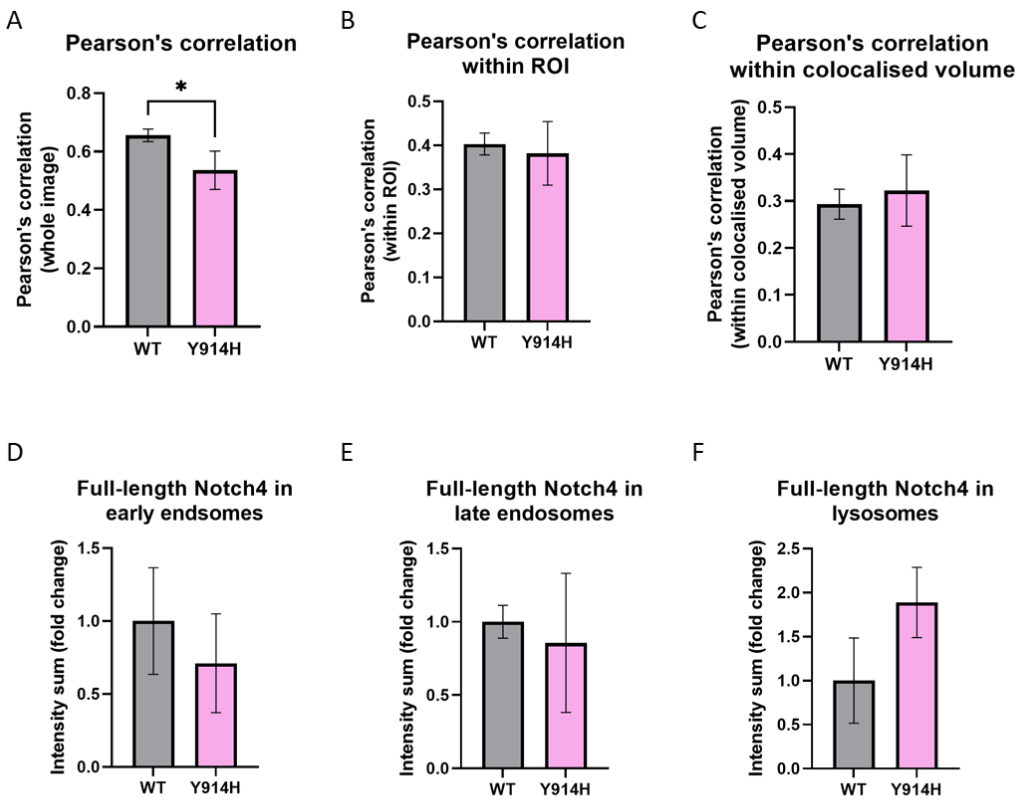

Figure 5-8: Quantification of ICD and ECD colocalisation and amount of full length Notch4 in endosomal compartments with WT and Y914H mutated Notch4. A+B+C) Pearson's correlation of colocalisation between Notch4 ICD and ECD channels in the whole image (A), within a defined Region of Interest (ROI) (B), and within the colocalised volume (C). D+E+F) Data intensity sum of full-length Notch4 within "surfaces" created to represent the endosomal compartments early endosomes (D), late endosomes (E) and lysosomes (F). Data are represented as mean ±SEM. Statistical tests: Unpaired t tests. *$p < 0.05$. A+B+C) N=7. D+E) N=3. F) N=2.

5.5 Y914H Notch4 gene mutation increased Notch4, Hey2 and DTX1 gene expression and decreased Mammosphere Forming Efficiency

Transiently transfecting MCF7s with wild-type Notch4 (Chapter 3) increased Hes1, Hey1 and Hey2 gene expression. To study the effect of the Y914H mutation on Notch4 signalling, RNA taken after transiently transfecting with WT or Y914H Notch4 was analysed for gene expression of Notch4, Notch target genes Hes1, Hey1 and Hey2, and DTX genes. Compared to wild-type, the Y914H mutant increased Notch4 gene expression ($P<0.0001$) (Figure 5-9A). It also increased Hey2 gene expression ($p<0.01$), but not Hes1 or Hey1 (Figure 5-9B+C+D). DTX2 and DTX4 gene expression was unchanged, but DTX1 was increased in the Y914H mutant ($p<0.05$) (Figure 5-9E+F+G). Taken together, these data suggest that reverting the ligand independent linked tyrosine residue in Notch4 to a histidine to match Notch1, 2 and 3 increases gene expression of Notch4, Hey2 and DTX1.

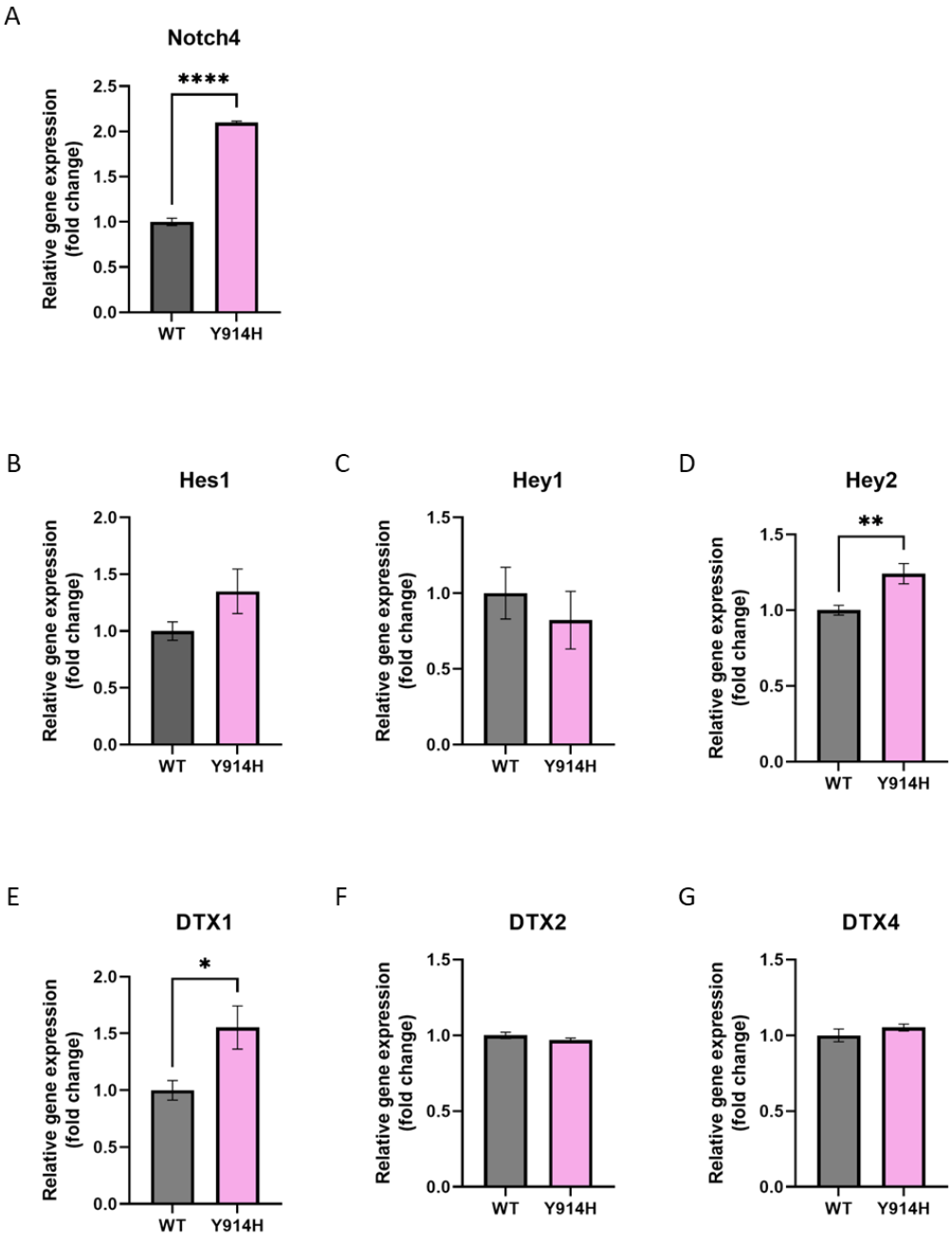

Figure 5-9: Y914H mutation of Notch4 increased Notch4, Hey2 and DTX1 gene expression, compared to WT Notch4. MCF7 cells were transiently transfected with WT or Y914H mutant Notch4, lysed for RNA after 24 hours and gene expression was analysed. Relative gene expression of Notch4 (A), Hes1 (B), Hey1 (C), Hey2 (D), DTX1 (E), DTX2 (F) DTX4 (G). N=3. Data are represented as mean ±SEM. Statistical tests: Unpaired t-tests. *p < 0.05. **p < 0.01. ****p<0.0001.

Following transfection with Y914H mutant and wild-type Notch4, MCF7 cells were plated out for a mammosphere assay to measure BCSC activity. It was found that compared to wild-type Notch4, the Y914H mutant Notch4 had slightly decreased mammosphere forming efficiency, although this did not reach significance (p=0.16) (Figure 5-10). This suggests that reverting the histidine found in Notch4 to a tyrosine which is found in Notch1/2/3 reduces Notch4's BCSC activity action.

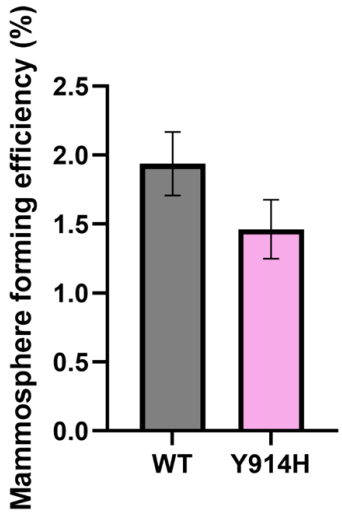

Figure 5-10: The Notch4 mutant Y914H slightly reduced mammosphere forming efficiency of MCF7 cells (compared to WT Notch4). Mammosphere forming efficiency of MCF7 cells transiently transfected with WT or Y914H mutant Notch4. N=3. Data are represented as mean ±SEM. Statistical test: Unpaired t-test.

5.6 Notch4 gene mutations affect Notch4 ICD and ECD colocalisation

Notch4 gene mutations that are found in breast cancers were mapped along the Notch4 domain structure and EGF repeat structure (Figure 5-1 and 5-2). Four of these mutations were selected, along with a mutation that blocks ligand binding in *Drosophila* (Baron et al, unpublished) (Whiteman et al., 2013) and plasmids containing the mutated Notch4 genes were created (Figure 5-4). To investigate how these mutations affect the Notch4 ICD and ECD colocalisation, the mutated plasmids were transiently transfected into MCF7 cells. These cells were fixed and stained for Notch4 ICD (green) and Notch4 ECD (red) (Figure 5-11). By eye, compared to wild-type, L491A and E511K mutations increase the colocalisation between Notch4 ICD and ECD, suggesting increased levels of full length Notch4 within the cell (Figure 5-11B+C). Some colocalisation between Notch4 ICD and ECD can be observed in the G924V mutant Notch4, although most of the staining shows separate green and red, indicating separate Notch4 ICD and ECD (Figure 5-11D). A similar situation can be observed with the E1009Q Notch4 mutant, although with more colocalisation, reaching a similar level of colocalisation to WT Notch4 (Figure 5-11E). In the E1836K mutated Notch4 image, the Notch4 is distributed within the cell more infrequently, with lots of colocalisation between ICD and ECD and very punctate dots, but with more space between the areas of full length Notch4 (Figure 5-11F).

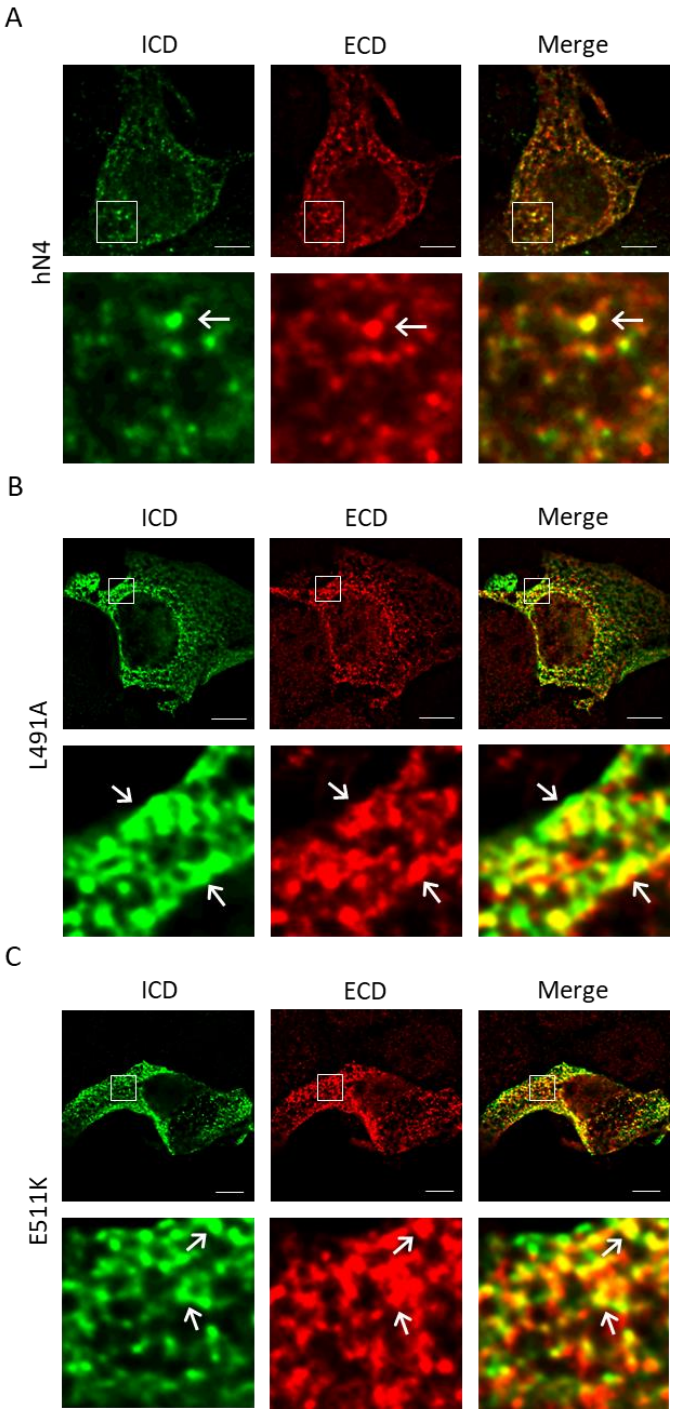
A
ICD
ECD
Merge
hN4
B
ICD
ECD
Merge
L491A
C
ICD
ECD
Merge
E511K

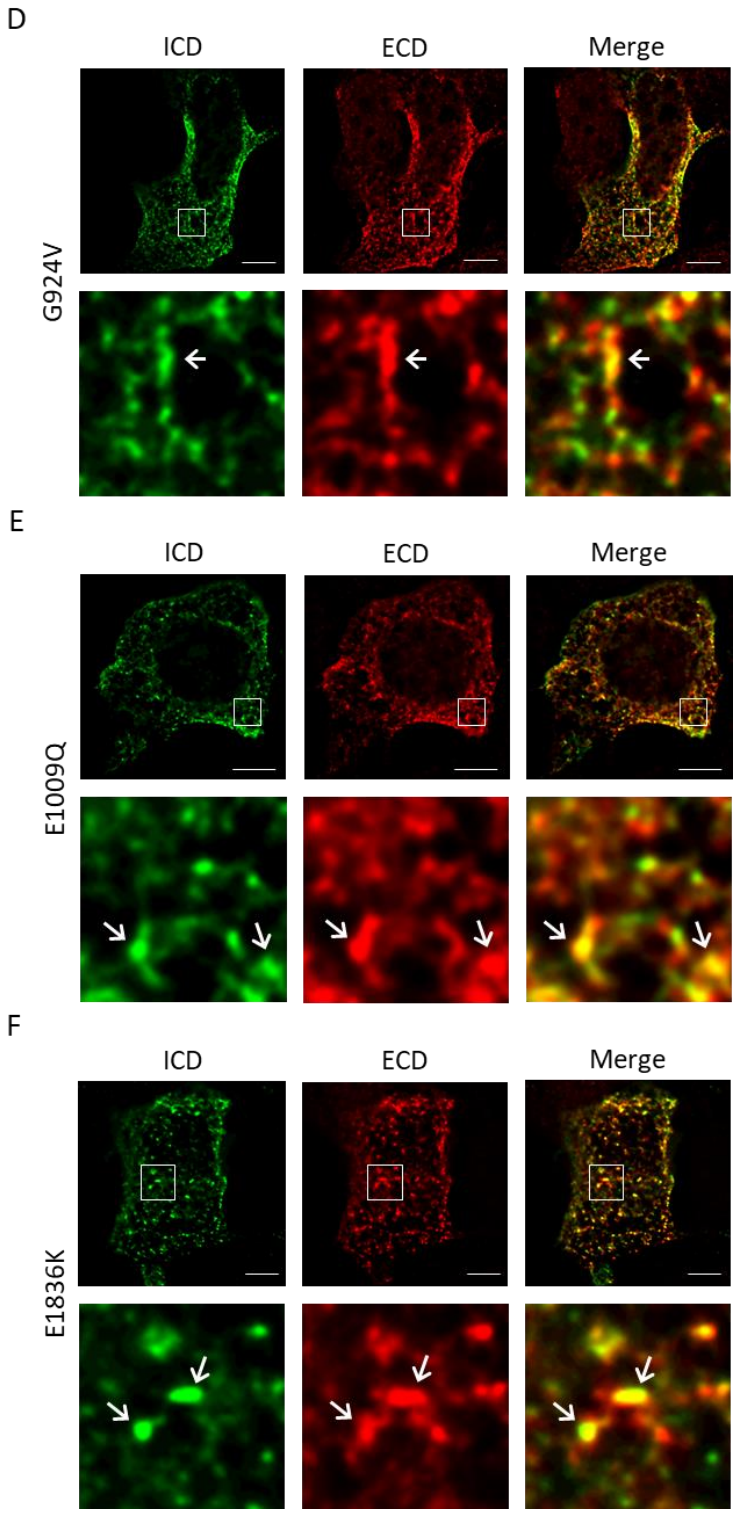

Figure 5-11: Notch4 mutations affect Notch4 ICD and ECD colocalisation. Immunofluorescence images of MCF7 cells transiently transfected with a WT Notch4 plasmid (A) or a Notch4 plasmid with a mutation at L491A (B), E511K (C), G924V (D), E1009Q (E), or E1836K (F). Images show Notch4 ICD (green), Notch4 ECD (red) and a merge of the three channels to demonstrate colocalisation. Areas of key colocalisation are indicated with arrows. Areas zoomed in to show detail in higher magnification, indicated by the white squares. Scale bars: 5µm.

5.7 Notch4 mutations affect full length Notch4 location in the endocytic trafficking pathway

As well as investigating the ICD and ECD colocalisation of the Notch4 mutants, they were also analysed for endocytic pathway location. MCF7 cells were stained with Notch4 ICD (green), Notch4 ECD (red) and EEA1/ CD63/ LAMP1 (blue), to stain for early endosomes, late endosomes, and lysosomes, respectively. The location of Notch4 within these compartments was compared to that of wild-type Notch4 (Figure 5-12).

With L491A mutant Notch4, there was little to no colocalisation observed between Notch4 ICD or ECD and EEA1. This was the same with CD63, although some colocalisation was observed between Notch4 ICD, ECD and LAMP1. Compared to WT Notch4, this is a reduced level of Notch4 found in all endocytic compartments, suggesting that the L491A mutant Notch4, which disrupts ligand binding, is not internalised into the endocytic pathway (Figure 5-12A+B+C).

The ICD and ECD of E511K mutant Notch4 had extensive colocalisation with the LAMP1 antibody, indicating that full length E511K Notch4 can be found in the lysosomes. There is a small amount a full length colocalisation with EEA1, and little to no colocalisation with CD63. This is greatly reduced in both cases compared to WT Notch4 (Figure 5-12D+E+F). These data suggest that the E511K mutant Notch4, found in breast cancers, is internalised into the endocytic pathway into lysosomes and also early endosomes, although at reduced rate compared to WT.

The G924V mutant Notch4 showed reduced early endosome and late endosome colocalisation compared to WT, although certain areas of full length Notch4 colocalised with CD63 (Figure 5-12G+H). This mutant had altered LAMP1 colocalisation compared to WT. The ICD portion of Notch4 extensively colocalised with LAMP1 (cyan areas in Figure 5-12I). There are also distinctive areas of Notch4 ECD colocalisation with LAMP1 (pink areas) as well as some full length Notch4 colocalisation. This suggests that G924V Abruptex domain mutated Notch4 is mostly located within the lysosomes, both as a full length protein and also in its cleaved form. This is a big change to the ICD localisation, and has similar effects to that of the Y914H reverted mutation.

The full length E1009Q Notch4 mutant has limited colocalisation with EEA1, although some colocalisation can be observed between Notch4 ECD and EEA1 (pink areas in Figure 5-12J). Little to no Notch4 colocalisation can be observed with CD63. However, there is extensive colocalisation between E1009Q mutant Notch4 and LAMP1, in both its full length version and

also the ICD form (Figure 5-12J+K+L). These data suggest that this mutant has similar effects on Notch4 localisation in the cell to that of the Y914H mutant.

E1836K PEST domain mutation of Notch4 altered mainly the full length Notch4 distribution. There were some areas of colocalisation with EEA1. CD63 and LAMP1 staining was limited in this situation, although when present, colocalisation with full length E1836K Notch4 was observed in both cases (Figure 5-12M+N+O). This indicates that whilst altering the cellular distribution of Notch4, the E1836K mutation in Notch4 does not reduce its presence in early endosomes, late endosomes and lysosomes.

The colocalisation was quantified as described previously, calculating Pearson's correlation for ICD and ECD colocalisation and intensity sum for amount of full length Notch4 within endocytic compartments (Figure 5-13). The E1009Q mutation significantly increased Pearson's correlation for Notch4 ICD and ECD in the whole image compared to wild-type ($p<0.05$) (Figure 5-13A), whilst E511K, G924V, E1009Q and E1836K mutations increased ROI Pearson's and colocalised volume Pearson's (Figure 5-13B+C). The G924V mutation increased full length Notch4 presence in early endosomes and lysosomes compared to wild-type Notch4 ($p<0.01$, $p<0.05$) (Figure 5-13D+F).

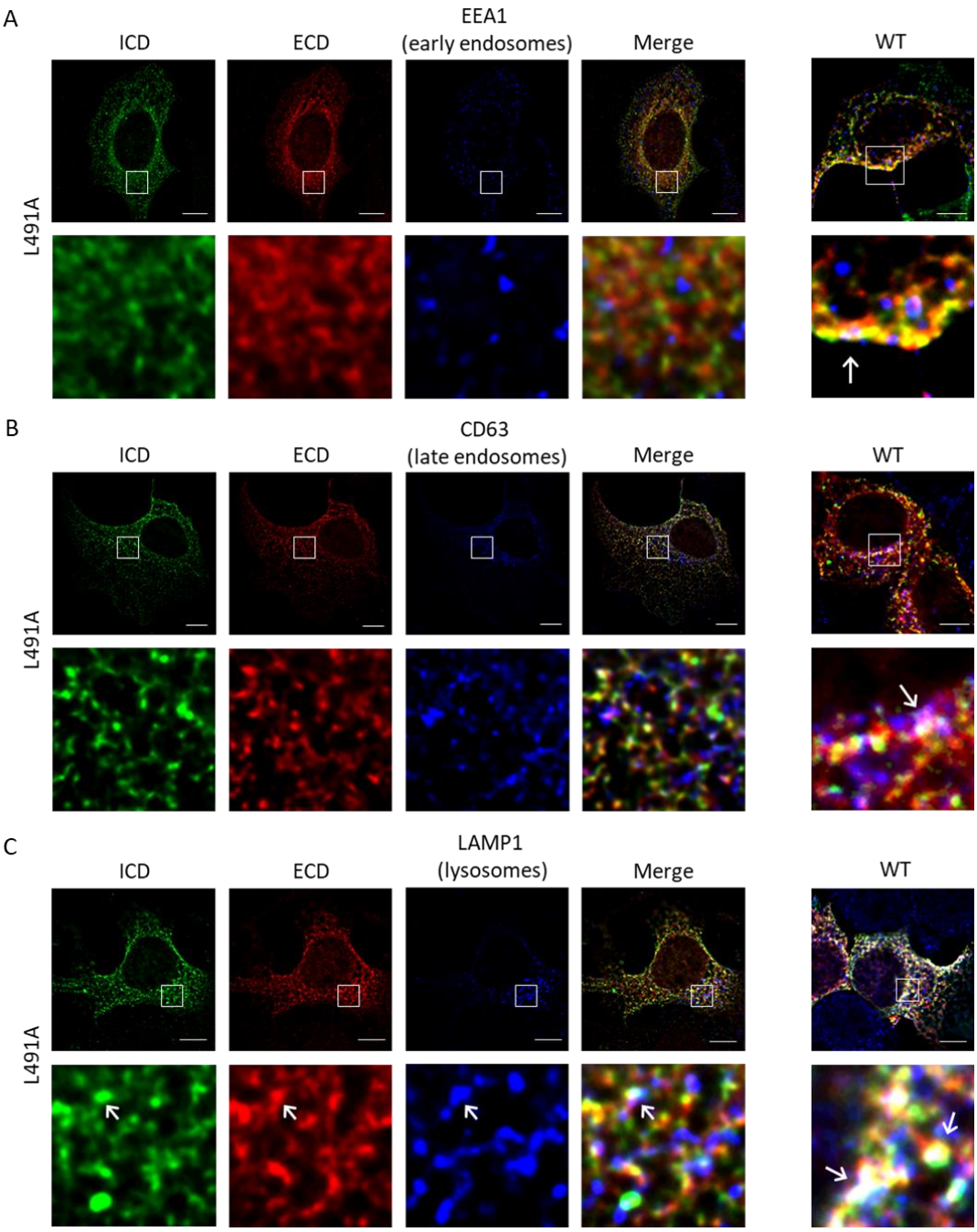
A
EEA1
(early endosomes)
ICD
ECD
Merge
WT
L491A
B
CD63
(late endosomes)
ICD
ECD
Merge
WT
L491A
C
LAMP1
(lysosomes)
ICD
ECD
Merge
WT
L491A

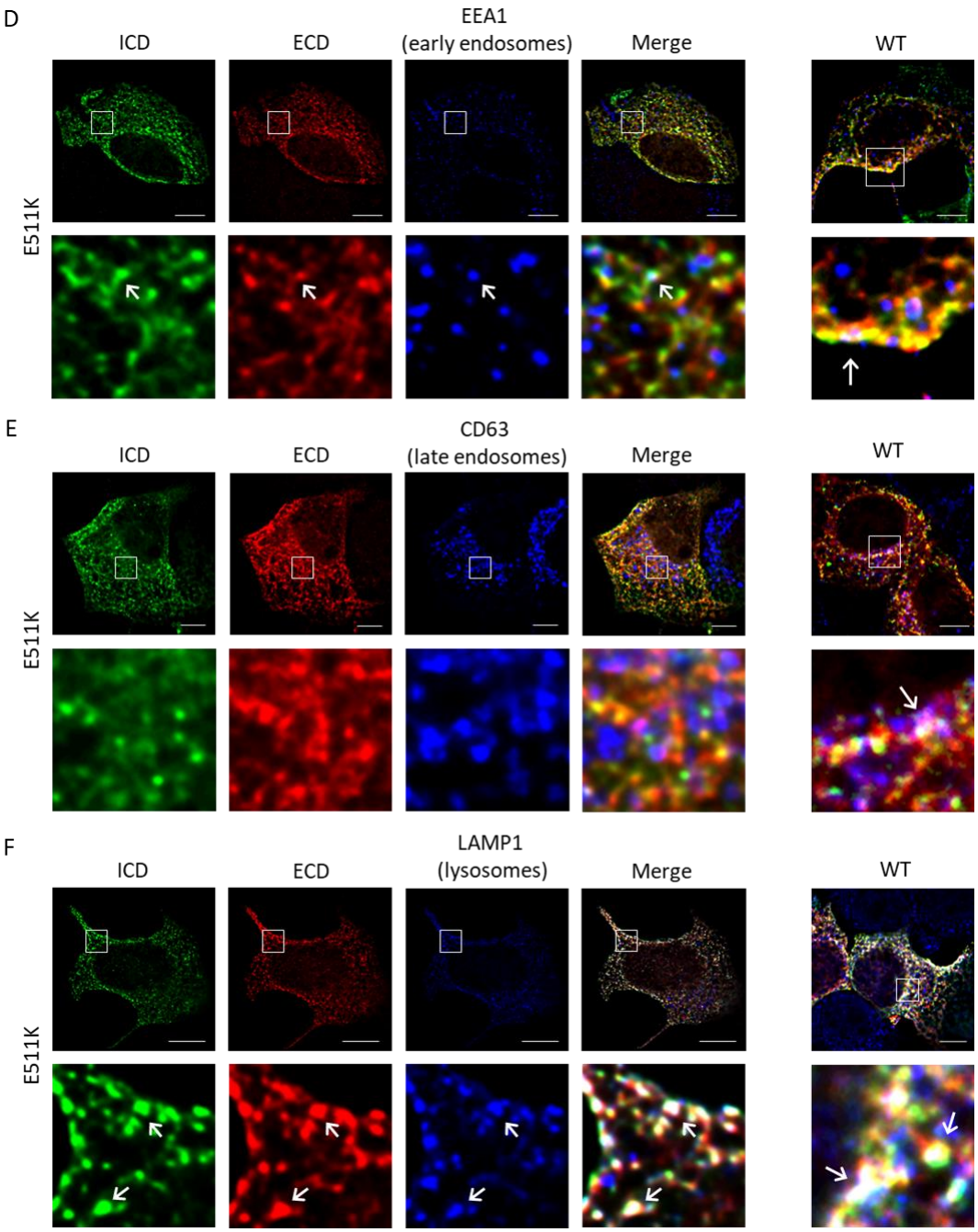
D
ICD
ECD
EEA1
(early endosomes)
Merge
WT
E511K
E
ICD
ECD
CD63
(late endosomes)
Merge
WT
E511K
F
ICD
ECD
LAMP1
(lysosomes)
Merge
WT
E511K

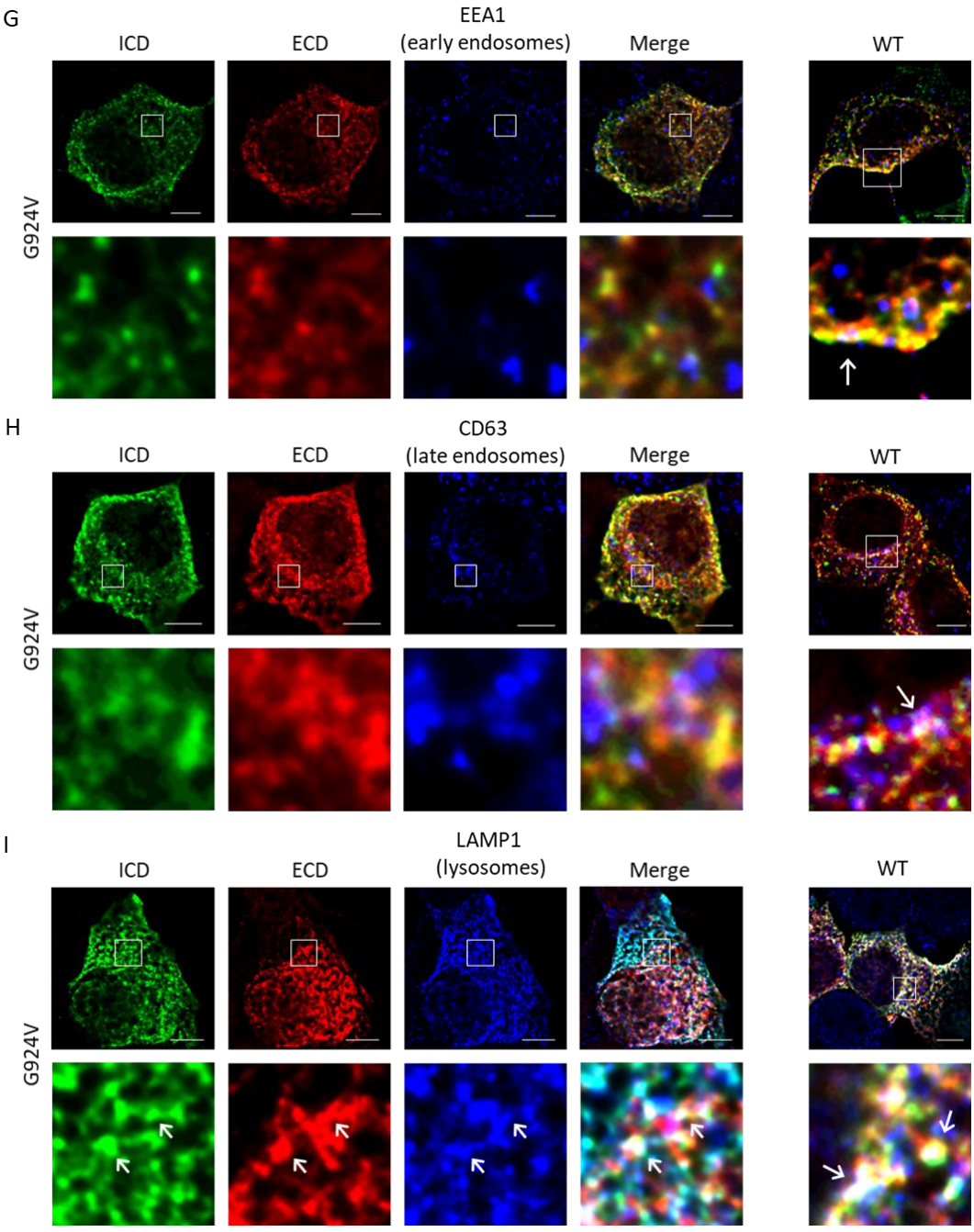
G
EEA1
(early endosomes)
ICD
ECD
Merge
WT
G924V
H
CD63
(late endosomes)
ICD
ECD
Merge
WT
G924V
I
LAMP1
(lysosomes)
ICD
ECD
Merge
WT
G924V

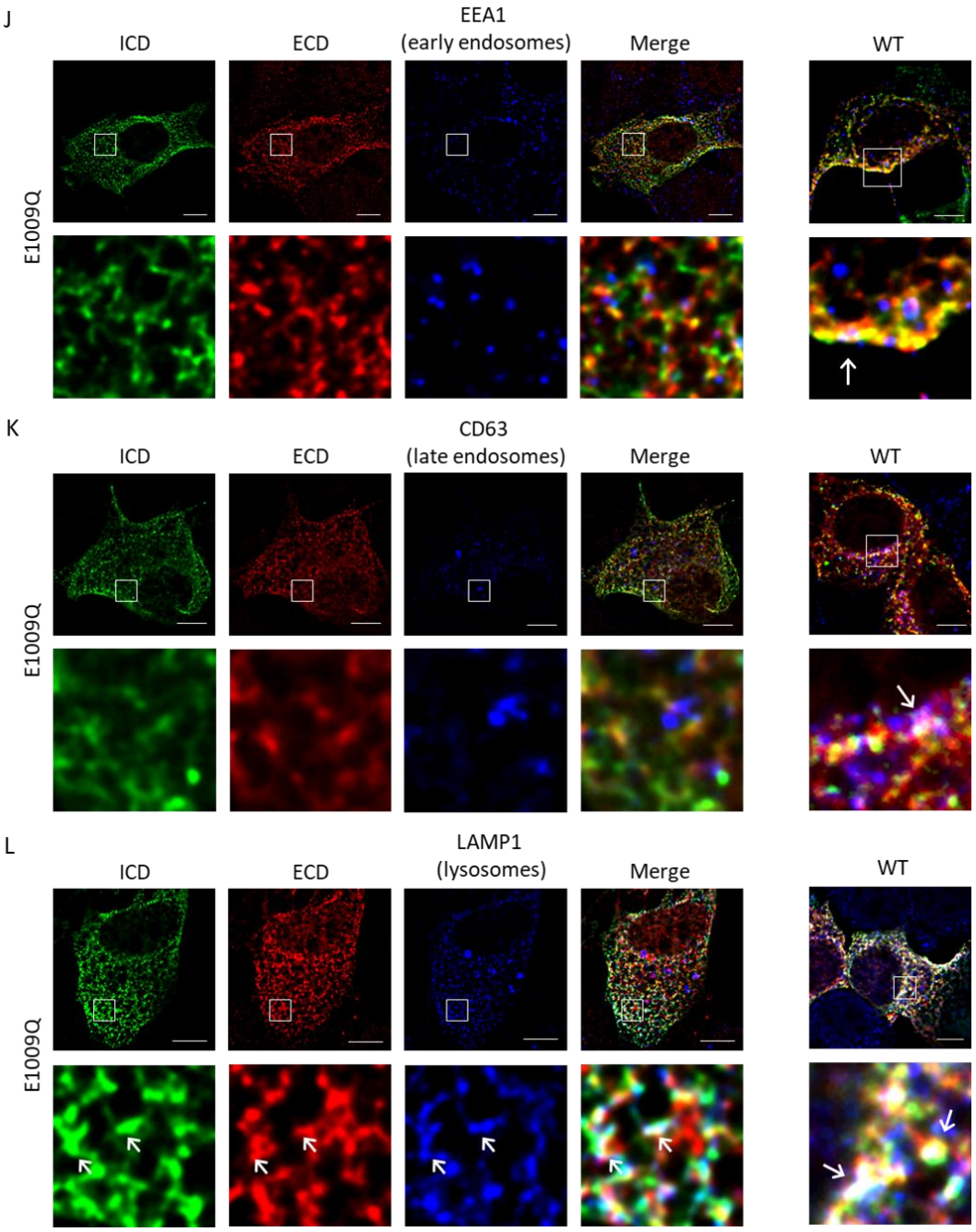
J
EEA1
(early endosomes)
ICD
ECD
Merge
WT
E1009Q
K
CD63
(late endosomes)
ICD
ECD
Merge
WT
E1009Q
L
LAMP1
(lysosomes)
ICD
ECD
Merge
WT
E1009Q

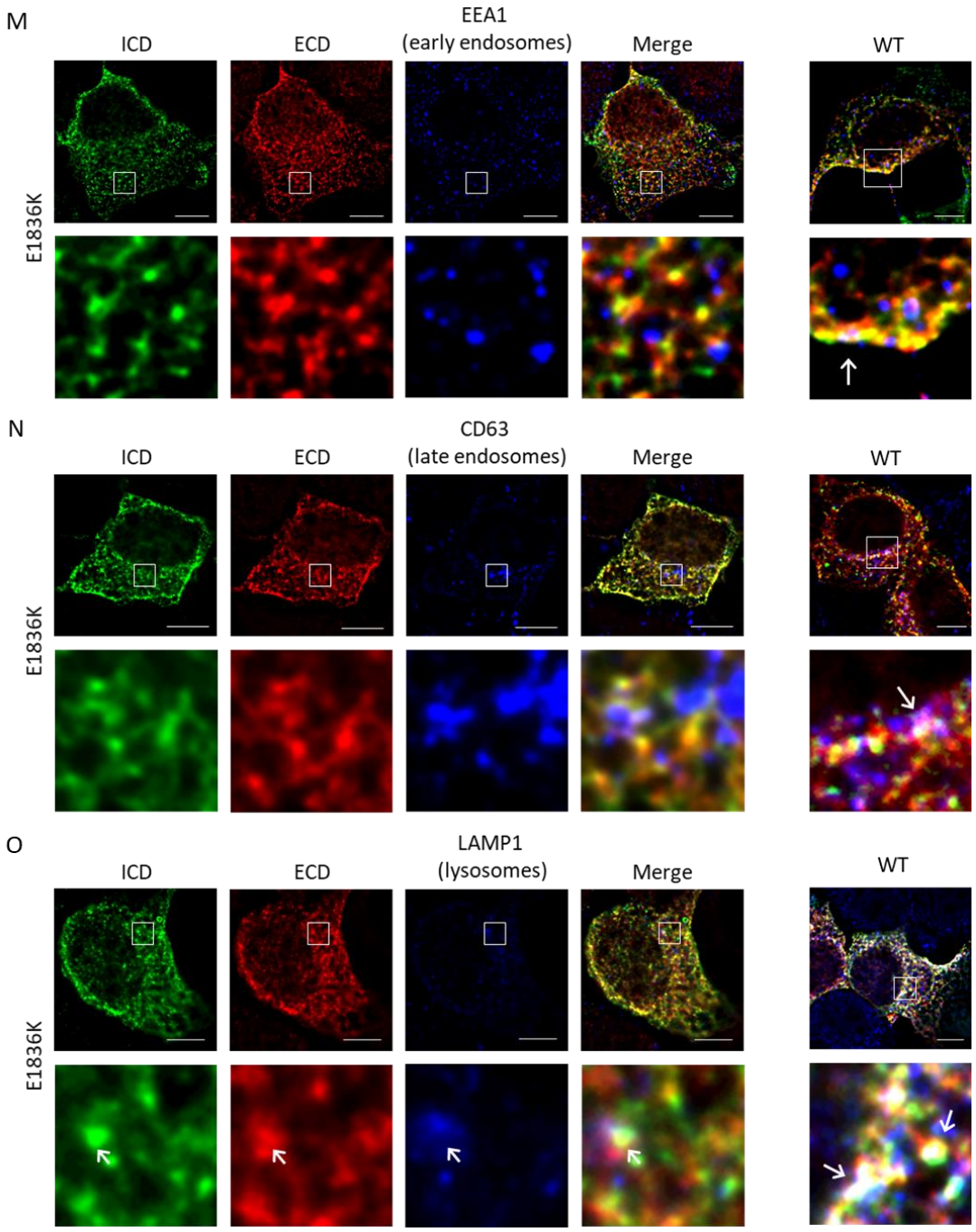

Figure 5-12: Notch4 mutations affect full length Notch4 location in the endocytic trafficking pathway. Immunofluorescence images of MCF7 cells transiently transfected with a Notch4 plasmid with a mutation at L491A (A,B,C), E511K (D,E,F), G924V (G,H,I), E1009Q (J,K,L) or E1836K (M,N,O). Images show Notch4 ICD (green), Notch4 ECD (red) and EEA1-early endosomes (blue) (A,D,G,J,M), CD63-late endosomes (blue) (B,E,H,K,N), LAMP1-lysosomes (blue) (C,F,I,L,O) and a merge of the three channels to demonstrate colocalisation. Areas of key colocalisation are indicated with arrows. Areas zoomed in to show detail in higher magnification, indicated by the white squares. Scale bars: 5µm. Panels from WT Notch4 from Figure 3-7 are shown for comparison.

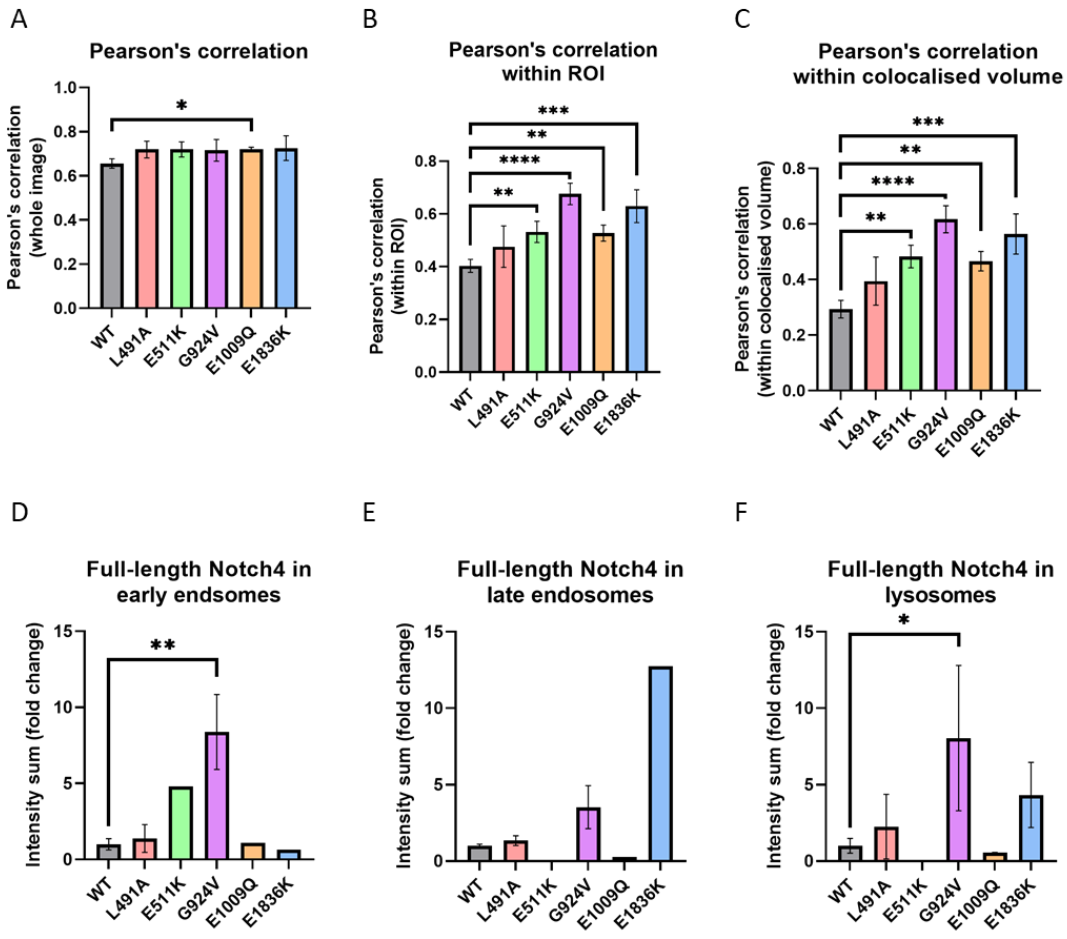

Figure 5-13: Quantification of ICD and ECD colocalisation and amount of full length Notch4 in endosomal compartments with WT and mutated Notch4 (L491A, E511K, G924V, E1009Q and E1836K). A+B+C) Pearson's correlation of colocalisation between Notch4 ICD and ECD channels in the whole image (A), within a defined Region of Interest (ROI) (B) and within the colocalised volume (C). D+E+F) Data intensity sum of full-length Notch4 within "surfaces" created to represent the endosomal compartments early endosomes (D), late endosomes (E) and lysosomes (F). Data are represented as mean ±SEM. Statistical tests: Unpaired t tests. *p < 0.05. **p < 0.01. ***p<0.001. ****p<0.0001. A+B+C) N=7. D+E) N=1. F) N=2.

5.8 Notch4 mutants affect target gene expression and Mammosphere Forming Efficiency

MCF7 cells were transfected with wild-type and mutated Notch4 and RNA was analysed for Notch target gene expression and DTX gene expression. The different mutants had different effects on Notch4 gene expression compared to the WT Notch4. L491A and E511K mutants caused decreased Notch4 gene expression compared to wild-type ($p<0.0001$ and $p<0.001$), whereas G924V and E1009Q mutants increased Notch4 gene expression ($p<0.05$ and $p<0.01$) (Figure 5-14A). The E1009Q mutant Notch4 decreased Hes1 gene expression ($p<0.05$) (Figure 5-14B). None of the five mutants affected Hey1 or Hey2 gene expression any differently than wild-type Notch4 (Figure 5-14C+D). DTX genes were also differently affected in some cases. E1009Q mutation increases DTX1 gene expression ($p<0.001$) (Figure 5-14E), E511K mutation increases expression of DTX2 ($p<0.01$), and both L491A and E511K mutation increase DTX4 expression compared to wild-type ($p<0.01$) (Figure 5-14F+G).

Combining these signalling results, we can determine that compared to wild-type Notch4, the L491A mutation increased DTX4 expression whilst decreasing Notch4 expression, the E511K mutation decreased Notch4 expression and increased DTX2 and DTX4, the G924V mutation decreased Hes1 and DTX4 expression and increased Notch4, and the E1009Q mutant increased Notch4 and DTX1 gene expression and decreased Hes1 expression.

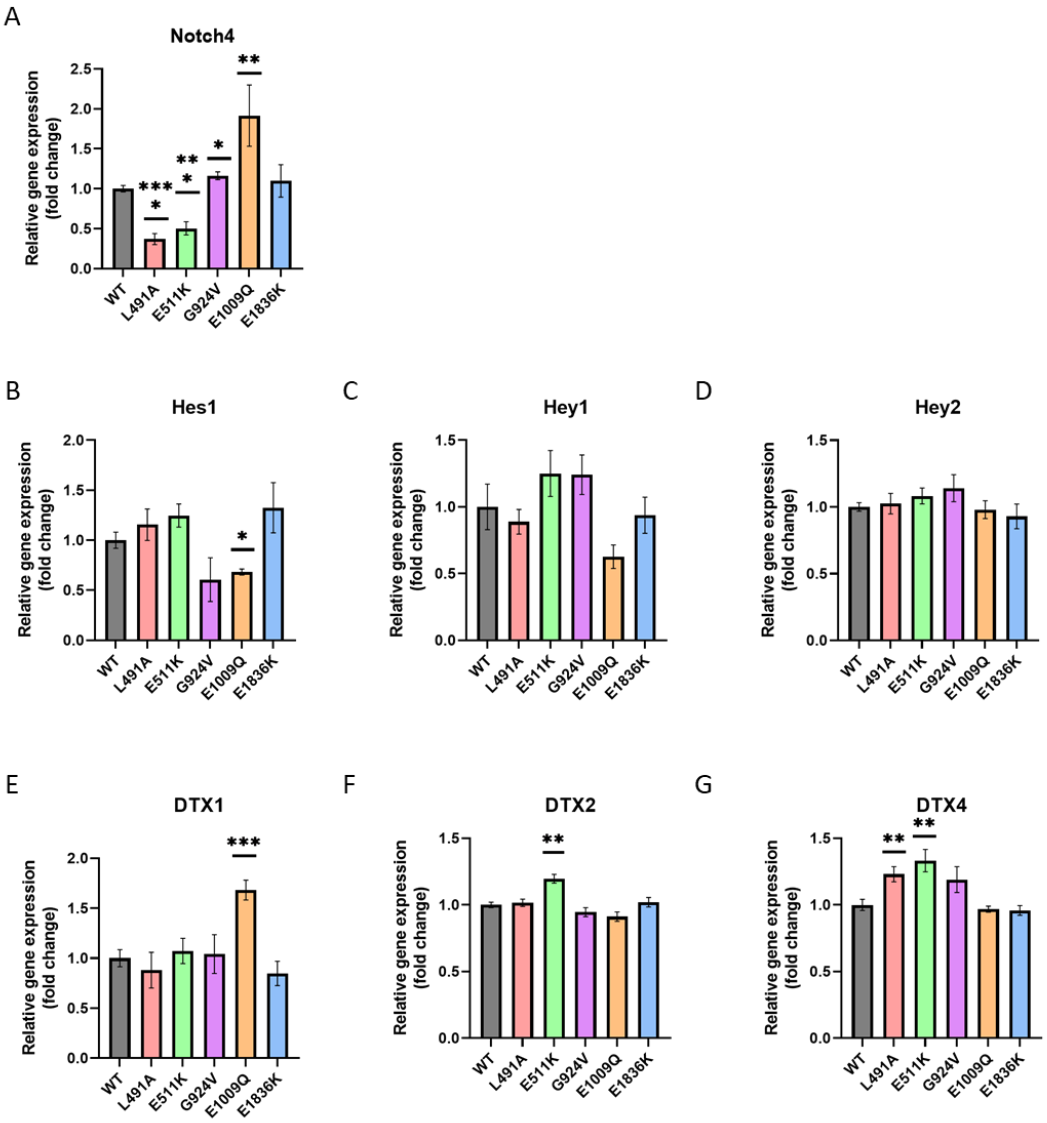

Figure 5-14: Notch4 mutants affect target gene expression in different ways. MCF7 cells were transiently transfected with WT or L491A, E511K, G924V, E1009Q or E1836K mutant Notch4 plasmids. Cells were lysed for RNA after 24 hours and gene expression was analysed. Relative gene expression of Notch4 (A), Hes1 (B), Hey1 (C), Hey2 (D), DTX1 (E), DTX2 (F) DTX4 (G). N=3. Data are represented as mean ±SEM. Statistical tests: Unpaired t-tests. *p < 0.05. **p < 0.01. ***p<0.001. ****p<0.0001.

MCF7 cells were also transfected with the five Notch4 mutants and plated out for mammospheres. Mammosphere forming efficiency was assessed after 5 days. G924V and E1009Q Notch4 mutations both slightly reduced mammosphere forming efficiency compared to wild-type Notch4, but this did not reach significance (p=0.08) (Figure 5-15).

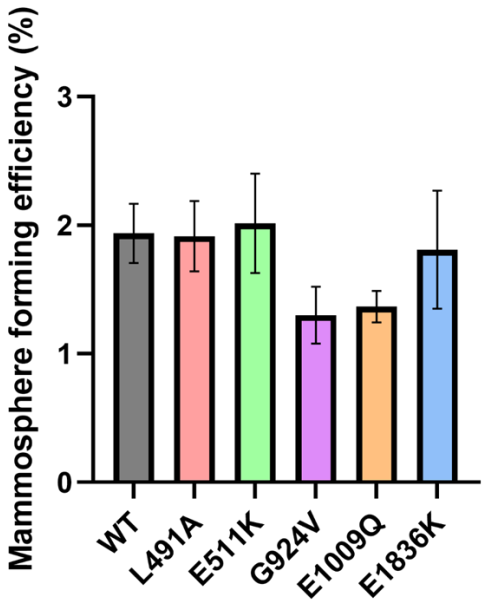

Figure 5-15: The Notch4 mutants G924V and E1009Q slightly reduced mammosphere forming efficiency of MCF7 cells (compared to WT Notch4). Mammosphere forming efficiency of MCF7 cells transiently transfected with WT or L491A, E511K, G924V, E1009Q or E1836K mutant Notch4. Data are represented as mean ±SEM. Statistical tests: Unpaired t-tests.

5.9 Analysis of putatively differentially expressed genes caused by mutations of Notch4

Next, we aimed to identify gene expression patterns and pathways that may be altered by the mutations of Notch4 (including the reverted residue). To do this, MCF7 cells were transiently transfected with a mutant or WT Notch4 plasmid, as described previously. 24 hours after transfection, the transfected cells were stained with the Notch4-AF647 antibody and sorted using FACS. The cells positive for Notch4 were discriminated from the negative cells using a stringent gating strategy (Appendix Figure 8-5). The RNA was extracted from these sorted cells and analysed by RNAseq by the CRUKMI Molecular Biology Core Facility. downstream analysis of this data was carried out by Matthew Roberts (CRUK) (Methods).

The genes that were found to have the greatest difference in expression between cells positive for WT Notch4 and those negative for Notch4 are plotted in a heatmap detailing gene expression differences, as well as the gene expression differences seen in the mutated Notch4 cells (Figure 5-16). Genes that were putatively differentially expressed with a log2 fold change of greater than 3.25 are included in the heatmap. Some genes, including Notch4, are consistently upregulated in all samples, with others consistently downregulated in all, including BOLA2B. Some of the genes identified in Figure 5-16 have an association with cancer and are listed in Table 5-1. These include TNF which has been extensively linked to breast cancer, as well as FGR which interacts with Src in cancers (H. S. Kim et al., 2011; Mercogliano et al., 2020). Interestingly, both of these genes are upregulated in the WT Notch4 population but are downregulated or less highly upregulated in the E1836K mutant Notch4 cells. The sample that diverges the most from the others using these genes of interest is the WT Notch4, with the Y914H and E1009Q mutants being the most similar to one another.

The user defined list of genes related to Notch that was used in Chapter 4, was used again for this dataset. The heatmap for gene expression, compared to Notch4 negative cells, for this set of genes is shown in Figure 5-17. The most upregulated genes in all samples include NOTCH4, CDKN1A, VPS33A and DTX3. The most downregulated genes in all samples include JAG2, HES6, GATA3 and HEY2. The main differences between samples occur in VPS18 and DTX4, which are upregulated in WT Notch4, but downregulated in Y914H, E1009Q and E1836K mutants, compared to Notch4 negative cells. The sample that diverges the most from the others using this gene set is the L491A mutant sample. Calculated fold change values of these genes are found in Appendix Table 8-2.

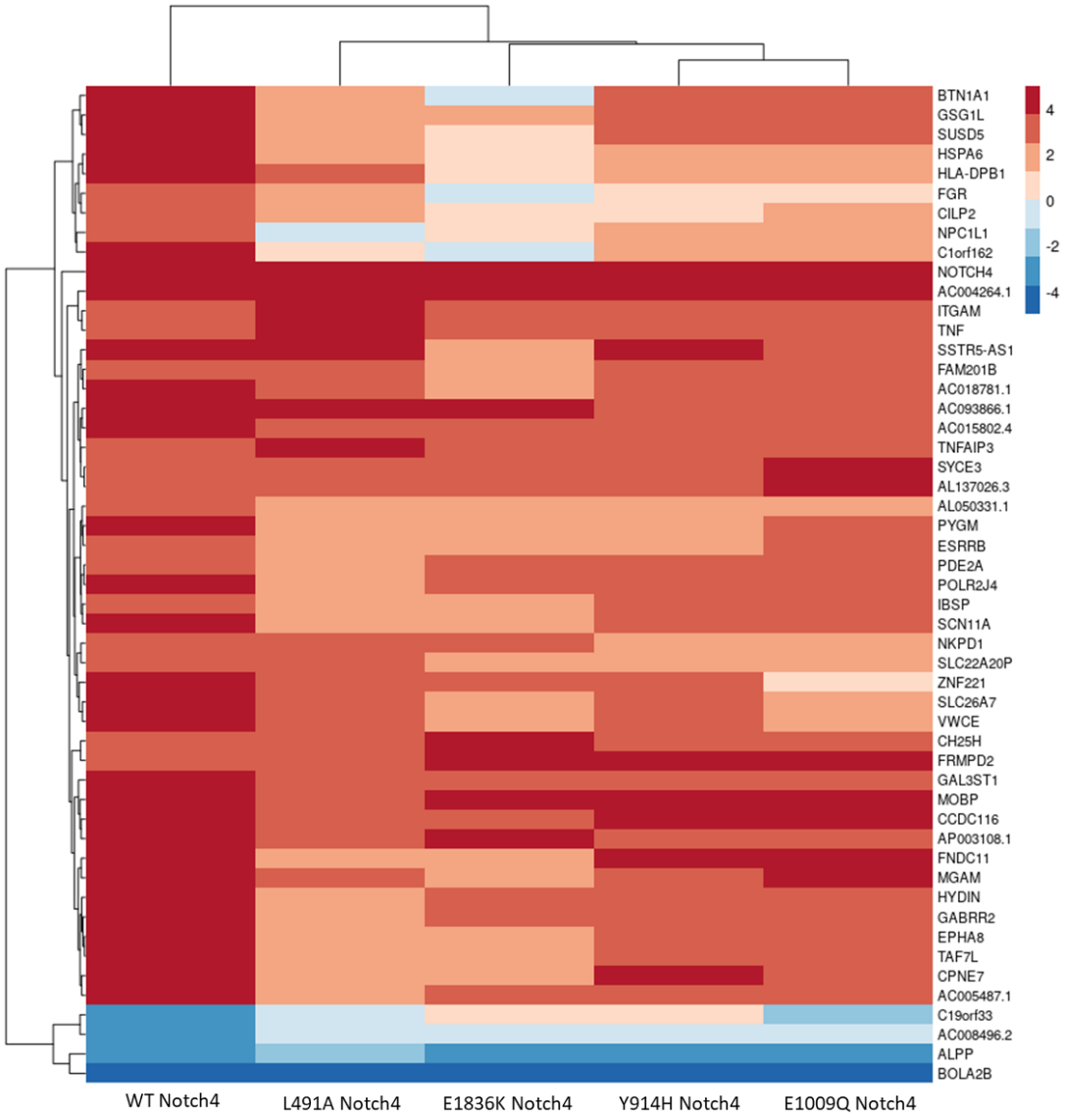

Figure 5-16: Genes putatively differentially expressed in WT, L491A, Y914H, E1009Q and E1836K Notch4 compared to an equivalent sorted population negative for Notch4. Includes genes above the log2 fold change 3.25 threshold in the WT Notch4 sample. Red corresponds to upregulated genes and blue to downregulated genes.

Gene ID	Gene name	Relevance/ association with cancer
HSPA6	Heat Shock Protein Family A (Hsp70) Member 6	Associated with Hepatocellular carcinoma. Inhibits migration and invasion of TNBC cells (Shen et al., 2021).
FGR	FGR Proto-Oncogene, Src Family Tyrosine Kinase	Involved with Src in various cancers, including ovarian (H. S. Kim et al., 2011).
TNF/ TNFAIP3	Tumour necrosis factor/ TNF Alpha Induced Protein 3	Extensively linked to cancers, including breast cancer (Mercogliano et al., 2020)

Table 5-1: Relevance/ association with cancer of some of the putatively differentially expressed genes identified in Figure 5-17.

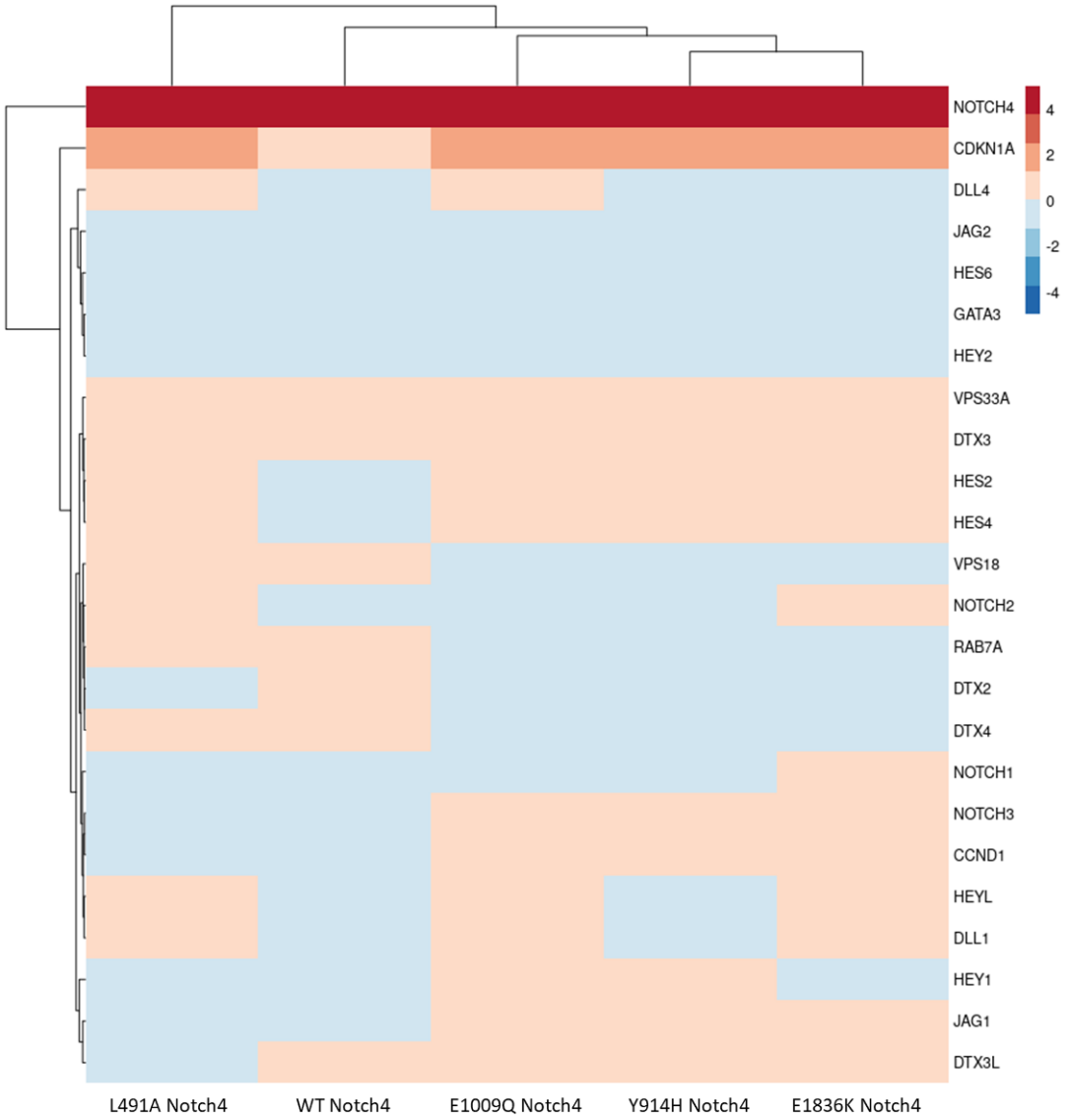

Figure 5-17: Expression level of genes related to Notch signalling including target genes and related genes. In WT, L491A, Y914H, E1009Q and E1836K Notch4 compared to an equivalent sorted population negative for Notch4. Expression level displayed as log2 fold change. Red corresponds to upregulated genes and blue to downregulated genes.

We then aimed to identify signalling pathways and networks that had associations with each mutated Notch4. As in chapter 4, KEGG pathway analysis was performed and genes that had a log2 fold change of greater than 1 were used in the analysis. These were compared to gene sets corresponding to certain signalling pathways. The pathways that have an association with the WT or mutated Notch4 populations that correspond to a p value of less than 0.01 are displayed in Table 5-2. WT Notch4 is associated with pathways including cytokine pathways and cell adhesion. Each mutant Notch4 shares some of these pathways, but each are associated with its own set of pathways. Of note, L491A Notch4 is uniquely associated with the TNF signalling pathway. Y914H Notch4 is associated with the cell cycle, p53 and JAK/STAT signalling pathways. The E1836K Notch4 is uniquely associated with pathways involved in DNA repair.

	P value				
Pathway	**WT Notch4**	**L491A**	**Y914H**	**E1009Q**	**E1836K**
Cytokine-cytokine receptor interaction	****	****	0.00056	****	0.00024
Hematopoietic cell lineage	****	****	0.00516		
Viral protein interaction with cytokine and cytokine receptor	0.00030	0.0028			
Cell adhesion molecules	0.00039	****			
Rheumatoid arthritis	0.0022	****	0.0081	0.00034	
Neuroactive ligand-receptor interaction	0.0028	0.0015	0.0095		
Phagosome	0.0041	****		0.00014	
Antigen processing and presentation		****			0.0032
TNF signaling pathway		****			
Complement and coagulation cascades		0.00017	0.0039		
Viral carcinogenesis		0.0035			0.0012
Transcriptional misregulation in cancer		0.0038			
Th1 and Th2 cell differentiation		0.0040			
Small cell lung cancer		0.0040	0.0075		
Cell cycle			****	****	****
DNA replication			0.00041		****
p53 signaling pathway			0.00029	0.00040	****
JAK-STAT signaling pathway			0.0031		
Gap junction				0.00019	

Mismatch repair					0.00012
Homologous recombination					0.00046
Cellular senescence					0.0015
Base excision repair					0.0018
Apoptosis					0.0034
Nucleotide excision repair					0.0053

Table 5-2: Pathways identified by KEGG pathway analysis that have an association with one or more of the cell populations expressing WT or mutant Notch4. Genes that had a log2 fold change of more than 1 compared to cells negative for Notch4 were included in the analysis. Pathways that are associated with these genes with a p value of less than 0.01 are included in the table. Pathways that are not relevant have been excluded from the table. **** $p<0.0001$.

We performed gene set enrichment analysis (GSEA) using genes of interest defined by log2 fold change of greater than 1. As in Chapter 4, enrichment analysis results using Gene Ontology terms from "Biological Processes" and "Molecular Functions" were produced. Gene sets that correspond to the processes and functions were compared to the genes of interest for each Notch4 population WT and mutant. The overview or "signature" of these functions or processes are summarised in Table 5-3 for each population of cells. Mutating the Notch4 changed the main theme of processes from extracellular response and movement related when WT, to cell cycle/ division related with L491A, Y914H and E1009Q mutants and to immune response related with E1836K mutants. The receptor activity themed functions associated with WT Notch4 was changed to DNA synthesis themed functions in Y914H and E1836K mutants.

Next, GSEA was performed to compare gene set collections from the Hallmark gene sets from MSigDB to the genes of interest, defined by a log2 fold change greater than 1 (Figure 5-18). The WT Notch4 population is negatively associated with E2F targets, mitotic spindle and G2M checkpoint gene sets, which are associated with cell proliferation and division. All mutant Notch4 populations are also similarly negatively associated with these gene sets (not shown). E1836K, Y914H and L491A mutant Notch4 cells are all associated with at least one immune/ inflammation related gene set. L491A has associations with multiple gene sets, additionally including IL6-STAT3 and K-Ras signalling gene sets.

Together, as these data are preliminary, it is difficult to draw any solid conclusions. However, what can be concluded is that mutating Notch4 alters the signalling pathways, functions and gene signatures of breast cancer cells.

	Biological Processes	Molecular Functions
WT Notch4	Extracellular response and movement	Receptor activity
L491A Notch4	Cell cycle/ cell division	Receptor activty
Y914H Notch4	Cell cylce/ cell division	DNA synthesis
E1009Q Notch4	Cell cycle/ cell division	Receptor activity/ binding
E1836K Notch4	Immune response	DNA synthesis

Table 5-3: Summary of Biological Processes and Molecular Functions identified as being most associated with each mutant or WT Notch4 expressing population of cells. Genes that had a log2 fold change of more than 1 compared to cells negative for Notch4 were included in the analysis. Full list of top 10 associated processes and functions can be found in Appendix Figures 8-6 and 8-7.

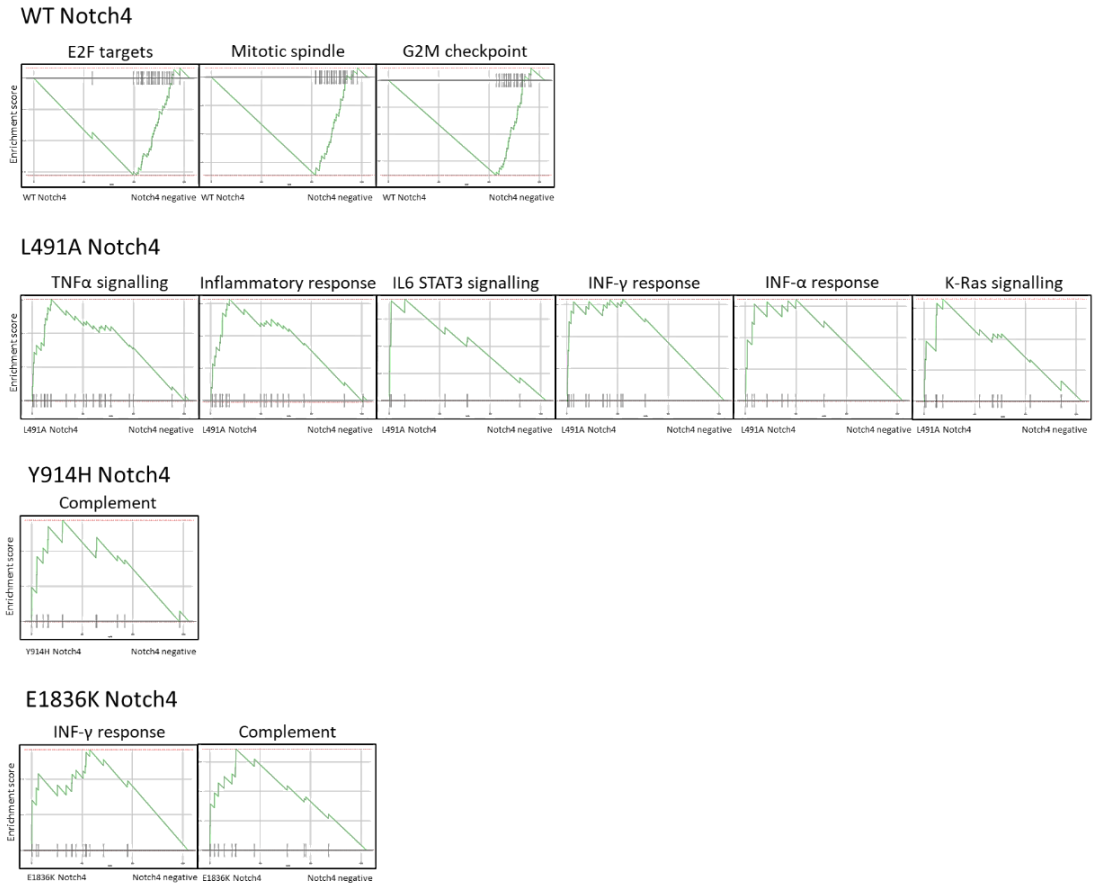

Figure 5-18: GSEA plots of Notch4 positive cells vs Notch4 negative cells using Hallmark gene sets from MSigDB. Genes that had a log2 fold change of more than 1 compared to cells negative for Notch4 were included in the analysis. Plots shown are those that overlap with the relevant WT or mutated Notch4 with a p-adjusted value of less than 0.05.

5.10 Discussion

The aim of this chapter has been to explore mutations of Notch4 in breast cancer and assess how these affect Notch4 signalling and trafficking, cellular gene expression signatures and Breast Cancer Stem Cell (BCSC) activity. This has been achieved by the site-directed mutagenesis of the Notch4 gene with key mutations identified in a thorough database search of primary and metastatic breast cancer samples. Site-directed mutagenesis was also employed to revert the amino acid residue in the Abruptex domain of Notch4 that has been hypothesised to play a part in Deltex dependent/ ligand independent signalling to match the conserved residue present in Notch1/2/3. Immunofluorescence, qRT-PCR and mammosphere experiments with cells expressing these mutated Notch4 receptors has found that the Y914H mutant reduces full length Notch4 levels in the cell and alters downstream signalling, indicating the tyrosine residue plays a key role in Notch4 signaling. It was also found that each mutant Notch4 has a different signature in trafficking, signalling and activity. Preliminary RNAseq analysis provided further insight into potential genes and pathways that are changed by the mutations. These further findings could be used for new research into mechanisms of Notch signalling, as well as being applicable in the clinic. As these mutations have been found in primary and metastatic breast cancers, the insights gained could be used to improve specific personalised treatment strategies in the future.

After searching for Notch4 mutations present in breast cancer samples in publicly available genomic databases, it was found that Notch4 mutation frequency was increased in metastatic samples compared to primary samples (3.84% compared to 2.89%). This suggests that these mutations contribute towards the progression and metastatic spread of breast cancers. The most common location for mutations was altered between primary and metastatic samples, from within the EGF repeats to within the stabilising PEST domain. This backs up the idea that the mutations are stabilising Notch4, allowing greater signalling capacity and driving metastasis. However, metastatic cancers tend to possess more mutations than primary, so this increase in mutation frequency could be as a result of the metastases, rather than the mutations helping drive metastasis (Gara et al., 2018; Paul et al., 2020). The Notch4 mutation data came from many different databases and studies which had not all published the same amount of data including subtype and grade of the cancer and patient information including survival. These data, had they been present, could be analysed further, sorting the mutations by subtype/ severity of the cancer and gaining insight into the grouping of mutations.

Clustering of mutations within the ligand binding domain (EGF repeats 8-12) seems paradoxical, since in other cancers, mutations in this area have been observed to be loss of function mutations (N. J. Wang et al., 2011). However, it could be possible that if the mutations remove the function of the ligand binding domain, this may increase the ligand independent signalling. Thus, these mutations could be driving ligand independent Notch4 signalling and potentially breast cancer stem cell activity.

The mutations used were selected for key reasons, including presence in multiple metastatic breast cancers and ligand binding disruption. For the scope of this project, only a limited number could be chosen. Other reasons that mutations may have been of interest is if they are located on an exposed loop or contact region of an EGF repeat, or correspond to other key mutations in other Notch receptors, either in breast cancer or other cancers. There is the chance that other mutations could have had more dramatic effects, and many other Notch4 mutations could potentially be investigated in the future.

The Y914H mutation reverts the tyrosine residue which in *Drosophila* has been linked to ligand independent and Deltex dependent signalling, to a histidine residue which matches the conserved residue in Notch1/2/3 and *Drosophila* Notch. We found that this mutation reduced full length Notch4 internalisation into the cell and reduced its trafficking through the endocytic pathway. Some extracellular domain (ECD) was detected in the early and late endosomes which suggests a small amount of trafficking took place. Both portions of the Notch4 receptor are found separately in the lysosomes which suggests they are likely to have been trafficked to the lysosome and subsequently degraded in the Multi Vesicular Bodies (MVB). To further explore this, other antibodies such as Rab5, Rab7 and GPI could have been used to stain other compartments within the endocytic pathway (discussed in Chapter 3).

The reversion mutation increased Notch4, Hey2 and DTX1 gene expression compared to WT. This reflects the link between Notch4 and Hey2 expression, and between DTX1 and Hey2 (discussed in Chapter 3). Perhaps the increased Notch4 gene expression is due to a positive feedback loop, allowing Notch4 to be transcribed more easily with the mutation. As previous results have shown, Hey2 is the Notch target gene most closely controlled by Notch4, so is expected to be the only one to be changed by this Y914H reversion, rather than Hes1 and Hey1 whose expression may be controlled by the other Notch receptors. The mutation may even stop Notch4 endocytic pathway activation (as observed in IF) and may lead to a switch to ligand activated signalling, causing the target gene repertoire to change. This highlights that Notch4 is involved in a tightly controlled fine balance in its signalling pathways. This

could be investigated by blocking ligand activated signalling to observe effects with Y914H Notch4. On the other hand, if the gene expression changes are normalised for the approximately 2-fold increase in Notch4 expression in the Y914H mutant, the results are different. Normalised for Notch4 gene expression, all Notch target genes and DTX genes have reduced expression after transfection with the Y914H mutant Notch4, compared to wild-type.

Y914H Notch4 decreased mammosphere forming efficiency slightly compared to wild-type Notch4, but it did not reach significance. It was performed after transient transfection so it is not expected that increased Notch4 expression was maintained for the entire duration of the experiment. This duration of the BCSC activity assay was one of the reasons that a Notch4 expressing stable cell line was produced in Chapter 4. However, stable cell lines were not produced for the Y914H Notch4 nor any of the mutants. Due to this, the mammosphere experiment observed here should be classed as preliminary as the non-significant decrease observed may have been enhanced if long term stable expression was achieved. Therefore, it is likely that the Y914 residue in Notch4 plays a part in its BCSC activity.

The preliminary RNAseq analysis that was undertaken compared Notch4 positive sorted cells that had been transfected with WT Notch4 or mutant Notch4 to cells negative for Notch4. This identified that the gene signature of Y914H Notch4 cells differed greatly from WT Notch4 cells. Interestingly, some pathways that were found to be upregulated in the Y914H Notch4 cells that differed from WT Notch4 cells were the cell cycle, DNA replication and the p53 and JAK/STAT signalling pathways. This suggests that the Y914 amino acid residue may have a role in cell cycle/ proliferation and also in preventing or enhancing crosstalks with classically cancer associated signalling pathways. The pathways identified are associated with genes that are differently expressed and it has not been identified if this is a positive or negative regulation. The RNAseq data is relatively preliminary, due to there being just one repeat for each sample.

The ligand binding domain mutant (L491A) of Notch4 was chosen as it should completely block binding of the ligand to the receptor (Whiteman et al., 2013). The Notch4 gene expression itself is slightly reduced but its target genes are signalling at a similar rate as WT Notch4 so it can be determined that ligand is likely not to play a major part in Notch4 target gene signalling. In fact, by immunofluorescence, more ICD and ECD colocalisation could be observed, although less localisation to the endocytic pathway components. When analysing the user defined Notch related genes in preliminary RNAseq, the L491A mutation was found

to be the mutant with an expression signature that differed most from the other mutants, perhaps highlighting the difference between this mutant and the others that were all found in breast cancers. This mutant had associations with the TNF, IL6-STAT3 and K-Ras signalling pathways and had multiple immune and inflammation related pathways upregulated compared to Notch4 negative cells, uniquely among the mutants. Future work would need to confirm that this mutant is definitely knocking out ligand-induced signalling, by creating a ligand induced signalling assay with WT Notch4 and comparing to L491A Notch4.

The E511K Notch4 mutant was selected due to its presence in multiple primary and metastatic breast cancer samples. It caused increased DTX2 and DTX4 gene expression compared to WT Notch4 but did not affect any other target genes. It had increased Notch4 ICD and ECD colocalisation, and localisation in the lysosome (although not apparent with quantification, potentially explained by limitations discussed below). These suggest that this mutation may push Notch4 to drive the expression of DTX, which may in turn may increase its internalisation via the endocytic pathway route. This could then lead to its signalling being increased in breast cancers that it is present in, driving BCSC activity and progression. The BCSC activity was not increased here, but as discussed, stable cell lines are preferable over transient transfection for longer term assays. This sample, as well as the G924V Notch4 cells were not able to be investigated by RNAseq as an insufficient level of RNA was isolated.

The G924V Abruptex mutation that was identified in two metastatic breast cancers was observed to have less Notch4 ICD and ECD colocalisation than WT, but more intensity in early endosomes and lysosomes by quantification. It did not affect gene expression of genes measured but slightly reduced mammosphere forming efficiency, not reaching significance. This mutation could act in a way to stabilise Notch4 in the endocytic compartments, but not allow its transport or cleavage, not increasing its signalling, and indirectly decreasing BCSC activity slightly.

The E1009Q Notch4 mutation is also within what is considered as the Abruptex domain and was found in primary and metastatic breast cancer samples. This was the only mutant Notch4 that was measured to have significantly increased colocalisation between ECD and ICD when quantified for the entire image. Some full length E1009Q Notch4 was found in lysosomes, but not exclusively. This mutant would benefit from a more extensive staining protocol, testing for its presence in other endocytic compartments. This mutant increased Notch4 gene expression the most, as well as increasing DTX1, whilst decreasing Hes1 expression, fortifying the link with DTX1 and suggesting that this mutation positively increases Notch4 signalling

through DTX1 expression. However, similarly to G924V, this mutation slightly reduced mammosphere formation, not reaching significance. Except for a switch to a cell division theme with identified genes, the preliminary RNAseq analysis did not identify any unique gene signatures associated with this mutation compared to WT Notch4. This mutation may prevent Notch4 from being released from the endocytic pathway, reducing its BCSC effects.

The E1836K had the highest frequency of mutation found in breast cancers across the whole of Notch4, with the majority of these being found in metastatic samples. This mutation was in the PEST domain which has been linked to stability of Notch and progression of triple negative breast cancers (K. Wang et al., 2015; Weng et al., 2004). This mutation changed the distribution of Notch4 to larger particles with a greater distance between them, whilst maintaining full length status within the cell and within endocytic compartments. In RNAseq analysis, DNA repair and synthesis pathways were activated, as well as immune response related genes. Perhaps this mutation is indeed stabilising the Notch4 receptor, allowing it to distribute in greater amounts through the endocytic pathway for activation, and on a cellular level leading to DNA repair and synthesis and ultimately survival of the breast cancer cells.

Although the Pearson's correlation quantification of colocalisation between Notch4 ICD and ECD channels did in some cases reflect what could be observed by eye, in some cases it showed a very different case. Another way that the colocalisation could have been quantified was to create "dots" to represent the punctate areas of staining in each channel. These could then be measured to assess whether they colocalised or not. This would negate the issues found when analysing images when Notch4 was distributed in dot forms, although may not have been effective in situations when the distribution was more spread out, not in dots. In theory, this could take place in the future, with these images and others.

In conclusion, we have found that mutating Notch4 by site-directed mutagenesis is a useful tool to study the specific actions of mutations found in breast cancer on cellular events such as gene expression and distribution of Notch4. However, stable cell lines expressing these mutated Notch4 proteins would be preferable for a consistent gene expression level as well as to allow for longer term assays such as BCSC activity assays. We have found that the Y914 residue, which was hypothesised to be responsible for the actions of Notch4 in endocytic trafficking and its link to endocrine resistance, is likely to be involved in all of these events. RNAseq analysis has proven to be a useful preliminary tool for evaluating gene signatures, pathways and processes that are altered by different mutations. In the future, these, and

other Notch4 breast cancer mutations could be investigated further, with effects *in vivo* giving a clearer picture to the actions across a whole organism, rather than within single cells.

6 Discussion and Future Perspectives

Estrogen Receptor positive (ER+) breast cancers make up 75% of all breast cancers (Smittenaar et al., 2016). Although mostly treated effectively, many of these cancers develop endocrine therapy resistance, rendering conventional treatments ineffective against resulting recurrence or metastasis (Early Breast Cancer Trialists' Collaborative Group (EBCTCG) et al., 2011; Pan et al., 2017). Most deaths occurring from ER+ breast cancer are caused by this resistant and metastatic spread (Smittenaar et al., 2016). Resistance is thought to arise from a small population of Breast Cancer Stem Cells (BCSCs) that survive treatment and can lay dormant. These can repopulate the tumour at a later date, leading to local relapse or travel to a distant site, causing metastasis (Q. Zheng et al., 2021).

Notch4 is a key member of the Notch family of receptors that have been linked to maintenance of stem cells, vascular development and mammary gland development (Dontu et al., 2004; Krebs et al., 2000; Pellegrinet et al., 2011). Notch4 itself is extensively linked to breast cancer. This relationship was first discovered when the MMTV third insertion site was found to be within the Notch4 gene (Gallahan & Callahan, 1997). More recently, Notch4 signalling has been found to be upregulated and activated in breast cancer stem cells, linking it strongly with endocrine resistance (Simões, O'Brien, et al., 2015).

Notch can be activated by two main pathways. The non-canonical, ligand independent pathway, which has been studied in *Drosophila*, involves internalisation of the Notch receptor through action of Deltex. The receptor is then trafficked through the endocytic pathway and the NICD is released into the cytoplasm, where it travels to the nucleus and induces target gene expression (Wilkin et al., 2008). This pathway does not require control by ligand for Notch activation, rendering it more susceptible to over-activation.

In *Drosophila*, the Notch AxE2 mutant is more dependent on Deltex for activity than WT Notch and is linked to Notch ligand independent/ endocytic pathway dependent signalling. Notch4 possesses the equivalent residue change to this mutant in its endogenous sequence. Therefore, it has been hypothesised that Notch4 signals via the ligand independent, Deltex dependent pathway, contributing to its links with endocrine resistance and BCSCs. It was the main aim of this thesis to investigate if this was the case, whilst gaining novel insight into the signalling mechanisms of Notch4. This is essential for the clinical field as gamma-secretase inhibitors (GSIs), which inhibit Notch signalling, have been trialled for treating breast cancer. They have been somewhat effective, but badly tolerated in terms of side effects. This is likely due to the essential functions that Notch is involved in throughout healthy tissue.

Improvements have come from combining GSIs with other drugs, as well as refining treatment to those that may respond. A current clinical trial is underway treating advanced breast cancers that are specifically Notch activated with a GSI (*A Study of AL101 Monotherapy in Patients With Notch Activated Triple Negative Breast Cancer ClinicalTrials.Gov*, 2022). This refining to those that will respond has been investigated in an *ex vivo* way, by creating PDX organoids from a patient's tumour and testing for sensitivity to GSI treatment (Guillen et al., 2021). If these PDX organoids are sensitive to treatment, it would indicate that the corresponding tumour may also be sensitive. If knowledge about the specific receptors and signalling pathways of Notch in breast cancer is improved to allow separate inhibition of receptors or signalling pathways, a more specific inhibition of the Notch activated breast cancers could occur, allowing for more personalised treatment strategies.

Our first aim was to investigate Notch4 signalling by identifying a signalling pathway and exploring its signalling requirements. To do this we used immunofluorescence. By staining both portions of the Notch4 receptor we could determine if Notch4 was present as a full length receptor in the cell, as well as investigate where in the cell it could be found. Analysis of gene expression was also undertaken, whilst knocking down potential signalling components to dissect requirements. From this, it was determined that Notch4 can signal via an endocytic pathway mechanism, Rab7a is involved in its gene expression and DTX1 and DTX4 are essential for its signalling. Both DTX1 and DTX4 are required for full length Notch4 internalisation into the endocytic pathway, DTX1 acts as a control over Notch4 and Hey2 gene expression, and DTX4 is required for BCSC activity of Notch4 cells. It remains to be answered whether this endocytic pathway signalling mechanism is the only or usual activation pathway of Notch4, or whether it is situation dependent and the ligand activated pathway is also involved. To further explore this in the future, the involvement of ligand and ligand expressing cells could be brought in, to explore any ligand requirements.

Our next aim was to apply this signalling knowledge to breast cancers by exploring the effects that Notch4 signalling has on BCSCs and endocrine resistance, whilst looking at this dependence on endocytic trafficking. This was done by creating a Notch4 expressing stable cell line that could be effectively used to explore BCSC activity. This helped fortify the signalling link of the target gene Hey2 specifically to Notch4. It was also determined that Notch4 contributes to BCSC activity and endocrine resistance. It remains to be fully understood whether Notch4 drives cells to become BCSCs or acts upon BCSCs as a separate population to increase their activity. The requirements of endocrine resistance on the endocytic pathway were dissected by using specific inhibitors that led to the conclusion that

endocrine resistant cells and Notch4 reliant cells require TRPML, but not ADAM10 for viability and BCSC activity. In the future, these requirements for TRPML could be combined with exploring the requirements for DTX, by combining the separate experiments performed to investigate each. Also, requirements for TRPML and ADAM10 could be investigated further using siRNA knockdown. This would allow for a more specific inhibition of their action as the inhibitors used may have other targets.

Our final aim was to identify Notch4 mutations present in breast cancers and investigate the effects that some of these mutations have on Notch4 signalling. Genomic changes were carried out by site-directed mutagenesis and allowed exploration of breast cancer related mutations. The residue that has been hypothesised to be responsible for Notch4's ligand independent signalling and link to endocrine resistance was altered to match the conserved residue of Notch1/2/3. These experiments fortified the link that this residue has with ligand independent signalling, showing that its reversion altered target gene expression, BCSC activity and cellular distribution of Notch4. The mutation that disrupted Notch4's ligand binding ability gave indication that Notch4 does not require ligand for signalling. The other mutation experiments determined that Notch4 mutations occurring in breast cancer have varying effects on Notch target gene expression and Notch4 trafficking. The results show that single point mutations can have large effects on target gene repertoire. Perhaps Notch4 activation from different locations in the cell has different preferences for nuclear activation complex assembly and therefore target gene activation. Further work on this topic could help to answer these questions. The mutation data shows that this method is a useful tool which could be expanded in the future to investigate many genomic changes in breast cancer. The mutations could also be linked with other requirements explored, including requirements for DTX and TRPML.

From results in Chapters 3 and 4, DTX1 and DTX4 are clearly involved in a complex gene expression crosstalk with Notch4 and target genes which relies on gene expression levels. The summary of the results of gene expression experiments carried out with transient and stable alteration of expression is shown schematically in Figure 6-1. When expression levels are high in a subset of cells for a short time (transient transfection), DTX1 and 4 have a positive effect on Notch4 and Notch4 has a positive effect on all 3 target genes. Transient knockdown shows DTX4 has positive effect on Hes1 but negative effect on Hey1 and Hey2, whilst DTX1 has a positive effect on both Hes1 and Hey2. In the situation where Notch4 is moderately overexpressed in all cells at an equal rate for a long time (stable cell line), it acts negatively on DTX1 and DTX4 and negatively on Hes1, whilst positively on Hey2. This shows

that the level and length of Notch4 expression changes its effect on target genes. This also suggests feedback loops with the DTXs. Over the short term, DTX has a positive effect on Hes1, but over the long term, Notch4's negative actions on DTX1 may reduce this, leading to an overall downregulation of Hes1 expression. A reciprocal action between Hes1 and DTX1 has been observed previously in mammalian cells, with Hes1 directly binding to the DTX1 promoter and inhibiting its transcription (P. Zhang et al., 2010). The feedback loops observed (Figure 6-1) could be DTX effects on Notch4 or direct effects on the target genes, or via a completely different signalling mechanism. These complex interactions could be further explored in the future, to gain deeper insight into Notch4 signalling.

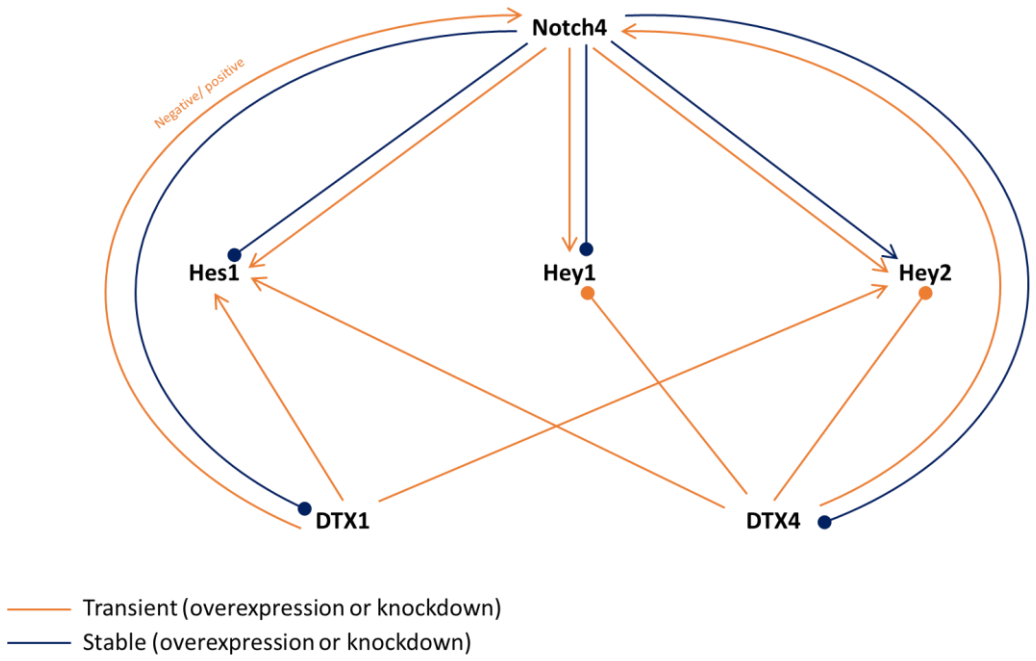

Figure 6-1: Summary of the gene expression interactions of Notch4, DTX1, DTX4 and Notch target genes Hes1, Hey1 and Hey2 in transient (overexpression or knockdown) and stable (overexpression or knockdown) expression experiments.

The analysis of BCSC activity has shown interesting results. The link between Notch4 and BCSC activity has been strengthened and DTX4 has also been shown to be required for BCSC activity. In endocrine resistant as well as Notch4 expressing cells, TRPML is linked to BCSC activity, whilst ADAM-10 is not. The Y914 key residue also has associations, and potential positive effects on BCSC activity. Whilst the mammosphere assay method of measuring stem cell activity does not discriminate between the mesenchymal-like and epithelial-like stem cells, the Aldefluor assay and FACS analysis methods begin to. Epithelial-like BCSCs tend to

express ALDH, whereas mesenchymal-like stem cells express $CD44^{+}/CD24^{-}$ (S. Liu et al., 2014). A recent paper explored Notch4 in TNBC cells and found extensive links between Notch4 and the mesenchymal population of BCSCs (Zhou et al., 2020). The flow cytometry data here agrees with this as the Notch4 cells were of a size and granularity that fits with the mesenchymal phenotype. There was also no large enrichment of ALDH+ cells with Notch4, suggesting no epithelial-like stem cell enrichment. However, this thesis did not include $CD44^{+}/CD24^{-}$ analysis which would be key for future confirmation of the link between Notch4 and mesenchymal BCSCs.

The expression levels of the Notch target genes Hes1, Hey1 and Hey2 were used consistently throughout this thesis as a signalling assay to determine Notch4 signalling. Another potentially more reliable and direct way to measure Notch4 signalling could be a luciferase assay. For this project, Notch4 signalling was unable to be measured with a luciferase assay but could be explored more meticulously in the future. RNAseq is also a robust method to analyse differential gene expression. With additional repeats in the future in order to convert the preliminary results explored here to a reliable form, further analysis could take place. This could include a PCA to observe potential clustering of mutations for roles and interactions.

To summarise, there are many future perspectives that could follow on from this research. This could include combining the investigation methods used here to improve knowledge about the Notch4 endocytic pathway signalling mechanism. For example, the TRPML and ADAM10 inhibitors could be used to investigate the Notch4 mutations to explore if a change in signalling pathway and requirements has occurred. Requirements for DTX could also be investigated with the mutant Notch4 receptors, as well as the use of stable cell lines created to comprehensively explore their effects on BCSC activity. The endocytic trafficking pathway of Notch4 could be scrutinised in a more detailed way with an antibody influx time course, allowing for a clearer comparison between the pathway of Notch4 in different situations. This could be utilised to investigate DTX and mutations further. Improvements could be made to the signalling assays by broadening target genes tested to create a more complex Notch4 target gene signature, which could then be investigated with the different situations researched here (lack of DTX, mutations etc). *In vivo* research could be expanded with the creation of an inducible Notch4 mouse line, to allow for the tight control of Notch4 signalling and therefore greater organism-wide investigation into its signalling. Ligand requirements could be investigated with the creation of Notch ligand expressing fibroblast cell lines which could be co-cultured with WT or mutant Notch4 expressing cells.

The preliminary RNAseq presented and analysed here should be expanded to include more repeats to increase the robustness of results. It could then be investigated further through validation of genes and pathways identified. For example, the mutation that produced a gene signature of DNA damage and repair could be investigated for chemotherapy and radiotherapy resistance. In addition, the mutation that had upregulated immune-related pathways could be investigated for sensitivity to immune targeting drugs. These insights could then be applied clinically to breast cancer in a predictive or prognostic way, to identify breast cancers that have a high Notch4 driven BCSC activity as well as those that may respond to Notch4 specific therapies. This could provide more personalised therapy for breast cancer.

It would be beneficial to repeat the experiments investigated in this thesis in more ER+ breast cancer cell lines or patient-derived samples to validate the findings. It would also be interesting to compare this to ER- cell lines and cell lines from other subtypes of breast cancer. Furthermore, it will be of interest to the wider research community to investigate Notch4 endocytic pathway dependent signalling in other cancers, other tissues that are reliant on Notch signalling including the vasculature, or other diseases. The investigation of endocytic pathway signalling by other Notch receptors is also important. Notch4's endocytic signalling activity is linked to the residue Y914 that is not present in other receptors, but the other Notch receptors may have the ability to signal in this way under certain conditions. Mutations of the other Notch receptors that alter the conserved histidine to a tyrosine as in Notch4, could occur in certain diseases or cancers, potentially driving them to signal in a similar way to Notch4.

In conclusion, we have found that Notch4 can signal via an endocytic pathway dependent route, which requires DTX1 and DTX4. DTX4 and TRPML are required for Notch4 mediated breast cancer stem cell activity in endocrine resistant cells and the Y914 residue, which has been linked to ligand independent signalling in *Drosophila*, is required for this Notch4 signalling and BCSC activity. Other results have provided the methods and preliminary data to identify components that are involved in this signalling pathway in BCSCs.

7 References

(EBCTCG), E. B. C. T. C. G. (2011). Effect of radiotherapy after breast-conserving surgery on 10-year recurrence and 15-year breast cancer death: meta-analysis of individual patient data for 10 801 women in 17 randomised trials. *Lancet*, *378*(9804), 1707.

(EBCTCG), E. B. C. T. C. G. (2018). Long-term outcomes for neoadjuvant versus adjuvant chemotherapy in early breast cancer: meta-analysis of individual patient data from ten randomised trials. *The Lancet. Oncology*, *19*(1), 27.

A Study of AL101 Monotherapy in Patients With Notch Activated Triple Negative Breast Cancer - Full Text View - ClinicalTrials.gov. (n.d.). Retrieved January 6, 2022, from https://clinicaltrials.gov/ct2/show/NCT04461600

Abel, S., Hundhausen, C., Mentlein, R., Schulte, A., Berkhout, T. A., Broadway, N., Hartmann, D., Sedlacek, R., Dietrich, S., Muetze, B., Schuster, B., Kallen, K.-J., Saftig, P., Rose-John, S., & Ludwig, A. (2004). The Transmembrane CXC-Chemokine Ligand 16 Is Induced by IFN-γ and TNF-α and Shed by the Activity of the Disintegrin-Like Metalloproteinase ADAM10. *The Journal of Immunology*, *172*(10), 6362–6372.

Ables, J. L., Breunig, J. J., Eisch, A. J., & Rakic, P. (2011). Not(ch) just development: Notch signalling in the adult brain. *Nature Reviews. Neuroscience*, *12*(5), 269–283.

Akhter, N., Dar, S. A., Haque, S., Wahid, M., Jawed, A., Akhtar, S., Alharbi, R. A., Sindi, A. A. A., Alruwetei, A., Zubair Choudhry, H. M., & Ahmad, A. (2021). Crosstalk of Cyclin-dependent kinase inhibitor 1A (CDKN1A) gene polymorphism with p53 and CCND1 polymorphism in breast cancer. *European Review for Medical and Pharmacological Sciences*, *25*(12), 4258–4273.

Al-Hajj, M., Wicha, M. S., Benito-Hernandez, A., Morrison, S. J., & Clarke, M. F. (2003). Prospective identification of tumorigenic breast cancer cells. *Proceedings of the National Academy of Sciences*, *100*(7), 3983–3988.

Anderson, K. N., Schwab, R. B., & Martinez, M. E. (2014). Reproductive Risk Factors and Breast Cancer Subtypes: A Review of the Literature. *Breast Cancer Research and Treatment*, *144*(1), 1.

Andersson, E. R., Sandberg, R., & Lendahl, U. (2011). Notch signaling: simplicity in design, versatility in function. *Development (Cambridge, England)*, *138*(17), 3593–3612.

Arpino, G., Green, S. J., Allred, D. C., Lew, D., Martino, S., Osborne, C. K., & Elledge, R. M. (2004). HER-2 Amplification, HER-1 Expression, and Tamoxifen Response in Estrogen Receptor-Positive Metastatic Breast Cancer: A Southwest Oncology Group Study. *Clinical Cancer Research*, *10*(17), 5670–5676.

Ayyanan, A., Civenni, G., Ciarloni, L., Morel, C., Mueller, N., Lefort, K., Mandinova, A., Raffoul, W., Fiche, M., Dotto, G. P., & Brisken, C. (2006). Increased Wnt signaling triggers oncogenic conversion of human breast epithelial cells by a Notch-dependent mechanism. *Proceedings of the National Academy of Sciences of the United States of America*, *103*(10), 3799.

Bache, S., & Wickham, H. (2020). *magrittr: A Forward-Pipe Operator for R. R package version 2.0.1.*

Banerji, S., Cibulskis, K., Rangel-Escareno, C., Brown, K. K., Carter, S. L., Frederick, A. M., Lawrence, M. S., Sivachenko, A. Y., Sougnez, C., Zou, L., Cortes, M. L., Fernandez-Lopez, J. C., Peng, S., Ardlie, K. G., Auclair, D., Bautista-Piña, V., Duke, F., Francis, J., Jung, J., …

Meyerson, M. (2012). Sequence analysis of mutations and translocations across breast cancer subtypes. *Nature*, *486*(7403), 405–409.

Baselga, J., Cortés, J., Kim, S.-B., Im, S.-A., Hegg, R., Im, Y.-H., Roman, L., Pedrini, J. L., Pienkowski, T., Knott, A., Clark, E., Benyunes, M. C., Ross, G., Swain, S. M., & CLEOPATRA Study Group. (2012). Pertuzumab plus Trastuzumab plus Docetaxel for Metastatic Breast Cancer. *New England Journal of Medicine*, *366*(2), 109–119.

Basudan, A., Priedigkeit, N., Hartmaier, R. J., Sokol, E. S., Bahreini, A., Watters, R. J., Boisen, M. M., Bhargava, R., Weiss, K. R., Karsten, M. M., Denkert, C., Blohmer, J. U., Leone, J. P., Hamilton, R. L., Brufsky, A. M., Elishaev, E., Lucas, P. C., Lee, A. V., & Oesterreich, S. (2019). Frequent ESR1 and CDK Pathway Copy-Number Alterations in Metastatic Breast Cancer. *Molecular Cancer Research*, *17*(2), 457–468.

Bazan-Peregrino, M., Sainson, R. C. A., Carlisle, R. C., Thoma, C., Waters, R. A., Arvanitis, C., Harris, A. L., Hernandez-Alcoceba, R., & Seymour, L. W. (2013). Combining virotherapy and angiotherapy for the treatment of breast cancer. *Cancer Gene Therapy 2013 20:8*, *20*(8), 461–468.

Bellavia, D., Checquolo, S., Campese, A. F., Felli, M. P., Gulino, A., & Screpanti, I. (2008). Notch3: from subtle structural differences to functional diversity. *Oncogene*, *27*(38), 5092–5098.

Bertucci, F., Finetti, P., Guille, A., Adélaïde, J., Garnier, S., Carbuccia, N., Monneur, A., Charafe-Jauffret, E., Goncalves, A., Viens, P., Birnbaum, D., & Chaffanet, M. (2016). Comparative genomic analysis of primary tumors and metastases in breast cancer. *Oncotarget*, *7*(19), 27208–27219.

Bhimani, J., Ball, K., & Stebbing, J. (2020). Patient-derived xenograft models—the future of personalised cancer treatment. *British Journal of Cancer 2020 122:5*, *122*(5), 601–602.

Biglia, N., Peano, E., Sgandurra, P., Moggio, G., Pecchio, S., Maggiorotto, F., & Sismondi, P. (2013). Body mass index (BMI) and breast cancer: impact on tumor histopatologic features, cancer subtypes and recurrence rate in pre and postmenopausal women. *Http://Dx.Doi.Org/10.3109/09513590.2012.736559*, *29*(3), 263–267.

Bladström, A., Anderson, H., & Olsson, H. (2003). Worse Survival in Breast Cancer Among Women with Recent Childbirth: Results from a Swedish Population-Based Register Study. *Clinical Breast Cancer*, *4*(4), 280–285.

Bolós, V., Mira, E., Martínez-Poveda, B., Luxán, G., Cañamero, M., Martínez-A, C., Mañes, S., & de la Pompa, J. L. (2013). Notch activation stimulates migration of breast cancer cells and promotes tumor growth. *Breast Cancer Research*, *15*(4), R54.

Bouras, T., Pal, B., Vaillant, F., Harburg, G., Asselin-Labat, M. L., Oakes, S. R., Lindeman, G. J., & Visvader, J. E. (2008). Notch Signaling Regulates Mammary Stem Cell Function and Luminal Cell-Fate Commitment. *Cell Stem Cell*, *3*(4), 429–441.

Bozorgi, A., Khazaei, M., & Khazaei, M. R. (2015). New Findings on Breast Cancer Stem Cells: A Review. *Journal of Breast Cancer*, *18*(4), 303–312.

Brennan, K., Tateson, R., Lewis, K., & Arias, A. M. (1997). A functional analysis of Notch mutations in Drosophila. *Genetics*, *147*(1), 177–188.

Brenton, J. D., Carey, L. A., Ahmed, A. A., & Caldas, C. (2005). Molecular Classification and Molecular Forecasting of Breast Cancer: Ready for Clinical Application? *Journal of Clinical Oncology*, *23*(29), 7350–7360.

Brugnoli, F., Grassilli, S., Al-Qassab, Y., Capitani, S., & Bertagnolo, V. (2019). CD133 in Breast Cancer Cells: More than a Stem Cell Marker. *Journal of Oncology*, *2019*.

Brunner, A., Cattaruzza, F., Yen, W.-C., Yeung, P., Fischer, M., Cancilla, B., O'Young, G., Tam, R., Liu, Y.-W., Gurney, A., Lewicki, J., Hoey, T., Wang, M., & Kapoun, A. M. (2016). Abstract 4652: Effects of anti-DLL4 treatment on non-small cell lung cancer (NSCLC) human xenograft tumors. *Cancer Research*, *76*(14 Supplement), 4652–4652.

Bui, Q. T., Im, J. H., Jeong, S. B., Kim, Y.-M., Lim, S. C., Kim, B., & Kang, K. W. (2017). *Essential role of Notch4/STAT3 signaling in epithelialemesenchymal transition of tamoxifen-resistant human breast cancer*.

Carey, L. A., Perou, C. M., Livasy, C. A., Dressler, L. G., Cowan, D., Conway, K., Karaca, G., Troester, M. A., Tse, C. K., Edmiston, S., Deming, S. L., Geradts, J., Cheang, M. C. U., Nielsen, T. O., Moorman, P. G., Earp, H. S., & Millikan, R. C. (2006). Race, Breast Cancer Subtypes, and Survival in the Carolina Breast Cancer Study. *JAMA*, *295*(21), 2492.

Carlson, M. (2019). *org.Hs.eg.db: Genome wide annotation for Human. R package version 3.8.2.*

Castro, N. P., Rangel, M. C., Merchant, A. S., MacKinnon, G., Cuttitta, F., Salomon, D. S., & Kim, Y. S. (2019). Sulforaphane Suppresses the Growth of Triple-negative Breast Cancer Stem-like Cells In vitro and In vivo. *Cancer Prevention Research*, *12*(3), 147–158.

Cerami, E., Gao, J., Dogrusoz, U., Gross, B. E., Sumer, S. O., Aksoy, B. A., Jacobsen, A., Byrne, C. J., Heuer, M. L., Larsson, E., Antipin, Y., Reva, B., Goldberg, A. P., Sander, C., & Schultz, N. (2012). The cBio Cancer Genomics Portal: An Open Platform for Exploring Multidimensional Cancer Genomics Data. *Cancer Discovery*, *2*(5), 401–404.

Chakrabarti, R., Celià-Terrassa, T., Kumar, S., Hang, X., Wei, Y., Choudhury, A., Hwang, J., Peng, J., Nixon, B., Grady, J. J., DeCoste, C., Gao, J., van Es, J. H., Li, M. O., Aifantis, I., Clevers, H., & Kang, Y. (2018). Notch ligand Dll1 mediates cross-talk between mammary stem cells and the macrophageal niche. *Science*, *360*(6396).

Chang, W., Cheng, J., Allaire, J., Sievert, C., Schloerke, B., Xie, Y., Allen, J., McPherson, J., Dipert, A., & Borges, B. (2021). *shiny: Web Application Framework for R. R package version 1.6.0.*

Chastagner, P., Rubinstein, E., & Brou, C. (2017). Ligand-activated Notch undergoes DTX4-mediated ubiquitylation and bilateral endocytosis before ADAM10 processing. *Science Signaling*, *10*(483).

Chen, C., Zhao, S., Karnad, A., & Freeman, J. W. (2018). The biology and role of CD44 in cancer progression: therapeutic implications. *Journal of Hematology & Oncology*, *11*(1).

Chiorean, E. G., LoRusso, P., Strother, R. M., Diamond, J. R., Younger, A., Messersmith, W. A., Adriaens, L., Liu, L., Kao, R. J., DiCioccio, A. T., Kostic, A., Leek, R., Harris, A., & Jimeno, A. (2015). A Phase I First-in-Human Study of Enoticumab (REGN421), a Fully Human Delta-like Ligand 4 (Dll4) Monoclonal Antibody in Patients with Advanced Solid Tumors. *Clinical Cancer Research*, *21*(12), 2695–2703.

Chun, S. Y., Kwon, Y. S., Nam, K. S., & Kim, S. (2015). Lapatinib enhances the cytotoxic effects of doxorubicin in MCF-7 tumorspheres by inhibiting the drug efflux function of ABC transporters. *Biomedicine & Pharmacotherapy*, *72*, 37–43.

Ciriello, G., Gatza, M. L., Beck, A. H., Wilkerson, M. D., Rhie, S. K., Pastore, A., Zhang, H., McLellan, M., Yau, C., Kandoth, C., Bowlby, R., Shen, H., Hayat, S., Fieldhouse, R., Lester,

S. C., Tse, G. M. K., Factor, R. E., Collins, L. C., Allison, K. H., … Zmuda, E. (2015). Comprehensive Molecular Portraits of Invasive Lobular Breast Cancer. *Cell*, *163*(2), 506–519.

Clarke, R., Tyson, J. J., & Dixon, J. M. (2015). Endocrine resistance in breast cancer--An overview and update. *Molecular and Cellular Endocrinology*, *418 Pt 3*(0 3), 220–234.

Cole, A. J., Fayomi, A. P., Anyaeche, V. I., Bai, S., & Buckanovich, R. J. (2020). An evolving paradigm of cancer stem cell hierarchies: therapeutic implications. *Theranostics*, *10*(7), 3083.

Collu, G. M., & Brennan, K. (2007). Cooperation between Wnt and Notch signalling in human breast cancer. *Breast Cancer Research*, *9*(3), 105.

Cortesi, L., Rugo, H. S., & Jackisch, C. (2021). An Overview of PARP Inhibitors for the Treatment of Breast Cancer. *Targeted Oncology*, *16*(3), 255–282.

Creighton, C. J., Fu, X., Hennessy, B. T., Casa, A. J., Zhang, Y., Gonzalez-Angulo, A. M., Lluch, A., Gray, J. W., Brown, P. H., Hilsenbeck, S. G., Osborne, C. K., Mills, G. B., Lee, A. V, & Schiff, R. (2010). Proteomic and transcriptomic profiling reveals a link between the PI3K pathway and lower estrogen-receptor (ER) levels and activity in ER+ breast cancer. *Breast Cancer Research*, *12*(3), R40.

Creighton, C. J., Li, X., Landis, M., Dixon, J. M., Neumeister, V. M., Sjolund, A., Rimm, D. L., Wong, H., Rodriguez, A., Herschkowitz, J. I., Fan, C., Zhang, X., He, X., Pavlick, A., Gutierrez, M. C., Renshaw, L., Larionov, A. A., Faratian, D., Hilsenbeck, S. G., … Chang, J. C. (2009). Residual breast cancers after conventional therapy display mesenchymal as well as tumor-initiating features. *Proceedings of the National Academy of Sciences of the United States of America*, *106*(33), 13820–13825.

Cui, X., Schiff, R., Arpino, G., Osborne, C. K., & Lee, A. V. (2005). Biology of progesterone receptor loss in breast cancer and its implications for endocrine therapy. *Journal of Clinical Oncology : Official Journal of the American Society of Clinical Oncology*, *23*(30), 7721–7735.

Curtis, C., Shah, S. P., Chin, S.-F., Turashvili, G., Rueda, O. M., Dunning, M. J., Speed, D., Lynch, A. G., Samarajiwa, S., Yuan, Y., Gräf, S., Ha, G., Haffari, G., Bashashati, A., Russell, R., McKinney, S., Caldas, C., Aparicio, S., Curtis†, C., … Aparicio, S. (2012). The genomic and transcriptomic architecture of 2,000 breast tumours reveals novel subgroups. *Nature*, *486*(7403), 346.

D'Angelo, R. C., Ouzounova, M., Davis, A., Choi, D., Tchuenkam, S. M., Kim, G., Luther, T., Quraishi, A. A., Senbabaoglu, Y., Conley, S. J., Clouthier, S. G., Hassan, K. A., Wicha, M. S., & Korkaya, H. (2015). Notch reporter activity in breast cancer cell lines identifies a subset of cells with stem cell activity. *Molecular Cancer Therapeutics*, *14*(3), 779–787.

D'Souza, B., Meloty-Kapella, L., & Weinmaster, G. (2010). Canonical and non-canonical Notch ligands. *Current Topics in Developmental Biology*, *92*, 73–129.

Dai, X., Chen, A., & Bai, Z. (2015). Integrative investigation on breast cancer in ER, PR and HER2-defined subgroups using mRNA and miRNA expression profiling. *Scientific Reports*, *4*(1), 6566.

Dai, X., Li, T., Bai, Z., Yang, Y., Liu, X., Zhan, J., & Shi, B. (2015). Breast cancer intrinsic subtype classification, clinical use and future trends. *American Journal of Cancer Research*, *5*(10), 2929–2943.

Dawson, S.-J., Rueda, O. M., Aparicio, S., & Caldas, C. (2013). Review A new genome-driven integrated classification of breast cancer and its implications. *The EMBO Journal*, *32*, 617–628.

Deng, H., Zhang, X.-T., Wang, M.-L., Zheng, H.-Y., Liu, L.-J., & Wang, Z.-Y. (2014). ER-α36-Mediated Rapid Estrogen Signaling Positively Regulates ER-Positive Breast Cancer Stem/Progenitor Cells. *PLoS ONE*, *9*(2), e88034.

Dent, S., Cortés, J., Im, Y. H., Diéras, V., Harbeck, N., Krop, I. E., Wilson, T. R., Cui, N., Schimmoller, F., Hsu, J. Y., He, J., De Laurentiis, M., Sousa, S., Drullinsky, P., & Jacot, W. (2021). Phase III randomized study of taselisib or placebo with fulvestrant in estrogen receptor-positive, PIK3CA-mutant, HER2-negative, advanced breast cancer: the SANDPIPER trial☆. *Annals of Oncology*, *32*(2), 197–207.

DeOme, K. B., Faulkin, L. J., Bern, H. A., & Blair, P. B. (1959). Development of Mammary Tumors from Hyperplastic Alveolar Nodules Transplanted into Gland-free Mammary Fat Pads of Female C3H Mice. *Cancer Research*, *19*(5).

Dexter, J. S. (1914). The Analysis of a Case of Continuous Variation in Drosophila by a Study of Its Linkage Relations. In *The American Naturalist* (Vol. 48, pp. 712–758). The University of Chicago PressThe American Society of Naturalists.

Dickler, M. N., Tolaney, S. M., Rugo, H. S., Cortés, J., Diéras, V., Patt, D., Wildiers, H., Hudis, C. A., O'Shaughnessy, J., Zamora, E., Yardley, D. A., Frenzel, M., Koustenis, A., & Baselga, J. (2017). MONARCH 1, A Phase II Study of Abemaciclib, a CDK4 and CDK6 Inhibitor, as a Single Agent, in Patients with Refractory HR $^{+}$ /HER2 $^{-}$ Metastatic Breast Cancer. *Clinical Cancer Research*, *23*(17), 5218–5224.

Dickson, B. C., Mulligan, A. M., Zhang, H., Lockwood, G., O'Malley, F. P., Egan, S. E., & Reedijk, M. (2007). High-level JAG1 mRNA and protein predict poor outcome in breast cancer. *Modern Pathology*, *20*(6), 685–693.

Domenici, G., Aurrekoetxea-Rodríguez, I., Simões, B. M., Rábano, M., Lee, S. Y., Millán, J. S., Comaills, V., Oliemuller, E., López-Ruiz, J. A., Zabalza, I., Howard, B. A., Kypta, R. M., & Vivanco, M. dM. (2019). A Sox2–Sox9 signalling axis maintains human breast luminal progenitor and breast cancer stem cells. *Oncogene*, *38*(17), 3151.

Dontu, G., Abdallah, W. M., Foley, J. M., Jackson, K. W., Clarke, M. F., Kawamura, M. J., & Wicha, M. S. (2003). In vitro propagation and transcriptional profiling of human mammary stem/progenitor cells. *Genes & Development*, *17*(10), 1253–1270.

Dontu, G., Jackson, K. W., McNicholas, E., Kawamura, M. J., Abdallah, W. M., & Wicha, M. S. (2004). Role of Notch signaling in cell-fate determination of human mammary stem/progenitor cells. *Breast Cancer Research*, *6*(6), 1–11.

Dowsett, M., Nicholson, R. I., & Pietras, R. J. (2005). Biological characteristics of the pure antiestrogen fulvestrant: overcoming endocrine resistance. *Breast Cancer Research and Treatment*, *93 Suppl 1*, S11-8.

Dufraine, J., Funahashi, Y., & Kitajewski, J. (2008). Notch signaling regulates tumor angiogenesis by diverse mechanisms. *Oncogene*, *27*(38), 5132–5137.

Early Breast Cancer Trialists' Collaborative Group (EBCTCG), E. B. C. T. C. G., Davies, C., Godwin, J., Gray, R., Clarke, M., Cutter, D., Darby, S., McGale, P., Pan, H. C., Taylor, C., Wang, Y. C., Dowsett, M., Ingle, J., & Peto, R. (2011). Relevance of breast cancer hormone receptors and other factors to the efficacy of adjuvant tamoxifen: patient-

level meta-analysis of randomised trials. *Lancet (London, England)*, *378*(9793), 771–784.

Edwards, A., & Brennan, K. (2021). Notch Signalling in Breast Development and Cancer. *Frontiers in Cell and Developmental Biology*, *0*, 1709.

Eirew, P., Stingl, J., Raouf, A., Turashvili, G., Aparicio, S., Emerman, J. T., & Eaves, C. J. (2008). A method for quantifying normal human mammary epithelial stem cells with in vivo regenerative ability. *Nature Medicine*, *14*(12), 1384–1389.

Ercan, C., Vermeulen, J. F., Hoefnagel, L., Bult, P., Van Der Groep, P., Van Der Wall, E., & Van Diest, P. J. (2012). HIF-1a and NOTCH signaling in ductal and lobular carcinomas of the breast. *Cellular Oncology*, *35*(6), 435–442.

Evans, D. G., Howell, S. J., & Howell, A. (2018). Personalized prevention in high risk individuals: Managing hormones and beyond. *The Breast*, *39*, 139–147.

Eyre, R., Alférez, D. G., Santiago-Gómez, A., Spence, K., McConnell, J. C., Hart, C., Simões, B. M., Lefley, D., Tulotta, C., Storer, J., Gurney, A., Clarke, N., Brown, M., Howell, S. J., Sims, A. H., Farnie, G., Ottewell, P. D., & Clarke, R. B. (2019). Microenvironmental IL1β promotes breast cancer metastatic colonisation in the bone via activation of Wnt signalling. *Nature Communications 2019 10:1*, *10*(1), 1–15.

Eyre, R., Alférez, D. G., Spence, K., Kamal, M., Shaw, F. L., Simões, B. M., Santiago-Gómez, A., Sarmiento-Castro, A., Bramley, M., Absar, M., Saad, Z., Chatterjee, S., Kirwan, C., Gandhi, A., Armstrong, A. C., Wardley, A. M., O'Brien, C. S., Farnie, G., Howell, S. J., & Clarke, R. B. (2016). Patient-derived Mammosphere and Xenograft Tumour Initiation Correlates with Progression to Metastasis. *Journal of Mammary Gland Biology and Neoplasia*, *21*(3–4), 99–109.

Fanfani, V., Zatopkova, M., Harris, A. L., Pezzella, F., & Stracquadanio, G. (2021). Dissecting the heritable risk of breast cancer: From statistical methods to susceptibility genes. *Seminars in Cancer Biology*, *72*, 175–184.

Farnie, G., Clarke, R. B., Spence, K., Pinnock, N., Brennan, K., Anderson, N. G., & Bundred, N. J. (2007). Novel cell culture technique for primary ductal carcinoma in situ: Role of notch and epidermal growth Factor Receptor Signaling Pathways. *Journal of the National Cancer Institute*, *99*(8), 616–627.

Ferrari, A., Vincent-Salomon, A., Pivot, X., Sertier, A.-S., Thomas, E., Tonon, L., Boyault, S., Mulugeta, E., Treilleux, I., MacGrogan, G., Arnould, L., Kielbassa, J., Le Texier, V., Blanché, H., Deleuze, J.-F., Jacquemier, J., Mathieu, M.-C., Penault-Llorca, F., Bibeau, F., … Thomas, G. (2016). A whole-genome sequence and transcriptome perspective on HER2-positive breast cancers. *Nature Communications*, *7*, 12222.

Fillmore, C. M., Gupta, P. B., Rudnick, J. A., Caballero, S., Keller, P. J., Lander, E. S., & Kuperwasser, C. (2010). Estrogen expands breast cancer stem-like cells through paracrine FGF/Tbx3 signaling. *Proceedings of the National Academy of Sciences*, *107*(50), 21737–21742.

Finegan, K. G., Perez-Madrigal, D., Hitchin, J. R., Davies, C. C., Jordan, A. M., & Tournier, C. (2015). ERK5 Is a Critical Mediator of Inflammation-Driven Cancer. *Cancer Research*, *75*(4), 742–753.

Finn, R. S., Martin, M., Rugo, H. S., Jones, S., Im, S.-A., Gelmon, K., Harbeck, N., Lipatov, O. N., Walshe, J. M., Moulder, S., Gauthier, E., Lu, D. R., Randolph, S., Diéras, V., & Slamon, D.

J. (2016). Palbociclib and Letrozole in Advanced Breast Cancer. *New England Journal of Medicine*, *375*(20), 1925–1936.

Frasor, J., Stossi, F., Danes, J. M., Komm, B., Lyttle, C. R., & Katzenellenbogen, B. S. (2004). Selective estrogen receptor modulators: discrimination of agonistic versus antagonistic activities by gene expression profiling in breast cancer cells. *Cancer Research*, *64*(4), 1522–1533.

Gallahan, D., & Callahan, R. (1997). The mouse mammary tumor associated gene INT3 is a unique member of the NOTCH gene family (NOTCH4). *Oncogene*, *14*(16), 1883–1890.

Gallahan, D., Jhappan, C., Robinson, G., Hennighausen, L., Sharp, R., Kordon, E., Callahan, R., Merlino, G., & Smith, G. H. (1996). Expression of a truncated Int3 gene in developing secretory mammary epithelium specifically retards lobular differentiation resulting in tumorigenesis. *Cancer Research*, *56*(8), 1775–1785.

Gao, J., Aksoy, B. A., Dogrusoz, U., Dresdner, G., Gross, B., Sumer, S. O., Sun, Y., Jacobsen, A., Sinha, R., Larsson, E., Cerami, E., Sander, C., & Schultz, N. (2013). Integrative Analysis of Complex Cancer Genomics and Clinical Profiles Using the cBioPortal. *Science Signaling*, *6*(269), pl1.

Gara, S. K., Lack, J., Zhang, L., Harris, E., Cam, M., & Kebebew, E. (2018). Metastatic adrenocortical carcinoma displays higher mutation rate and tumor heterogeneity than primary tumors. *Nature Communications*, *9*(1).

Garg, V., Muth, A. N., Ransom, J. F., Schluterman, M. K., Barnes, R., King, I. N., Grossfeld, P. D., & Srivastava, D. (2005). Mutations in NOTCH1 cause aortic valve disease. *Nature*, *437*(7056), 270–274.

Garza-Treviño, E. N., Said-Fernández, S. L., & Martínez-Rodríguez, H. G. (2015). Understanding the colon cancer stem cells and perspectives on treatment. *Cancer Cell International*, *15*(1), 2.

Gasca, J., Flores, M. L., Jiménez-Guerrero, R., Sáez, M. E., Barragán, I., Ruíz-Borrego, M., Tortolero, M., Romero, F., Sáez, C., & Japón, M. A. (2020). EDIL3 promotes epithelial–mesenchymal transition and paclitaxel resistance through its interaction with integrin αVβ3 in cancer cells. *Cell Death Discovery 2020 6:1*, *6*(1), 1–14.

Gelsomino, L., Panza, S., Giordano, C., Barone, I., Gu, G., Spina, E., Catalano, S., Fuqua, S., & Andò, S. (2018). Mutations in the estrogen receptor alpha hormone binding domain promote stem cell phenotype through notch activation in breast cancer cell lines. *Cancer Letters*, *428*, 12–20.

Ginestier, C., Hur, M. H., Charafe-Jauffret, E., Monville, F., Dutcher, J., Brown, M., Jacquemier, J., Viens, P., Kleer, C. G., Liu, S., Schott, A., Hayes, D., Birnbaum, D., Wicha, M. S., & Dontu, G. (2007). ALDH1 Is a Marker of Normal and Malignant Human Mammary Stem Cells and a Predictor of Poor Clinical Outcome. *Cell Stem Cell*, *1*(5), 555–567.

Ginestier, C., Liu, S., Diebel, M. E., Korkaya, H., Luo, M., Brown, M., Wicinski, J., Cabaud, O., Charafe-Jauffret, E., Birnbaum, D., Guan, J. L., Dontu, G., & Wicha, M. S. (2010). CXCR1 blockade selectively targets human breast cancer stem cells in vitro and in xenografts. *The Journal of Clinical Investigation*, *120*(2), 485.

Gordon, W. R., Roy, M., Vardar-Ulu, D., Garfinkel, M., Mansour, M. R., Aster, J. C., & Blacklow, S. C. (2009). Structure of the Notch1-negative regulatory region: implications for normal activation and pathogenic signaling in T-ALL. *Blood*, *113*(18), 4381–4390.

Gridley, T. (2003). Notch signaling and inherited disease syndromes. *Human Molecular Genetics*, *12 Spec No 1*, R9-13.

Grossman, R. L., Heath, A. P., Ferretti, V., Varmus, H. E., Lowy, D. R., Kibbe, W. A., & Staudt, L. M. (2016). Toward a Shared Vision for Cancer Genomic Data. *New England Journal of Medicine*, *375*(12), 1109–1112.

Guillen, K. P., Fujita, M., Butterfield, A. J., Scherer, S. D., Bailey, M. H., Chu, Z., Derose, Y. S., Zhao, L., Cortes-Sanchez, E., Yang, C.-H., Toner, J., Wang, G., Qiao, Y., Huang, X., Greenland, J. A., Vahrenkamp, J. M., Lum, D. H., Factor, R. E., Nelson, E. W., … Welm, A. L. (2021). *A breast cancer patient-derived xenograft and organoid platform for drug discovery and precision oncology*.

Gupta, P. B., Onder, T. T., Jiang, G., Tao, K., Kuperwasser, C., Weinberg, R. A., & Lander, E. S. (2009). Identification of selective inhibitors of cancer stem cells by high-throughput screening. *Cell*, *138*(4), 645.

Guruharsha, K. G., Kankel, M. W., & Artavanis-Tsakonas, S. (2012). The Notch signalling system: Recent insights into the complexity of a conserved pathway. *Nature Reviews Genetics*, *13*(9), 654–666.

Győrffy, B. (2021). Survival analysis across the entire transcriptome identifies biomarkers with the highest prognostic power in breast cancer. *Computational and Structural Biotechnology Journal*, *19*, 4101–4109.

Haapasalo, A., & Kovacs, D. M. (2011). The Many Substrates of Presenilin/γ-Secretase. *Journal of Alzheimer's Disease*, *25*(1), 3.

Hamajima, N., Hirose, K., Tajima, K., Rohan, T., Friedenreich, C. M., Calle, E. E., Gapstur, S. M., Patel, A. V., Coates, R. J., Liff, J. M., Talamini, R., Chantarakul, N., Koetsawang, S., Rachawat, D., Marcou, Y., Kakouri, E., Duffy, S. W., Morabia, A., Schuman, L., … Fukao, A. (2012). Menarche, menopause, and breast cancer risk: Individual participant meta-analysis, including 118 964 women with breast cancer from 117 epidemiological studies. *The Lancet Oncology*, *13*(11), 1141–1151.

Han, J., Hendzel, M. J., & Allalunis-Turner, J. (2011). Notch signaling as a therapeutic target for breast cancer treatment? *Breast Cancer Research : BCR*, *13*(3), 210.

Han, L., Diehl, A., Nguyen, N. K., Korangath, P., Teo, W., Cho, S., Kominsky, S., Huso, D. L., Feigenbaum, L., Rein, A., Argani, P., Landberg, G., Gessler, M., & Sukumar, S. (2014). The Notch pathway inhibits TGF-β signaling in breast cancer through HEYL-mediated crosstalk. *Cancer Research*, *74*(22), 6509.

Hanker, A. B., Sudhan, D. R., & Arteaga, C. L. (2020). Cancer Cell Review Overcoming Endocrine Resistance in Breast Cancer. *Cancer Cell*, *37*, 496–513.

Harb, H., Stephen-Victor, E., Crestani, E., Benamar, M., Massoud, A., Cui, Y., Charbonnier, L.-M., Arbag, S., Baris, S., Cunnigham, A., Leyva-Castillo, J. M., Geha, R. S., Mousavi, A. J., Guennewig, B., Schmitz-Abe, K., Sioutas, C., Phipatanakul, W., & Chatila, T. A. (2020). A regulatory T cell Notch4–GDF15 axis licenses tissue inflammation in asthma. *Nature Immunology 2020 21:11*, *21*(11), 1359–1370.

Harbeck, N., Penault-Llorca, F., Cortes, J., Gnant, M., Houssami, N., Poortmans, P., Ruddy, K., Tsang, J., & Cardoso, F. (2019). Breast cancer. *Nature Reviews Disease Primers 2019 5:1*, *5*(1), 1–31.

Harrison, H., Farnie, G., Howell, S. J., Rock, R. E., Stylianou, S., Brennan, K. R., Bundred, N. J.,

& Clarke, R. B. (2010). Regulation of breast cancer stem cell activity by signaling through the Notch4 receptor. *Cancer Research*, *70*(2), 709–718.

Harrison, H., Rogerson, L., Gregson, H. J., Brennan, K. R., Clarke, R. B., & Landberg, G. (2013). Contrasting Hypoxic Effects on Breast Cancer Stem Cell Hierarchy Is Dependent on ER-α Status. *Cancer Research*, *73*(4), 1420–1433.

Harrison, H., Simões, B. M., Rogerson, L., Howell, S. J., Landberg, G., & Clarke, R. B. (2013). Oestrogen increases the activity of oestrogen receptor negative breast cancer stem cells through paracrine EGFR and Notch signalling. *Breast Cancer Research : BCR*, *15*(2), R21.

Haughian, J. M., Pinto, M. P., Harrell, J. C., Bliesner, B. S., Joensuu, K. M., Dye, W. W., Sartorius, C. A., Tan, A. C., Heikkilä, P., Perou, C. M., & Horwitz, K. B. (2012). Maintenance of hormone responsiveness in luminal breast cancers by suppression of Notch. *Proceedings of the National Academy of Sciences of the United States of America*, *109*(8), 2742–2747.

Hellström, M., Phng, L.-K., Hofmann, J. J., Wallgard, E., Coultas, L., Lindblom, P., Alva, J., Nilsson, A.-K., Karlsson, L., Gaiano, N., Yoon, K., Rossant, J., Iruela-Arispe, M. L., Kalén, M., Gerhardt, H., & Betsholtz, C. (2007). Dll4 signalling through Notch1 regulates formation of tip cells during angiogenesis. *Nature*, *445*(7129), 776–780.

Heo, T. H., Wahler, J., & Suh, N. (2016). Potential therapeutic implications of IL-6/IL-6R/gp130-targeting agents in breast cancer. *Oncotarget*, *7*(13), 15460.

Hong, C. C., Tang, B. K., Hammond, G. L., Tritchler, D., Yaffe, M., & Boyd, N. F. (2004). Cytochrome P450 1A2 (CYP1A2) activity and risk factors for breast cancer: a cross-sectional study. *Breast Cancer Research*, *6*(4), R352.

Hori, K., Sen, A., Kirchhausen, T., & Artavanis-Tsakonas, S. (2011). Synergy between the ESCRT-III complex and Deltex defines a ligand-independent Notch signal. *The Journal of Cell Biology*, *195*(6), 1005–1015.

Hortobagyi, G. N., Stemmer, S. M., Burris, H. A., Yap, Y.-S., Sonke, G. S., Paluch-Shimon, S., Campone, M., Blackwell, K. L., André, F., Winer, E. P., Janni, W., Verma, S., Conte, P., Arteaga, C. L., Cameron, D. A., Petrakova, K., Hart, L. L., Villanueva, C., Chan, A., … O'Shaughnessy, J. (2016). Ribociclib as First-Line Therapy for HR-Positive, Advanced Breast Cancer. *New England Journal of Medicine*, *375*(18), 1738–1748.

Howell, A., Robertson, J. F. R., Abram, P., Lichinitser, M. R., Elledge, R., Bajetta, E., Watanabe, T., Morris, C., Webster, A., Dimery, I., & Osborne, C. K. (2004). Comparison of Fulvestrant Versus Tamoxifen for the Treatment of Advanced Breast Cancer in Postmenopausal Women Previously Untreated With Endocrine Therapy: A Multinational, Double-Blind, Randomized Trial. *Journal of Clinical Oncology*, *22*(9), 1605–1613.

Howell, S. J., Campone, M., Cortés, J., Duhoux, F. P., Ross, S., Morris, T., & Franklin, S. (2019). 341P Final results of the STEM trial: SFX-01 in the treatment and evaluation of ER1 Her2-metastatic breast cancer (mBC). *Abstract Book of the 44th ESMO Congress (ESMO 2019) 27 September – 1 October 2019, Barcelona, Spain*, *30*, v122.

Howell, S. J., Johnston, S. R. D., & Howell, A. (2004). The use of selective estrogen receptor modulators and selective estrogen receptor down-regulators in breast cancer. *Best Practice & Research. Clinical Endocrinology & Metabolism*, *18*(1), 47–66.

Hsu, T. S., Mo, S. T., Hsu, P. N., & Lai, M. Z. (2018). c-FLIP is a target of the E3 ligase deltex1 in gastric cancer. *Cell Death & Disease 2018 9:2*, *9*(2), 1–12.

Hu, C., Diévart, A., Lupien, M., Calvo, E., Tremblay, G., & Jolicoeur, P. (2006). Overexpression of activated murine Notch1 and Notch3 in transgenic mice blocks mammary gland development and induces mammary tumors. *American Journal of Pathology*, *168*(3), 973–990.

Hu, Y., & Smyth, G. K. (2009). ELDA: Extreme limiting dilution analysis for comparing depleted and enriched populations in stem cell and other assays. *Journal of Immunological Methods*, *347*(1–2), 70–78.

Hu, Z., Fan, C., Oh, D. S., Marron, J., He, X., Qaqish, B. F., Livasy, C., Carey, L. A., Reynolds, E., Dressler, L., Nobel, A., Parker, J., Ewend, M. G., Sawyer, L. R., Wu, J., Liu, Y., Nanda, R., Tretiakova, M., Orrico, A., … Perou, C. M. (2006). The molecular portraits of breast tumors are conserved across microarray platforms. *BMC Genomics*, *7*(1), 96.

Huang, C.-C., Tu, S.-H., Lien, H.-H., Jeng, J.-Y., Huang, C.-S., Huang, C.-J., Lai, L.-C., & Chuang, E. Y. (2013). Concurrent Gene Signatures for Han Chinese Breast Cancers. *PLOS ONE*, *8*(10), e76421.

Huber, R. M., Rajski, M., Sivasankaran, B., Moncayo, G., Hemmings, B. A., & Merlo, A. (2013). Deltex-1 Activates Mitotic Signaling and Proliferation and Increases the Clonogenic and Invasive Potential of U373 and LN18 Glioblastoma Cells and Correlates with Patient Survival. *PLOS ONE*, *8*(2), e57793.

Huntly, B. J. P., & Gilliland, D. G. (2005). Timeline: Leukaemia stem cells and the evolution of cancer-stem-cell research. *Nature Reviews Cancer*, *5*(4), 311–321.

James, A. C., Szot, J. O., Iyer, K., Major, J. A., Pursglove, S. E., Chapman, G., & Dunwoodie, S. L. (2014). Notch4 reveals a novel mechanism regulating Notch signal transduction. *Biochimica et Biophysica Acta (BBA) - Molecular Cell Research*, *1843*(7), 1272–1284.

Jawaid, W. (2021). *enrichR: Provides an R Interface to 'Enrichr'. R package version 3.0.*

Jerusalem, G., De Boer, R. H., Hurvitz, S., Yardley, D. A., Kovalenko, E., Ejlertsen, B., Blau, S., Özgüroğlu, M., Landherr, L., Ewertz, M., Taran, T., Fan, J., Noel-Baron, F., Louveau, A. L., & Burris, H. (2018). Everolimus Plus Exemestane vs Everolimus or Capecitabine Monotherapy for Estrogen Receptor-Positive, HER2-Negative Advanced Breast Cancer: The BOLERO-6 Randomized Clinical Trial. *JAMA Oncology*, *4*(10), 1367–1374.

Jiang, H., Zhou, C., Zhang, Z., Wang, Q., Wei, H., Shi, W., Li, J., Wang, Z., Ou, Y., Wang, W., Wang, H., Zhang, Q., Sun, W., Sun, P., & Yang, S. (2020). Jagged1-Notch1-deployed tumor perivascular niche promotes breast cancer stem cell phenotype through Zeb1. *Nature Communications 2020 11:1*, *11*(1), 1–16.

Jin, S., Mutvei, A. P., Chivukula, I. V., Andersson, E. R., Ramsköld, D., Sandberg, R., Lee, K. L., Kronqvist, P., Mamaeva, V., Östling, P., Mpindi, J. P., Kallioniemi, O., Screpanti, I., Poellinger, L., Sahlgren, C., & Lendahl, U. (2013). Non-canonical Notch signaling activates IL-6/JAK/STAT signaling in breast tumor cells and is controlled by p53 and IKKα/IKKβ. *Oncogene*, *32*(41), 4892–4902.

Jones, R. H., Casbard, A., Carucci, M., Cox, C., Butler, R., Alchami, F., Madden, T. A., Bale, C., Bezecny, P., Joffe, J., Moon, S., Twelves, C., Venkitaraman, R., Waters, S., Foxley, A., & Howell, S. J. (2020). Fulvestrant plus capivasertib versus placebo after relapse or progression on an aromatase inhibitor in metastatic, oestrogen receptor-positive breast

cancer (FAKTION): a multicentre, randomised, controlled, phase 2 trial. *The Lancet Oncology*, *21*(3), 345–357.

Jubb, A. M., Soilleux, E. J., Turley, H., Steers, G., Parker, A., Low, I., Blades, J., Li, J. L., Allen, P., Leek, R., Noguera-Troise, I., Gatter, K. C., Thurston, G., & Harris, A. L. (2010). Expression of vascular Notch ligand delta-like 4 and inflammatory markers in breast cancer. *American Journal of Pathology*, *176*(4), 2019–2028.

Kabos, P., Haughian, J. M., Wang, X., Dye, W. W., Finlayson, C., Elias, A., Horwitz, K. B., & Sartorius, C. A. (2011). Cytokeratin 5 positive cells represent a steroid receptor negative and therapy resistant subpopulation in luminal breast cancers. *Breast Cancer Research and Treatment*, *128*(1), 45–55.

Kakuda, S., & Haltiwanger, R. S. (2017). Deciphering the Fringe-mediated Notch Code: Identification of activating and inhibiting sites allowing discrimination between ligands. *Developmental Cell*, *40*(2), 193.

Kan, Z., Ding, Y., Kim, J., Jung, H. H., Chung, W., Lal, S., Cho, S., Fernandez-Banet, J., Lee, S. K., Kim, S. W., Lee, J. E., Choi, Y. La, Deng, S., Kim, J. Y., Ahn, J. S., Sha, Y., Mu, X. J., Nam, J. Y., Im, Y. H., … Park, Y. H. (2018). Multi-omics profiling of younger Asian breast cancers reveals distinctive molecular signatures. *Nature Communications 2018 9:1*, *9*(1), 1–13.

Kan, Z., Jaiswal, B. S., Stinson, J., Janakiraman, V., Bhatt, D., Stern, H. M., Yue, P., Haverty, P. M., Bourgon, R., Zheng, J., Moorhead, M., Chaudhuri, S., Tomsho, L. P., Peters, B. A., Pujara, K., Cordes, S., Davis, D. P., Carlton, V. E. H., Yuan, W., … Seshagiri, S. (2010). Diverse somatic mutation patterns and pathway alterations in human cancers. *Nature*, *466*(7308), 869–873.

Kangsamaksin, T., Murtomaki, A., Kofler, N. M., Cuervo, H., Chaudhri, R. A., Tattersall, I. W., Rosenstiel, P. E., Shawber, C. J., & Kitajewski, J. (2015). NOTCH decoys that selectively block DLL/NOTCH or JAG/NOTCH disrupt angiogenesis by unique mechanisms to inhibit tumor growth. *Cancer Discovery*, *5*(2), 182–197.

Kim, H. S., Han, H. D., Armaiz-Pena, G. N., Stone, R. L., Nam, E. J., Lee, J. W., Shahzad, M. M. K., Nick, A. M., Lee, S. J., Roh, J. W., Nishimura, M., Mangala, L. S., Bottsford-Miller, J., Gallick, G. E., Lopez-Berestein, G., & Sood, A. K. (2011). Functional Roles of Src and Fgr in Ovarian Carcinoma. *Clinical Cancer Research*, *17*(7), 1713–1721.

Kim, S.-L., Choi, H. S., Kim, J.-H., & Lee, D.-S. (2020). The Antiasthma Medication Ciclesonide Suppresses Breast Cancer Stem Cells through Inhibition of the Glucocorticoid Receptor Signaling-Dependent YAP Pathway. *Molecules 2020, Vol. 25, Page 6028*, *25*(24), 6028.

Knowlden, J. M., Hutcheson, I. R., Jones, H. E., Madden, T., Gee, J. M. W., Harper, M. E., Barrow, D., Wakeling, A. E., & Nicholson, R. I. (2003). Elevated Levels of Epidermal Growth Factor Receptor/c-erbB2 Heterodimers Mediate an Autocrine Growth Regulatory Pathway in Tamoxifen-Resistant MCF-7 Cells. *Endocrinology*, *144*(3), 1032–1044.

Koboldt, D. C., Fulton, R. S., McLellan, M. D., Schmidt, H., Kalicki-Veizer, J., McMichael, J. F., Fulton, L. L., Dooling, D. J., Ding, L., Mardis, E. R., Wilson, R. K., Ally, A., Balasundaram, M., Butterfield, Y. S. N., Carlsen, R., Carter, C., Chu, A., Chuah, E., Chun, H.-J. E., … Palchik, J. D. (2012). Comprehensive molecular portraits of human breast tumours. *Nature*, *490*(7418), 61–70.

Kolde, R. (2019). *pheatmap: Pretty Heatmaps. R package version 1.0.12.*

Kopan, R., & Ilagan, M. X. G. (2009). The canonical Notch signaling pathway: unfolding the activation mechanism. *Cell*, *137*(2), 216–233.

Kordon, E. C., & Smith, G. H. (1998). An entire functional mammary gland may comprise the progeny from a single cell. *Development (Cambridge, England)*, *125*(10), 1921–1930.

Korotkevich, G., Sukhov, V., & Sergushichev, A. (2019). *Fast gene set enrichment analysis. bioRxiv*.

Krawczyk, N., Meier-Stiegen, F., Banys, M., Neubauer, H., Ruckhaeberle, E., & Fehm, T. (2014). Expression of stem cell and epithelial-mesenchymal transition markers in circulating tumor cells of breast cancer patients. *BioMed Research International*, *2014*.

Krebs, L. T., Xue, Y., Norton, C. R., Shutter, J. R., Maguire, M., Sundberg, J. P., Gallahan, D., Closson, V., Kitajewski, J., Callahan, R., Smith, G. H., Stark, K. L., & Gridley, T. (2000). Notch signaling is essential for vascular morphogenesis in mice. *Genes & Development*, *14*(11), 1343–1352.

Krug, K., Jaehnig, E. J., Satpathy, S., Blumenberg, L., Karpova, A., Anurag, M., Miles, G., Mertins, P., Geffen, Y., Tang, L. C., Heiman, D. I., Cao, S., Maruvka, Y. E., Lei, J. T., Huang, C., Kothadia, R. B., Colaprico, A., Birger, C., Wang, J., … Zimmerman, L. J. (2020). Proteogenomic Landscape of Breast Cancer Tumorigenesis and Targeted Therapy. *Cell*, *183*(5), 1436-1456.e31.

Kumar, S., Srivastav, R. K., Wilkes, D. W., Ross, T., Kim, S., Kowalski, J., Chatla, S., Zhang, Q., Nayak, A., Guha, M., Fuchs, S. Y., Thomas, C., & Chakrabarti, R. (2018). Estrogen-dependent DLL1-mediated Notch signaling promotes luminal breast cancer. *Oncogene 2018 38:12*, *38*(12), 2092–2107.

Lamy, M., Ferreira, A., Dias, J. S., Braga, S., Silva, G., & Barbas, A. (2017). Notch-out for breast cancer therapies. *New Biotechnology*, *39*, 215–221.

Lawrence, M. S., Stojanov, P., Mermel, C. H., Robinson, J. T., Garraway, L. A., Golub, T. R., Meyerson, M., Gabriel, S. B., Lander, E. S., & Getz, G. (2014). Discovery and saturation analysis of cancer genes across 21 tumour types. *Nature 2014 505:7484*, *505*(7484), 495–501.

Lawson, D. A., Bhakta, N. R., Kessenbrock, K., Prummel, K. D., Yu, Y., Takai, K., Zhou, A., Eyob, H., Balakrishnan, S., Wang, C.-Y., Yaswen, P., Goga, A., & Werb, Z. (2015). Single-cell analysis reveals a stem-cell program in human metastatic breast cancer cells. *Nature 2015 526:7571*, *526*(7571), 131–135.

Layman, R. M., & Arun, B. (2021). PARP Inhibitors in Triple-Negative Breast Cancer including Those with BRCA Mutations. *Cancer Journal (United States)*, *27*(1), 67–75.

Lee, H.-R., Kim, T.-H., & Choi, K.-C. (2012). Functions and physiological roles of two types of estrogen receptors, ERα and ERβ, identified by estrogen receptor knockout mouse. *Laboratory Animal Research*, *28*(2), 71–76.

Lee, J. H., Shin, K. M., Lee, S. Y., Hong, M. J., Choi, J. E., Kang, H. G., Do, S. K., Lee, W. K., Lee, E. B., Seok, Y., Jeong, J. Y., Yoo, S. S., Lee, J., Cha, S. I., Kim, C. H., Cho, S., Jheon, S., Kim, Y. C., Oh, I. J., … Park, J. Y. (2019). Genetic Variant of Notch Regulator DTX1 Predicts Survival After Lung Cancer Surgery. *Annals of Surgical Oncology*, *26*(11), 3756–3764.

Lee, J. J. X., Loh, K., & Yap, Y. S. (2015). PI3K/Akt/mTOR inhibitors in breast cancer. *Cancer Biology & Medicine*, *12*(4), 342.

Lefebvre, C., Bachelot, T., Filleron, T., Pedrero, M., Campone, M., Soria, J.-C., Massard, C., Lévy, C., Arnedos, M., Lacroix-Triki, M., Garrabey, J., Boursin, Y., Deloger, M., Fu, Y., Commo, F., Scott, V., Lacroix, L., Dieci, M. V., Kamal, M., … André, F. (2016). Mutational Profile of Metastatic Breast Cancers: A Retrospective Analysis. *PLOS Medicine*, *13*(12), e1002201.

Lei, J. T., Anurag, M., Haricharan, S., Gou, X., & Ellis, M. J. (2019). Endocrine therapy resistance: new insights. *Breast (Edinburgh, Scotland)*, *48*(Suppl 1), S26.

Lei, J. T., Shao, J., Zhang, J., Iglesia, M., Chan, D. W., Cao, J., Anurag, M., Singh, P., He, X., Kosaka, Y., Matsunuma, R., Crowder, R., Hoog, J., Phommaly, C., Goncalves, R., Ramalho, S., Peres, R. M. R., Punturi, N., Schmidt, C., … Ellis, M. J. (2018). Functional Annotation of ESR1 Gene Fusions in Estrogen Receptor-Positive Breast Cancer. *Cell Reports*, *24*(6), 1434.

Leong, K. G., Niessen, K., Kulic, I., Raouf, A., Eaves, C., Pollet, I., & Karsan, A. (2007). Jagged1-mediated Notch activation induces epithelial-to-mesenchymal transition through Slug-induced repression of E-cadherin. *Journal of Experimental Medicine*, *204*(12), 2935–2948.

Leriche, G., Chen, A. C., Kim, S., Selkoe, D. J., & Yang, J. (2016). A Fluorescent Analog of Batimastat Enables Imaging of α-Secretase in Living Cells HHS Public Access. *ACS Chem Neurosci*, *7*(1), 40–45.

Levine, M. E., Suarez, J. A., Brandhorst, S., Balasubramanian, P., Cheng, C.-W., Madia, F., Fontana, L., Mirisola, M. G., Guevara-Aguirre, J., Wan, J., Passarino, G., Kennedy, B. K., Cohen, P., Crimmins, E. M., & Longo, V. D. (2014). Low Protein Intake is Associated with a Major Reduction in IGF-1, Cancer, and Overall Mortality in the 65 and Younger but Not Older Population. *Cell Metabolism*, *19*(3), 407.

Li, L., Zhao, F., Lu, J., Li, T., Yang, H., Wu, C., & Liu, Y. (2014). Notch-1 Signaling Promotes the Malignant Features of Human Breast Cancer through NF-κB Activation. *PLoS ONE*, *9*(4), e95912.

Li, Y., Welm, B., Podsypanina, K., Huang, S., Chamorro, M., Zhang, X., Rowlands, T., Egeblad, M., Cowin, P., Werb, Z., Tan, L. K., Rosen, J. M., & Varmus, H. E. (2003). Evidence that transgenes encoding components of the Wnt signaling pathway preferentially induce mammary cancers from progenitor cells. *Proceedings of the National Academy of Sciences of the United States of America*, *100*(26), 15853.

Liang, Y., Han, H., Liu, L., Duan, Y., Yang, X., Ma, C., Zhu, Y., Han, J., Li, X., & Chen, Y. (2018). CD36 plays a critical role in proliferation, migration and tamoxifen-inhibited growth of ER-positive breast cancer cells. *Oncogenesis 2018 7:12*, *7*(12), 1–14.

Lin, X., Sun, B., Zhu, D., Zhao, X., Sun, R., Zhang, Y., Zhang, D., Dong, X., Gu, Q., Li, Y., & Liu, F. (2016). Notch4+ cancer stem-like cells promote the metastatic and invasive ability of melanoma. *Cancer Science*, *107*(8), 1079.

Liu, B. Y., McDermott, S. P., Khwaja, S. S., & Alexander, C. M. (2004). The transforming activity of Wnt effectors correlates with their ability to induce the accumulation of mammary progenitor cells. *Proceedings of the National Academy of Sciences of the United States of America*, *101*(12), 4158.

Liu, J., Pan, S., Hsieh, M. H., Ng, N., Sun, F., Wang, T., Kasibhatla, S., Schuller, A. G., Li, A. G., Cheng, D., Li, J., Tompkins, C., Pferdekamper, A. M., Steffy, A., Cheng, J., Kowal, C., Phung, V., Guo, G., Wang, Y., … Harris, J. L. (2013). Targeting Wnt-driven cancer through

the inhibition of Porcupine by LGK974. *Proceedings of the National Academy of Sciences of the United States of America*, *110*(50), 20224–20229.

Liu, L., Yin, B., Yi, Z., Liu, X., Hu, Z., Gao, W., Yu, H., & Li, Q. (2018). Breast cancer stem cells characterized by CD70 expression preferentially metastasize to the lungs. *Breast Cancer 2018 25:6*, *25*(6), 706–716.

Liu, S., Cong, Y., Wang, D., Sun, Y., Deng, L., Liu, Y., Martin-Trevino, R., Shang, L., McDermott, S. P., Landis, M. D., Hong, S., Adams, A., D'Angelo, R., Ginestier, C., Charafe-Jauffret, E., Clouthier, S. G., Birnbaum, D., Wong, S. T., Zhan, M., … Wicha, M. S. (2014). Breast cancer stem cells transition between epithelial and mesenchymal states reflective of their normal counterparts. *Stem Cell Reports*, *2*(1), 78–91.

Liu, S., Dontu, G., Mantle, I. D., Patel, S., Ahn, N., Jackson, K. W., Suri, P., & Wicha, M. S. (2006). Hedgehog Signaling and Bmi-1 Regulate Self-renewal of Normal and Malignant Human Mammary Stem Cells. *Cancer Research*, *66*(12), 6063–6071.

Liu, S., Dontu, G., & Wicha, M. S. (2005). Mammary stem cells, self-renewal pathways, and carcinogenesis. *Breast Cancer Research*, *7*(3), 86–95.

Liu, W. M., Laux, H., Henry, J. Y., Bolton, T. B., Dalgleish, A. G., & Galustian, C. (2010). A microarray study of altered gene expression in colorectal cancer cells after treatment with immunomodulatory drugs: Differences in action in vivo and in vitro. *Molecular Biology Reports*, *37*(4), 1801–1814.

Lombardo, Y., Faronato, M., Filipovic, A., Vircillo, V., Magnani, L., & Coombes, R. C. (2014). Nicastrin and Notch4 drive endocrine therapy resistance and epithelial to mesenchymal transition in MCF7 breast cancer cells. *Breast Cancer Research*, *16*(3), 1–14.

Lopez, M., Di Lauro, L., Viola, G., Foggi, P., Conti, F., Corsetti, S., Sergi, D., Botti, C., Di Filippo, F., & Vici, P. (2009). [Adjuvant chemotherapy in hormone-receptor positive HER2-negative early breast cancer]. *La Clinica Terapeutica*, *160*(6), 481–488.

Low, J. A., Johnson, M. D., Bone, E. A., & Dickson, R. B. (1996). The matrix metalloproteinase inhibitor batimastat (BB-94) retards human breast cancer solid tumor growth but not ascites formation in nude mice. *Clinical Cancer Research*, *2*(7).

Luan, F., Li, X., Cheng, X., Huangfu, L., Han, J., Guo, T., Du, H., Wen, X., & Ji, J. (2020). TNFRSF11B activates Wnt/β-catenin signaling and promotes gastric cancer progression. *International Journal of Biological Sciences*, *16*(11), 1956.

Luca, V. C., Jude, K. M., Pierce, N. W., Nachury, M. V., Fischer, S., & Garcia, K. C. (2015). Structural basis for Notch1 engagement of Delta-like 4. *Science*, *347*(6224), 847–853.

Luca, V. C., Kim, B. C., Ge, C., Kakuda, S., Wu, D., Roein-Peikar, M., Haltiwanger, R. S., Zhu, C., Ha, T., & Garcia, K. C. (2017). Notch-Jagged complex structure implicates a catch bond in tuning ligand sensitivity. *Science*, *355*(6331), 1320–1324.

Luo, W. (2020). *gageData: Auxillary data for gage package. R package version 2.28.0.*

Luo, W., & Brouwer, C. (2013). Pathview: an R/Bioconductor package for pathway-based data integration and visualization. *Bioinformatics*, *29*(14), 1830–1831.

Luo, W., Friedman, M. S., Shedden, K., Hankenson, K. D., & Woolf, P. J. (2009). GAGE: generally applicable gene set enrichment for pathway analysis. *BMC Bioinformatics*, *10*, 161.

Macaulay, V., O'Byrne, K., Saunders, M., Braybrooke, J., Long, L., Gleeson, F., Mason, C.,

Harris, A., Brown, P., & Talbot, D. (1999). Phase I study of intrapleural batimastat (BB-94), a matrix metalloproteinase inhibitor, in the treatment of malignant pleural effusions. *Undefined*.

Magnani, L., Stoeck, A., Zhang, X., Lánczky, A., Mirabella, A. C., Wang, T. L., Gyorffy, B., & Lupien, M. (2013). Genome-wide reprogramming of the chromatin landscape underlies endocrine therapy resistance in breast cancer. *Proceedings of the National Academy of Sciences of the United States of America*, *110*(16).

Magnifico, A., Albano, L., Campaner, S., Delia, D., Castiglioni, F., Gasparini, P., Sozzi, G., Fontanella, E., Menard, S., & Tagliabue, E. (2009). Tumor-initiating cells of HER2-positive carcinoma cell lines express the highest oncoprotein levels and are sensitive to trastuzumab. *Clinical Cancer Research*, *15*(6), 2010–2021.

Mallmann, M. R., Staratschek-Jox, A., Rudlowski, C., Braun, M., Gaarz, A., Wolfgarten, M., Kuhn, W., & Schultze, J. L. (2010). Prediction and prognosis: impact of gene expression profiling in personalized treatment of breast cancer patients. *The EPMA Journal*, *1*(3), 421.

Maraver, A., Fernandez-Marcos, P. J., Herranz, D., Cañamero, M., Muñoz-Martin, M., Gómez-López, G., Mulero, F., Megías, D., Sanchez-Carbayo, M., Shen, J., Sanchez-Cespedes, M., Palomero, T., Ferrando, A., & Serrano, M. (2012). Therapeutic Effect of γ-Secretase Inhibition in KrasG12V-Driven Non-Small Cell Lung Carcinoma by Derepression of DUSP1 and Inhibition of ERK. *Cancer Cell*, *22*(2), 222–234.

Marini, F. (2020). *ideal: an R/Bioconductor package for Interactive Differential Expression Analysis, bioRxiv*.

Martorana, F., Motta, G., Pavone, G., Motta, L., Stella, S., Vitale, S. R., Manzella, L., & Vigneri, P. (2021). AKT Inhibitors: New Weapons in the Fight Against Breast Cancer? *Frontiers in Pharmacology*, *12*, 546.

Masiero, M., Li, D., Whiteman, P., Bentley, C., Greig, J., Hassanali, T., Watts, S., Stribbling, S., Yates, J., Bealing, E., Li, J. L., Chillakuri, C., Sheppard, D., Serres, S., Sarmiento-Soto, M., Larkin, J., Sibson, N. R., Handford, P. A., Harris, A. L., & Banham, A. H. (2019). Development of Therapeutic Anti-JAGGED1 Antibodies for Cancer Therapy. *Molecular Cancer Therapeutics*, *18*(11), 2030–2042.

Maurer, C., Martel, S., Zardavas, D., & Ignatiadis, M. (2017). New agents for endocrine resistance in breast cancer. *The Breast*, *34*, 1–11.

Mavaddat, N., Peock, S., Frost, D., Ellis, S., Platte, R., Fineberg, E., Evans, D. G., Izatt, L., Eeles, R. A., Adlard, J., Davidson, R., Eccles, D., Cole, T., Cook, J., Brewer, C., Tischkowitz, M., Douglas, F., Hodgson, S., Walker, L., … EMBRACE, on behalf of. (2013). Cancer Risks for BRCA1 and BRCA2 Mutation Carriers: Results From Prospective Analysis of EMBRACE. *JNCI: Journal of the National Cancer Institute*, *105*(11), 812–822.

Mazzone, M., Selfors, L. M., Albeck, J., Overholtzer, M., Sale, S., Carroll, D. L., Pandya, D., Lu, Y., Mills, G. B., Aster, J. C., Artavanis-Tsakonas, S., & Brugge, J. S. (2010). Dose-dependent induction of distinct phenotypic responses to Notch pathway activation in mammary epithelial cells. *Proceedings of the National Academy of Sciences of the United States of America*, *107*(11), 5012.

McCarthy, D. J., Chen, Y., & Smyth, G. K. (2012). Differential expression analysis of multifactor RNA-Seq experiments with respect to biological variation. *Nucleic Acids Research*, *40*(10), 4288.

McClelland, R. A., Barrow, D., Madden, T. A., Dutkowski, C. M., Pamment, J., Knowlden, J. M., Gee, J. M. W., & Nicholson, R. I. (2001). Enhanced Epidermal Growth Factor Receptor Signaling in MCF7 Breast Cancer Cells after Long-Term Culture in the Presence of the Pure Antiestrogen ICI 182,780 (Faslodex). *Endocrinology*, *142*(7), 2776–2788.

McGill, M. A., Dho, S. E., Weinmaster, G., & McGlade, C. J. (2009). Numb Regulates Post-endocytic Trafficking and Degradation of Notch1. *Journal of Biological Chemistry*, *284*(39), 26427–26438.

McTiernan, A., Kooperberg, C., White, E., Wilcox, S., Coates, R., Adams-Campbell, L. L., Woods, N., & Ockene, J. (2003). Recreational Physical Activity and the Risk of Breast Cancer in Postmenopausal Women: The Women's Health Initiative Cohort Study. *JAMA*, *290*(10), 1331–1336.

Mead, R. (Roger). (1988). *The design of experiments : statistical principles for practical applications*. Cambridge University Press.

Means-Powell, J. A., Mayer, I. A., Ismail-Khan, R., Valle, L. Del, Tonetti, D., Abramson, V. G., Sanders, M. S., Lush, R. M., Sorrentino, C., Majumder, S., & Miele, L. (2021). A Phase Ib Dose Escalation Trial of RO4929097 (a γ-secretase inhibitor) in Combination with Exemestane in Patients with ER + Metastatic Breast Cancer (MBC). *Clinical Breast Cancer*.

Mercogliano, M. F., Bruni, S., Elizalde, P. V., & Schillaci, R. (2020). Tumor Necrosis Factor α Blockade: An Opportunity to Tackle Breast Cancer. *Frontiers in Oncology*, *10*, 584.

Meriranta, L., Pasanen, A., Louhimo, R., Cervera, A., Alkodsi, A., Autio, M., Taskinen, M., Rantanen, V., Karjalainen-Lindsberg, M. L., Holte, H., Delabie, J., Lehtonen, R., Hautaniemi, S., & Leppä, S. (2017). Deltex-1 mutations predict poor survival in diffuse large B-cell lymphoma. *Haematologica*, *102*(5), e195–e198.

Meurette, O., & Mehlen, P. (2018). Notch Signaling in the Tumor Microenvironment. *Cancer Cell*, *34*(4), 536–548.

Meurette, O., Stylianou, S., Rock, R., Collu, G. M., Gilmore, A. P., & Brennan, K. (2009). Notch activation induces Akt signaling via an autocrine loop to prevent apoptosis in breast epithelial cells. *Cancer Research*, *69*(12), 5015–5022.

Milano, J., McKay, J., Dagenais, C., Foster-Brown, L., Pognan, F., Gadient, R., Jacobs, R. T., Zacco, A., Greenberg, B., & Ciaccio, P. J. (2004). Modulation of Notch Processing by γ-Secretase Inhibitors Causes Intestinal Goblet Cell Metaplasia and Induction of Genes Known to Specify Gut Secretory Lineage Differentiation. *Toxicological Sciences*, *82*(1), 341–358.

Miller, T. W., Balko, J. M., Fox, E. M., Ghazoui, Z., Dunbier, A., Anderson, H., Dowsett, M., Jiang, A., Smith, R. A., Maira, S.-M., Manning, H. C., González-Angulo, A. M., Mills, G. B., Higham, C., Chanthaphaychith, S., Kuba, M. G., Miller, W. R., Shyr, Y., & Arteaga, C. L. (2011). ERα-dependent E2F transcription can mediate resistance to estrogen deprivation in human breast cancer. *Cancer Discovery*, *1*(4), 338.

Min, A., Kim, J. E., Kim, Y. J., Lim, J. M., Kim, S., Kim, J. W., Lee, K. H., Kim, T. Y., Oh, D. Y., Bang, Y. J., & Im, S. A. (2018). Cyclin E overexpression confers resistance to the CDK4/6 specific inhibitor palbociclib in gastric cancer cells. *Cancer Letters*, *430*, 123–132.

Mittal, S., Subramanyam, D., Dey, D., Kumar, R. V, & Rangarajan, A. (2009). Cooperation of Notch and Ras/MAPK signaling pathways in human breast carcinogenesis. *Molecular*

Cancer, *8*(1), 128.

Miyamoto, Y., Maitra, A., Ghosh, B., Zechner, U., Argani, P., Iacobuzio-Donahue, C. A., Sriuranpong, V., Iso, T., Meszoely, I. M., Wolfe, M. S., Hruban, R. H., Ball, D. W., Schmid, R. M., & Leach, S. D. (2003). Notch mediates TGF alpha-induced changes in epithelial differentiation during pancreatic tumorigenesis. *Cancer Cell*, *3*(6), 565–576.

Mokbel, K. (2002). The evolving role of aromatase inhibitors in breast cancer. *International Journal of Clinical Oncology*, *7*(5), 279–283.

Mollen, E. W. J., Ient, J., Tjan-Heijnen, V. C. G., Boersma, L. J., Miele, L., Smidt, M. L., & Vooijs, M. A. G. G. (2018). Moving breast cancer therapy up a notch. *Frontiers in Oncology*, *8*, 518.

Morotti, M., Bridges, E., Valli, A., Choudhry, H., Sheldon, H., Wigfield, S., Gray, N., Zois, C. E., Grimm, F., Jones, D., Teoh, E. J., Cheng, W. C., Lord, S., Anastasiou, D., Haider, S., McIntyre, A., Goberdhan, D. C. I., Buffa, F., & Harris, A. L. (2019). Hypoxia-induced switch in SNAT2/SLC38A2 regulation generates endocrine resistance in breast cancer. *Proceedings of the National Academy of Sciences of the United States of America*, *116*(25), 12452–12461.

Müller, B. M., Keil, E., Lehmann, A., Winzer, K.-J., Richter-Ehrenstein, C., Prinzler, J., Bangemann, N., Reles, A., Stadie, S., Schoenegg, W., Eucker, J., Schmidt, M., Lippek, F., Jöhrens, K., Pahl, S., Sinn, B. V., Budczies, J., Dietel, M., & Denkert, C. (2013). The EndoPredict Gene-Expression Assay in Clinical Practice - Performance and Impact on Clinical Decisions. *PloS One*, *8*(6), e68252.

Müller, K., & Wickham, H. (2021). *tibble: Simple Data Frames. R package version 3.1.2.*

Mutvei, A. P., Fredlund, E., & Lendahl, U. (2015). Frequency and distribution of Notch mutations in tumor cell lines. *BMC Cancer*, *15*(1), 1–11.

Nagamatsu, I., Onishi, H., Matsushita, S., Kubo, M., Kai, M., Imaizumi, A., Nakano, K., Hattori, M., Oda, Y., Tanaka, M., & Katano, M. (2014). NOTCH4 is a potential therapeutic target for triple-negative breast cancer. *Anticancer Research*, *34*(1), 69–80.

Narayan, P., Prowell, T. M., Gao, J. J., Fernandes, L. L., Li, E., Jiang, X., Qiu, J., Fan, J., Song, P., Yu, J., Zhang, X., King-Kallimanis, B. L., Chen, W., Ricks, T. K., Gong, Y., Wang, X., Windsor, K., Rhieu, S. Y., Geiser, G., … Beaver, J. A. (2021). FDA Approval Summary: Alpelisib Plus Fulvestrant for Patients with HR-positive, HER2-negative, PIK3CA-mutated, Advanced or Metastatic Breast Cancer. *Clinical Cancer Research : An Official Journal of the American Association for Cancer Research*, *27*(7), 1842–1849.

Nazari, S. S., & Mukherjee, P. (2018). An overview of mammographic density and its association with breast cancer. *Breast Cancer 2018 25:3*, *25*(3), 259–267.

Nemetschke, L., & Knust, E. (2016). Drosophila Crumbs prevents ectopic Notch activation in developing wings by inhibiting ligand-independent endocytosis. *Development*, *143*(23), 4543–4553.

Neuwirth, E. (2014). *RColorBrewer: ColorBrewer Palettes. R package version 1.1-2.*

Nik-Zainal, S., Davies, H., Staaf, J., Ramakrishna, M., Glodzik, D., Zou, X., Martincorena, I., Alexandrov, L. B., Martin, S., Wedge, D. C., Van Loo, P., Ju, Y. S., Smid, M., Brinkman, A. B., Morganella, S., Aure, M. R., Lingjærde, O. C., Langerød, A., Ringnér, M., … Stratton, M. R. (2016). Landscape of somatic mutations in 560 breast cancer whole-genome sequences. *Nature*, *534*(7605), 47–54.

Nixon, M. J., Formisano, L., Mayer, I. A., Estrada, M. V., González-Ericsson, P. I., Isakoff, S. J., Forero-Torres, A., Won, H., Sanders, M. E., Solit, D. B., Berger, M. F., Cantley, L. C., Winer, E. P., Arteaga, C. L., & Balko, J. M. (2019). PIK3CA and MAP3K1 alterations imply luminal A status and are associated with clinical benefit from pan-PI3K inhibitor buparlisib and letrozole in ER+ metastatic breast cancer. *Npj Breast Cancer 2019 5:1*, *5*(1), 1–9.

Nowell, C. S., & Radtke, F. (2017). Notch as a tumour suppressor. *Nature Reviews Cancer*, *17*(3), 145–159.

Oon, C. E., Bridges, E., Sheldon, H., Sainson, R. C. A., Jubb, A., Turley, H., Leek, R., Buffa, F., Li, J. L., & Harris, A. L. (2014). Functional comparison of Notch ligands in tumour angiogenesis. *Asian Pacific Journal of Tropical Disease*, *4*(3), 229.

Osborne, C. K., & Schiff, R. (2011). Mechanisms of Endocrine Resistance in Breast Cancer. *Annual Review of Medicine*, *62*(1), 233–247.

Osipo, C., Golde, T. E., Osborne, B. A., & Miele, L. A. (2008). Off the beaten pathway: The complex cross talk between Notch and NF-κB. *Laboratory Investigation*, *88*(1), 11–17.

Pagès, H., Carlson, M., Falcon, S., & Li, N. (2020). *AnnotationDbi: Manipulation of SQLite-based annotations in Bioconductor. R package version 1.52.0.*

Paik, S., Shak, S., Tang, G., Kim, C., Baker, J., Cronin, M., Baehner, F. L., Walker, M. G., Watson, D., Park, T., Hiller, W., Fisher, E. R., Wickerham, D. L., Bryant, J., & Wolmark, N. (2009). A Multigene Assay to Predict Recurrence of Tamoxifen-Treated, Node-Negative Breast Cancer. *Http://Dx.Doi.Org/10.1056/NEJMoa041588*.

Pal, D., Kolluru, V., Chandrasekaran, B., Baby, B. V, Aman, M., Suman, S., Sirimulla, S., Sanders, M. A., Alatassi, H., Ankem, M. K., & Damodaran, C. (2017). Targeting aberrant expression of Notch-1 in ALDH+ cancer stem cells in breast cancer. *Molecular Carcinogenesis*, *56*(3), 1127.

Pan, H., Gray, R., Braybrooke, J., Davies, C., Taylor, C., McGale, P., Peto, R., Pritchard, K. I., Bergh, J., Dowsett, M., & Hayes, D. F. (2017). 20-Year Risks of Breast-Cancer Recurrence after Stopping Endocrine Therapy at 5 Years. *Http://Dx.Doi.Org/10.1056/NEJMoa1701830*, *377*(19), 1836–1846.

Patrawala, L., Calhoun, T., Schneider-Broussard, R., Zhou, J., Claypool, K., & Tang, D. G. (2005). Side population is enriched in tumorigenic, stem-like cancer cells, whereas ABCG2+ and ABCG2- cancer cells are similarly tumorigenic. *Cancer Research*, *65*(14), 6207–6219.

Paul, M. R., Pan, T. C., Pant, D. K., Shih, N. N. C., Chen, Y., Harvey, K. L., Solomon, A., Lieberman, D., Morrissette, J. J. D., Soucier-Ernst, D., Goodman, N. G., Stavropoulos, S. W., Maxwell, K. N., Clark, C., Belka, G. K., Feldman, M., DeMichele, A., & Chodosh, L. A. (2020). Genomic landscape of metastatic breast cancer identifies preferentially dysregulated pathways and targets. *The Journal of Clinical Investigation*, *130*(8), 4252–4265.

Pece, S., Serresi, M., Santolini, E., Capra, M., Hulleman, E., Galimberti, V., Zurrida, S., Maisonneuve, P., Viale, G., & Di Fiore, P. P. (2004). Loss of negative regulation by Numb over Notch is relevant to human breast carcinogenesis. *The Journal of Cell Biology*, *167*(2), 215–221.

Pece, S., Tosoni, D., Confalonieri, S., Mazzarol, G., Vecchi, M., Ronzoni, S., Bernard, L., Viale, G., Pelicci, P. G., & Di Fiore, P. P. (2010). Biological and Molecular Heterogeneity of

Breast Cancers Correlates with Their Cancer Stem Cell Content. *Cell*, *140*(1), 62–73.

Pellegrinet, L., Rodilla, V., Liu, Z., Chen, S., Koch, U., Espinosa, L., Kaestner, K. H., Kopan, R., Lewis, J., & Radtke, F. (2011). Dll1- and Dll4-Mediated Notch Signaling Are Required for Homeostasis of Intestinal Stem Cells. *Gastroenterology*, *140*(4), 1230-1240.e7.

Peng, D., Tanikawa, T., Li, W., Zhao, L., Vatan, L., Szeliga, W., Wan, S., Wei, S., Wang, Y., Liu, Y., Staroslawska, E., Szubstarski, F., Rolinski, J., Grywalska, E., Stanisławek, A., Polkowski, W., Kurylcio, A., Kleer, C., Chang, A. E., … Kryczek, I. (2016). Myeloid-Derived Suppressor Cells Endow Stem-like Qualities to Breast Cancer Cells through IL6/STAT3 and NO/NOTCH Cross-talk Signaling. *Cancer Research*, *76*(11), 3156–3165.

Perou, C. M., Sørlie, T., Eisen, M. B., van de Rijn, M., Jeffrey, S. S., Rees, C. A., Pollack, J. R., Ross, D. T., Johnsen, H., Akslen, L. A., Fluge, Ø., Pergamenschikov, A., Williams, C., Zhu, S. X., Lønning, P. E., Børresen-Dale, A.-L., Brown, P. O., & Botstein, D. (2000). Molecular portraits of human breast tumours. *Nature*, *406*(6797), 747–752.

Piva, M., Domenici, G., Iriondo, O., Rábano, M., Simões, B. M., Comaills, V., Barredo, I., López-Ruiz, J. A., Zabalza, I., Kypta, R., & Vivanco, M. D. M. (2014). Sox2 promotes tamoxifen resistance in breast cancer cells. *EMBO Molecular Medicine*, *6*(1), 66–79.

Politi, K., Feirt, N., & Kitajewski, J. (2004). Notch in mammary gland development and breast cancer. *Seminars in Cancer Biology*, *14*(5), 341–347.

Ponti, D., Costa, A., Zaffaroni, N., Pratesi, G., Petrangolini, G., Coradini, D., Pilotti, S., Pierotti, M. A., & Daidone, M. G. (2005). Isolation and in vitro propagation of tumorigenic breast cancer cells with stem/progenitor cell properties. *Cancer Research*, *65*(13), 5506–5511.

Proia, T., Jiang, F., Bell, A., Nicoletti, R., Kong, L., Kreuter, K., Poling, L., Winston, W. M., Flaherty, M., Weiler, S., Perino, S., O'Hagan, R., Lin, J., Gyuris, J., & Okamura, H. (2015). 23814, an Inhibitory Antibody of Ligand-Mediated Notch1 Activation, Modulates Angiogenesis and Inhibits Tumor Growth without Gastrointestinal Toxicity. *Molecular Cancer Therapeutics*, *14*(8), 1858–1867.

Pu, M., Messer, K., Davies, S. R., Vickery, T. L., Pittman, E., Parker, B. A., Ellis, M. J., Flatt, S. W., Marinac, C. R., Nelson, S. H., Mardis, E. R., Pierce, J. P., & Natarajan, L. (2020). Research-based PAM50 signature and long-term breast cancer survival. *Breast Cancer Research and Treatment*, *179*(1), 197–206.

R Core Team. (2020). *R: A language and environment for statistical computing. R Foundation for Statistical Computing, Vienna, Austria.*

R Studio Team. (2021). *RStudio: Integrated Development Environment for R. RStudio, PBC, Boston, MA*.

Rakha, E. A., Reis-Filho, J. S., & Ellis, I. O. (2008). Basal-like breast cancer: a critical review. *Journal of Clinical Oncology : Official Journal of the American Society of Clinical Oncology*, *26*(15), 2568–2581.

Ramakrishnan, G., Davaakhuu, G., Chung, W. C., Zhu, H., Rana, A., Filipovic, A., Green, A. R., Atfi, A., Pannuti, A., Miele, L., & Tzivion, G. (2015). AKT and 14-3-3 Regulate Notch4 Nuclear Localization. *Scientific Reports*, *5*(1), 8782.

Razavi, P., Chang, M. T., Xu, G., Bandlamudi, C., Ross, D. S., Vasan, N., Cai, Y., Bielski, C. M., Donoghue, M. T. A., Jonsson, P., Penson, A., Shen, R., Pareja, F., Kundra, R., Middha, S., Cheng, M. L., Zehir, A., Kandoth, C., Patel, R., … Baselga, J. (2018). The Genomic Landscape of Endocrine-Resistant Advanced BreastCancers. *Cancer Cell*, *34*(3), 427.

Reedijk, M., Odorcic, S., Chang, L., Zhang, H., Miller, N., McCready, D. R., Lockwood, G., & Egan, S. E. (2005). High-level Coexpression of JAG1 and NOTCH1 Is Observed in Human Breast Cancer and Is Associated with Poor Overall Survival. *Cancer Research*, *65*(18), 8530–8537.

Reedijk, M., Pinnaduwage, D., Dickson, B. C., Mulligan, A. M., Zhang, H., Bull, S. B., O'Malley, F. P., Egan, S. E., & Andrulis, I. L. (2008). *JAG1 expression is associated with a basal phenotype and recurrence in lymph node-negative breast cancer*. 439–448.

Renehan, A. G., Zwahlen, M., Minder, C., O'Dwyer, S. T., Shalet, S. M., & Egger, M. (2004). Insulin-like growth factor (IGF)-I, IGF binding protein-3, and cancer risk: systematic review and meta-regression analysis. *The Lancet*, *363*(9418), 1346–1353.

Reynolds, B. A., & Weiss, S. (1996). Clonal and population analyses demonstrate that an EGF-responsive mammalian embryonic CNS precursor is a stem cell. *Developmental Biology*, *175*(1), 1–13.

Rich, J. N. (2016). Cancer stem cells: understanding tumor hierarchy and heterogeneity. *Medicine*, *95*(Suppl 1), S2–S7.

Rizzo, P., Miao, H., D'Souza, G., Osipo, C., Yun, J., Zhao, H., Mascarenhas, J., Wyatt, D., Antico, G., Hao, L., Yao, K., Rajan, P., Hicks, C., Siziopikou, K., Selvaggi, S., Bashir, A., Bhandari, D., Marchese, A., Lendahl, U., … Miele, L. (2008). Cross-talk between Notch and the Estrogen Receptor in Breast Cancer Suggests Novel Therapeutic Approaches. *Cancer Research*, *68*(13), 5226–5235.

Robbins, J., Blondel, B. J., Gallahan, D., & Callahan, R. (1992). Mouse mammary tumor gene int-3: a member of the notch gene family transforms mammary epithelial cells. *Journal of Virology*, *66*(4), 2594–2599.

Rojas, K., & Stuckey, A. (2016). Breast Cancer Epidemiology and Risk Factors. *Clinical Obstetrics and Gynecology*, *59*(4), 651–672.

Royce, M. E., & Osman, D. (2015). Everolimus in the Treatment of Metastatic Breast Cancer. *Breast Cancer : Basic and Clinical Research*, *9*, 73.

Sales-Dias, J., Silva, G., Lamy, M., Ferreira, A., & Barbas, A. (2019). The Notch ligand DLL1 exerts carcinogenic features in human breast cancer cells. *PLoS ONE*, *14*(5).

Samie, M., Wang, X., Zhang, X., Goschka, A., Li, X., Cheng, X., Gregg, E., Azar, M., Zhuo, Y., Garrity, A. G., Gao, Q., Slaugenhaupt, S., Pickel, J., Zolov, S. N., Weisman, L. S., Lenk, G. M., Titus, S., Bryant-Genevier, M., Southall, N., … Xu, H. (2013). A TRP Channel in the Lysosome Regulates Large Particle Phagocytosis via Focal Exocytosis. *Developmental Cell*, *26*(5), 511–524.

Santiago-Gómez, A., Kedward, T., Simões, B. M., Dragoni, I., NicAmhlaoibh, R., Trivier, E., Sabin, V., Gee, J. M., Sims, A. H., Howell, S. J., & Clarke, R. B. (2019). PAK4 regulates stemness and progression in endocrine resistant ER-positive metastatic breast cancer. *Cancer Letters*, *458*, 66–75.

Sarmiento-Castro, A., Caamaño-Gutiérrez, E., Sims, A. H., Hull, N. J., James, M. I., Santiago-Gómez, A., Eyre, R., Clark, C., Brown, M. E., Brooks, M. D., Wicha, M. S., Howell, S. J., Clarke, R. B., & Simões, B. M. (2020). Increased Expression of Interleukin-1 Receptor Characterizes Anti-estrogen-Resistant ALDH+ Breast Cancer Stem Cells. *Stem Cell Reports*, *15*(2), 307–316.

Schiff, R., Massarweh, S. A., Shou, J., Bharwani, L., Mohsin, S. K., & Osborne, C. K. (2004).

Cross-talk between estrogen receptor and growth factor pathways as a molecular target for overcoming endocrine resistance. *Clinical Cancer Research : An Official Journal of the American Association for Cancer Research*, *10*(1 Pt 2), 331S-6S.

Scholzen, T., & Gerdes, J. (2000). The Ki-67 protein: From the known and the unknown. *Journal of Cellular Physiology*, *182*(3), 311–322.

Sethi, N., Dai, X., Winter, C. G., & Kang, Y. (2011). Tumor-Derived Jagged1 Promotes Osteolytic Bone Metastasis of Breast Cancer by Engaging Notch Signaling in Bone Cells. *Cancer Cell*, *19*(2), 192–205.

Shackleton, M., Vaillant, F., Simpson, K. J., Stingl, J., Smyth, G. K., Asselin-Labat, M.-L., Wu, L., Lindeman, G. J., & Visvader, J. E. (2006). Generation of a functional mammary gland from a single stem cell. *Nature*, *439*(7072), 84–88.

Shen, S., Wei, C., & Fu, J. (2021). RNA-Sequencing Reveals Heat Shock 70-kDa Protein 6 (HSPA6) as a Novel Thymoquinone-Upregulated Gene That Inhibits Growth, Migration, and Invasion of Triple-Negative Breast Cancer Cells. *Frontiers in Oncology*, *11*, 1518.

Sherratt, M. J., McConnell, J. C., & Streuli, C. H. (2016). Raised mammographic density: causative mechanisms and biological consequences. *Breast Cancer Research 2016 18:1*, *18*(1), 1–9.

Shi, W., & Harris, A. L. (2006). Notch signaling in breast cancer and tumor angiogenesis: Cross-talk and therapeutic potentials. *Journal of Mammary Gland Biology and Neoplasia*, *11*(1), 41–52.

Shiino, S., Kinoshita, T., Yoshida, M., Jimbo, K., Asaga, S., Takayama, S., & Tsuda, H. (2016). Prognostic Impact of Discordance in Hormone Receptor Status Between Primary and Recurrent Sites in Patients With Recurrent Breast Cancer. *Clinical Breast Cancer*, *16*(4), e133–e140.

Shimizu, H., Woodcock, S. A., Wilkin, M. B., Trubenová, B., Monk, N. A. M., & Baron, M. (2014). Compensatory flux changes within an endocytic trafficking network maintain thermal robustness of Notch signaling. *Cell*, *157*(5), 1160–1174.

Siersbæk, R., Scabia, V., Nagarajan, S., Chernukhin, I., Papachristou, E. K., Broome, R., Johnston, S. J., Joosten, S. E. P., Green, A. R., Kumar, S., Jones, J., Omarjee, S., Alvarez-Fernandez, R., Glont, S., Aitken, S. J., Kishore, K., Cheeseman, D., Rakha, E. A., D'Santos, C., … Carroll, J. S. (2020). IL6/STAT3 Signaling Hijacks Estrogen Receptor α Enhancers to Drive Breast Cancer Metastasis. *Cancer Cell*, *38*(3), 412-423.e9.

Simões, B. M., Alferez, D. G., Howell, S. J., & Clarke, R. B. (2015). The role of steroid hormones in breast cancer stem cells. *Endocrine-Related Cancer*, *22*(6), T177–T186.

Simões, B. M., O'Brien, C. S., Eyre, R., Silva, A., Yu, L., Sarmiento-Castro, A., Alférez, D. G., Spence, K., Santiago-Gómez, A., Chemi, F., Acar, A., Gandhi, A., Howell, A., Brennan, K., Rydén, L., Catalano, S., Andó, S., Gee, J., Ucar, A., … Clarke, R. B. (2015). Anti-estrogen Resistance in Human Breast Tumors Is Driven by JAG1-NOTCH4-Dependent Cancer Stem Cell Activity. *Cell Reports*, *12*(12), 1968–1977.

Simões, B. M., Piva, M., Iriondo, O., Comaills, V., López-Ruiz, J. A., Zabalza, I., Mieza, J. A., Acinas, O., & Vivanco, M. d. M. (2011). Effects of estrogen on the proportion of stem cells in the breast. *Breast Cancer Research and Treatment*, *129*(1), 23–35.

Simões, B. M., Santiago-Gómez, A., Chiodo, C., Moreira, T., Conole, D., Lovell, S., Alferez, D., Eyre, R., Spence, K., Sarmiento-Castro, A., Kohler, B., Morisset, L., Lanzino, M., Andò, S.,

Marangoni, E., Sims, A. H., Tate, E. W., Howell, S. J., & Clarke, R. B. (2020). Targeting STAT3 signaling using stabilised sulforaphane (SFX-01) inhibits endocrine resistant stem-like cells in ER-positive breast cancer. *Oncogene 2020 39:25*, *39*(25), 4896–4908.

Sleeman, K. E., Kendrick, H., Ashworth, A., Isacke, C. M., & Smalley, M. J. (2005). CD24 staining of mouse mammary gland cells defines luminal epithelial, myoepithelial/basal and non-epithelial cells. *Breast Cancer Research*, *8*(1), R7.

Smith, G. H., Gallahan, D., Diella, F., Jhappan, C., Merlino, G., & Callahan, R. (1995). Constitutive expression of a truncated INT3 gene in mouse mammary epithelium impairs differentiation and functional development. *Cell Growth & Differentiation : The Molecular Biology Journal of the American Association for Cancer Research*, *6*(5), 563–577.

Smith, G. H., Gallahan, D., Zwiebel, J. A., Freeman, S. M., Bassin, R. H., & Callahan, R. (1991). Long-term in vivo expression of genes introduced by retrovirus-mediated transfer into mammary epithelial cells. *Journal of Virology*, *65*(11), 6365–6370.

Smith, N. G., Gyanchandani, R., Shah, O. S., Gurda, G. T., Lucas, P. C., Hartmaier, R. J., Brufsky, A. M., Puhalla, S., Bahreini, A., Kota, K., Wald, A. I., Nikiforov, Y. E., Nikiforova, M. N., Oesterreich, S., & Lee, A. V. (2019). Targeted mutation detection in breast cancer using MammaSeq™. *Breast Cancer Research 2019 21:1*, *21*(1), 1–11.

Smittenaar, C. R., Petersen, K. A., Stewart, K., & Moitt, N. (2016). Cancer incidence and mortality projections in the UK until 2035. *British Journal of Cancer*, *115*(9), 1147–1155.

Song, X., Call, G. B., Kirilly, D., & Xie, T. (2007). Notch signaling controls germline stem cell niche formation in the Drosophila ovary. *Development*, *134*(6), 1071–1080.

Sørlie, T., Perou, C. M., Tibshirani, R., Aas, T., Geisler, S., Johnsen, H., Hastie, T., Eisen, M. B., van de Rijn, M., Jeffrey, S. S., Thorsen, T., Quist, H., Matese, J. C., Brown, P. O., Botstein, D., Lønning, P. E., & Børresen-Dale, A. L. (2001). Gene expression patterns of breast carcinomas distinguish tumor subclasses with clinical implications. *Proceedings of the National Academy of Sciences of the United States of America*, *98*(19), 10869–10874.

Spring, L. M., Wander, S. A., Zangardi, M., & Bardia, A. (2019). CDK 4/6 Inhibitors in Breast Cancer: Current Controversies and Future Directions. *Current Oncology Reports*, *21*(3), 25.

Sprinzak, D., Lakhanpal, A., Lebon, L., Santat, L. A., Fontes, M. E., Anderson, G. A., Garcia-Ojalvo, J., & Elowitz, M. B. (2010). Cis-interactions between Notch and Delta generate mutually exclusive signalling states. *Nature*, *465*(7294), 86–90.

Steinbuck, M. P., & Winandy, S. (2018). A Review of Notch Processing With New Insights Into Ligand-Independent Notch Signaling in T-Cells. *Frontiers in Immunology*, *9*(JUN), 1.

Stojanov, D., Grozdanović, D., Petrović, S., Benedeto-Stojanov, D., Stefanović, I., Stojanović, N., & Ilić, D. N. (2014). De novo mutation in the NOTCH3 gene causing CADASIL. *Bosnian Journal of Basic Medical Sciences*, *14*(1), 48–50.

Stylianou, S., Clarke, R. B., & Brennan, K. (2006). Aberrant activation of notch signaling in human breast cancer. *Cancer Research*, *66*(3), 1517–1525.

Sun, Y., Lowther, W., Kato, K., Bianco, C., Kenney, N., Strizzi, L., Raafat, D., Hirota, M., Khan, N. I., Bargo, S., Jones, B., Salomon, D., & Callahan, R. (2005). Notch4 intracellular domain binding to Smad3 and inhibition of the TGF-β signaling. *Oncogene 2005 24:34*, *24*(34), 5365–5374.

Tate, J. G., Bamford, S., Jubb, H. C., Sondka, Z., Beare, D. M., Bindal, N., Boutselakis, H., Cole, C. G., Creatore, C., Dawson, E., Fish, P., Harsha, B., Hathaway, C., Jupe, S. C., Kok, C. Y., Noble, K., Ponting, L., Ramshaw, C. C., Rye, C. E., … Forbes, S. A. (2019). COSMIC: the Catalogue Of Somatic Mutations In Cancer. *Nucleic Acids Research*, *47*(D1), D941–D947.

Taurin, S., & Alkhalifa, H. (2020). Breast cancers, mammary stem cells, and cancer stem cells, characteristics, and hypotheses. *Neoplasia*, *22*(12), 663–678.

Tegally, H., Kensler, K. H., Mungloo-Dilmohamud, Z., Ghoorah, A. W., Rebbeck, T. R., & Baichoo, S. (2020). Discovering novel driver mutations from pan-cancer analysis of mutational and gene expression profiles. *PLOS ONE*, *15*(11), e0242780.

Thomas, R., Al-Khadairi, G., & Decock, J. (2021). Immune Checkpoint Inhibitors in Triple Negative Breast Cancer Treatment: Promising Future Prospects. *Frontiers in Oncology*, *10*, 3464.

Tirino, V., Desiderio, V., Paino, F., Rosa, A. De, Papaccio, F., Noce, M. La, Laino, L., Francesco, F. De, & Papaccio, G. (2013). Cancer stem cells in solid tumors: an overview and new approaches for their isolation and characterization. *The FASEB Journal*, *27*(1), 13–24.

Tosello, V., & Ferrando, A. A. (2013). The NOTCH signaling pathway: role in the pathogenesis of T-cell acute lymphoblastic leukemia and implication for therapy. *Therapeutic Advances in Hematology*, *4*(3), 199–210.

Toy, W., Shen, Y., Won, H., Green, B., Sakr, R. A., Will, M., Li, Z., Gala, K., Fanning, S., King, T. A., Hudis, C., Chen, D., Taran, T., Hortobagyi, G., Greene, G., Berger, M., Baselga, J., & Chandarlapaty, S. (2013). ESR1 ligand-binding domain mutations in hormone-resistant breast cancer. *Nature Genetics*, *45*(12), 1439–1445.

Tremblay, I., Paré, E., Arsenault, D., Douziech, M., & Boucher, M. J. (2013). The MEK/ERK Pathway Promotes NOTCH Signalling in Pancreatic Cancer Cells. *PLoS ONE*, *8*(12).

Turnbull, A. K., Arthur, L. M., Renshaw, L., Larionov, A. A., Kay, C., Dunbier, A. K., Thomas, J. S., Dowsett, M., Sims, A. H., & Dixon, J. M. (2015). Accurate Prediction and Validation of Response to Endocrine Therapy in Breast Cancer. *Journal of Clinical Oncology*, *33*(20), 2270–2278.

Turner, N. C., & Reis-Filho, J. S. (2006). Basal-like breast cancer and the BRCA1 phenotype. *Oncogene*, *25*(43), 5846–5853.

Turner, N. C., Ro, J., André, F., Loi, S., Verma, S., Iwata, H., Harbeck, N., Loibl, S., Huang Bartlett, C., Zhang, K., Giorgetti, C., Randolph, S., Koehler, M., & Cristofanilli, M. (2015). Palbociclib in Hormone-Receptor–Positive Advanced Breast Cancer. *New England Journal of Medicine*, *373*(3), 209–219.

Ursin, G., Bernstein, L., Lord, S. J., Karim, R., Deapen, D., Press, M. F., Daling, J. R., Norman, S. A., Liff, J. M., Marchbanks, P. A., Folger, S. G., Simon, M. S., Strom, B. L., Burkman, R. T., Weiss, L. K., & Spirtas, R. (2005). Reproductive factors and subtypes of breast cancer defined by hormone receptor and histology. *British Journal of Cancer*, *93*(3), 364.

Van't Veer, L. J., Dai, H., Van de Vijver, M. J., He, Y. D., Hart, A. A. M., Mao, M., Peterse, H. L., Van Der Kooy, K., Marton, M. J., Witteveen, A. T., Schreiber, G. J., Kerkhoven, R. M., Roberts, C., Linsley, P. S., Bernards, R., & Friend, S. H. (2002). Gene expression profiling predicts clinical outcome of breast cancer. *Nature 2002 415:6871*, *415*(6871), 530–536.

van de Vijver, M. J., He, Y. D., van 't Veer, L. J., Dai, H., Hart, A. A. M., Voskuil, D. W., Schreiber, G. J., Peterse, J. L., Roberts, C., Marton, M. J., Parrish, M., Atsma, D., Witteveen, A., Glas,

A., Delahaye, L., van der Velde, T., Bartelink, H., Rodenhuis, S., Rutgers, E. T., … Bernards, R. (2002). A Gene-Expression Signature as a Predictor of Survival in Breast Cancer. *New England Journal of Medicine*, *347*(25), 1999–2009.

Venkatachalam, K., Wong, C. O., & Zhu, M. X. (2015). The role of TRPMLs in endolysosomal trafficking and function. *Cell Calcium*, *58*(1), 48–56.

Versini, A., Colombeau, L., Hienzsch, A., Gaillet, C., Retailleau, P., Debieu, S., Müller, S., Cañeque, T., & Rodriguez, R. (2020). Salinomycin Derivatives Kill Breast Cancer Stem Cells by Lysosomal Iron Targeting. *Chemistry – A European Journal*, *26*(33), 7416–7424.

Viatour, P., Ehmer, U., Saddic, L. A., Dorrell, C., Andersen, J. B., Lin, C., Zmoos, A. F., Mazur, P. K., Schaffer, B. E., Ostermeier, A., Vogel, H., Sylvester, K. G., Thorgeirsson, S. S., Grompe, M., & Sage, J. (2011). Notch signaling inhibits hepatocellular carcinoma following inactivation of the RB pathway. *The Journal of Experimental Medicine*, *208*(10), 1963.

Voduc, K. D., Cheang, M. C. U., Tyldesley, S., Gelmon, K., Nielsen, T. O., & Kennecke, H. (2010). Breast cancer subtypes and the risk of local and regional relapse. *Journal of Clinical Oncology : Official Journal of the American Society of Clinical Oncology*, *28*(10), 1684–1691.

Wahba, H. A., & El-Hadaad, H. A. (2015). Current approaches in treatment of triple-negative breast cancer. *Cancer Biology & Medicine*, *12*(2), 106–116.

Wang, K., Zhang, Q., Li, D., Ching, K., Zhang, C., Zheng, X., Ozeck, M., Shi, S., Li, X., Wang, H., Rejto, P., Christensen, J., & Olson, P. (2015). PEST domain mutations in Notch receptors comprise an oncogenic driver segment in triple-negative breast cancer sensitive to a γ-secretase inhibitor. *Clinical Cancer Research : An Official Journal of the American Association for Cancer Research*, *21*(6), 1487–1496.

Wang, L., Sun, X., He, J., & Liu, Z. (2021). Functions and Molecular Mechanisms of Deltex Family Ubiquitin E3 Ligases in Development and Disease. *Frontiers in Cell and Developmental Biology*, *9*, 2355.

Wang, N. J., Sanborn, Z., Arnett, K. L., Bayston, L. J., Liao, W., Proby, C. M., Leigh, I. M., Collisson, E. A., Gordon, P. B., Jakkula, L., Pennypacker, S., Zou, Y., Sharma, M., North, J. P., Vemula, S. S., Mauro, T. M., Neuhaus, I. M., LeBoit, P. E., Hur, J. S., … Cho, R. J. (2011). Loss-of-function mutations in Notch receptors in cutaneous and lung squamous cell carcinoma. *Proceedings of the National Academy of Sciences of the United States of America*, *108*(43), 17761–17766.

Wang, Z., Zhang, X., Shen, P., Loggie, B. W., Chang, Y., & Deuel, T. F. (2005). Identification, cloning, and expression of human estrogen receptor-α36, a novel variant of human estrogen receptor-α66. *Biochemical and Biophysical Research Communications*, *336*(4), 1023–1027.

Weigelt, B., Geyer, F. C., & Reis-Filho, J. S. (2010). Histological types of breast cancer: How special are they? *Molecular Oncology*, *4*(3), 192–208.

Weng, A. P., Ferrando, A. A., Lee, W., Morris, J. P., Silverman, L. B., Sanchez-Irizarry, C., Blacklow, S. C., Look, A. T., & Aster, J. C. (2004). Activating Mutations of NOTCH1 in Human T Cell Acute Lymphoblastic Leukemia. *Science*, *306*(5694), 269–271.

Whiteman, P., De Madrid, B. H., Taylor, P., Li, D., Heslop, R., Viticheep, N., Tan, J. Z., Shimizu, H., Callaghan, J., Masiero, M., Li, J. L., Banham, A. H., Harris, A. L., Lea, S. M., Redfield,

C., Baron, M., & Handford, P. A. (2013). Molecular Basis for Jagged-1/Serrate Ligand Recognition by the Notch Receptor. *The Journal of Biological Chemistry*, *288*(10), 7305.

Wickham, H. (2009). ggplot2. *Ggplot2*.

Wickham, H. (2021). *tidyr: Tidy Messy Data. R package version 1.1.3. https://CRAN.R-project.org/package=tidyr*.

Wickham, H., François, R., Henry, L., & Müller, K. (2021). *dplyr: A Grammar of Data Manipulation. R package version 1.0.6.*

Wilkin, M., Tongngok, P., Gensch, N., Clemence, S., Motoki, M., Yamada, K., Hori, K., Taniguchi-Kanai, M., Franklin, E., Matsuno, K., & Baron, M. (2008). Drosophila HOPS and AP-3 Complex Genes Are Required for a Deltex-Regulated Activation of Notch in the Endosomal Trafficking Pathway. *Developmental Cell*, *15*(5), 762–772.

Wilson, J. J., & Kovall, R. A. (2006). Crystal Structure of the CSL-Notch-Mastermind Ternary Complex Bound to DNA. *Cell*, *124*(5), 985–996.

Woodward, W. A., Chen, M. S., Behbod, F., & Rosen, J. M. (2005). On mammary stem cells. *Journal of Cell Science*, *118*(Pt 16), 3585–3594.

Wu, L., & Yang, X. (2018). Targeting the Hippo Pathway for Breast Cancer Therapy. *Cancers*, *10*(11).

Wu, Y., Cain-Hom, C., Choy, L., Hagenbeek, T. J., De Leon, G. P., Chen, Y., Finkle, D., Venook, R., Wu, X., Ridgway, J., Schahin-Reed, D., Dow, G. J., Shelton, A., Stawicki, S., Watts, R. J., Zhang, J., Choy, R., Howard, P., Kadyk, L., … Siebel, C. W. (2010). Therapeutic antibody targeting of individual Notch receptors. *Nature 2010 464:7291*, *464*(7291), 1052–1057.

Xu, M., Almasi, S., Yang, Y., Yan, C., Sterea, A. M., Rizvi Syeda, A. K., Shen, B., Richard Derek, C., Huang, P., Gujar, S., Wang, J., Zong, W. X., Trebak, M., El Hiani, Y., & Dong, X. P. (2019). The lysosomal TRPML1 channel regulates triple negative breast cancer development by promoting mTORC1 and purinergic signaling pathways. *Cell Calcium*, *79*, 80–88.

Xu, T., & Artavanis-Tsakonas, S. (1990). deltex, a locus interacting with the neurogenic genes, Notch, Delta and mastermind in Drosophila melanogaster. *Genetics*, *126*(3), 665–677.

Yamada, K., Fuwa, T. J., Ayukawa, T., Tanaka, T., Nakamura, A., Wilkin, M. B., Baron, M., & Matsuno, K. (2011). Roles of Drosophila Deltex in Notch receptor endocytic trafficking and activation. *Genes to Cells*, *16*(3), 261–272.

Yan, Y., Liu, F., Han, L., Zhao, L., Chen, J., Olopade, O. I., He, M., & Wei, M. (2018). HIF-2α promotes conversion to a stem cell phenotype and induces chemoresistance in breast cancer cells by activating Wnt and Notch pathways. *Journal of Experimental & Clinical Cancer Research : CR*, *37*(1).

Yao, K., Rizzo, P., Rajan, P., Albain, K., Rychlik, K., Shah, S., & Miele, L. (2011). Notch-1 and Notch-4 receptors as prognostic markers in breast cancer. *International Journal of Surgical Pathology*, *19*(5), 607–613.

Yao, W., Shan, Z., Gu, A., Fu, M., Shi, Z., & Wen, W. (2018). WW domain–mediated regulation and activation of E3 ubiquitin ligase Suppressor of Deltex. *The Journal of Biological Chemistry*, *293*(43), 16697.

Yates, L. R., Knappskog, S., Wedge, D., Farmery, J. H. R., Gonzalez, S., Martincorena, I., Alexandrov, L. B., Van Loo, P., Haugland, H. K., Lilleng, P. K., Gundem, G., Gerstung, M.,

Pappaemmanuil, E., Gazinska, P., Bhosle, S. G., Jones, D., Raine, K., Mudie, L., Latimer, C., … Campbell, P. J. (2017). Genomic Evolution of Breast Cancer Metastasis and Relapse. *Cancer Cell*, *32*(2), 169-184.e7.

Ye, F., Zhong, X., Qiu, Y., Yang, L., Wei, B., Zhang, Z., & Bu, H. (2017). CD49f Can Act as a Biomarker for Local or Distant Recurrence in Breast Cancer. *Journal of Breast Cancer*, *20*(2), 142.

Yoon, K., & Gaiano, N. (2005). Notch signaling in the mammalian central nervous system: insights from mouse mutants. *Nature Neuroscience*, *8*(6), 709–715.

Yu, D., Holm, R., Goscinski, M. A., Trope, C. G., Nesland, J. M., & Suo, Z. (2016). Prognostic and clinicopathological significance of Cacna2d1 expression in epithelial ovarian cancers: a retrospective study. *American Journal of Cancer Research*, *6*(9), 2088.

Yu, G., & He, Q. Y. (2016). ReactomePA: an R/Bioconductor package for reactome pathway analysis and visualization. *Molecular BioSystems*, *12*(2), 477–479.

Yu, L., Fan, Z., Fang, S., Yang, J., Gao, T., Simões, B. M., Eyre, R., Guo, W., & Clarke, R. B. (2016). Cisplatin selects for stem-like cells in osteosarcoma by activating Notch signaling. *Oncotarget*, *7*(22), 33055–33068.

Yun, J., Pannuti, A., Espinoza, I., Zhu, H., Hicks, C., Zhu, X., Caskey, M., Rizzo, P., D'Souza, G., Backus, K., Denning, M. F., Coon, J., Sun, M., Bresnick, E. H., Osipo, C., Wu, J., Strack, P. R., Tonetti, D. A., & Miele, L. (2013). Crosstalk between PKCα and Notch-4 in endocrine-resistant breast cancer cells. *Oncogenesis*, *2*(8).

Zeevi, D. A., Frumkin, A., & Bach, G. (2007). TRPML and lysosomal function. *Biochimica et Biophysica Acta (BBA) - Molecular Basis of Disease*, *1772*(8), 851–858.

Zehir, A., Benayed, R., Shah, R. H., Syed, A., Middha, S., Kim, H. R., Srinivasan, P., Gao, J., Chakravarty, D., Devlin, S. M., Hellmann, M. D., Barron, D. A., Schram, A. M., Hameed, M., Dogan, S., Ross, D. S., Hechtman, J. F., DeLair, D. F., Yao, J., … Berger, M. F. (2017). Mutational landscape of metastatic cancer revealed from prospective clinical sequencing of 10,000 patients. *Nature Medicine*, *23*(6), 703–713.

Zeng, Q., Li, S., Chepeha, D. B., Giordano, T. J., Li, J., Zhang, H., Polverini, P. J., Nor, J., Kitajewski, J., & Wang, C. Y. (2005). Crosstalk between tumor and endothelial cells promotes tumor angiogenesis by MAPK activation of Notch signaling. *Cancer Cell*, *8*(1), 13–23.

Zhang, P., Yang, Y., Nolo, R., Zweidler-McKay, P. A., & Hughes, D. P. M. (2010). Regulation of NOTCH signaling by reciprocal inhibition of HES1 and Deltex 1 and its role in osteosarcoma invasiveness. *Oncogene 2010 29:20*, *29*(20), 2916–2926.

Zhang, Z., & Richmond, A. (2021). The Role of PI3K Inhibition in the Treatment of Breast Cancer, Alone or Combined With Immune Checkpoint Inhibitors. *Frontiers in Molecular Biosciences*, *8*, 286.

Zheng, L., & Conner, S. D. (2018). PI5P4Kγ functions in DTX1-mediated notch signaling. *Proceedings of the National Academy of Sciences of the United States of America*, *115*(9), E1983–E1990.

Zheng, Q., Zhang, M., Zhou, F., Zhang, L., & Meng, X. (2021). The Breast Cancer Stem Cells Traits and Drug Resistance. *Frontiers in Pharmacology*, *0*, 2120.

Zheng, Z. Y., Anurag, M., Lei, J. T., Cao, J., Singh, P., Peng, J., Kennedy, H., Nguyen, N. C., Chen,

Y., Lavere, P., Li, J., Du, X. H., Cakar, B., Song, W., Kim, B. J., Shi, J., Seker, S., Chan, D. W., Zhao, G. Q., … Chang, E. C. (2020). Neurofibromin is an Estrogen Receptor-α Transcriptional Co-repressor in Breast Cancer. *Cancer Cell*, *37*(3), 387.

Zhou, L., Wang, D., Sheng, D., Xu, J., Chen, W., Qin, Y., Du, R., Yang, X., He, X., Xie, N., Liu, S., & Zhang, L. (2020). NOTCH4 maintains quiescent mesenchymal-like breast cancer stem cells via transcriptionally activating SLUG and GAS1 in triple-negative breast cancer. *Theranostics*, *10*(5), 2405–2421.

8 Appendix

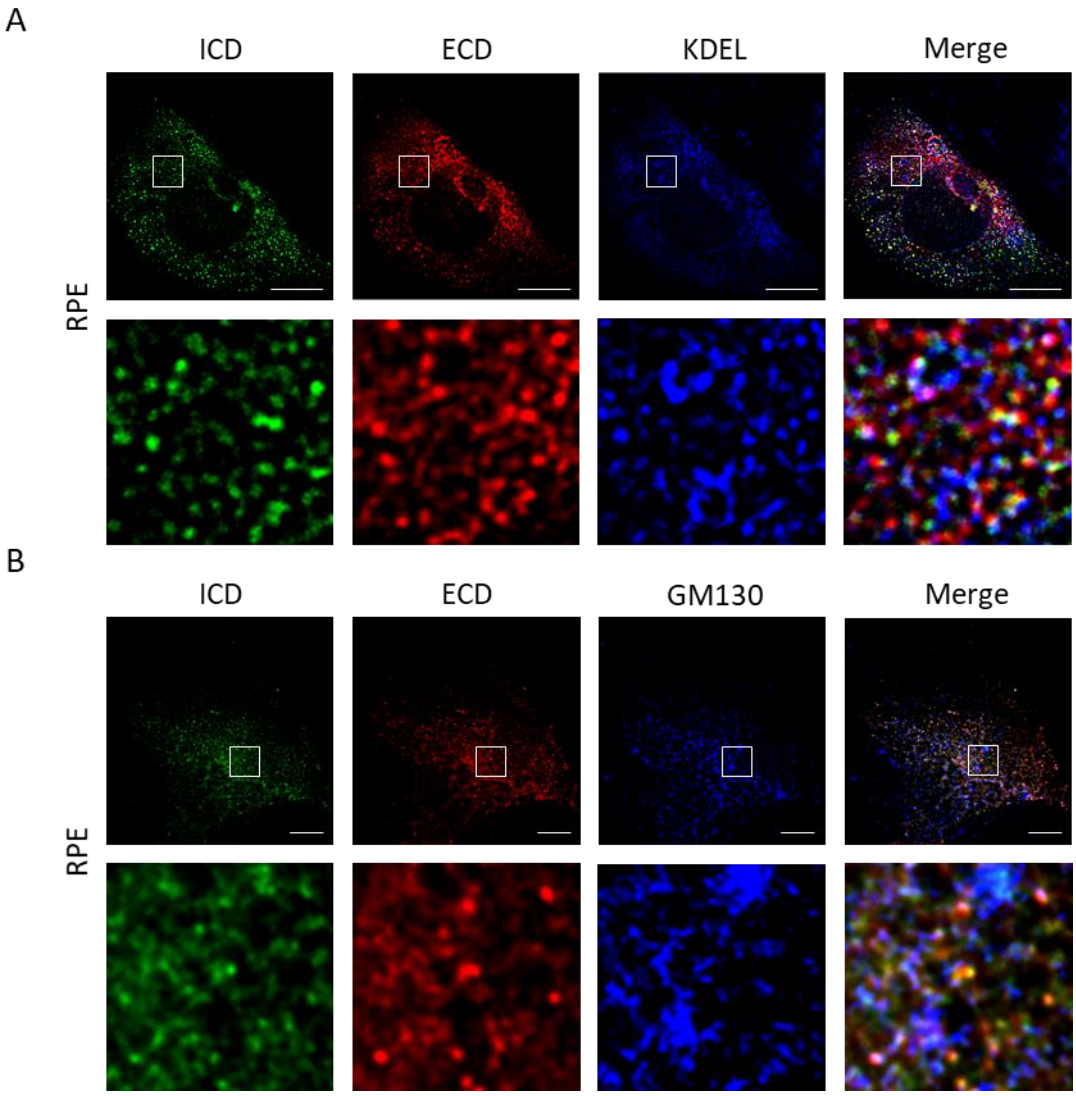

Figure 8-1: Full length Notch4 is not found predominantly in the Endoplasmic Reticulum or the Golgi. Immunofluorescence images of RPE cells transiently transfected with a Notch4 plasmid using GeneJuice® showing one plane of Notch4 ICD (green), Notch4 ECD (red) and (A) KDEL- Endoplasmic Reticulum marker (blue) and (B) GM130 – Golgi marker (blue) and a merge of the three channels to demonstrate colocalisation. Areas zoomed in to show detail in higher magnification, indicated by the white squares. Scale bars: 5µm.

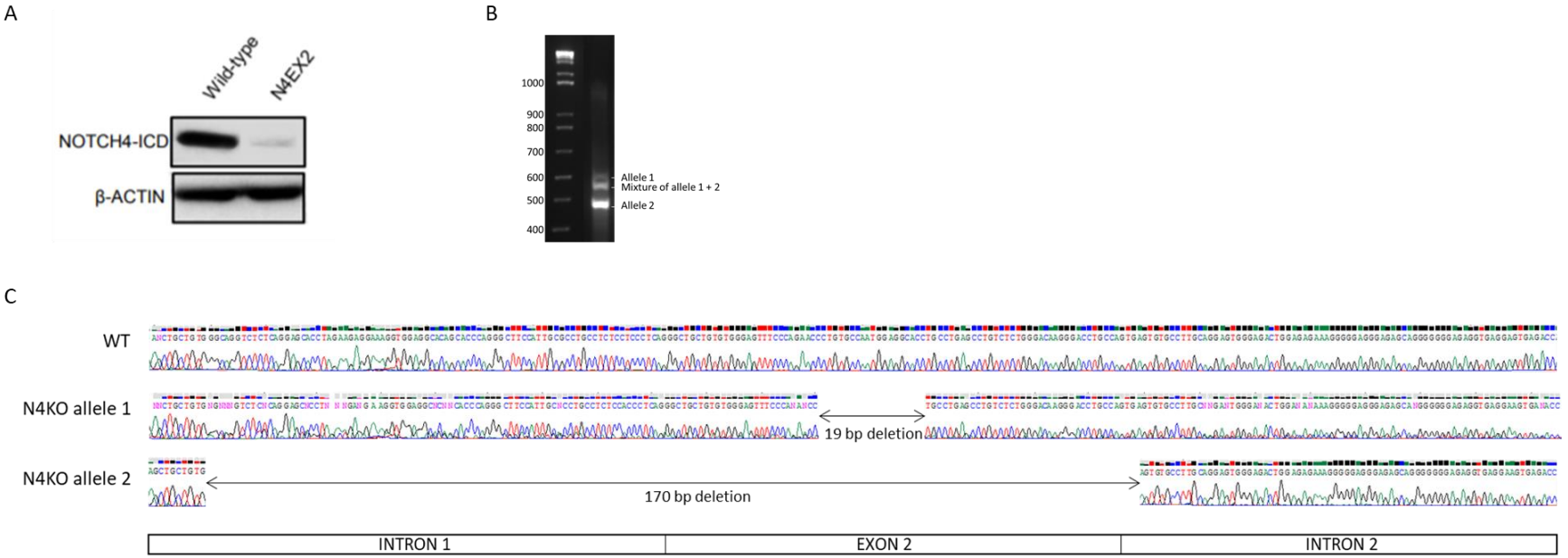

Figure 8-2: N4KO cells characterisation. A) Western blot comparing wildtype and N4KO cells showing reduction in Notch4 ICD protein levels in N4KO cells. B) Agarose gel of a portion of DNA in the Notch4 gene N4KO cells showing two fragments (2 allelic variants) containing deletions, and a further fragment which is a PCR product containing a mixture of the two alleles. C) Representation of the DNA sequence of the wildtype NOTCH4 gene and two deletions found in two alleles of the N4KO MCF7 cells. This is compared to the relative position of introns and exons along the sequence.

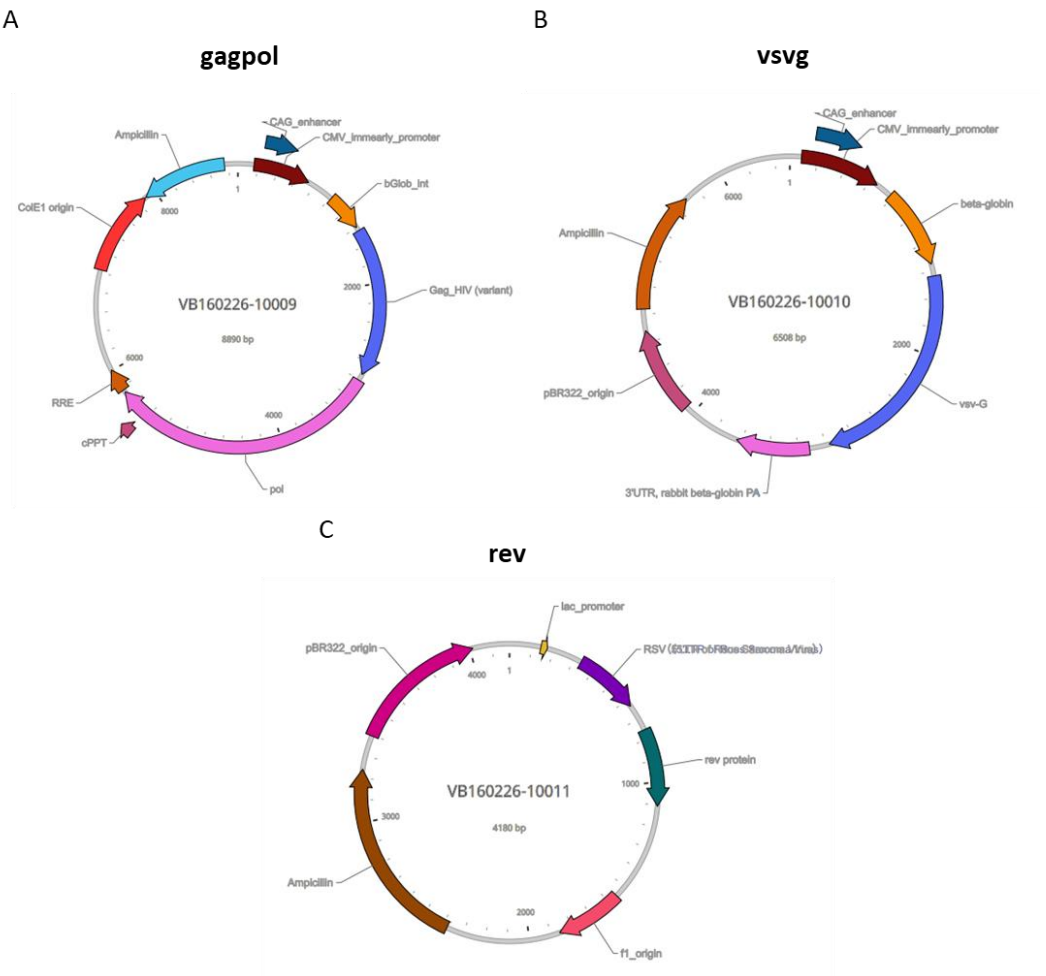

Figure 8-3: Plasmids used for lentivirus production- "gagpol", "vsvg" and "rev". Plasmids obtained from VectorBuilder for use in production of lentivirus.

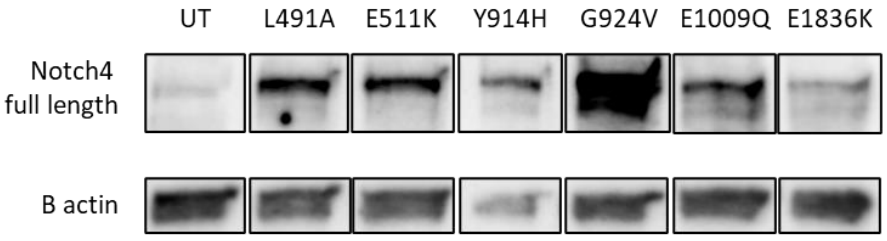

Figure 8-4: Transient transfection of MCF7 cells with mutated Notch4 plasmids leads to increased protein expression of Notch4, detected by western blot. Cells were transfected with Notch4 plasmids for 24 hours, after which, protein was extracted and analysed by western blot for Notch4.

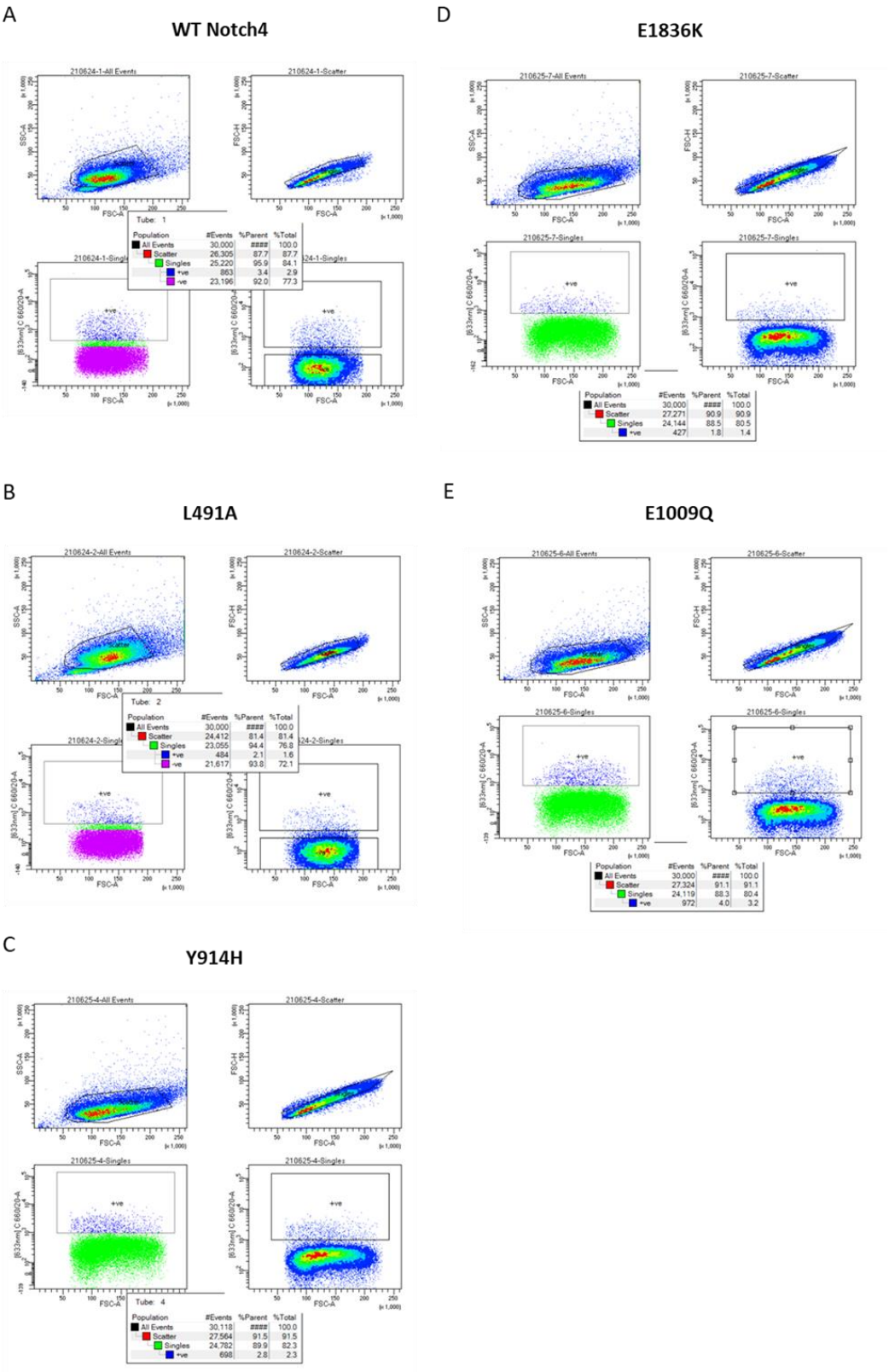

Figure 8-5: FACS plots showing sorting protocol for mutant Notch4 MCF7 cells. MCF7 cells were transiently transfected with different mutant Notch4 plasmids- L491A, E511K, Y914H, G924V, E1009Q, E1836K and WT Notch4. After 24 hours they were stained with Notch4-AF647 antibody and sorted for cells positive for Notch4 (and negative cells in the case of hN4).

Gene ID	Calculated fold change of gene expression N4KO-N4 vs N4KO-CON
JAG1	2.84
HEY1	2.82
HES2	2.35
JAG2	2.33
HES6	1.86
DLL1	1.66
NOTCH1	1.53
HES1	1.49
NOTCH4	1.49
CDKN1A	1.44
VPS18	1.31
HES4	1.29
DLL4	1.21
GATA3	1.20
RAB7A	1.19
DTX2	1.05
VPS33A	1.02
NOTCH2	0.98
NOTCH3	0.96
CCND1	0.91
DTX4	0.88
HEYL	0.83
DTX3L	0.78
DTX3	0.71
HEY2	0.42

Table 8-1: Calculated fold change of gene expression between N4KO-N4 and N4KO-CON cells of a Notch related user defined list of genes.

Gene ID	Calculated fold change of gene expression (vs sorted Notch4 negative cells)				
	WT Notch4	L491A	Y914H	E1009Q	E1836K
NOTCH4	82.74	14.98	47.81	63.60	42.38
CDKN1A	2.12	2.45	2.59	2.48	3.24
VPS18	1.09	1.29	0.84	0.80	0.94
DTX4	1.09	1.06	0.95	0.78	0.91
DTX3	1.07	1.18	1.32	1.10	1.39
DTX3L	1.06	0.88	1.33	1.35	1.29
VPS33A	1.06	1.29	1.10	1.02	1.05
DTX2	1.02	0.98	0.87	0.81	0.86
RAB7A	1.01	1.01	0.99	0.89	0.89
HES2	1.00	1.08	1.14	1.10	1.39
NOTCH2	1.00	1.07	0.85	0.93	1.04
CCND1	0.99	0.95	1.03	1.03	1.08
HES4	0.98	1.19	1.15	1.20	1.21
JAG2	0.98	0.91	0.63	0.53	0.56
HES6	0.92	0.71	0.73	0.83	0.77
JAG1	0.92	0.94	1.55	1.57	1.65
NOTCH3	0.91	0.87	1.02	1.01	1.16
HEY1	0.88	0.73	1.39	1.65	0.80
HEY2	0.87	0.58	0.66	0.66	0.62
NOTCH1	0.86	0.91	0.75	0.86	1.11
DLL1	0.85	1.04	0.93	1.19	1.05
HES1	0.85	1.04	0.48	0.45	0.50
HEYL	0.81	1.00	0.94	1.02	1.20
GATA3	0.79	0.64	0.73	0.66	0.69
DLL4	0.70	1.03	0.63	1.27	0.61

Table 8-2: Calculated fold change of gene expression between WT, L491A, Y914H, E1009Q, E1836K Notch4 and sorted Notch4 negative cells of a Notch related user defined list of genes.

Biological Processes

WT Notch4

Extracellular matrix organization
Response to external stimulus
Response to chemical
Extracellular structure organization
Metal ion transport
Locomotion
Muscle organ development
Cell surface receptor signaling pathway
Response to cytokine
Cell motility

L491A Notch4

mit+A23:A49otic cell cycle process
Cell cycle process
Cell cycle
Mitotic cell cycle
Mitotic cell cycle phase transition
Cell cycle phase transition
Nuclear division
Organelle fission
DNA-dependent DNA replication
Cell division

Y914H Notch4

Mitotic cell cycle
Mitotic cell cycle process
Cell cycle
Cell division
Cell cycle process
Nuclear division
Mitotic sister chromatid segregation
Mitotic nuclear division
Nuclear chromosome segregation
Sister chromatid segregation

E1009Q Notch4

Mitotic cell cycle
Mitotic cell cycle process
Cell cycle process
Cell cycle
Cell division
Nuclear division
Chromosome segregation
Nuclear chromosome segregation
Mitotic sister chromatid segregation
Sister chromatid segregation

E1836K Notch4

Immune response
Innate immune response
Cell surface receptor signaling pathway
Defense response
Immune system process
Positive regulation of immune system process
Positive regulation of immune response
Response to cytokine
Positive regulation of response to stimulus
Cytokine-mediated signaling pathway

Figure 8-6: Biological processes that are enriched in WT or each mutant Notch4 expressing population of cells. The 10 most highly associated biological processes are included. Differentially expressed genes with a log2 fold change of more than 1 were included in the analysis.

Molecular Functions

WT Notch4

Signalling receptor binding
Phenanthrene 9,10-monooxygenase activity

L491A Notch4

Signalling receptor binding
Peptide antigen binding
Receptor ligand activity
Receptor regulator activity
MHC class II receptor activity
Cytokine activity
MHC class II protein complex binding
Monovalent inorganic cation transmembrane transporter activity
Phenanthrene 9,10-monooxygenase activity
MHC protein complex binding

Y914H Notch4

Protein binding
Tubulin binding
Microtubule binding
Microtubule motor activity
Single-stranded DNA-dependent ATP-dependent DNA helicase activity
Single-stranded DNA-dependent ATPase activity
ATPase activity
ATP-dependent DNA helicase activity
ATP-dependent helicase activity
Purine NTP-dependent helicase activity

E1009Q Notch4

Signalling receptor binding
Extracellular matrix structural constituent
Microtubule motor activity
Receptor regulator activity
Receptor ligand activity
Cytokine activity
Protein binding
Microtubule binding
Tubulin binding
Motor activity

E1836K Notch4

Protein binding
Catalytic activity, acting on DNA
DNA helicase activity
Single-stranded DNA-dependent ATP-dependent DNA helicase activity
Single-stranded DNA-dependent ATPase activity
ATP-dependent DNA helicase activity
ATP-dependent helicase activity
Purine NTP-dependent helicase activity
Microtubule motor activity
DNA-dependent ATPase activity

Figure 8-7: Molecular functions that are enriched in WT or each mutant Notch4 expressing population of cells. The 10 most highly associated molecular functions are included. Differentially expressed genes with a log2 fold change of more than 1 were included in the analysis.